Design and characterization of direct compression excipients

Patel, Chaitanya I.

Award date:
1986

Awarding institution:
University of Bath

Design and Characterization of Direct Compression Excipients.

A thesis submitted by
Chaitanya. I. Patel
for the degree of PhD
at the University of Bath
1986

ProQuest LLC
789 East Eisenhower Parkway
P.O. Box 1346
Ann Arbor, MI 48106-1346

SUMMARY

Quantitative differences in plasticity of several direct compression excipients were found to be distinguishable using normalised work of failure determinations. New parameters were developed to account for changes in strain rate application during diametral crushing. Failure viscosity was found to have a similar sensitivity to changes in excipient plasticity to that obtained using NWF determinations. However, power of failure lacked the sensitivity required to distinguish small changes in plastic behaviour. A test to determine the fatigue strength of tablets was developed and was found to differentiate the ability of Avicel, Microtal and Emcompress tablets to relieve stress at crack tips. Monitoring the acoustic emissions which occurred during fatigue testing showed that different modes of fatigue failure were produced prior to brittle fracture in Emcompress and ductile fracture in Avicel or Microtal tablets.

Creep compliance curves for the powders studied could be differentiated into three distinct types of behaviour: elastic, visco-elastic and plastic deformation. Such curves were found useful in describing the rheological characteristics of direct compression excipients.

An assumption, reported in the literature, - namely that work performed during 2nd compression may be used to represent work required for elastic deformation, was found to be invalid. Determination of the true work of compaction was found not to be a good measure of an excipients' tendency to undergo irreversible deformation. It was also found that the method used to determine true work of compaction influenced power of compaction determinations.

A method of particle engineering is described for the production of physico-mechanically modified sucrose crystals for use as direct compression excipients. Crystallization of sucrose by a co-transformation process, in the presence of polymeric materials such as maltodextrin, gelatins and celluloses, increased the inherent plasticity of transformed sucrose. The inherent plasticity of sucrose co-transformed with 1% and 3% w/w maltodextrin or 1% w/w gelatin was found to be greater than direct compression excipients such as Dipac, Nutab, Emcompress, Tablettose, Fast-Flo and anhydrous lactose.

ACKNOWLEDGEMENTS

In the course of this study, the author has drawn on the time and experience of many people.

Firstly, the author would like to thank his academic supervisor Dr. J.N. Staniforth, for his guidance, encouragement, critical discussion and understanding throughout the whole of this study. The help and discussions with Professor J.E. Rees are also very much appreciated.

The author deeply appreciates and acknowledges the expert technical assistance, critical discussions and friendship of Mrs. J.P. Hart. The assistance of Mrs S. Carter is also acknowledged.

The author would like to thank his industrial supervisor, Dr. M.G. Lindley, for his encouragement and use of facilities during the part of this study conducted at the Tate & Lyle Research Laboratories in Reading. The help and assistance of other Tate & Lyle personnel, especially, Mr. J. Bateman, Dr. C. Goodacre, and Mr. K. Sinclair is also acknowledged.

The author would also like to thank Professor B. Harris of the School of Materials Science, University of Bath, for use of acoustic emission equipment. The assistance of numerous post-graduates in the School of Materials Science, especially Mr. M. Moghisi; Mr. B. Chapman, of the School of Physics and Mrs. K. Powell, of the Electron Optics Centre, University of Bath is also acknowledged.

The author would like to thank Dr. Reiter and Dr. W. Arnold of the Fraunhofer-Institute for Non-Destructive Testing, Saarbrucken, Federal Republic of Germany, for the use of a Scanning Laser Acoustic Microscope and discussions.

Lastly, the author would like to thank Science and Engineering Research Council and Tate & Lyle for funding this work.

To my wife and my parents

CONTENTS Page No.

CONTENTS Page No.

CONTENTS Page No.

CONTENTS Page No.

LIST OF FIGURES

Table No. LIST OF TABLES Page No.

1. INTRODUCTION.

1.1 Compressed Tablets.

The compressed tablet is the most widely used form of oral drug dosage form in both human and veterinary medicine. Numerous advantages are offered to both the patient and the manufacturer. The tablet provides an economical and simple method for large batch production of reproducibly accurate dosage forms. It is also convenient for purposes of storage, packaging and dispensing and thus tablets have largely replaced other unit dosage forms of solid drugs.

1.2 Methods of Tablet Preparation.

Three different techniques are commonly used in tablet preparation: wet granulation; dry granulation and direct compression. Wet granulation was the first method to be described for production of compressed tablets and is still the most widely used. The technique can be separated into distinct stages: preliminary blending; preparation of binder solution; wet massing; wet screening; drying; dry screening; addition of lubricants and disintegrants and finally, tablet compression. Dry granulation provides an alternative method for drugs which are sensitive to moisture or heat. Mixed dry powders are compressed into large weak tablets known as "slugs" which are then milled and compressed into tablets. Alternatively, small granular compacts can be produced directly using a technique known as roller compaction. The method of direct compression

provides the simplest possible technique for tablet compression, the only process necessary prior to tablet compression being a dry mixing stage for drug and excipient powders.

1.3 Advantages and Disadvantages of Direct Compression Excipients.

The direct compression technique eliminates the time consuming wet-massing and screening processes used in wet granulation, as well as the energy consuming drying process and has been shown to be both an extremely efficient and effective alternative to conventional tablet production methods (Cohn et al., 1966; Mendell, 1972; Ingale, 1979). The use of a direct compression technique avoids contact between chemically unstable drugs and granulating solutions, thus minimising the risk of accelerated decomposition in the presence of excipients. There are also some potential disadvantages associated with use of the direct compression technique. Wet granulation can be used to improve the processing behaviour of raw materials, so that precise control of physico-mechanical properties of the excipients, may be of minor importance. In contrast, direct compression excipients must possess well defined physico-mechanical properties since no major alterations to tablet performance can be brought about during subsequent processing.

Although individual excipients may have a weakness in one particular area, direct compression excipients as a whole have two major disadvantages. Gunsel et al. (1976) considered that unless the drug itself was easily compressible, the amount of

drug which can be added to the excipient is restricted to about 30% of the compression weight. It is for this reason that the direct compression technique is often confined to tableting low-dose, high potency drugs. This leads to the second disadvantage, which is the tendency for the excipient to segregate from drug particles in a free flowing mix. Selkirk (1974) and Spring (1977), have shown that segregation of drugs from excipients can also occur with wet granulations, but the completely free movement of particles in a direct compression mix means that any segregation tendency during processing will almost inevitably lead to dosage variations.

1.3.1 Direct Compression Excipients.

Kanig (1970) has listed fourteen properties that an ideal direct compression excipient should possess: high fluidity; high compressibility; physiological inertness; compatibility with all types of active ingredients; showing no physical or chemical change on ageing and stable to air, moisture and heat; high capacity; colourlessness and tastelessness; ability to accept colourants uniformly; relatively low in cost; possession of proper mouth feel; non-interference with the biological availability of the active ingredients, unless specifically designed to do so; particle size range which should be equivalent to most active ingredients; capable of being reworked without loss of flow or compressibility; a good pressure-hardness (sic) profile.

The suitability of a direct compression formulation depends

primarily on the "capacity" of the main diluent excipient. The capacity of a diluent excipient can be defined as the ability to produce a tablet with acceptable physico-mechanical properties especially crushing forces, when blended with drug powders. The capacity of the excipient is limited by its inherent physical and mechanical properties. Physical properties influence the tendency for drug segregation to occur following mixing which may lead to unacceptable tablet content uniformity. Mechanical properties govern the ability of an excipient to form a tablet in the presence of an inherently poorly compactible drug.

1.3.2 Physico-mechanical Properties of Some Direct Compression Excipients.

1.3.2.1 Cellulose.

Battista and Smith (1962) reported the preparation of a microcrystalline cellulose (Avicel, American Viscose Corp., U.S.A.) by the acid hydrolysis of a soluble pulp. Lamberson and Raynor (1976) stated that the high purity of microcyrstalline cellulose (mcc) was due to the acid hydrolysis process. Studies carried out by Battista and Smith (1962) showed the compressional, self-lubrication and disintegration qualities exhibited by this mcc product to be excellent.

In studies carried out by Fox et al. (1963) the major advantage of this product was considered to be its ability to act as a dry binder. The excellent combination of compaction and disintegration properties of mcc has been attributed to the

presence of hydrogen bonds between the particles (Reier and Shangraw, 1966) although the presence of such bonds was not demonstrated until work reported by Huettenrauch (1971).

The flow properties of mcc have drawn some attention in the literature, where perhaps surprisingly, Fox et al. (1963) and Livingstone (1970) have stated mcc possesses good flow properties. However, Mendell (1972) reported that mcc exhibited the poorest flowability of all the excipients studied. The reason for this discrepancy is that the flow rate measured by Fox et al. (1963) and Livingstone (1970) is based on bulk volumetric rates (ml/s) and consequently, powders with low bulk density were misleadingly found to possess high flow rates. Mendell (1972) used the conventional, mass rate measurements (kg/s), to determine the flow rate of mcc.

Richman et al. (1965) have described the use of mcc in the preparation of stable glycerin trinitrate tablets by direct compression. More recently Graf and Sakr (1978) found Avicel PH101 and Avicel PH102 to be the most efficient excipients for Stomach Extract tablets. But the greatest use of the Avicels has been as a dry binder.

Wells and Langridge (1981) evaluated binary mixes of mcc and dicalcium phosphate dihydrate with microfine paracetamol as the drug. Their study revealed that good compression mixes contained between 66-90% mcc and 10-33% dicalcium phosphate dihydrate with 0.5% magnesium stearate as the lubricant. Laakso et al. (1982) used mcc as a binder with xylitol in their acetylsalicylic acid (ASA) formulation and showed that mcc had a

greater influence on the release of ASA than xylitol and that mcc combined with xylitol was more suitable for use as an excipient in direct compression than in wet granulation procedures. Bangudu and Pilpel (1985) reported that as the percentage of mcc in a mixture was increased the tensile strength of the tablets also increased. This observation was attributed to a decrease in the elastic recovery to stress relaxation ratio. Their results also explain the use of approximately 25% of mcc, by Lieberman and Lachman (1980) in commercial paracetamol tablets.

In the studies where mcc has been used as a dry binder, no further investigations have been carried out by the workers in an attempt to design an excipient with the high plastic deformation characteristics which their studies indicated to be desirable for direct compression excipients.

1.3.2.2 Starch.

Paronen and Juslin (1983) studied the compressional properties of four starches. From the compressional data these workers showed that the tendency of the starches to undergo plastic flow during compaction was dependent on particle size, size distribution and particle shape. Spherical potato and maize starch particles were found to be more prone to plastic deformation than the plate-like barley and wheat starch particles. Ideally, the study should have been conducted with a single-sourced starch in order to investigate the influence of particle shape on particle plasticity so as to eliminate possible differences due to the origin of the starch. Their results also

showed that maize starch undergoes considerable plastic flow and only a little elastic recovery. Barley and wheat starches undergo more elastic deformation than maize and potato starches during compaction.

Sakr et al. (1974) evaluated some direct compression excipients in an acetylsalicylic acid formulation and stated that Starch 1500 was the "ideal excipient" among the starches studied. They also reported that Starch 1500 was "better" than mcc and anhydrous lactose U.S.P. Their results show that Starch 1500 has a fairly high degree of cohesiveness, is self lubricating and self disintegrating.

Kassem (1981) found that Starch 1500 could be used to produce direct compression Aluminium Aspirin tablets with satisfactory uniformity of weight and mechanical properties. The other excipients used in the formulation, Avicel PH101, Emdex, anhydrous lactose and Emcompress, improved mechanical properties as their concentration was increased, but unlike Starch 1500 tablets, all failed the B.P. disintegration test.

1.3.2.3 Lactose.

Castello and Mattocks (1962) and later Gunsel and Lachman (1963) reported that tablets prepared using spray-dried lactose tended to discolour much more than conventionally processed lactose following storage. Castello and Mattocks (1962) concluded from their stability studies that the browning was a result of a reaction of lactose with alkaline lubricants at high temperatures and humidity levels. Brownley and Lachman (1964)

showed that the browning reaction was due to presence of 5-(hydoxymethyl)-2-furaldehyde (HMF) which reacted with any amine groups present in the powders of the formulation.

Studies carried out by Newton and Fell (1970, 1971a, 1971b, 1971c) using different drying, feed rate and stirring conditions showed that various grades of spray-dried lactose could be produced, giving a range of tablet strengths. These workers reported that the presence of alpha-lactose monohydrate in a mixture of alpha- and beta-lactose increased tensile strength. It was assumed that alpha-monohydrate created a greater number of intimate contacts there by increasing the degree of inter-particle bonding.

Commercially available direct compression lactoses include Tablettose, a pure form of alpha-monohydrate (Meggle Milchindustrie) and two forms of spray dried lactoses, Fast-Flo (Foremost Whey Products) and Zeparox (Dairy Crest), both of which are composed of a high proportion of alpha-monohydrate. However, these lactoses are still widely used in combination with dry binders, (Armstrong and Lowndes, 1984) suggesting that the lactose excipients lack the high degree of plastic deformation necessary for satisfactory tablets to be produced by direct compression techniques.

1.3.2.4 Dextrose.

Henderson and Bruno (1970) compared the physical properties and direct compression characteristics of lactose USP monohydrate and anhydrous lactose USP with lactose USP (beadlets)

and dextrose (PAF2011, available as Emdex). They concluded that the compressional characteristics of Emdex were superior to those of the lactoses, although no reason has been put forward by these workers to account for this difference. Emdex is the product of starch hydrolysis and consists of approximately 90-92% dextrose with 3-5% maltose and the remainder is higher glucose saccharide units (Mendell, 1972). The maltose and the higher saccharides may act as plasticizers, thus accounting for the higher crushing force of Emdex.

Bolhuis et al. (1974) stated that Emdex required a minimum of 1% magnesium stearate as a lubricant due to the high degree of friction between the tablet and die walls.

1.3.2.5 Sucrose.

The monoclinic crystal characteristic of granular sucrose is free-flowing but compresses poorly (Shangraw et al., 1981). Various workers (Hardman and Lilley, 1970; Rees and Hersey, 1971) have demonstrated that sucrose particles undergo irreversible deformation by extensive particle fragmentation when compressed. Consequently sucrose crystals tend to form tablets with low mechanical resistance so that "granular" sucrose is infrequently used as a direct compression excipient.

Ondari et al. (1983) have compared the fundamental properties of two commercially available sucrose-based excipients, Dipac (sucrose co-crystallized with modified dextrins) and Nutab (processed sucrose with 4% invert sugar and approximately 0.2% maize starch and magnesium stearate), with two

grades of California and Hawaiian Sugars (C & H). These workers found that the two grades of C & H sugars possessed higher crushing forces and lower friability than either Dipac or Nutab. However, the workers do not state the nature of the two grades of C & H products.

1.3.3 Design of Direct Compression Excipients.

In order to obtain an excipient having optimum flow, mixing and compression properties, some physical or chemical modifications of the raw materials may be required. This modification process has been termed "Particle Engineering" by Staniforth (1984). Probably the most useful particle engineering method is crystallization; where alteration of conditions can yield a wide variety of physical and/or chemical forms which have different bulk properties.

Kanig (1964) co-crystallized mannitol with various carbohydrates in order to improve the flow and compressional properties of mannitol. He found a difference in the lubricant requirement of co-crystallized products and admixes of the powders. This difference may be attributed to the shape of the particles:- co-crystallized powder particles were observed to be smooth, regular spheres while those of the admixes were irregular. Although mannitol has been co-crystallised with polymeric materials such as beeswax, polyethylene glycol 4000 and carboxymethylcellulose by Kanig there is no published data describing the mechanical properties of these tablets.

Newton and Fell (1970, 1971a, 1971b and 1971c) found that

changes in crystal structure during spray drying could alter the direct compression properties of spray-dried lactose. They used a polarimetric technique to distinguish between alpha- and beta-lactose and thermogravimetry was used to quantify the proportion of alpha-lactose monohydrate. They obtained several batches of spray-dried lactose by controlling the drying conditions and thus were able to vary the proportion of each form of lactose.

With specific interest in the design of direct compression excipients, Staniforth et al. (1981) used six different crystallization methods to modify crystal habit in order to produce a new mannitol excipient which formed non-segregating ordered mixes with drug particles. They reported that the recrystallized mannitol was more resistant to vibrational segregation than anhydrous lactose, due to the highly irregular surface of recrystallized mannitol which was sufficiently porous to entrap drug particles. However, these workers did not comment on the compactibility of their product.

In an attempt to produce a cellulose-based direct compression excipient with surface properties similar to those of habit-modified mannitol, as described above, Staniforth and McCluskey (1982) prepared a co-precipitated cellulose powder (C.P.C.). When compared with four commercially available cellulose products, C.P.C. was found to be highly porous, having relatively large volumes of macro-, meso-, and micro-pores. In addition, C.P.C. and Elcema G250 possessed faster flow rates than the finer-particle excipients such as Avicel and Elcema P100. These workers have reported the physical properties of their

powder, but again no data regarding the compressional behaviour of their powder was obtained.

Unlike Newton and Fell (1970) who produced polymorphs of lactose, Staniforth (1984), by careful control of crystallization conditions, was able to produce various crystal polytypes so that all crystals were composed of only alpha-stable lactose monohydrate. The physical properties of lactose polytypes such as flow, porosity, surface area, roughness and shape, were found to be optimal for spherulites crystallized from a solution containing 80% ethanol. However, it would have been of interest to compare the compressional behaviour of this powder with commercial direct compression excipients, but no data was presented by Staniforth (1984).

A major objective of the present study was to investigate the use of a particle engineering technique in changing the compressional behaviour of a carbohydrate-based powder.

1.4 Sucrose.

Sucrose is a non-reducing disaccharide carbohydrate: systematic name, beta-D-fructofuranosyl-alpha-D-glucopyranoside. The structure of sucrose has been established both by enzymic synthesis (Hassid and Doudoroff, 1944 and 1950), and chemical synthesis (Lemieux and Huber, 1953; Iley and Fraser-Reid, 1975). The precise molecular structure of sucrose has been determined by physical methods such as x-ray crystallography (Beevers and Cochran, 1947; Gilardi and Flippen, 1975) and neutron diffraction (Brown and Levy, 1963 and 1973).

1.4.1 Sucrose Crystallization.

Crystalline sucrose is commonly produced by preparing hot concentrated syrup in pans, followed by evacuation to remove water. Residual liquor is seeded with pure sucrose crystals which initiates nucleation and secondary growth produces crystal agglomerates which gradually form in the mother liquor. The sucrose agglomerates are separated, usually by centrifugation. The mother liquor is then reboiled and the cycle repeated to produce a second crop of crystals. This process may be repeated a number of times, the final residue left when the last crop of crystals has been separated is known as molasses. One of the advantages of this process is that an extremely pure sucrose is obtained in the first crop. However the process is very slow, energy and equipment intensive and complex to control.

An alternative process for sucrose crystallization is called "transformation" (Nicol, 1974)

1.4.2 Transformation of Sucrose.

Sucrose transformation is a continuous process of crystallization with no by-products. A hot sucrose syrup is stored in a tank (A, Fig. 1) and usually has a solids content between 50% and 80% by weight. From this tank the syrup is passed to a plate evaporator (B, Fig. 1) where it is concentrated by removal of water, to form a sucrose syrup which may have a solids content of 90% or more by weight. This is then passed through a second evaporator (C, Fig. 1), which is heated by steam, where

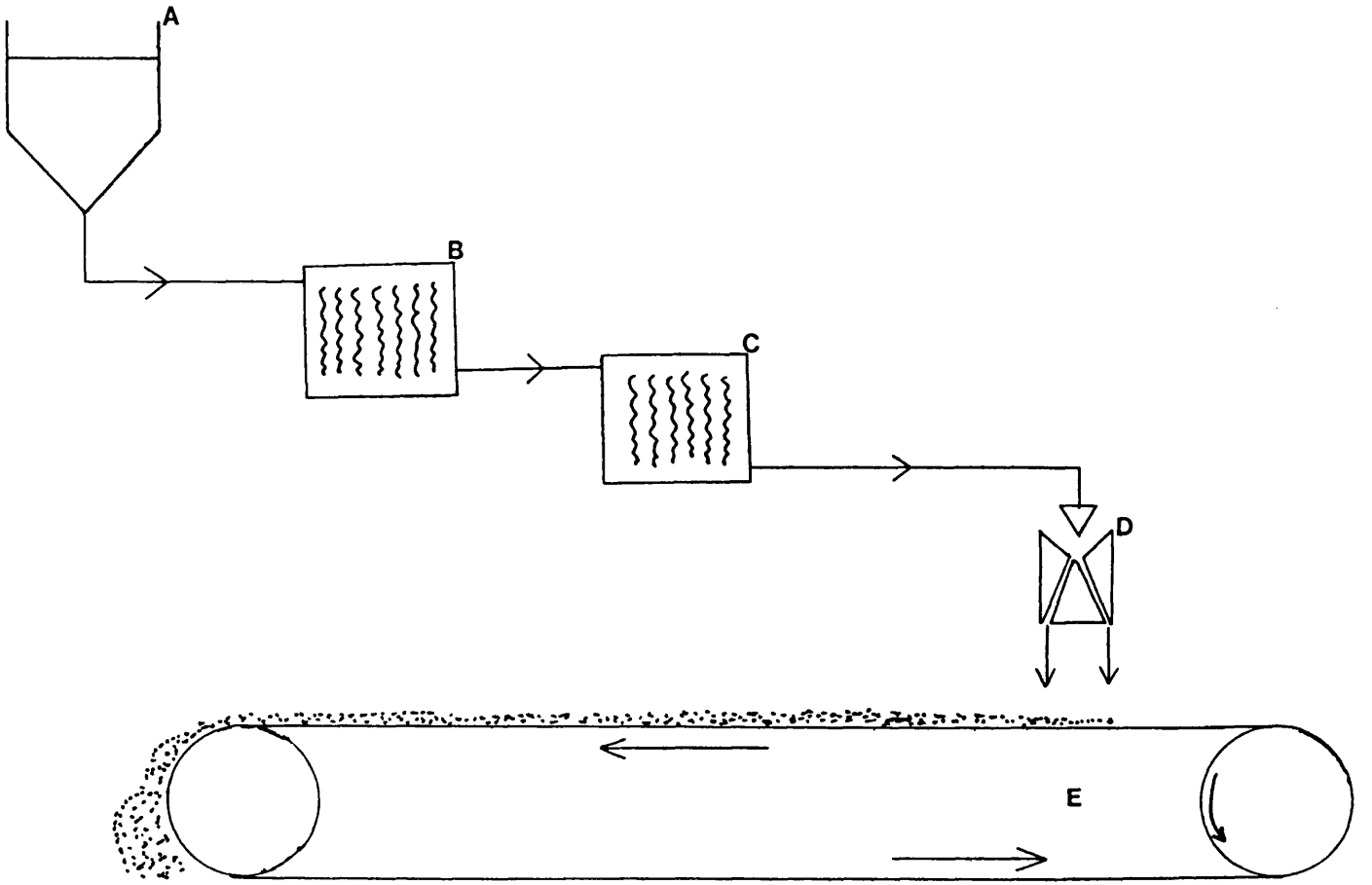

Figure 1. Continuous sucrose crystallization process (Tate & Lyle Plc., U.K. Patent No. 14606 14).

the syrup is further concentrated by removal of water. The highly concentrated syrup, at a temperature greater than 123°C (C, Fig. 1) is passed through a colloid mill (D, Fig. 1) which applies a sufficiently high shear to induce nucleation. The syrup emerges as a concentrated slurry in which crystals are in the process of forming and flows onto a heated conveyor band (E, Fig. 1). Sucrose crystallization is an exothermic reaction and the heat generated during this stage of crystal formation aids drying of the final product, which can be milled to the desired particle size range.

1.5 Powder Compaction.

The main influences on tablet compaction include material properties and machine conditions. Material properties can be subdivided into intrinsic rheological characteristics or properties of additives (Yarton and Davis, 1963) and particulate properties such as particle size and size distribution (Huffine and Bonilla, 1963; Vijayan and Venkateswarlue, 1969), particle shape (Nystrðm and Alderborn ,1982) or moisture content (Rees and Shotton, 1966 and 1971). Machine conditions influencing tablet compression include the nature and rate of load application (Train and Hersey, 1960) and die/punch condition and geometry. The interaction between material characteristics and applied mechanical conditions determine the ultimate properties of the compact.

Tablet compression follows a volumetric die filling step and the initial configuration of particles in the die will be of

relatively low packing density. Thus initial volume reduction on contact of tablet machine punch with powder will probably be due to particle rearrangement to give a more closely packed unit. Further volume reduction can only occur through elastic deformation of particles and when the elastic limit is reached, irreversible deformation such as plastic and brittle deformation will take place. Finally, at higher loads elastic deformation of the compact may occur (Seelig and Wulff, 1946; Birks and Muzaffar, 1971). Several factors may be envisaged to oppose volume reduction including inter-particle friction, die wall friction, bonding between adjacent particles, and the pneumatic resistance of air.

1.5.1 Deformation of Particles.

Endersby (1940) postulated that the resistance offered by a powder to an applied force is caused by the formation of temporary struts, columns and vaults which protect small voids and generally support the applied load. But when a sufficiently high force is applied the temporary structures collapse and elastic deformation of the particles then follows. This deformation depends upon the physical properties of the particles and also upon the magnitude, rate of application and duration of loading. If the modulus of elasticity is large, any resulting deformation will be very small. However, if the modulus is low, deformation will take place, but the system may recover when the force is released.

If the elastic limit is exceeded, destructive

(irreversible) deformation of the particles will take place. This type of deformation will also be accompanied by an elastic deformation component which will be recovered on removal of force. Two types of destructive deformation can be identified: plastic deformation and brittle deformation.

1.5.1.1 Plastic Deformation.

The "block slip theory", (Fig. 2), can be used to explain plastic deformation, which takes place by the movement of large blocks of atoms sliding relative to one another across certain areas within crystals called slip planes. Fig. 2(a) shows an unstressed condition while Fig. 2(b) shows elastic deformation taking place. On removal of the load the structure will revert to that shown in Fig 2(a). Fig. 2(c) shows both elastic and plastic deformation taking place and Fig. 2(d) shows the permanent plastic deformation having taken place with elastic recovery (Cottrell, 1953). One of the main disadvantages of the block slip theory is that large discrepancies exist between predicted theoretical values and measured values of yield strengths. This led to the development of the "dislocation theory" which accepts the existence of small imperfections, or defects, within crystal lattices. Plastic deformation is thus usually considered to be due to the movement of dislocations across the slip planes of a crystal under the action of an applied force.

1.5.1.1.1 Slip Planes.

The crystal planes across which slip generally occurs are

those which possess the highest degree of atomic packing and the direction of slip within a crystal plane is the direction of greatest atomic line density. If the slip planes are aligned either normal to (Fig 3a), or parallel to the stress axis (Fig. 3b), failure tends to occur in a brittle manner (1.5.1.2). If however the slip planes are inclined an angle θ, other than 0°or 90° , plastic deformation tends to occur (Fig. 3c). Plastic deformation can occur by a process termed "twinning" (Fig. 4). Twin formation is often a result of impact or shock loading conditions (Sinnott, 1958). The atoms in each plane undergo some displacement and a revised lattice arrangement is formed (Fig. 4).

1.5.1.1.2 Dislocations.

The presence of line or point defects in a crystal lattice leads to plastic deformation. The line defects are termed dislocations and there are two main types of dislocations: one of which is known as edge dislocation - this type of dislocation can be regarded as due to the presence of an additional half row of atoms within the crystal lattice (Fig. 5). Application of a shear stress F causes dislocation to move along the slip plane until it leaves this section of the lattice giving an increased plastic deformation. Under the action of a shear stress, movement occurs along a slip plane in the direction of the applied force. The second type of line defect is called screw dislocation - where the movement of a dislocation occurs in a direction normal to the lines of stress. In practice,

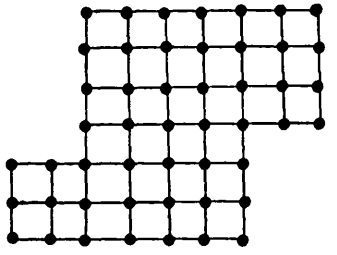

a. unstressed condition

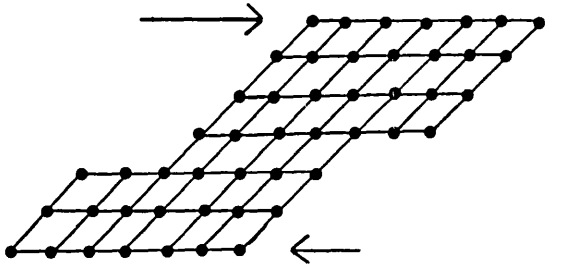

b. elastic deformation taking place

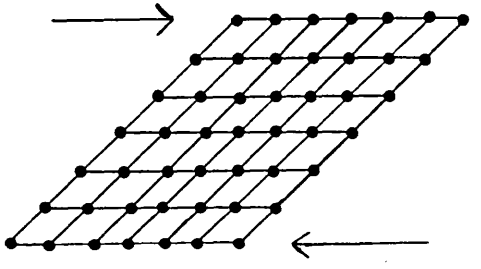

c. combination of elastic and plastic deformation

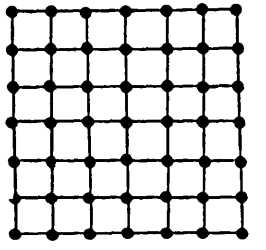

d. unstressed condition after elastic recovery.

Figure 2. Plastic deformation according to "Block Slip Theory" (from Cottrell 1953).

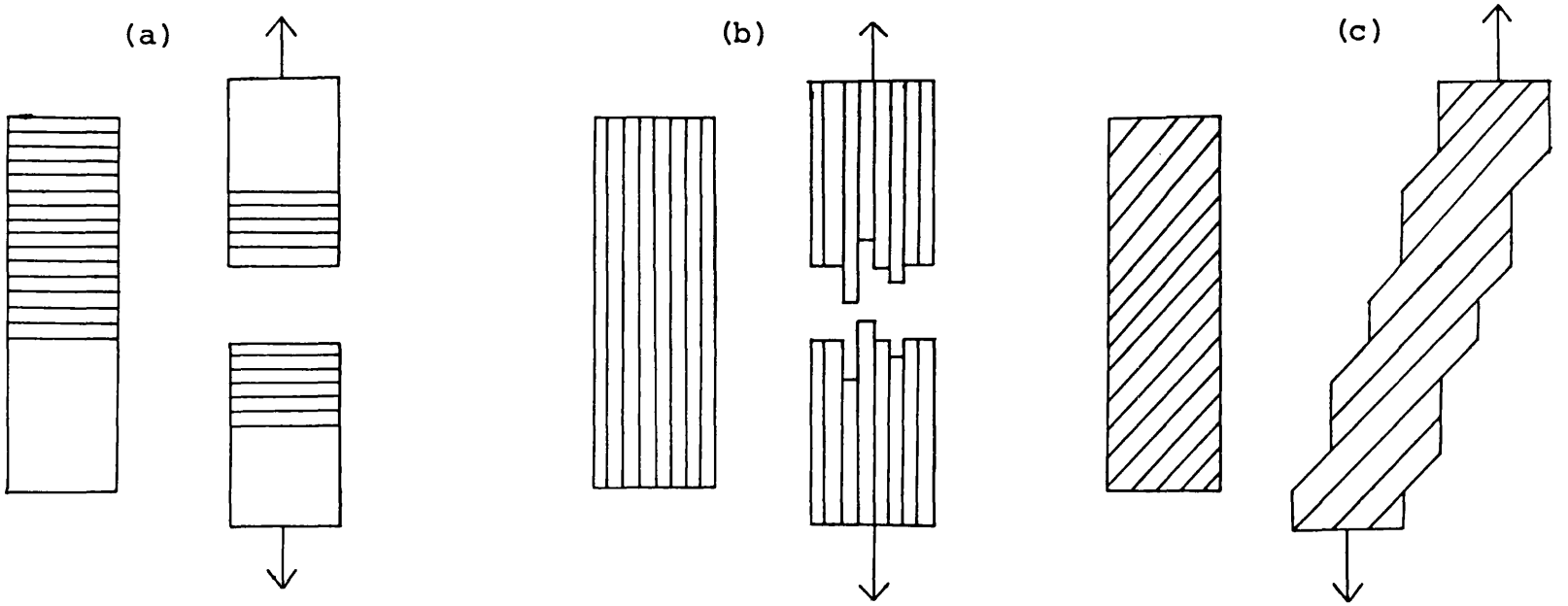

Figure 3. Influence of the slip planes on the fracture mode of single crystals (from John 1972)
(a) slip planes normal to applied force,
(b) slip planes parallel to applied force,
(c) slip planes inclined at an angle other than 0 or 90 degrees

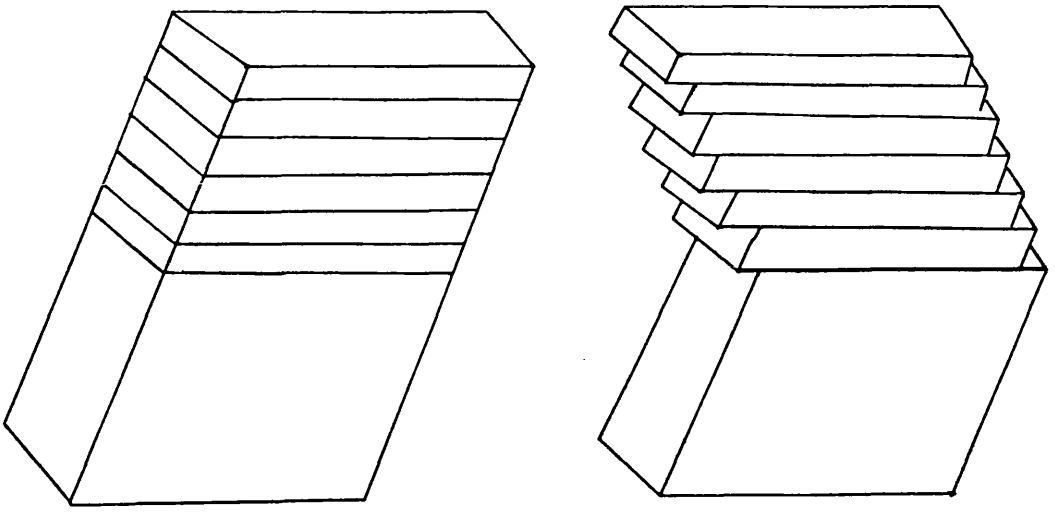

Figure 4.. Deformation by twinning (Sinnott 1958)

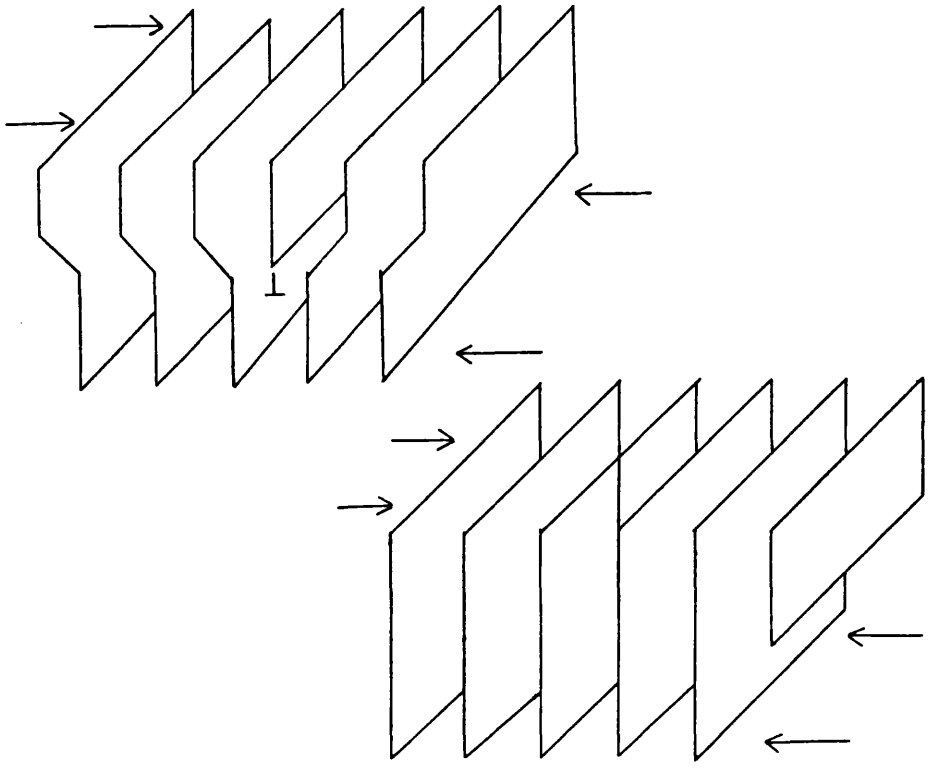

Figure 5. Edge dislocation (from John 1972)

dislocations in crystals are rarely of the pure edge or pure screw type but are mixed dislocations. Plastic deformation is caused by the movement of these dislocation lines under the action of a force, which is considerably less than that which would be required to bring about block slip (John, 1972).

1.5.1.2 Brittle Deformation (Fragmentation).

If the rate of load application is sufficiently rapid, the material is incapable of deforming plastically at a rate sufficient to accommodate the induced strain and fracture of the particles occurs. Brittle deformation was first explained by Griffith (1920) (see also section 1.6.2). In materials that show brittle deformation, the degree of local deformation around a crack tip is very small, thus the energy required for the crack to propagate will also be small and this gives rise to rapid crack propagation across the particle. This theory can be used to explain the increase in numbers of finer particles resulting in the filling of inter-particle voids. Fragmentation of particles also results in the creation of fresh, clean particle surfaces which can bond by van der Waals interactions if areas of intimate contact between particles are established.

The mechanical properties of compacts depend on the type of deformation, plastic or brittle, which predominates during the compaction process.

1.5.2 Evidence of Particle Deformation.

Higuchi et al. (1953) attributed surface area changes which

occurred during compaction of sulphathiazole granules to a process of brittle deformation (Fig. 6). They postulated that the initial increase in specific surface area was due to brittle deformation of particles. The decrease in surface area at higher pressures was then due to formation of aggregates by cold bonding between the fragmented particles. The mechanism suggested by Higuchi et al. (1953) was supported by Armstrong and Haines-Nutt (1970) who studied the disintegration of magnesium carbonate compacts in water. The resultant particle suspension was analysed using a Coulter counter and it was found that these surface area changes corresponded to changes in the geometric mean diameter of the particles in the compacts. They found a gradual increase in the number of small particles (20-30 μm diameter) and a gradual decrease in the number of large particles (90-100 μm diameter), with increasing compaction pressure indicative of fragmentation.

Unlike Higuchi et al. (1953), Griffiths and Armstrong (1970) found a second rise in specific surface area of tablets at high compressional pressure (Fig. 6). These workers attributed the second rise to new surfaces formed during elastic recovery of the compact on force removal, such as that which occurs as a result of capping or lamination.

Gregory (1962) used an optical microscope to examine briquetted coal and concluded that plastic deformation of the coal particles had taken place. Optical microscopy does not offer sufficiently high resolution to allow accurate analysis to be carried out and consequently it was considered impossible to draw firm conclusions regarding plastic deformation of coal particles.

Hardman and Lilley (1970) using a scanning electron microscope examined sodium chloride, sucrose and coal before and after compaction. Their micrographs show no evidence of fragmentation in sodium chloride. In the case of sucrose, extensive fragmentation of particles was observed with each crystal losing its original discrete identity. The behaviour of coal was found to be intermediate between that of sodium chloride and sucrose, but the fragmentation was considered less than in sucrose.

Hardman and Lilley (1973), using the same powders, examined changes in specific surface area, pore volume and scanning electron micrographs with increase in pressure. They concluded that fragmentation of sodium chloride was minimal and that reduction in the relative volume of a compact was achieved mainly by plastic deformation of particles. Sucrose was found to undergo considerable fragmentation and in this case the reduction in relative volume was considered to be due to movement of particle fragments although at high pressures there is likely to be some plastic deformation of very small particles.

From their dissolution studies, Smith et al. (1971) suggested that for a dissolution-compression pressure profile, dissolution rate is dependent on changes in particle size or specific surface area during the compression process. Armstrong and Haines-Nutt (1973) were later able to show that the dissolution rate of disintegrated phenacetin tablets reached a maximum value at approximately the same pressure as that at which the surface area was maximal.

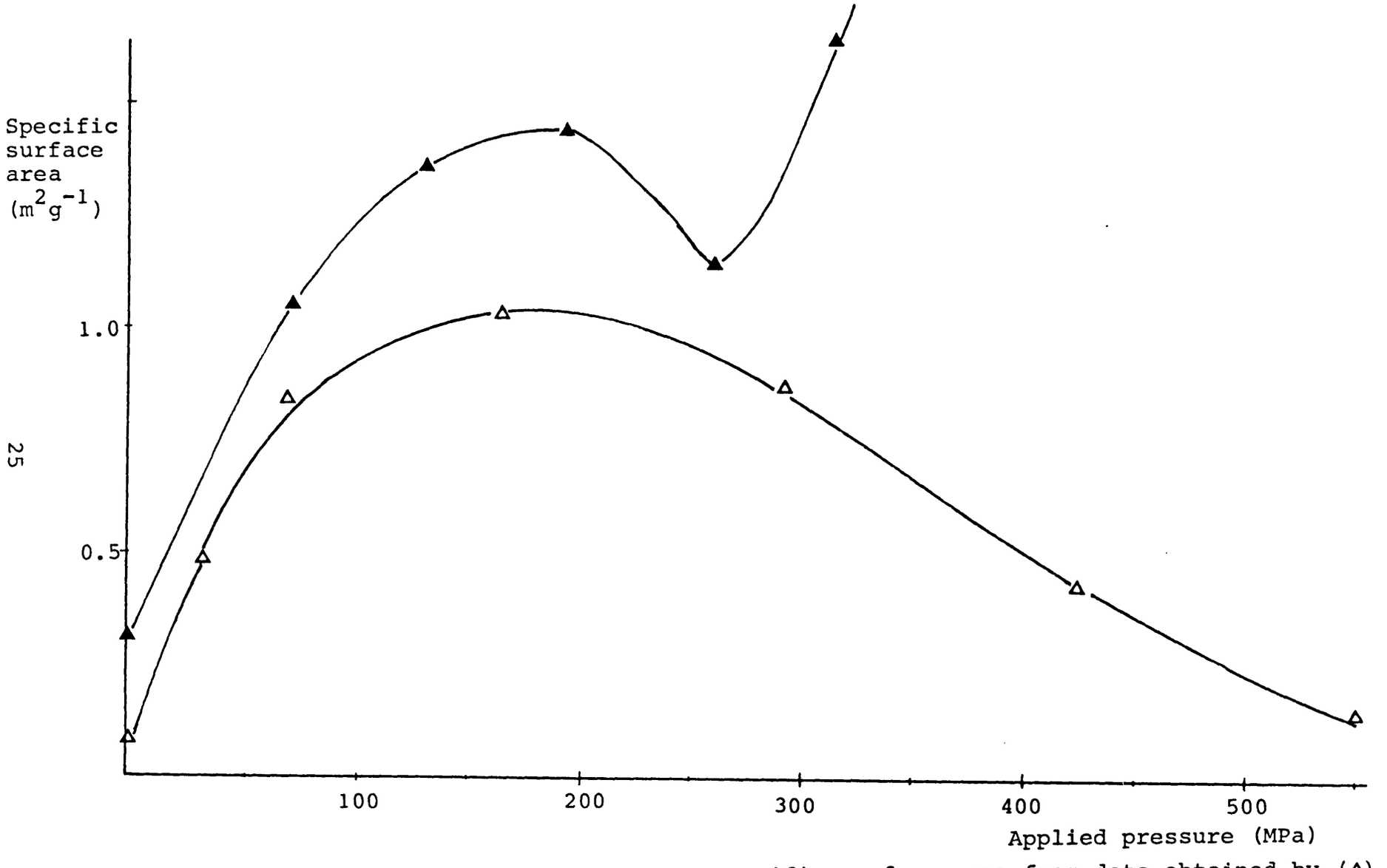

Figure 6. Effect of compressional pressure on specific surface area from data obtained by (△) Higuchi et al. (1953) and Griffiths and Armstrong, (1970) (▲).

1.5.3 Mechanism of Bonding.

A coherent compact with adequate strength will only be formed provided that bonding occurs between adjacent particles. The ultimate reason for application of force is to bring the adjacent particle surfaces into close proximity.

1.5.3.1 Interatomic Forces.

When particles are in sufficiently close proximity inter-particle adhesion may occur by electrostatic attraction, van der Waals forces or hydrogen bonding, depending on the material and conditions. During compaction, certain materials undergo fragmentation, creating clean, new surfaces. Bowden and Tabor (1954) stated that absolutely clean surfaces adhere with a strength equal to the bulk strength of the material. However surface contamination, such as that due to adsorbed gases, moisture, oxide layers or lubricant films will all tend to reduce the bond strength. Rees and Shotton (1966) found that an increase in moisture content decreased the crushing strength of sodium chloride tablets, presumably by reducing inter-particle bonding. To enable asperities on particle surfaces to penetrate surface films, Train and Hersey (1960) have suggested the application of shear forces to attain maximum contact between surfaces thus promoting extensive and improved bonding.

Fragmentation of particles alone is not the only method of establishing bonds between particles. Materials which undergo plastic deformation also produce compacts of adequate strength. Bonding following plastic deformation occurs by increasing

individual inter-particle contact areas. Hardman and Lilley (1973) showed that sodium chloride compacts possessed greater strengths than those of either coal or sucrose and these workers stated that the strength of the bond between two surfaces was determined mainly by the area of intimate contact. During plastic deformation, intimate contact occurs between particles leading to extensive areas of true contact of the particles. Consequently, the magnitude of van der Waals forces across these interfaces is large thus providing higher bond strengths compared with fragmenting materials. Rees et al. (1975) attributed the low strength of lactose tablets to the large number of contact points which support the applied load so that the stress on each point contact is low. Thus the plastic deformation of the contact is very small, the number of van der Waals bonds will be much smaller and hence the strength of the bond formed during compaction will be relatively low.

1.5.3.2 Inter-particle Bridging.

During the compaction process, temperature may increase at inter-particle points of contact, leading to localised melting of the material. Hanus and King (1968) reported a linear relationship between rise in temperature of sodium chloride tablets with compaction force. They also showed a similar linear relationship between the reciprocal of machine speed and the logarithm of tablet temperature. York and Pilpel (1972), studied the effect of temperature on the mechanical properties of some pharmaceutical powders. Their results showed that the tensile

strength of powders increased with an increase in temperature. Later it was suggested by York and Pilpel (1973) that the heat generated during compression, due to frictional effects, may be sufficient to cause asperity melting. Any such molten material would solidify on decompression, as the heat was dissipated to form solid bridges of material between particles. They also suggested that such a melting and solidification process may contribute to the tensile strength of tablets, particularly where one or more of the components of the formulation had a low melting point.

Rees and Shotton (1966) reported that the recrystallization of dissolved materials was responsible for the increase in strength of sodium chloride compacts. They compressed sodium chloride of known moisture content and then dried the samples, thus enabling them to compare the wet and dry strengths of the compacts. Their results showed that the dried compacts were stronger than the wet compacts. Examination of dried compacts using a microscope suggested that recrystallization of sodium chloride had occurred from solution, forming solid inter-particle bridges which could have produced the increased strength of this material.

1.5.3.3 Mechanical Interlocking.

Seth (1956) has reported that mechanical interlocking may contribute to tablet strength. However, such interlocking will only be effective if the surfaces of the particles are irregularly shaped or possess projections, which need to be very

strong to avoid being sheared off during compaction. This is not the case for most pharmaceutical powders and hence this mechanism is unlikely to play a major role in improving tablet strength.

Formation of a tablet with adequate mechanical strength is not only dependent on the extent of bonding, but also on the degree of stored elastic energy which is recovered during the decompression phase of the compaction process. During the decompression phase any elastic recovery will break a proportion of bonds formed during compression. The extent to which bond disruption occurs depends on the elastic properties of the material and the magnitude and rate of force application and removal.

In order to assess the suitability of a powder as an excipient, various parameters have been measured. The measurement of these parameters can be performed during the compaction of the powder or after the compaction process, on the compressed tablet.

1.5.4 Assessment of Powder Compactibility.

When a powder in a confined space is subjected to a load, volume reduction takes place and the powder is said to be compressible. When a powder is compressed and a coherent compact of reproducible mechanical strength is produced, then the powder is said to be compactible. The more compressible and compactible a powder, such as an excipient, the more useful it will be in aiding the formation of pharmaceutical tablets.

1.5.4.1 Parameters Measured During Powder Compaction.

1.5.4.1.1 Axial-Radial Forces.

When powder is compressed in a die by application of an axial force this results in the formation of a radial force which gives rise to an ejection force when the tablet is expelled from the die. Long (1960) measured both the radial and axial pressures of a complete compression cycle and was able to describe two possible compaction profiles for an ideal non-porous isotropic system. A material having a constant yield stress in shear, exhibited slope OA equal to BC (Fig. 7a), which was equal to Poisson's ratio ν. Slope AB is equal to slope CD, which equals 1. This is considered by Long to represent a material which undergoes plastic deformation. The second type of profile suggested is that shown in Fig. 7(b), where the material behaves like a Mohr's body, i.e the yield in shear is a function of the normal stress on the plane of shear and here the consolidation mechanism is considered to be by fragmentation. Slope OA' is equal to B'C', which is equal to Poisson's ratio, while

$$\text{slope } A'B' = \frac{1 - \mu}{1 + \mu} \quad \text{and} \qquad \text{-------- Equation 1.}$$

$$\text{slope } C'D' = \frac{1 + \mu}{1 - \mu} \qquad \text{-------- Equation 2.}$$

where μ is coefficient of friction.

Application of these profiles to tablet compaction studies has inevitably led to confusion since tablets are porous

anisotropic structures. Inconsistencies have been observed in sodium chloride studies, where Obiorah (1978) concluded that sodium chloride behaved like a Mohr's body. However, Leigh et al. (1967) had shown previously that at low compaction forces sodium chloride behaved like a perfect model of a body with a constant yield stress in shear, but at higher forces, it more closely resembled a Mohr's body. These results are in conflict with microscope analysis by Hardman and Lilley (1970) and Heckel plots by Rees et al. (1970 and 1971), where sodium chloride has been shown to undergo plastic deformation.

More recently Krycer et al. (1982) examined four pharmaceutical powders and two model materials by plotting axial versus radial pressure profiles. The compaction behaviour of lead spheres was found to resemble a body with a constant yield stress in shear as lead compacts mainly by plastic flow. In contrast, porcelain powder did not form a coherent compact and was reported by the workers to exhibit behaviour akin to a Mohr's body, due to compaction by fragmentation. The pharmaceutical powders, compressed at high and low forces, were reported to exhibit behaviour somewhere between these two extremes, but more closely resembling the porcelain powder than the lead spheres. These workers stated that there was no discernable difference in the overall shape of these plots for the materials studied (Avicel, Dipac, mannitol and paracetamol). Determination of the yield point (point A, Fig. 7) was said to be impossible because only small changes of gradient occurred in the profiles. This led to the conclusion that axial-radial profiles do not provide a very

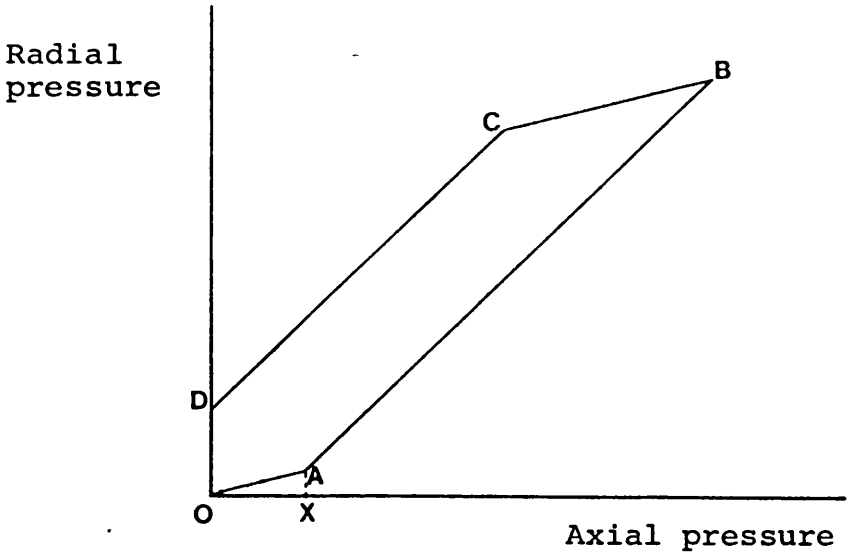

a. Compact exhibiting behaviour like a body with a constant yield stress in shear.

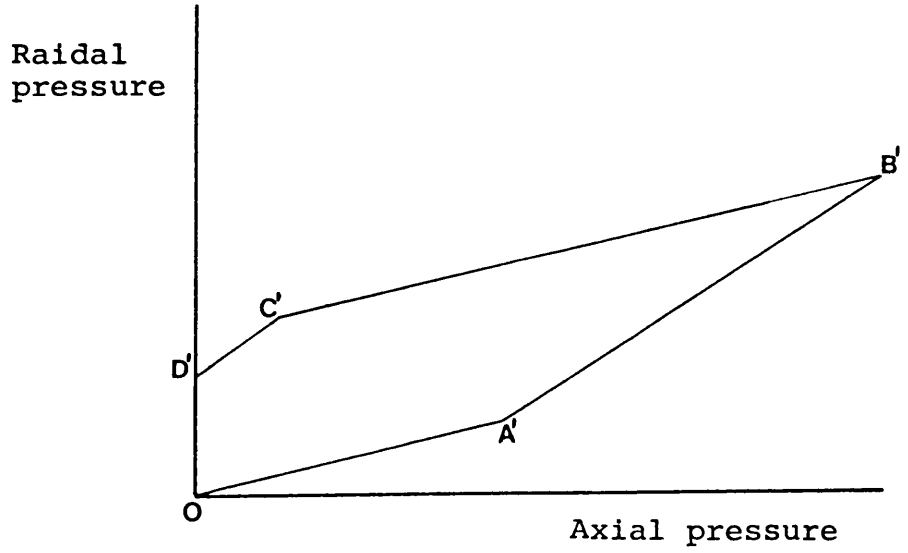

b. Compact exhibiting behaviour akin to a Mohr body.

Figure 7 (a and b). Theoretical radial versus axial pressure cycles (after Long 1960).

useful assessment of compaction behaviour.

1.5.4.1.2 Stress Relaxation.

Measurement of stress relaxation is achieved by stopping the compression process at the point of maximum compression and observing the decay of compression force with time. This decay in force or stress is due to plastic deformation allowing stress to be relieved through flow into interstitial spaces in the compact.

The compression of powder involves time dependent deformation and Shlanta and Milosovich (1964) concluded that stress relaxation measurements appeared to be valuable since they provided information regarding the degree of plastic deformation of powders likely to take place on compaction.

Rees et al. (1975) reported that the largest stress relaxation in pharmaceutical materials studied occurred in sodium chloride and potassium chloride. Compacts of these materials were found to possess high mechanical strength and particle size analyses of these two materials showed no evidence of fragmentation, they therefore concluded that these two materials probably deformed plastically during compaction. They also reported that lactose and potassium citrate showed small stress relaxation, suggesting that these materials deformed principally by fragmentation. Particle size analysis confirmed their hypothesis and lactose was found to undergo more fragmentation than potassium citrate.

David and Augsburger (1977) analysed stress relaxation data using the Maxwell model of visco-elastic behaviour in an

attempt to quantify the rate of plastic deformation of some direct compression excipients. They derived the relationship shown in equation 3.

$$\ln \Delta F = \ln \Delta Fo - kt \qquad \text{------- Equation 3.}$$

where ΔF is the force left in the visco-elastic region (this is the stage where plastic flow and fracture takes place), t is the time, ΔFo is the total magnitude of this force at $t = 0$ and k is the visco-elastic slope. These workers stated that visco-elastic slope could be quantitatively used to determine the degree of plastic flow. Their results showed that direct compression excipients such as compressible starch and microcrystalline cellulose exhibited higher visco-elastic slope than compressible sugar and dicalcium phosphate. They also reported that direct compression excipients with the largest visco-elastic slopes exhibited higher tensile strength values.

Results obtained by Rees and Rue (1978b) contradict those of David and Augsburger (1977). A probable explanation, as suggested by Rees and Rue (1978b) for these differences is that the strain conditions were not identical. Hiestand et al. (1977) analaysed their stress relaxation data in a different manner, by plotting upper punch force against the logarithm of time. Differences in the slopes of the initial segments of these plots were found to reflect the ability of the material to relieve stresses i.e. undergo plastic deformation.

1.5.4.1.3 Work of Compaction.

Examination of the various terms of energy involved in the compaction process can give an indication of the behaviour of a powder. The approaches used by various workers to determine the energy of compaction have differed.

Hanus and King (1968), related tablet temperature to the speed and force applied to form the tablet. Extrapolation of a plot of decrease in tablet temperature with time enabled tablet temperature during compaction to be determined. From these measurements Hanus and King converted thermal energy to a mechanical work equivalent which was used to represent the useful work required in compaction. However, it should be noted that the relationship between useful work and temperature is not fully elucidated yet. The work performed in the creation of clean new surfaces for subsequent bonding is useful, but it is unlikely that a significant temperature rise will be associated with a fragmentation process.

More recently, Coffin-Beach and Hollenbeck (1983) devised a compression calorimeter which used glass fibre punches and allowed energy changes during tableting to be measured. Formation of a tablet was found to be associated with a decrease in the energy of the system and these workers termed this the "energy of formation". Not surprisingly they found that when energy of formation was small (0.52 J) the tablet formed has a low tensile strength, for example acetaminophen. In contrast, Avicel was found to have an energy of formation of 10.6 J and had the largest tensile strength values. In both cases, the powders were

compressed to the same maximum compression force (30kN). These workers suggest the use of such a compression calorimeter in order to quantitatively determine differences in energy of formation.

A widely used method of determining energy of compaction is based on calculation of the area under the force-displacement (FD) curves during compression. Several workers, (Higuchi et al., 1952; Fuehrer, 1962; Polderman et al., 1969), have used the FD curve to show the qualitative aspects of the compaction process. The reason for lack of quantitative results was due to use of either XY or oscilloscope recorders which provide very little data which could be accurately analysed.

The first quantitative evaluation of an FD curve was carried out by Polderman and de Blaey (1970), to examine the action of tablet lubricants. They described a new device enabling them to perform double compression for each die fill, without ejection. The areas under the FD curve were calculated by photographing the curves from the screen of an oscilloscope and quantitative determination of the area under the FD curve was carried out by planimetery. The data analysis was not only laborious but introduced errors. The workers stated that even when the tableting machine was at the lowest possible speed (15 cycles/minute), data acquisition was incomplete. The same workers reported in 1971(a) the use of a small digital computer to enable a more precise determination of the FD curves. These workers recognised the following energy consuming process during tablet compaction: particle rearrangement; inter-particle

friction; particle-die wall friction; elastic deformation and in cases where the elastic limit is exceeded, irreversible deformation leading to bond formation. They showed that work performed during the first two steps was negligible. They also introduced some terms to enable work performed during the various compaction steps to be calculated. These terms were more clearly defined by Polderman and de Blaey (1971b) when they carried out compressional studies on sulphadimidine granulations. The terms were:

$$\text{gross work} = \int_{Ds}^{Dm} UPF.dD \quad \text{----- Equation 4.}$$

$$\text{lower punch work} = \int_{Ds}^{Dm} LPF.dD \quad \text{----- Equation 5.}$$

$$\text{expansion work} = \int_{Dm}^{De} UPF.dD \quad \text{----- Equation 6.}$$

where UPF = upper punch force; LPF = lower punch force; D = displacement; Ds = displacement where force deviates from zero; De = displacement at which force returns to zero; Dm = maximum displacement of the upper punch.

The gross work (Equation 4) comprises of: a, the die-wall frictional work; b, the work required for elastic deformation and c, work for irreversible deformation of the particles (true work). To permit the calculation of true work of compaction of powders, Polderman and de Blaey (1971b) introduced additional

formulae:

$$\text{friction work} = \int_{Ds}^{Dm} (UPF - LPF).dD \quad \text{---- Equation 7.}$$

$$\text{elastic deformation} = \int_{Ds}^{Dm} LPF_2 .dD \quad \text{---- Equation 8.}$$

$$\text{net (true) work} = \int_{Ds}^{Dm} (LPF_1 - LPF_2).dD \quad \text{---- Equation 9.}$$

where subscripts 1 and 2 refer to the first and second compressions respectively.

Earlier Polderman and de Blaey (1970) suggested that it was necessary to perform a second compression, without ejection of the tablet in order to measure the work required for elastic deformation. The reasons for this second compression can be explained with reference to Fig. 8. Area Ds-Fm-Dm (Fig. 8) represents the gross work performed which has been referred to, by Juslin and Jarvinen (1971) as the "apparent work". The term "apparent" was used because there is incomplete registration of the expansion work (area represented by DeFmDm). The latter area represents expansion of the tablet due to its elastic properties and is work which the tablet performs on the ascending punch. However, since the tablet does not elastically recover at the same rate as the ascending upper punch, area DeFmDm is only part of the expansion work. Thus a second compression is performed without ejection and the total area under the second FD curve is

used as a measure of work required for elastic deformation. This value, together with the frictional work (Equation 7), is subtracted from the gross work to determine the work required for irreversible deformation (true work). Polderman and de Blaey (1971b) suggested that the net (true) work of compaction can be calculated according to equation 9, where the force transmitted to the lower punch is monitored instead of the upper punch force, thus taking work lost due to die-wall friction into account.

There are two assumptions made by all the workers who have used FD curves quantitatively, (Polderman et al., 1970; Polderman and de Blaey, 1971a, 1971b and 1971c; Ragnarsson and Sjogren, 1983, 1984a, 1984b and 1985; Rubinstein et al., 1982; Armstrong and Morton, 1979; Doelker et al., 1980 and Krycer et al., 1982), these are:

1. There is complete elastic expansion of the tablet in the die prior to recompression,
2. Work performed during the second compression is purely elastic.

Both assumptions should be treated with caution. Carless and Leigh (1974) have shown that elastic expansion of the tablet still occurs even after the tablet has been completely removed from the die. In addition, the assumption that no irreversible deformation takes place on recompression is questionable since it contradicts all known stress relaxation data. David and Augsburger (1977) have shown that tablet strength increases with increase in dwell time. Newton and Fell (1971d) have also shown that decreasing the compaction speed - effectively increasing

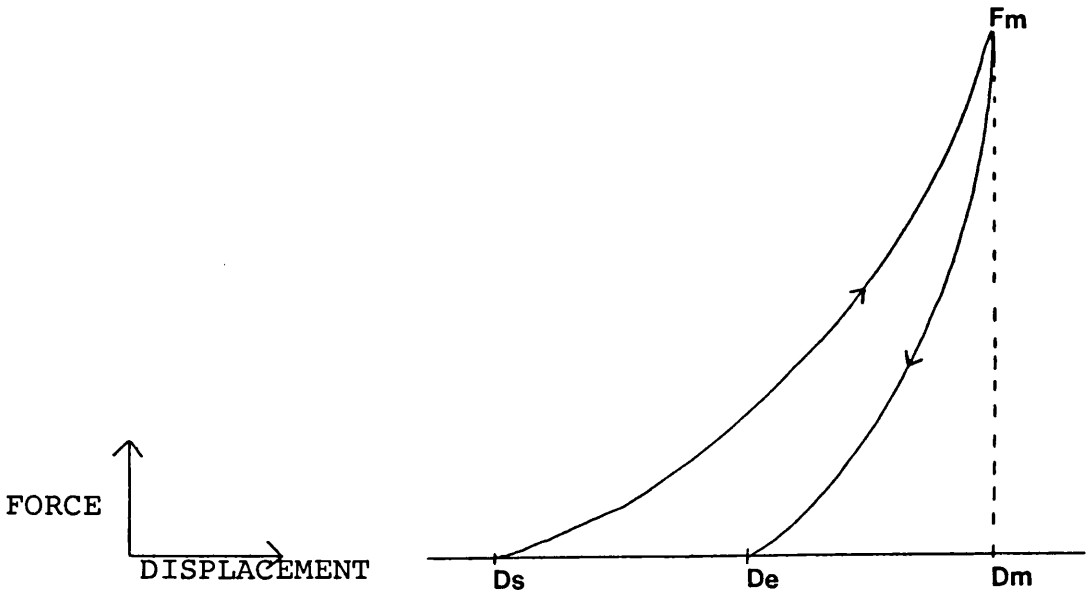

Figure 8. Theoretical force-displacement profile during tablet compaction,
where Fm = maximum force applied,
Ds = first displacement reading as force deviates above threshold,
De = displacement reading as force deviates below threshold,
Dm = displacement reading at maximum force.

dwell time - leads to an increase in tablet densification.

Guyot (1978) stated that the slope and shape of the FD curve will vary according to the deformation properties of the powder. He suggested that if excipients and drugs were compressed under identical conditions on a single punch machine, using the same adjustment of the eccentric strap and the same depth of the compression chamber, the FD curves obtained would have different characteristics for each set of powders. An FD curve which approaches the shape of a right angled triangle can be taken as an indication that a powder will produce tablets having acceptable mechanical qualities and sodium chloride was given as an example which supported this hypothesis (Guyot, 1978)

Rubinstein et al. (1982), examined the variations in work during compaction of a binary mixture of lactose and polyethylene on a tensile testing machine. They reported that for polyethylene alone, 70% of the energy was used in elastic deformation and thus explained the poor consolidation. This elastic behaviour was observed to decrease with an increase in lactose concentration in the binary mix.

Several workers (Durr et al., 1972; Stamm and Mathis, 1976; Kala et al., 1981) have correlated a high net work or a high ratio between the net work and the gross work with the ability of a material to deform plastically and to form a strong compact.

Ragnarsson and Sjogren (1985) varied the inter-particle friction and bonding and studied their effects on net work of compaction and Heckel plots. Increasing the mixing time of magnesium stearate with Starch 1500 and Emcompress reduced the

crushing strength and the net work. These workers stated that the ability of the material to deform plastically was not altered as indicated by the constant yield pressure values. Reduction in the particle size of sodium chloride and saccharose caused an increase in the net work and a corrseponding increase in crushing strength. However, the yield pressure values were found to be approximately constant, hence these workers stated that the effect of the particle size on the net work is not due to differences in plasticity but is caused by differences in the particle interactions. They concluded that net work of compaction appeared to be more useful in detecting variations in the compaction properties rather than for general evaluation of inherent deformation properties of materials.

1.5.4.1.4 Heckel Plots.

Heckel (1961a, 1961b) considered the compaction process analogous to a first order reaction, with pores replacing reactants and densified powder replacing product and was described according to equation 10.

$$\ln \frac{1}{1-D} = KP + A \qquad \text{--------- Equation 10.}$$

where D = relative density, P = applied stress and K,A are constants which are determined from the Heckel plot.

Compaction behaviour, using Heckel plots, was divided into 2 main types by Rees and Hersey (1970). These workers stated that type A behaviour (Fig 9a) was obtained for a powder which had different initial bulk densities, depending on particle size. In

such a material, densification under pressure after particle slippage or repacking is by plastic deformation. For type B behaviour (Fig. 9b), the material consolidates largely by fragmentation. In this case when different size fractions of lactose were compressed above a certain pressure a coincident linear relationship was obtained. A third type of compaction behaviour, has been reported by York and Pilpel (1973), (Fig. 9c), when they studied the compressional properties of four fatty acids and showed that there was an initial steep linear incline which was dependent on the individual fatty acid concerned. The densification of the powder is probably due to both plastic deformation and possibly asperity melting. Evidence for the latter was shown when an increase in melting point of the fatty acid caused a decrease in the initial linear portion.

It was noted by Rees and Rue (1978a) that for Elcema G250, the Heckel profile showed a continual decrease in slope so that it was not possible to determine a value for the yield pressure by this technique. It is ironic that the workers who originally proposed the classification of materials by using Heckel plots (Rees and Hersey, 1970; York and Pilpel, 1973) should later show concern about the use of such plots (Rees and Rue, 1978a and York, 1979). When classifying materials into distinct types, caution is necessary since for many materials the type of plot varies, depending on the experimental compaction conditions, such as the time over which the upper punch applies a force to the die contents (Jones, 1977).

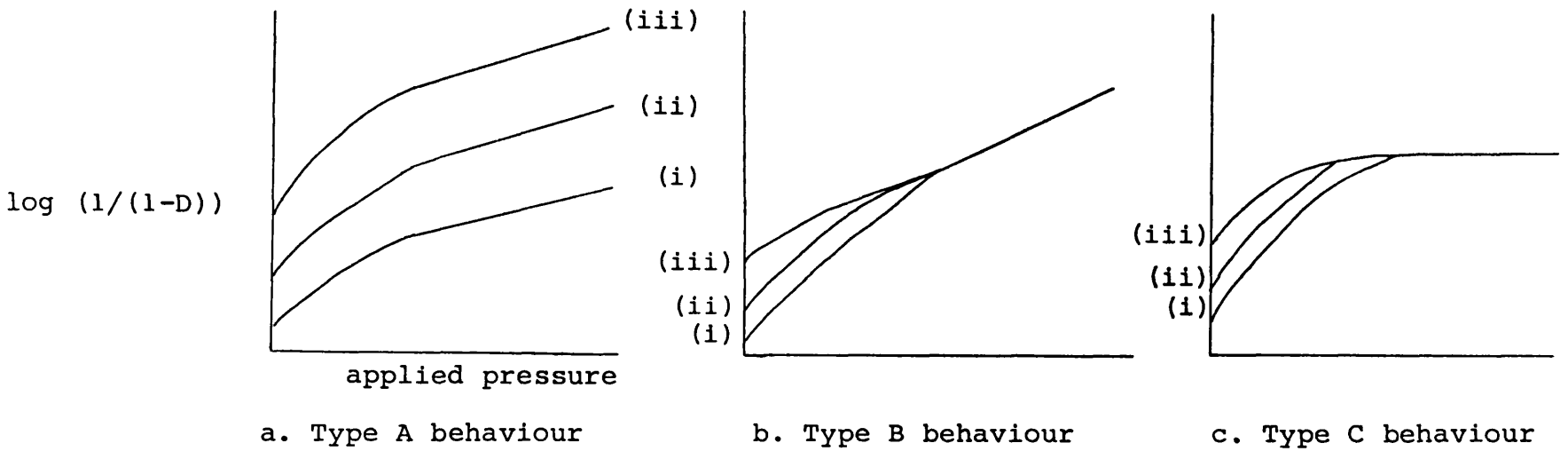

Figure 9. Classification of compaction behaviour by Heckel plots. In plot (a) and (b) line (i) to (iii) refer to increasing particle size, in plot (c) line (i) to (iii) refer to increasing fatty acid concentration.

1.5.4.2 Parameters Measured Following Tablet Compaction.

A second general method of investigating powder compactibility is to subject finished compressed tablets to mechanical testing such as indentation hardness, diametral breaking strength and friability measurements.

The most widely used method for characterizing tablet properties is the diametral crushing test. A tablet is placed between two parallel platens one of which moves to apply a load across the diameter, or the longest axis in the case of a cylindrical tablet, until the tablet fails. The force required to cause tablet failure is measured. Such measurements are widely used both for in-process monitoring and quality assurance testing at the end of production. However, such tests do not give any direct quantitative assessment of powder compactibility, but various parameters are sometimes derived from the measurements performed during the test, including tensile strength and toughness.

Barcellos and Carneiro (1954) developed a tension test for concrete and this was first used for testing pharmaceutical tablets by Newton and Fell (1968), where the tensile strength of tablets was calculated according to equation 11, when a tablet was placed along its edge between 2 flat platens.

$$\sigma = \frac{2P}{\pi Dt} \qquad \text{---------- Equation 11.}$$

where σ = tensile strength, P = load required to cause tensile failure, D = tablet diameter, t = tablet thickness.

It should be noted that equation 11 is only valid when

tablet failure occurs in tension as a single fracture along the loaded diameter (Fig 10e). Tablet failure may also take place in different modes as illustrated in Fig. 10 (Newton et al., 1971). The application of a load by two platens to a cylindrical tablet results in stress distribution across the loaded diameter (Fig. 11) at points A and B. The applied load can be resolved into three components: tensile stress, acting normal to the loaded diameter; compressive stress and shear stress. In ideal line loading the compressive and shear stress are high immediately below the load points thus preventing the initiation of failure in tension. Newton and Fell (1970) have stated that ideal line loading is never obtained in practice and the load will actually be distributed over a contact area. Pharmaceutical tablets are relatively soft compared to the metal platen, causing the load to be spread at the contact points and preventing ideal line loading which reduces both the compressive and shear stresses. Consequently the tablet will fail in tension and equation 11 may be applied. This method of characterizing tablets has been used by numerous workers including York and Pilpel (1973), Summers et al., (1977) and Newton et al., (1985).

Newton et al. (1971) suggested a correction to equation 11 to allow for the average porosity of the tablet. This correction is shown in equation 12.

$$\sigma = \frac{2P}{\pi Dt\,(1-e)} \qquad \text{--------- Equation 12.}$$

where e = fractional voidage.

Equation 12 has been applied by Rowe et al. (1973) to

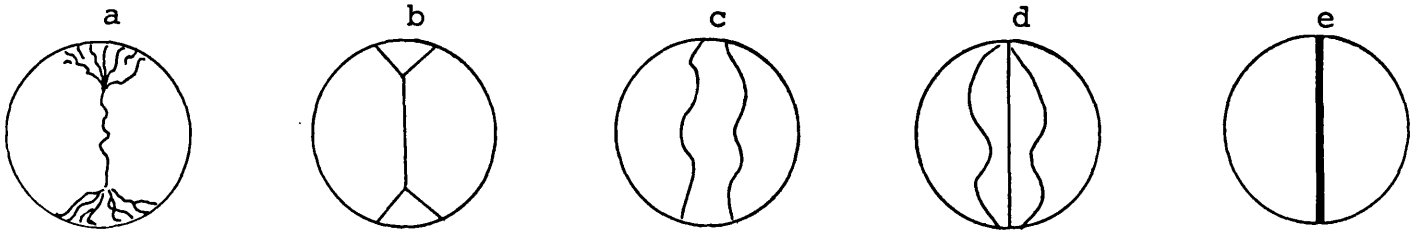

Figure 10. Failure of tablets subjected to diametral compression. (a) Compression failure locally at the loading points, (b) failure under local shear at and near the loading points, (c) failure along maximum loci when point loading is applied, (d) "triple-cleft" fracture due to transfer of load to each half-disc after breakage along the vertical diameter, (e) ideal tensile fracture.

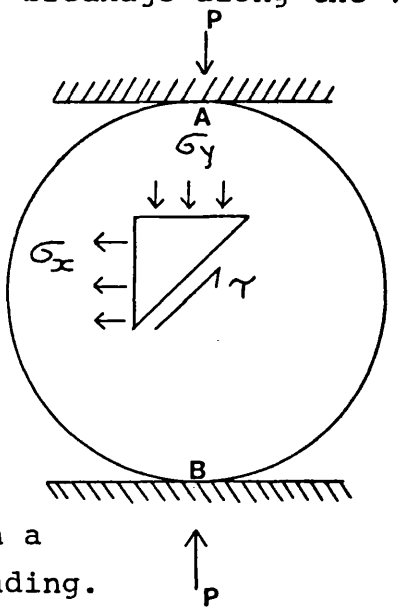

Figure 11. Stress conditions in a tablet under ideal tensile loading.

where,

σ_x = tensile stress,
σ_y = compressive stress,
τ = shear stress.

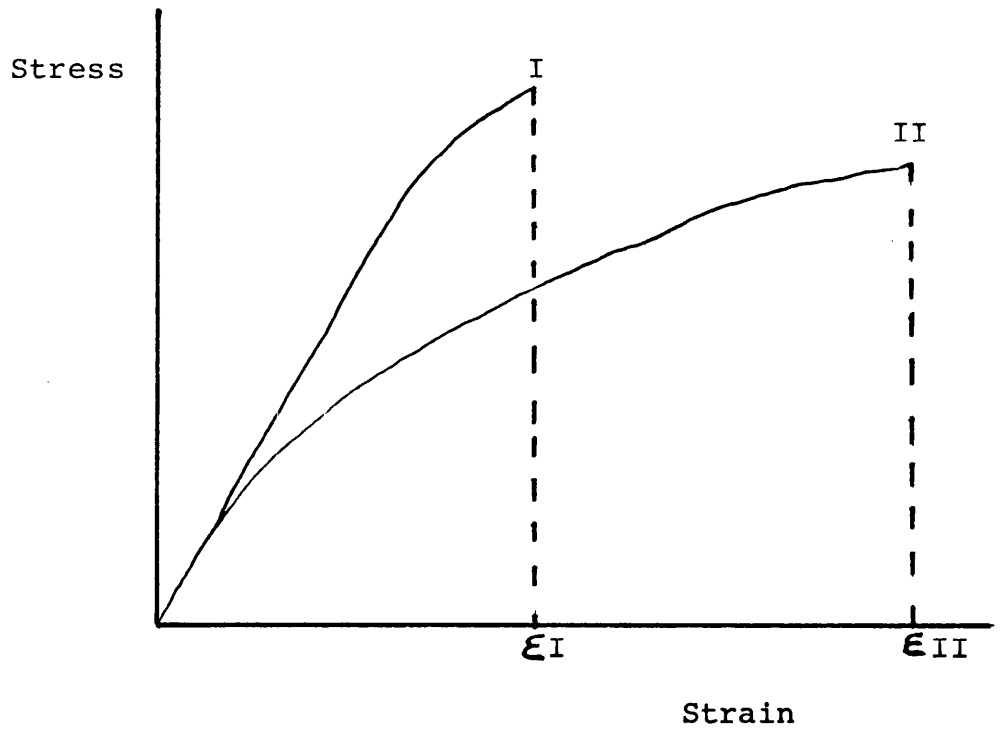

Figure 12. Stress-strain profiles of two materials in a true tensile test.

calculate the tensile strength of plastic matrix tablets. However, Newton (1974) later criticised the correction factor since it does not correct for the true area of inter-particle contact and does not allow for the distribution of porosity within the tablet. Consequently, equation 12 has found restricted use since most pharmaceutical powders are not well defined systems.

Schubert et al. (1975) suggested that it is useful to study stress-strain behaviour in order to fully characterize materials. While studying mechanical properties of agglomerates these workers stated that if the strain at maximum load (fracture strain) is small, an agglomerate will be more sensitive to cracking than if the fracture strain is large, although the tensile strengths may be identical.

If a material is tested in a true tensile test (using a test specimen), differences in behaviour can be observed (Fig. 12). For example, assume material I has a slightly higher tensile strength than material II, but a considerably lower fracture strain, EI. The area under the stress-strain curve for material II is therefore larger than for material I, illustrating that work done to cause fracture of material II is larger than that for material I. Thus material II is considered to be tougher than material I. Toughness has been described by Dieter (1961) as the ability to absorb energy in the plastic range and can be quantified by measuring the area under the stress-strain curve.

Rees and Rue (1978c) applied this principal to diametral testing of pharmaceutical tablets. They continuously monitored

the force applied to the tablet and the distance moved by the lower platen. The latter effectively measured the deformation undergone by the tablet during the diametral test. The measured deformation of the tablet is not a tensile strain, but a deformation of the tablet in the direction of the compressive loading. Integration, using the trapezoidal rule, gives the area under the force-displacement curve (Equation 13) and this parameter is related to the toughness of the tablet as defined by Dieter (1961). Rees and Rue (1978c) termed the calculated area "work of failure" (W.F).

$$W.F = \int_0^{xmax} F\,dx \qquad \text{--------- Equation 13.}$$

where F_{max} = force required to cause tensile failure, x = tablet deformation, xmax = tablet deformation at failure.

The tensile strength of Elcema tablets was shown to be about three times that found for Emcompress whereas the work of failure for Elcema tablets was about ten times that for Emcompress, and these ratios increased with increase in compaction force. The explanation given for this behaviour was that Elcema underwent a greater degree of deformation than Emcompress during the period before failure in the diametral test. Rees and Rue found that this deformation increased with increase in compaction force for Elcema, presumably due to the creation of large areas of inter-particle bonding at higher compaction forces. They also reported that compaction force had little effect on the deformation of Emcompress and lactose since

increase in compaction force only increased the number of brittle inter-particle bonds, rather than the area of existing points of contact. Thus these workers concluded that materials that deform plastically during compaction are associated with high work of failure values, whereas materials in which particle fragmentation is the main process of compaction, are associated with low work of failure values.

Rees et al. (1977) related the work of failure values of tablets to friability or abrasion resistance as determined in a Roche friabilator (Shafer et al., 1959). Rees et al. (1977) found that tablets with high work of failure values could accommodate the shear and impact stresses induced in such a test much more readily than tablets with lower work of failures. Hall and Rees (1978) monitored the effect of addition of a plastically deforming dry binder, methyl cellulose, in tablets of Emcompress by testing the compressed tablets in a diametral compression test. These workers found that increasing the concentration of methyl cellulose resulted in an increase in the work of failure values, thus confirming its usefulness as a binder, even though the actual tensile strength values were found to decrease slightly.

The assessment of the bonding mechanisms in compression of paracetamol granules prepared by precompression, wet granulation and spray drying techniques has been studied by Seager et al. (1980). These workers reported that tablets compressed from spray dried granules possessed the largest work of failure values and this value was about 2.5 times larger than that for tablets

prepared by wet granulation. However, the tensile strength of tablets compressed from spray dried granules was only 1.8 times that of the wet granulation technique. The former tablets possessed higher tablet deformation values than the latter. It was suggested that spray drying concentrated the polymeric binder at the granule surface thus inducing greater plasticity in the paracetamol granules. Further confirmation of the fact that increased plasticity leads to an increase in the work of failure values was illustrated by stress relaxation experiments. The relaxation behaviour of tablets prepared from spray dried granules was the largest and most rapid compared with those prepared from wet massed and pre-compressed granules.

Studies carried out by Parrott and Jarosz (1982) appear to support the hypothesis made by Rees and Rue (1978c). Addition of 0.25% magnesium stearate to microcrystalline cellulose was found to dramatically reduce the work of failure values. The most probable mechanism for this reduction is that magnesium stearate interferes with inter-particle bonding by forming a physical barrier thus reducing the amount of clean reactive surface produced during compaction. A less drastic reduction in work of failure values of microcrystalline cellulose tablets was observed when stearic acid and hydrogenated vegetable oil were used as lubricants.

1.6 Fatigue Strength.

Fatigue is a phenomenon in which a crack develops and extends under fluctuating stresses or strains, possibly resulting in complete fracture. The subject of fatigue has been studied in depth by both design engineers and metallurgists (Plumbridge, 1972); the former being concerned with the endurance or lifetime of components under given fluctuating stresses or strains, the latter investigating the structural changes involved. There are a number of tests that can be performed in order to predict the probable lifetime of a component, the most commonly used tests involve cyclic load application (Deighton and Mead, 1978).

1.6.1 Fatigue Testing Procedures.

Components are subjected to a particular stress amplitude until either the specimen fails or a predetermined endurance has been achieved. Application and removal of load can be sinusoidal as shown in Fig 13. Other commonly used waveforms for load application are schematically represented in Figs. 14(a - d). In order to predict the safe working stress of a component, a "stress-number curve" (S-N curve), Fig. 15, is constructed by testing several components at different levels of stresses.

1.6.2 Fatigue Crack Propagation (FCP).

The single application of a stress, in excess of the yield value, to a crystalline material results in the production and movement of dislocations, which form slip bands or slip lines where they intersect the surface of the component (Plumbridge,

1972). On repeated stressing the subsequent deformation is concentrated into specific slip lines, which become broader and deeper until eventually a micro-crack is initiated (Forsyth, 1963). Very thin folds of material known as "extrusions" are pushed out of the surface and they are generally associated with small crevices, termed "intrusions" (Plumbridge and Ryder, 1969). This marks the initiation of a crack and its subsequent rate of propagation will be largely material dependent.

1.6.2.1 Fracture Mechanics.

An important precursor to the study of fracture behaviour made by Griffith (1920) was that reported by Inglis (1913). Griffith used a reversible thermodynamic process as a model for a crack system. Fig. 16 illustrates the important elements of the system: an elastic body, E, containing an internal crack S of length 2c, is subjected to loads applied at the outer boundary L. Griffith simply sought the state which minimised the total free energy of the system; the crack would then be in a state of equilibrium and thus on the verge of extension. He developed the relationship shown in equation 14 for the total energy (U) of the system for a static crack.

$$U = (-W1 + Ue) + Us \qquad \text{-------- Equation 14.}$$

where W1 = work done on the system due to applied load; Ue = strain potential energy stored in the elastic medium, which will be sensitive to any variations in the system geometry, Us = free surface energy expended to create new crack surfaces. The composite term in brackets (equation 14) represents the

mechanical energy of the system. Thermodynamic equilibrium is attained by balancing the mechanical and surface energy terms over a crack extension δc Fig. 16. He suggested that instability of the crack occurred when the strain energy release rate associated with an incremental advance of the crack was greater than the energy necessary to create the free surfaces of the newly generated crack increment. Griffith showed that a crack, in an ideally brittle solid, would grow unstable according to equation 15.

$$\sigma = \sqrt{(2Eys/\pi a)} \qquad \text{------- Equation 15.}$$

where σ = applied stress, E = modulus of elasticity, ys = the surface energy of the solid, a = half the crack length.

He also derived a relationship (Equation 16) to calculate the maximum stress, (σmax) at the tip of an elliptical crack in a brittle solid.

$$\sigma\text{max} = \sqrt{(a/r)} \ .2\ \sigma \qquad \text{------- Equation 16.}$$

where r = the radius of curvature at the crack tip. Thus, the maximum stress at the crack tip is inversely proportional to the radius of curvature at the crack tip. Hence the smaller the radius of curvature greater the will be the stress concentrations and the larger the possibility of crack propagation. Orowan (1948) suggested that equation 15 could be extended to metals with the addition of another energy term, the energy associated with plastic deformation. This modification is described in equation 17.

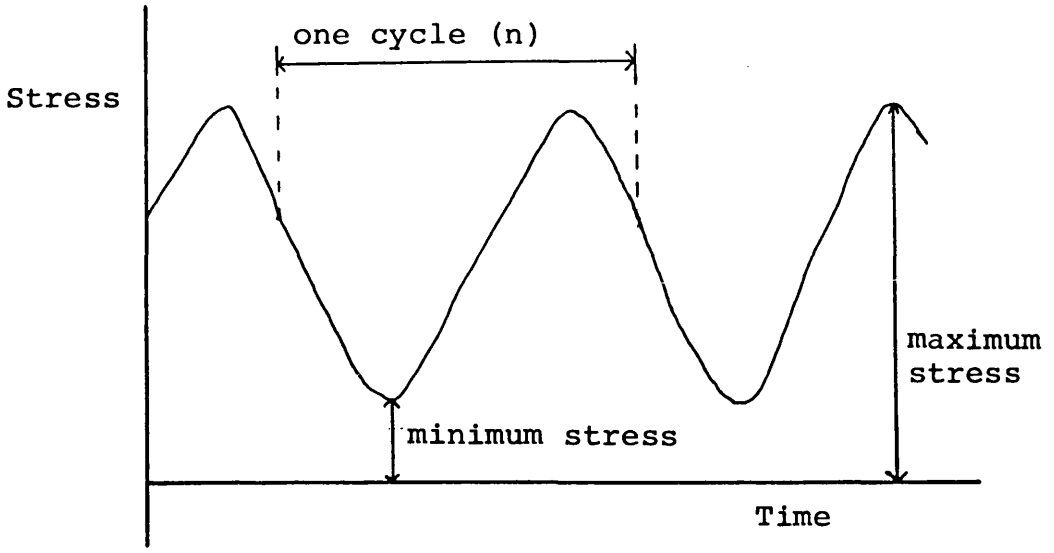

Figure 13. Fatigue-stress cycle.

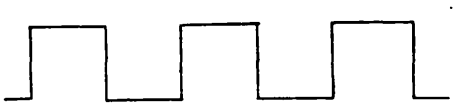

a. Square

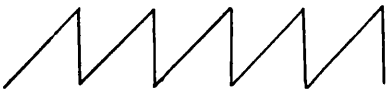

b. Positive sawtooth

c. Negative sawtooth

d. Triangular

Figure 14. Waveforms of load application in a fatigue test.

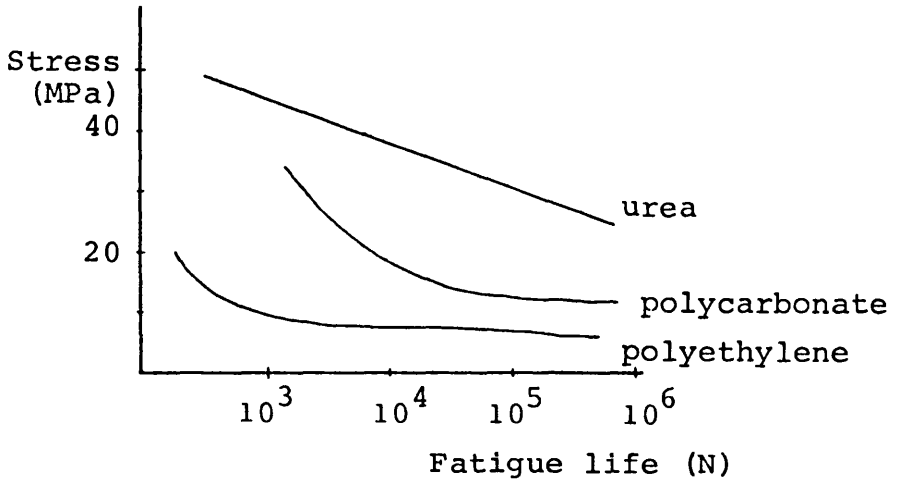

Figure 15. Typical S-N curve for polymers (from Riddell, 1974)

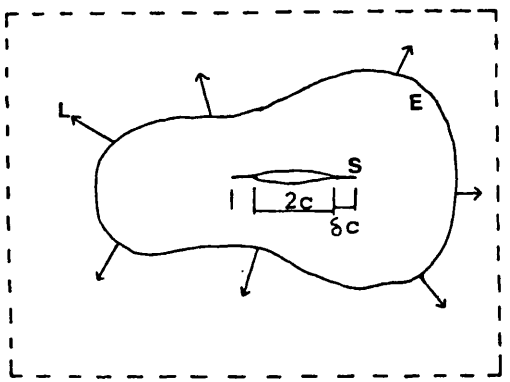

Figure 16. Static crack system: L = applied load, δc = crack extension, E = elastic medium, S = crack surface.

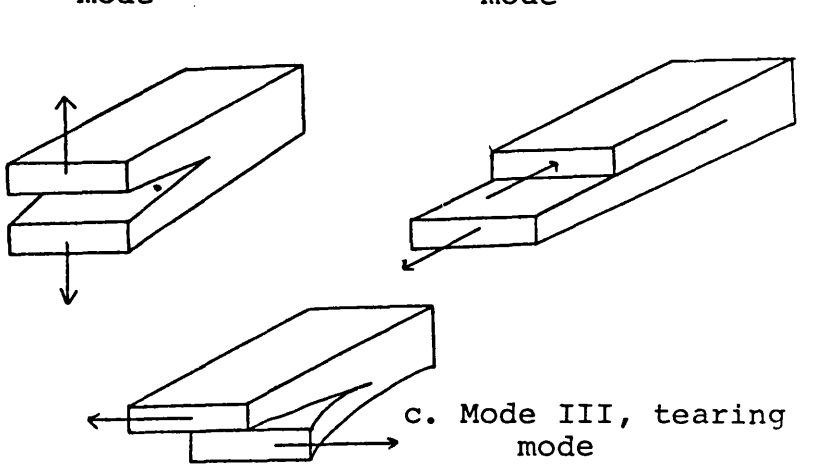

Figure 17. Three modes of fracture.

$$\sigma = \sqrt{2E\,(ys + yp)/\pi a}$$ ------- Equation 17.

where yp = plastic deformation energy term and yp>> ys.

1.6.2.2 Modes of Crack Propagation.

There are three basic modes of crack-surface displacement, as illustrated in Fig 17 (a,b and c). Mode I (Fig 17a), often referred to as "opening mode", corresponds to normal separation of the crack walls under the action of tensile stress; mode II, (Fig. 17b) "sliding mode", corresponds to mutual shearing of the crack walls in a direction normal to the crack front; mode III (Fig. 17c), "tearing mode", corresponds to mutual shearing parallel to the crack tip.

1.6.2.3 Crack-tip Zones.

Both Orowan (1955) and Irwin (1958), proposed the hypothetical division of the crack system into two well-defined zones: the "outer", surrounding zone, consisting of exclusively linear elastic material, which transmits the applied force to the "inner", crack tip zone, where the non-linear separation processes operate. The crack tip zone model can be used to explain the two general types of fracture:

(i) Ductile fracture

Material localized near a crack tip (Fig. 18a) can be considered as a minute tensile specimen, the ductility in tension of such a material is of considerable importance to the subsequent type of failure. If the ductility is high, crack tip

blunting is extensive, effectively increasing the radius of curvature at the crack tip (Fig. 18b). This leads to distribution of the stress over a larger area hence reducing the possibility of crack propagation: this represents the situation in ductile fracture.

(ii) Brittle fracture

For materials with low ductility (Fig. 18c), no crack tip blunting will occur and therefore the stress concentration at the tip will be large. The possibility of crack propagation will be increased as a result and the rate of crack propagation will be rapid: this represents the situation in brittle fracture. This concept can be used to explain both the brittle fracture (fragmentation) which occurs during tablet compaction and during subsequent diametral tablet testing.

1.6.2.4 Fatigue Crack Propagation (FCP) Equation.

The kinetics of FCP process have been examined by measuring the change in crack length of a pre-cracked sample as a function of the total number of loading cycles (Hertzberg and Manson, 1980). A typical plot of such data is shown in Fig. 19, where crack length increases with number of loading cycles. Increasing the stress results in an increase in the fatigue crack growth (da/dn), where "a" is the crack length and "n" is the number of cycles at any stage of the fatigue test. Using the principles of fracture mechanics, Paris (1964) postulated that the stress intensity factor, K, was a major controlling factor in the FCP process, where K is a function of the stress and crack length

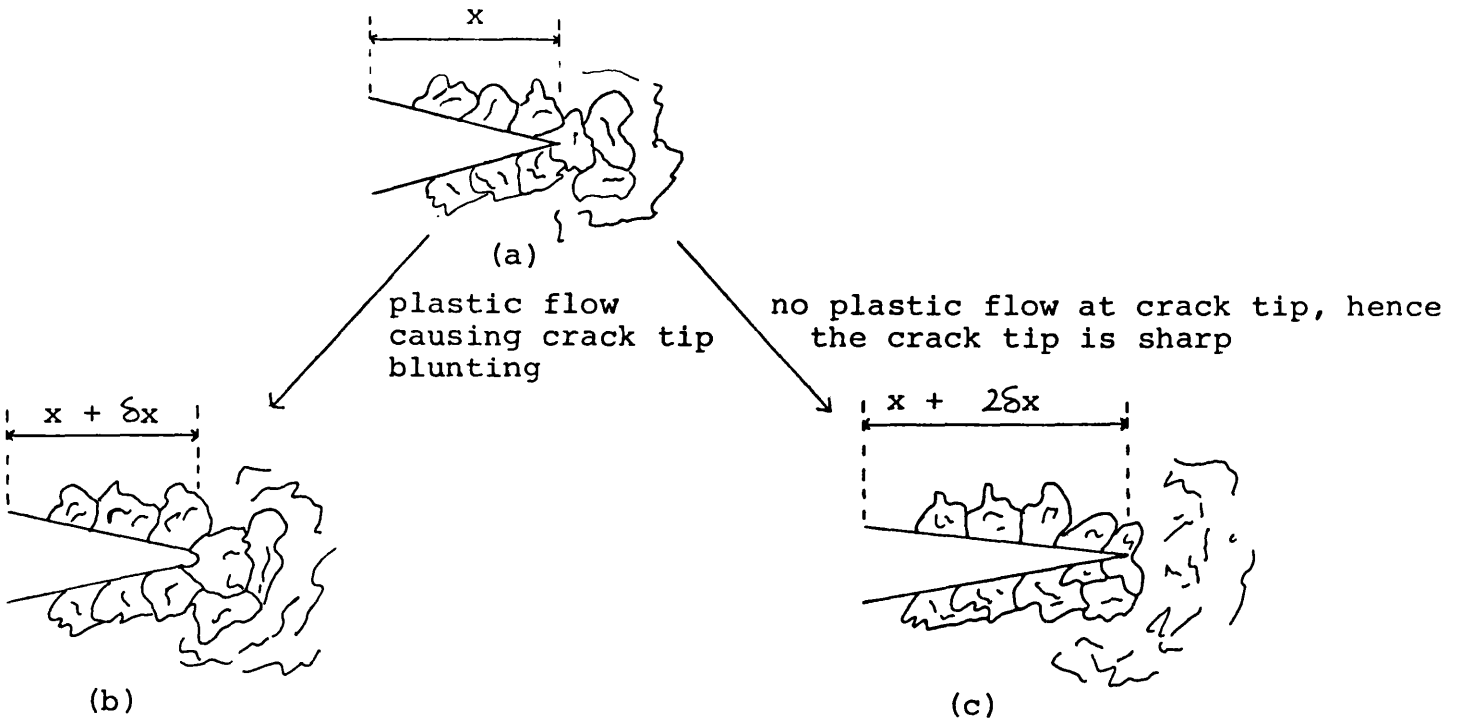

Figure 18. Model to represent behaviour of material at crack tip, where,
x = crack length,
δx = increment in crack length.

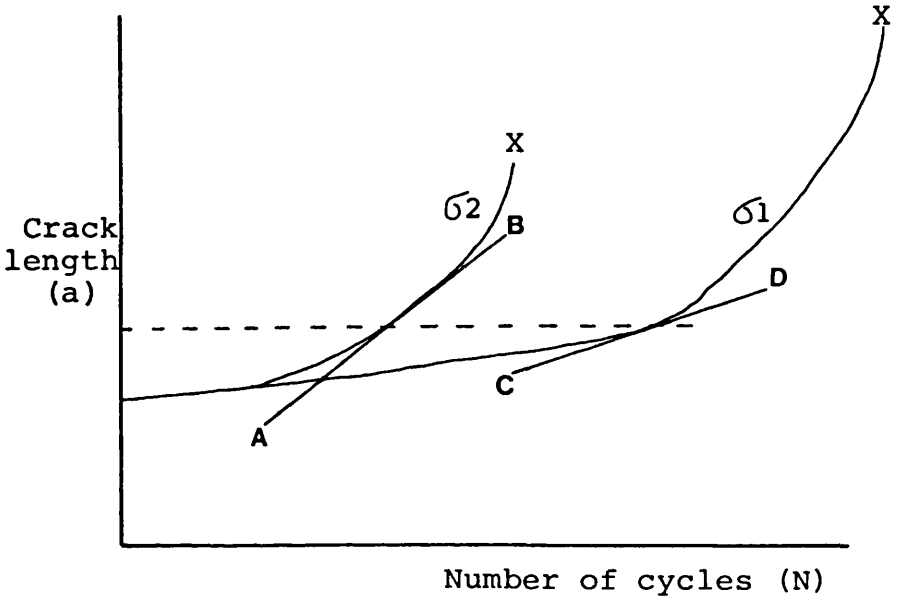

Figure 19. Crack length versus number of loading cycles where σ2 is much greater than σ1, hence slope AB is greater than slope CD. Fatigue crack growth (da/dN) at any particular time, will be greater at σ2 (from Hertberg et al., 1980).
X = point where crack has propagated across the component resulting in fracture.

according to the relationship in equation 20.

$$da/dn = f(\sigma, a) \qquad \text{-------- Equation 20.}$$

Paris found that the most important variable was the stress range (σ max - σ min) and therefore described fatigue crack growth rate per cycle in terms of a stress intensity factor range, according to equation 21.

$$da/dn = A(\Delta K)^m \qquad \text{--------- Equation 21.}$$

where ΔK = stress intensity factor range given by Kmax - Kmin; A,m = functions of material and test variables such as temperature, cycling frequency, stress ratio and environment.

1.6.2.5 Effect of Test Frequency on Fatigue Crack Propagation.

There have been numerous studies into the effect of test frequency on FCP. When pre-notched samples were tested over a range of cyclic frequencies from 0.1 to 100 Hz, the associated FCP rates for several polymers such as poly(methyl methacrylate), (Walters, 1966; Mukherjee and Burns, 1971), polystyrene (Hertzberg et al., 1975), decreased with increasing frequency. Other polymers such as nylon 6,6 (Hertzberg et al., 1979), polycarbonate (Manson et al., 1973) showed no apparent sensitivity. A change in test frequency not only alters the strain rate but also the integrated time under load for each load excursion. A study of strain rate effects on FCP behaviour might better be examined by conducting fatigue tests at a fixed

frequency but with different waveforms.

1.6.2.6 Effect of Temperature on Fatigue Crack Propagation.

There is very little information in the literature to identify the effect of test temperature on FCP behaviour. Kurobe et al. (1970, 1972), have reported that FCP rates in poly(methyl methacrylate) decreased with increasing temperature over a testing range of 263 to 323 K. However, Radon and Culver (1975) found that FCP rates increased with increasing temperatures. Both, Pearson (1968) and Hill and Smith (1969) have shown that in steel the FCP rate at 773 K is 137% greater than that at 293 K.

1.6.2.7 Effect of Stress Ratio (R) on Fatigue Crack Propagation.

Generally, an increase in the mean stress leads to an increase in the FCP, but Frost and Dugdale (1958) and Frost (1962) have reported no measurable effect on FCP. Relaxation at the crack tip is a possible explanation for the latter.

1.6.2.8 Effect of Material Variables on Fatigue Crack Propagation.

Hertzberg et al. (1970) noted dramatic differences in behaviour among polymers possessing a wide range of structures and morphologies. The materials examined by these workers ranged from crystalline polymers such as nylon 66 to amorphous, glassy polymers such as poly (methyl methacrylate) and polycarbonate.

These workers equated the FCP with the damping characteristics of the polymers and have stated that best resistance to crack propagation is achieved when substantial internal energy dissipation mechanisms exist. Studies by Sauer (1978) revealed a marked decrease of FCP in polystyrene when molecular weight was increased.

1.7 Visco-elastic Analysis of Semi-solids.

Pharmaceutical dosage forms range in consistency from fluid through semi-solid to solid. Rheological measurements may be carried out on such materials for a number of reasons: a, to aid fundamental understanding of a system; b, quality control of raw materials and final products; c, to study the influence of changes in formulation; d, to determine the effect on the bioavailability of a drug.

One test which has been used to examine visco-elastic behaviour of semi-solids is the creep test. The process of creep may be defined as the slow and progressive deformation of a material with time, under a constant stress.

1.7.1 Creep Test.

A constant stress is applied to a sample, contained in a suitable apparatus and the strain response with time is followed. The application of the stress should be instantaneous and it is important that the sample remains in the linear region of strain, hence obeying the Boltzmann principle (Leaderman, 1925; Ferry, 1970). A concentric cylinder air turbine viscometer has been

designed by Barry and Warburton (1968) and later by Barry and Grace (1971b) in order to carry out compliance measurements on semi-solids such as creams and ointments.

1.7.1.1 Creep Analysis.

Creep analysis can be achieved by graphical methods, as used by Barry and Warburton (1968) and Sherman (1968, 1970), or by computer using a modification described by Davis and Warburton (1968). According to convention, compliance is plotted with respect to time and a typical curve obtained for many semi-solids such as creams or ointments is illustrated in Fig. 20. The numerical value of compliance (J) is calculated according to equation 22 and has the units 1/Pa.

J = strain / stress ------- Equation 22.

Visco-elastic behaviour can be represented in the form of a mechanical model. Barry and Grace (1971a) used a Maxwell unit in series with several Voigt units. They separated the spring and dashpot of the Maxwell unit using three Voigt units connected in series, (Fig. 21). The total strain in the Voigt units is the sum of the strains in the individual elements and thus compliances in series are additive (Barry and Warburton, 1968).

$$J(t) = \sum_{i=1}^{i} Ji\ (1 - \exp(-t/\tau i)) \quad \text{------ Equation 23.}$$

where J(t) = compliance at time t, Ji = compliance at the i'th element and τi = retardation time. The Voigt model described by equation 23 represents a visco-elastic solid. Barry and Warburton

(1968) extended the equation to visco-elastic liquids by including the compliance of the viscous dashpot, which is calculated according to equation 24.

$$Jn(t) = t/\eta o \qquad \text{-------- Equation 24.}$$

where $Jn(t)$ = compliance of viscous dashpot and ηo = viscosity of liquid in dashpot. Thus for a real visco-elastic liquid, these workers derived equation 25.

$$J(t) = Jo + \sum_{i=1}^{i} Ji(1 - \exp(-t/\tau i) + t/\eta o) \qquad \text{----- Equation 25.}$$

where Jo = compliance of the elastic spring and ηo = residual shear viscosity of liquid in the dashpot of the Maxwell model. Sherman (1970) divided the creep compliance-time curve into three regions (Fig. 20).

1. A-B is the region of instantaneous compliance (Jo) and its value can be determined according to equation 26.

$$Jo = 1/Go = \Delta yo(t)/\sigma \qquad \text{------ Equation 26.}$$

where Go = instantaneous elastic modulus, Δyo = instantaneous strain (as t--> 0) and σ = constant applied shear stress. A simple method for determining the value of Jo is to measure it directly using an experimental creep plot. A-B region represents the elastic deformation of the powder during compaction and is modelled by spring stretching in the Maxwell unit (Fig. 21).

2. B-C is the time-dependent retarded elastic region with a compliance of Jr. For more than one Voigt unit the summation given in equation 27 can be used. This is modelled by the retarded stretching of the spring caused by the dashpot

connected in parallel (Fig. 21).

$$Jr = \sum_{i} Ji \left(1 - \exp(-t/\tau i) \right) \qquad \text{------ Equation 27.}$$

3. C-D is the linear region of Newtonian compliance, Jn, calculated according to equation 28 and represents residual viscous flow which is modelled by the viscosity of the liquid in the dash-pot of the Maxwell unit.

$$Jn = t/\eta o = \Delta yn\,(t)/\sigma \qquad \text{------ Equation 28.}$$

where yn = the strain in region C-D.

A creep recovery curve, represented by D-F, is observed on removal of the stress when instantaneous elastic recovery (D-E) takes place, which is of the same magnitude as A-B. Residual shear viscosity (ηo) is determined by regression of the linear portion of C-D, represented by equation 28.

1.7.2 Creep Compliance Studies.

Several workers have studied the visco-elastic properties of semi-solids by applying equation 25. The stability of liquid paraffin in water emulsions with different emulsifiers has been studied using creep compliance curves by Barry (1970). The use of sodium dodecyl sulphate-stearyl alcohol was found to produce emulsions with higher creep compliance than those produced using either sodium dodecyl sulphate-cetyl alcohol or sodium dodecyl sulphate-cetostearyl alcohol.

Investigation of the visco-elastic properties of powders has been carried out by several workers, as mentioned above in section 1.5.4.1.2, but there are no reports of creep analysis

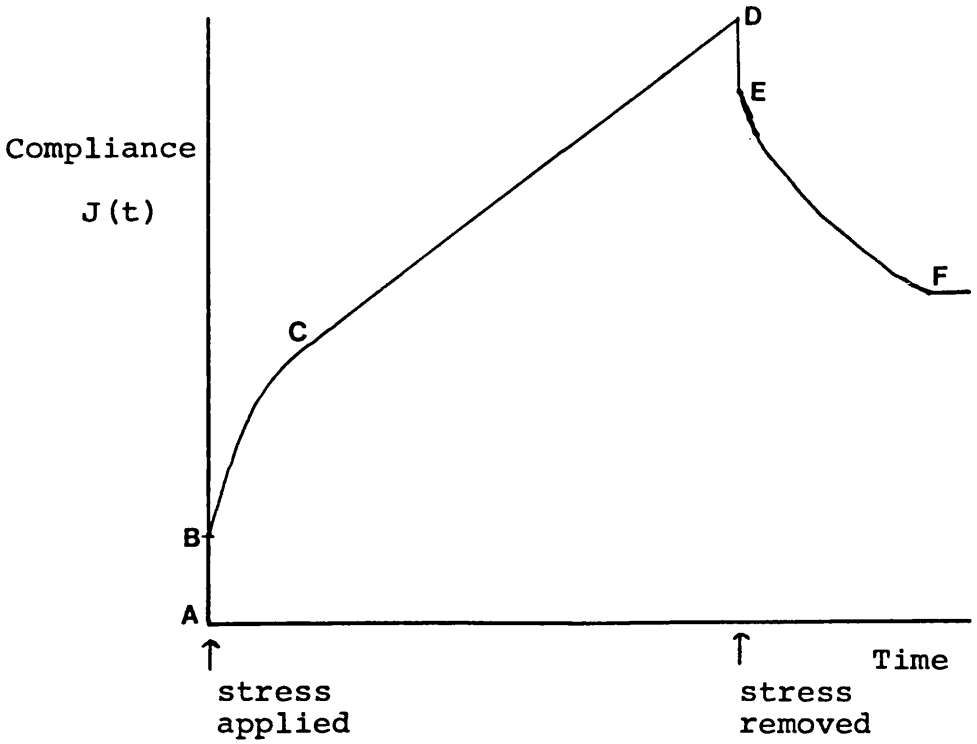

Figure 20. Creep compliance curve (from Sherman, 1970).

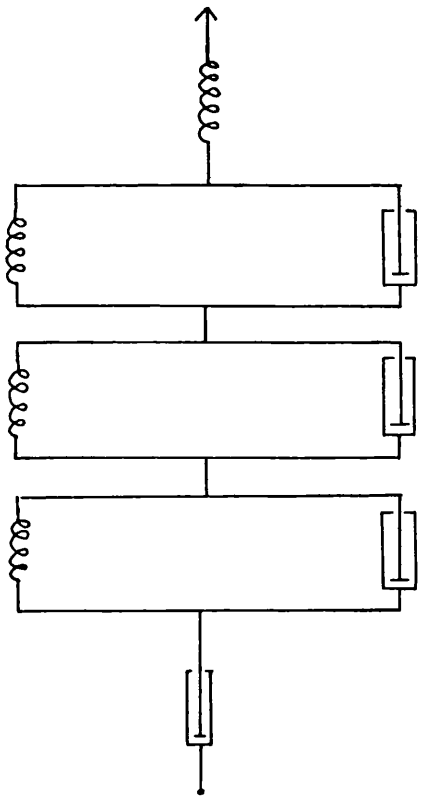

Figure 21. Mechanical model used to describe creep curve.

relating to pharmaceutical powders or tablets.

1.8 Non-destructive Tests (NDT).

Non-destructive testing is the name given to processes of inspection which do not render the component examined unfit for further use. There are a wide range of techniques available for use in NDT for example optical, radiography and acoustic microscopy techniques. In the present study an acoustic microscopy technique has been empolyed for the inspection of cracks in compacts, which are optically opaque.

1.8.1 Acoustic Microscopy.

Sokolov (1936) was the first to propose a device for producing magnified views of structure with 3000 MHz sound waves, but due to technological limitations at the time, no such instrument could be constructed. The principle of such a device is to place an acoustic (ultrasonic) transmitter on one end of the test object and a receiving device on the other end. The presence of any discontinuities create an obstacle in the path of the acoustic waves, through which they can penetrate only partially. Any defect interrupting the path of the acoustic waves will therefore cast an "acoustic shadow" on the receiver, causing a drop in the received signal. More recently Kessler and Yuhas (1979) have described two techniques, Scanning acoustic microscopy (SAM) and Scanning laser acoustic microscopy (SLAM), both of which are commercially available.

In SLAM, a specimen is viewed by placing it on a stage

where it is insonified with plane acoustic waves and illuminated with laser light (Kessler et al., 1971). Within the sample, the sound is scattered and absorbed according to the internal elastic microstructure. The principle on which the laser beam is employed as a detector is based upon the minute displacements which occur as the elastic waves propagate through the component. Fig. 22 shows the principle of the SLAM. An optically reflective surface placed in the sound field will become distorted in proportion to the localised sound pressure. The distortions are dynamic in that the pressure wave is periodic and the mirror displacements accurately follow the wave amplitude and phase. At every instant of time the mirror surface is an optical phase replica of the sound field (Kessler and Yuhas, 1979). The laser is used to measure the degree of regional distortion. By electronically magnifying the area of the laser scan to the size of the screen monitor and by brightness modulating the display, the acoustic micrograph is made visible.

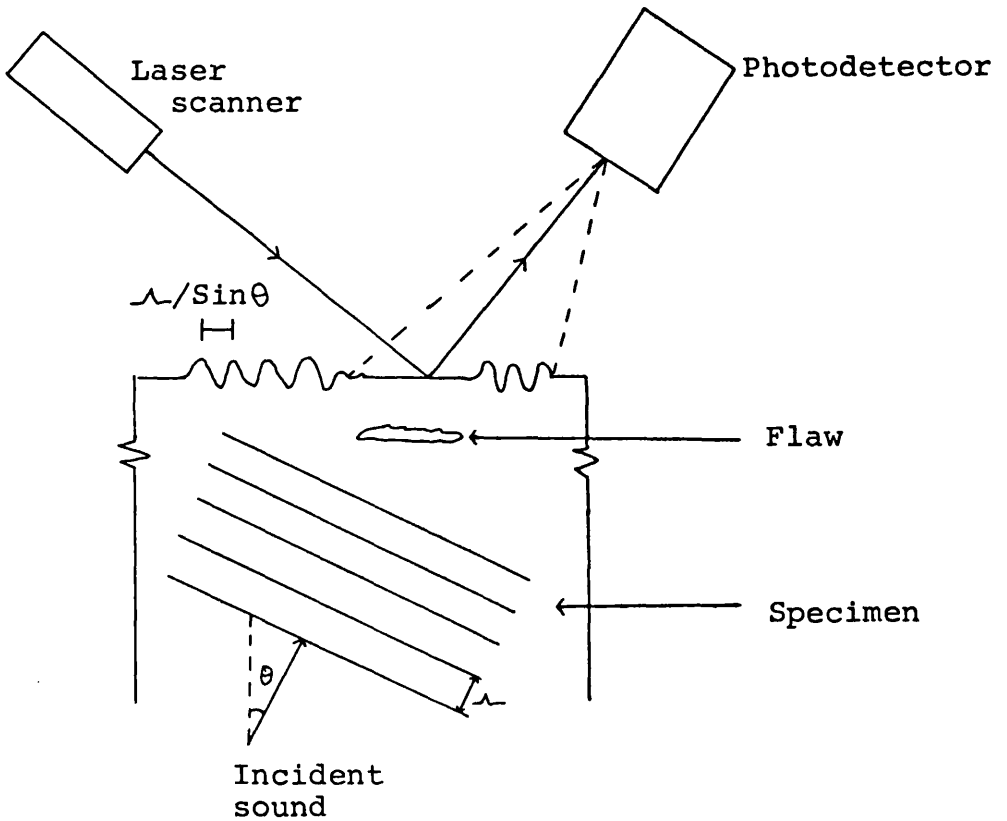

Figure 22. Laser detection of acoustic energy at an interface (from Keseler and Yuhas, 1979).

Chapter 2. MATERIALS AND METHODS.

2.1 Characterization of the Physico-mechanical Behaviour of Direct Compression Excipients.

2.1.1 Materials.

Anhydrous lactose (Humko Sheffield Chem. Co., New Jersey, U.S.A.)

Fast-Flo (spray dried alpha lactose monohydrate), lot 2RL209, (Foremost Whey Corp., San Francisco, U.S.A.)

Tablettose (pure alpha lactose monohydrate, Meggle Milchindustrie GmbH, Reitmehring, F.R.G.)

Dipac (co-crystallized sucrose and modified dextrins, Amstar Corp., New York, U.S.A.)

Nu-tab (sucrose with 4% invert sugar, 0.2% maize starch and magnesium stearate, Ingredient Technology Corp., New Jersey, U.S.A.)

Microtal D.C.E. (co-transformed sucrose with 3% maltodextrin 20DE, Tate & Lyle Plc., Plaistow, Wharf, U.K.)

Starch 1500 (maize starch), batch No. 112014, (Colorcon Ltd., Orpington. U.K.)

Avicel (microcrystalline cellulose), type PH102, lot 7242, (FMC Corp., Philadelphia, U.S.A.).

Emcompress (dibasic calcium phosphate dihydrate), lot 105, (Edward Mendell Co., Inc. Carmel, U.S.A.)

Magnesium stearate, lot 9516382E, (BDH Chemicals, Poole, U.K.)

2.1.2 METHODS.

2.1.2.1 Tablet Compression.

2.1.2.1.1 Tableting Machine.

A single station reciprocating tableting machine (type E2, Manesty Ltd., Speke, Liverpool, U.K.), fitted with 12.7mm diameter flat-faced punches was used in this study. Fig. 23 illustrates the complete system used for tablet compression and the necessary instrumentation and interfacing to determine the force applied during compaction.

2.1.2.1.2 Instrumentation of the Punches.

Two pairs of minature foil strain gauges (type EA06 062TT 350) were fitted and bonded by Welwyn Strain Measurements Ltd., Basingstoke, U.K., to the body of the upper punch such that at maximum travel during compression, both sets of strain gauges would remain outside the die. Two pairs of strain gauges were employed to compensate for any out of plane bending moments. The foil material used was Constantan, an alloy of 45% nickel and 55% copper, having a thickness of 2.5*E-5 m and heat treated to provide self-temperature compensation. Similarly two pairs of strain gauges were bonded by Welwyn Strain Measurements Ltd., on the lower punch holder.

2.1.2.1.3 Data Acquisition and Manipulation.

A 5 volt d.c. power supply (Central power module 2110,

Vishay Measurements, Raleigh, U.S.A) was used to energize the strain gauges. The resistance of each "active" strain gauge was passed to a conditioning amplifier (type 2120, Vishay Measurements) where changes in resistance were converted into voltage changes. Subsequently the analogue voltage signals were passed via a specially constructed fast analogue-digital converter (ADC) connected to a small microcomputer (Model B, BBC Microcomputer System, Acorn Ltd., Cambridge, U.K.), through the 1MHz BUS (Fig. 23).

The fast ADC converts analogue signals from the instrument to a digital form which can be input directly to a microcomputer. The ADC board has the potential for eight differential inputs into a multiplexer which is used to select one of these inputs for conversion by the AD 574 (Analogue to Digital conversion semiconductor). The board has a facility for selection of three input ranges; 2, 4 or 8 volts full scale. Also available is a read/write address selection for data output via the 1MHz BUS, thus allowing the data manipulation to be conducted by the microcomputer.

The calibration values (see 2.1.2.1.4) for the upper and lower strain gauges were included in a program written in BASIC computer language, thus allowing the forces applied by the upper punch and transmitted to the lower punch to be monitored with respect to time. The data acquisition subroutine was written in 6502 Assembler code to improve the rate of data acquisition. A total of 1000 points were sampled during each tablet compression cycle, 500 points from the upper and 500 points from the lower

punch. The peak digital value of the upper and lower punch was converted to force values which were printed out. The peak upper punch forces were used as one of the parameters for characterizing tablet production conditions.

2.1.2.1.4 Calibration of Strain Gauges.

The calibration of both sets of strain gauges was conducted in situ on the tableting machine. A pre-calibrated piezo-electric load cell (type 9021, peak force 35kN, Kistler Ltd., Switzerland) was subjected to compressive loading. A load distribution device was constructed in order to reduce the development of bending forces and to have ideal application of uniform surface forces on the load cell. Fig. 24 illustrates the basic design and dimensions of the load distribution device, the piezo-electric load cell was sandwiched between two such devices.

The converted analogue signals from the two sets of strain gauges were acquired as described above in 2.1.2.1.3, the analogue signals from the load cell were also fed into the fast analogue-digital converter, via a modular charge amplifier card (type 5054A2430, Kistler Ltd.), which was powered by a 15 volt d.c. supply. The digital outputs from the fast analogue-digital converter were processed by a BBC microcomputer via the 1MHz BUS. A short program was written in BASIC in order to collect three different digital outputs from the fast ADC. 100 points were collected at each magnitude of load application and the means were plotted versus values from the load cell (Fig. 25). Slopes, corresponding correlation coefficients and intercepts from the

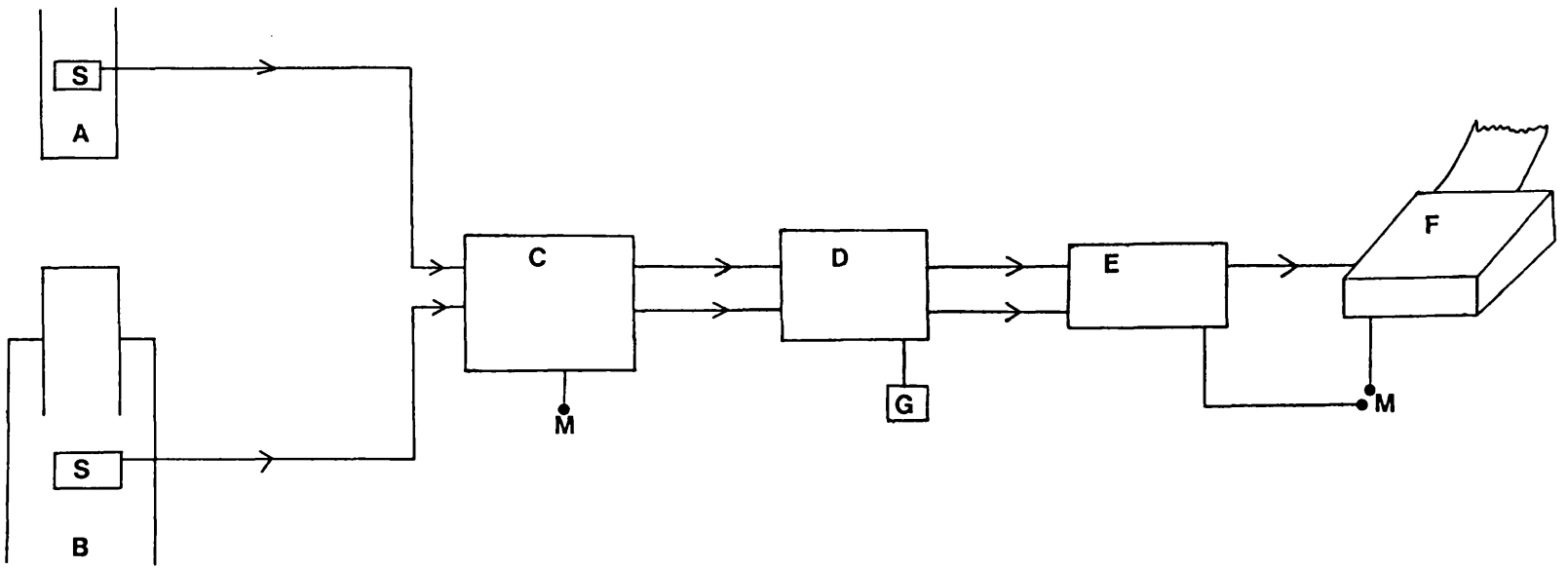

Figure 23. Block diagram to illustrate the complete system for determining force applied during tablet compaction.

A = upper punch,
B = lower punch block,
C = conditioning/amplifier,
D = analogue to digital converter,
E = BBC microcomputer system,
F = dot-matrix printer,
G = 15V d.c power supply,
M = mains supply,
S = minature strain gauges.

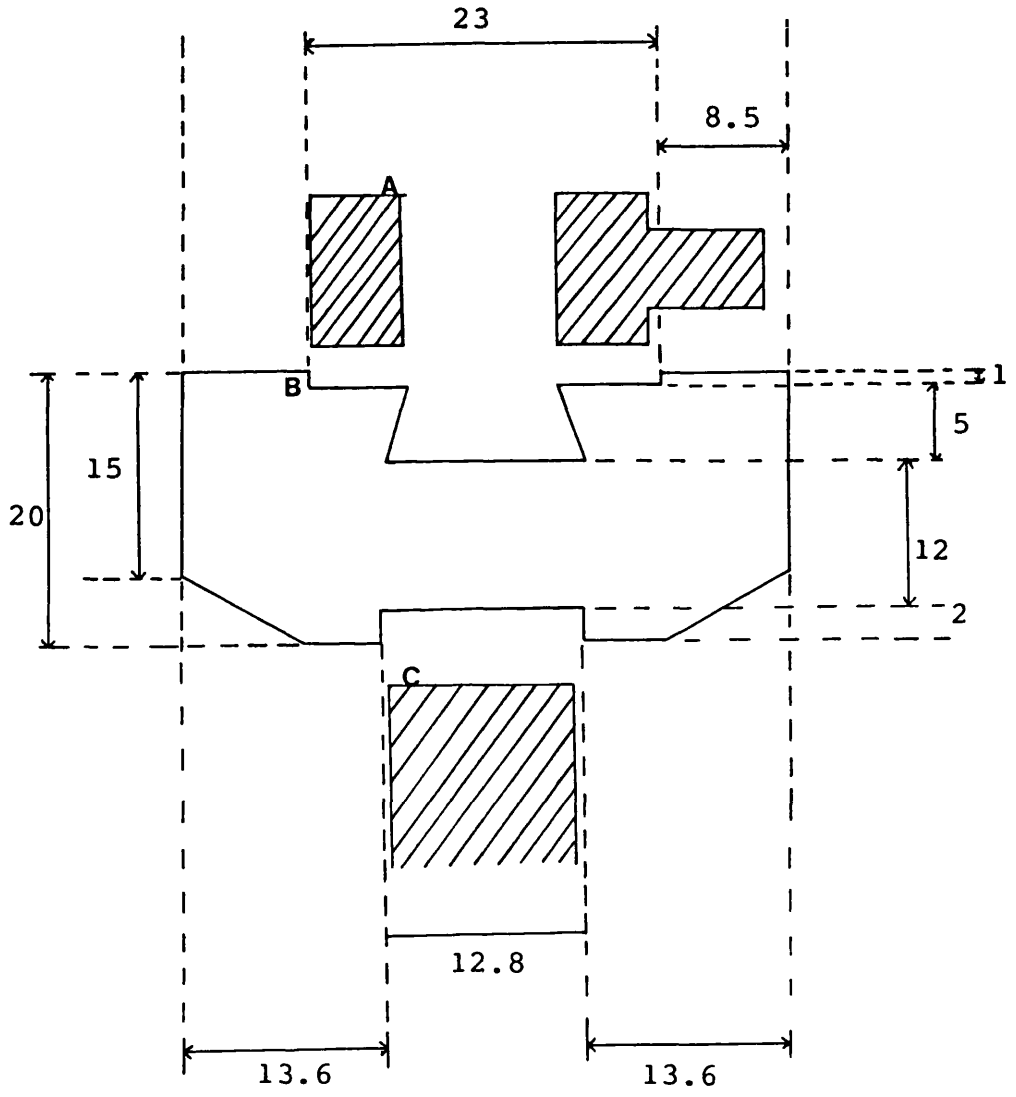

Figure 24. Design of load distribution device.
A = piezoelectric washer,
B = bottom half of the load distribution device,
C = lower punch of tableting machine.
An identical structure to that of B is placed above A.
All dimensions are in mm.

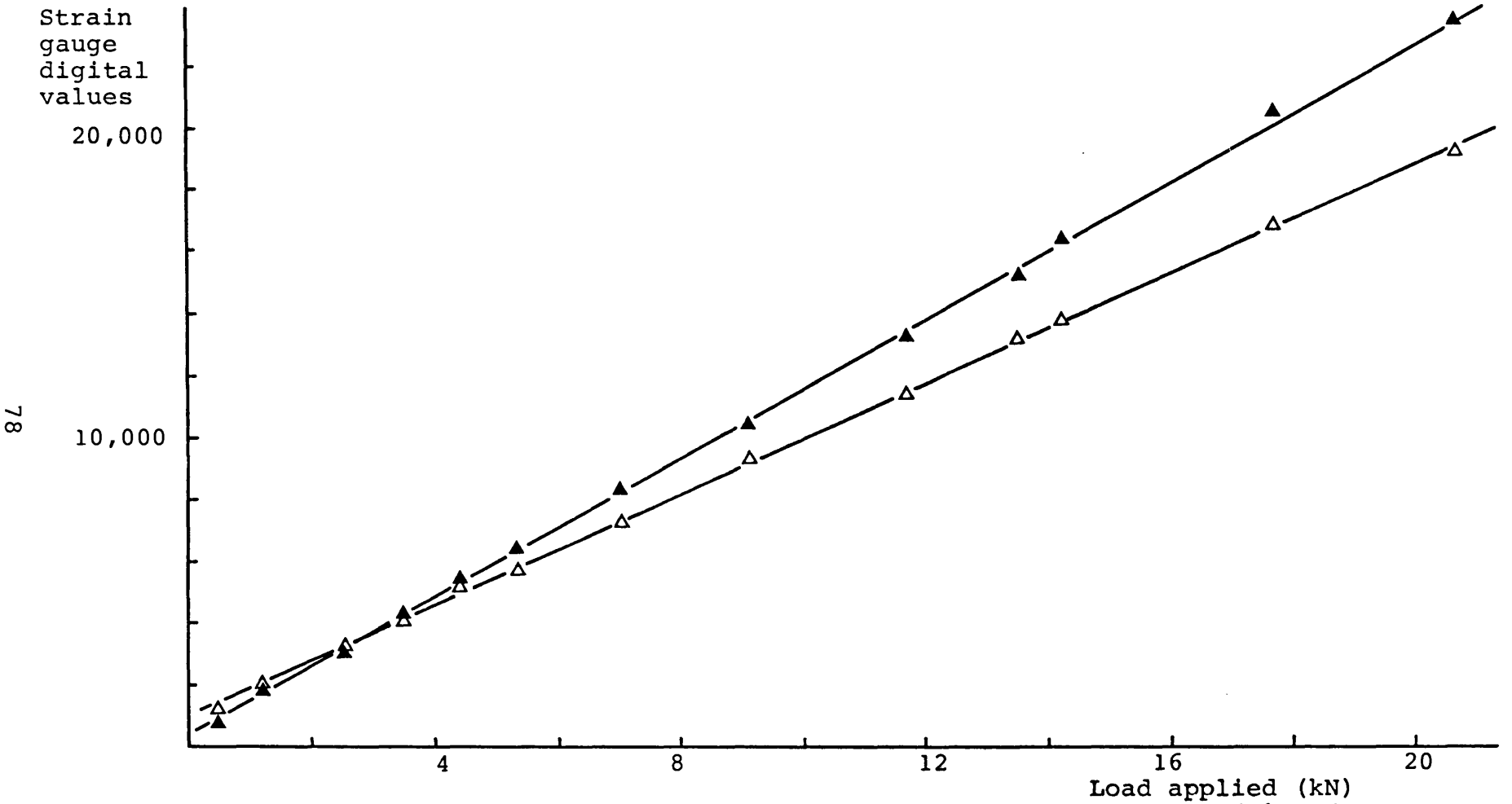

Figure 25. Calibration plot of the strain gauges bonded on the upper punch (▲) and lower punch (△) using a precalibrated piezoelectric load cell with a load distribution washer. The slope, intercept and correlation coefficient values are shown in Table 1.

Upper punch	Zero time	Zero time plus six months
slope	1.159	1.188
intercept	-982.6	-1277.5
c.c	0.9998	0.9997
Lower punch		
slope	0.8938	0.8961
intercept	262.1	344.4
c.c	0.9999	0.9996

Table 1. Calibration data of the strain gauges attached to the upper punch and lower punch block of the tableting machine. The calibration plot is shown in figure 25 and the slopes, correlation coefficient (c.c) and intercept of the strain gauge calibrations at time zero and six months later are tabulated above.

calibration plots are shown in Table 1. The values after six months of continuous use are also given.

2.1.2.1.5 Tableting Conditions.

Fine particle magnesium stearate powder was screened through a 110 μm aperture sieve and mixed at a concentration of 1% w/w with the conditioned powder for approximately 60 seconds. Each mixture was compressed at a compaction rate of 75 tablets per minute to produce tablets each weighing 500mg at a range of compaction forces, between 4kN and 25kN. The compaction force was increased by increasing the depth of penetration of the upper punch. Compressed tablets were conditioned, as described below in section 2.2.6, for 48 hours prior to testing.

2.1.2.2 Mechanical Testing of Tablets.

2.1.2.2.1 Caleva Tensile Tester.

A tensile tester specifically designed for determining the tensile strength of pharmaceutical tablets was used in preliminary studies (type 25, Caleva Ltd., Sunninghill, Berkshire, U.K.). A power driven ram acts on a 250N load cell, thus allowing the peak crushing force to be monitored. In addition a LVDT was used to determine diametral deformation. To calculate the area under the force-displacement curve according to Rees and Rue (1978c), it was found imperative that the force and tablet deformation should be almost simultaneously monitored. This is most accurately and easily accomplished when the signals

from the BCD output of the tensile tester are converted to analogue voltage and fed to the microcomputer through the analogue input. It was found that in the Caleva 25 tensile tester, the sampling rate was too slow to give consistent results for brittle powders, for example Emcompress. It was impossible to increase sampling rate as the data acquisition semiconductor also drove the LED display. The force values displayed by the LED at peak crushing force also failed to correspond to those obtained via the BCD output. Accurate recalibration of the 250N load cell was found to be impossible and for these reasons this tensile tester was not employed in further studies of mechanical properties of tablets.

2.1.2.2.2 JJ Lloyd Tensile Tester.

A type T22K (JJ Lloyd Instr., Ltd., Southampton, U.K.) tensile tester, (Fig. 26), was used for the determination of tensile strengths and work of failure values according to Rees and Rue (1978c). The moving crosshead was moved by two parallel screw drives rotated by two synchronous electric motors which could be accurately controlled by an electronic thyristor drive unit. The crosshead speeds possible with this arrangement gave a variable rate of strain from 0.5-75mm per minute.

The tester could be operated in either tension or compression modes, although in this part of the study the tester was used in the compression mode at a crosshead speed of 2mm per min. The load cell located in the driven crosshead was interchangeable and two cells with different force ranges were used,

one up to 500N and the other up to 1000N; both were Grade B load cells, calibrated by JJ Lloyd Instr., such that at each load cell magnification the maximum full scale deflection was 2 volts. The load cell was fitted such that it was in the centre of the crosshead and the tip of each load cell had a flat-faced surface parallel to the fixed lower platen (Fig. 26). Placing a tablet between the movable crosshead and lower platen allowed the determination of the forces required to cause tensile failure of a tablet, together with the deformation of the tablet during testing.

2.1.2.2.3 Data Acquisition.

The analogue signals from the force and crosshead displacement outputs were fed via an ADC connected to the 1MHz BUS of a microcomputer. Due to electrical noise on the highest magnification of the crosshead displacement, a LVDT (type AG 2.5mm, Sangamo Instr., Ltd., Bognor Regis, U.K.) was fitted directly on to the crosshead, thus allowing the tablet deformation during the diametral test to be determined with greater precision and accuracy. The signals from the LVDT were fed via a card amplifier (type CA2 series, Sangamo Instr., Ltd.) into an ADC and processed by the microcomputer. The amplifier card was powered by a 15 volt d.c power supply pack. The card carried out the signal conditioning from the LVDT output and thus allowed interfacing with the data acquisition system and processing by microcomputer. The data acquisition subroutine and that for data manipulation (see 2.1.2.2.5) were both

incorporated into a menu-driven program.

2.1.2.2.4 Calibration of 2.5mm Linear Variable Displacement Transducer.

Calibration was carried out in situ on the tensile tester, the calibration of the LVDT was checked by placing feeler gauges previously cleaned in acetone, between the LVDT head and a highly polished, hard metal surface. A set of 10 feeler gauges of various thickness were employed. The output from the LVDT was conditioned using a card amplifier (see 2.1.2.2.3) into the 2 volt channel of the ADC and calibration data processing was achieved by feeding the signals into the BBC microcomputer through the 1MHz BUS. A short program was written in BASIC to collect 100 digitized points for every gauge thickness and the mean digital value was plotted against true gauge thickness measured using a micrometer (Fig. 27). The results are given below in Table 2.

2.1.2.2.5 Data Manipulation.

1000 digitized points were acquired during each tensile test: 500 digitized points recording the changes in force and 500 digitized points recording tablet deformation. The analogue output from the load cell and LVDT was sampled by the ADC and then converted to digital form. The sampling rate was governed by the time taken for tensile failure to occur in each test. Using the appropriate calibrations each digitized point was converted to an equivalent force or displacement value and

displayed on the monitor. Using a menu-driven program, data processing was performed after each complete tensile test and the values shown below were calculated and a print out made for comparison later.

a. Peak crushing force (N),

b. Deformation undergone by the tablet (mm),

c. Time elapsed from initial loading to tablet failure (s),

d. Integration of the area under the force versus tablet deformation curve using trapezoidal rule (J). Note this value will be referred to subsequently as "Work of Failure" (WF) and is calculated, as described above in section 1.5.4.2, using equation 13.

e. The value calculated in (d) was normalised to account for changes in cross-sectional areas between tablet specimens, caused by dimensional differences resulting from compression and storage. This value will be referred to as "Normalised Work of Failure" (NWF), J/m2, and was calculated according to equation 29, (Rees et al., 1977).

$$NWF = \frac{2}{\pi Dt} \int_0^{xmax} F.dx \qquad \text{-------- Equation 29.}$$

where D is the tablet diameter, t is the tablet thickness (m).

f. Radial tensile strength was calculated using equation 11 as proposed by Newton and Fell (1968).

g. Power of failure, which was obtained by dividing work of failure values, obtained in (d), by the time required for tablet failure, in (c), (J/s or W).

Figure 26. JJ Lloyd tensile tester with a LVDT attached to determine tablet deformation during diametral testing of tablets.

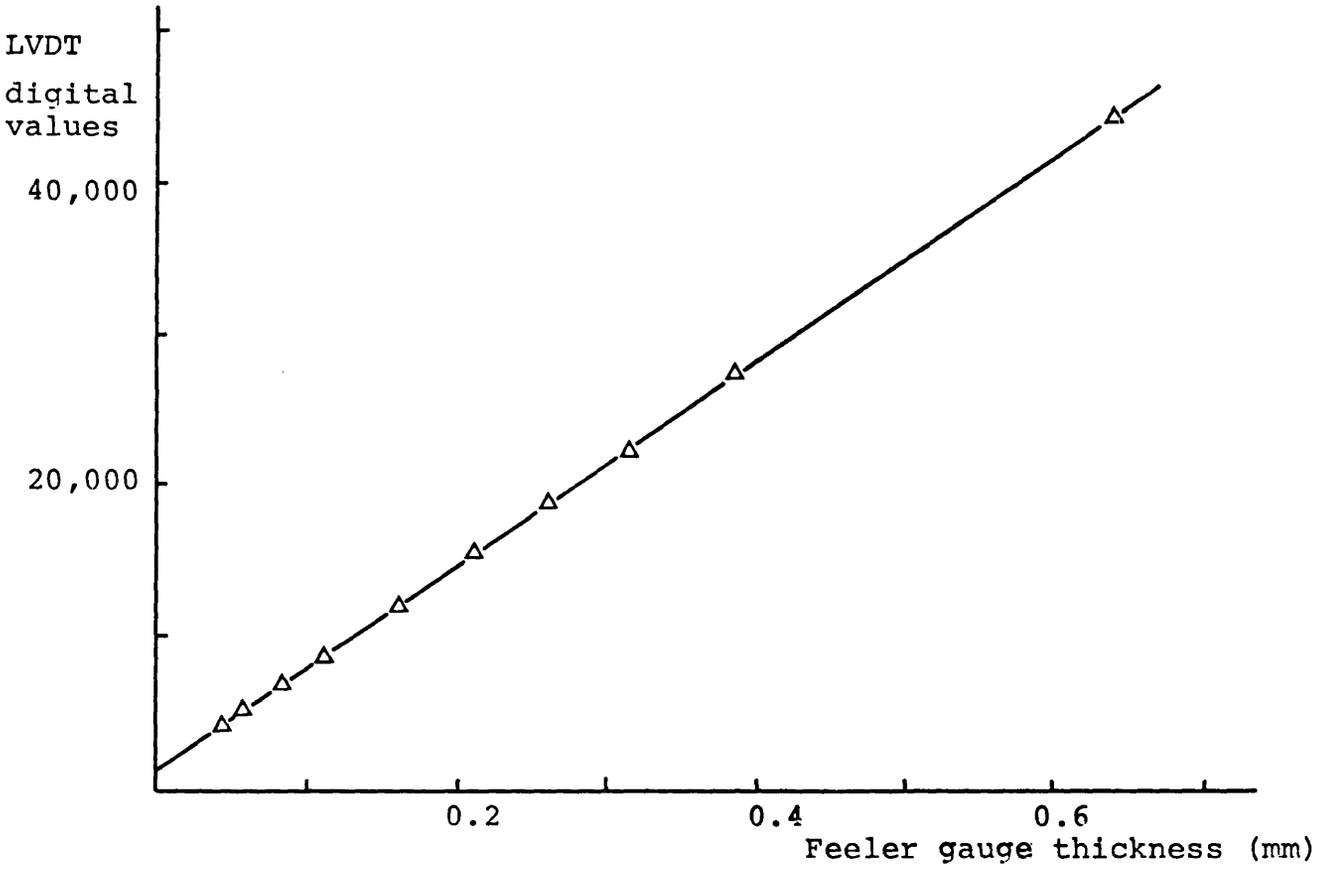

Figure 27. Calibration of the LVDT used with the tensile tester, by plotting LVDT digital values versus feeler gauge thickness. The slope, intercept and correlation coefficient values are shown in Table 2.

slope	= 67240
intercept	= 1397.3
correlation coefficient	= 0.99998

Table. 2 showing the calibration data for the 2.5mm LVDT attached on the tensile tester in order to monitor tablet deformation during the diametral test. Calibration plot is shown in figure 27.

2.1.2.2.6 Fatigue Strength Determination of Tablets Produced by Direct Compression.

2.1.2.2.6.1 Tablet Mass.

The mass required to produce a tablet of 2.5mm thickness at zero theoretical porosity was calculated from a knowledge of the volume which the tablet should occupy and the true density of the powder, according to equation 30:

$$m = pv \qquad \text{---------- Equation 30.}$$

where m = tablet mass, v = volume, p = true density.

2.1.2.2.6.2 Determination of True Density.

A Helium Pycnometer (model 1302, Micromeritics Instr., Corp., Norcross, U.S.A.) was employed in the true density determination. The samples were dried for 2 hours at 60°C and allowed to cool under vacuum prior to density determinations.

Instructions according to those detailed in "Service and Operation of Helium Pycnometer Model 1302" were followed. A mean of five consecutive readings was accepted. The values in parentheses are the corresponding standard deviations.

Materials	True density kg/L
Avicel PH102	1.59 (0.06)
Dipac	1.56 (0.04)
Emcompress	2.39 (0.03)
Microtal	1.57 (0.04)
Tablettose	1.54 (0.03)
Starch 1500	1.54 (0.04)

2.1.2.2.6.3 Tablet Compression.

Tablets were produced manually using a lever mechanism to turn the fly wheel smoothly and reproducibly. The compressed tablets were conditioned as before prior to testing (section 2.2.6). The reason for compressing the tablets manually was to reduce the deviations of individual compaction forces from the mean and increase compaction force reproducibility. A block diagram of the complete system used is shown in figure 23.

2.1.2.2.6.4 Fatigue Failure Testing.

Tablets of five direct compression excipients were examined using a fatigue failure test. A tablet was placed on edge between two platens as shown in Fig. 28 and the tablet was subjected to cyclic load application and removal at a constant frequency of 0.23Hz between a maximum load equivalent to 80% of the mean peak

crushing force and a minimum load equivalent to 20% of mean peak crushing force, giving a constant stress ratio of 0.25. Crushing forces were obtained as the mean value of ten tablets determined using a diametral test, after Newton and Fell (1968).

The cycling was performed using a sinusoidal waveform for the rate of load application and removal, governed by the cycling frequency. The frequency was maintained constant (0.23Hz) by altering the strain rate. Fatigue failure was considered to have occurred when crack propagation had taken place vertically across the tablet diameter, usually splitting the tablet in two halves. At this point the number of cycles required to cause failure was noted. The surfaces in contact with the tablet during the test were smooth and highly polished thus eliminating possible indentations due to rough platen surfaces. Experimental work was performed under ambient conditions.

2.1.2.2.6.4.1 Fatigue Failure Testing Instruments.

An Instron, screw driven tensile tester (type 1122, Instron Ltd., High Wycombe U.K.) was used in the preliminary studies. The Instron was interfaced with an Instron Electronic Integrator which allowed the maximum and minimum load limits to be accurately pre-set. The number of cycles required for fatigue failure are calculated from knowledge of the cycling frequency and total fatigue time.

A JJ Lloyd tensile tester, (type T22K, JJ Lloyd Instr., Southampton, U.K.) as described above (section 2.1.2.2.2) was employed. An additional facility available on the T22K is the

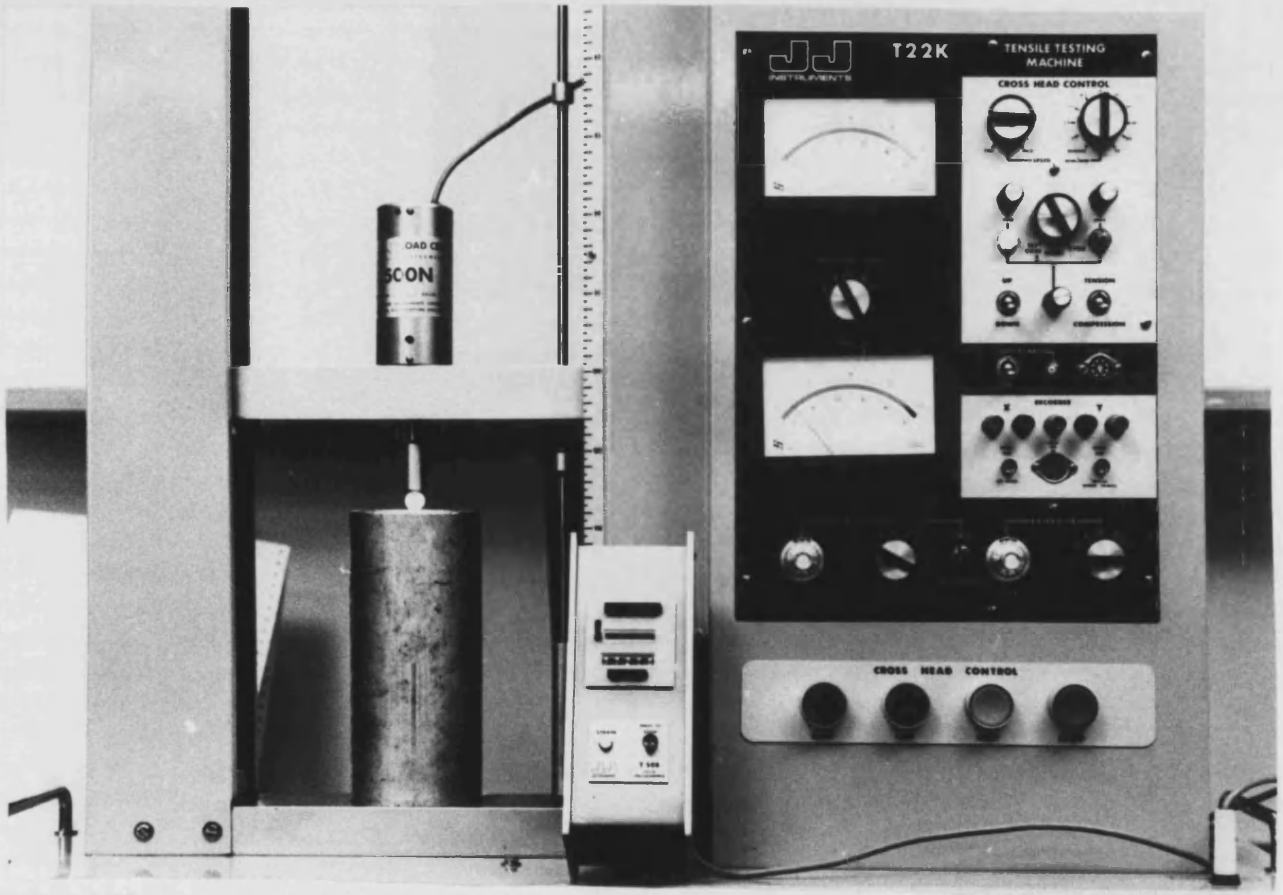

FIGURE 28 FATIGUE TESTING SET-UP

capacity for cyclic load application in either compression or tension mode (Fig. 28). Interfacing the T22K to a small microcomputer described above section (2.1.2.2.3) allows accurate setting of the maximum and minimum load limits for cycling. An automatic counter, (type T508, JJ Lloyd Instr.,) was interfaced to the T22K, thus enabling automatic recording of the number of reversals during cycling of the specimen (Fig. 28). For this reason the JJ Lloyd instrument was used in preference to the Instron tensile tester.

2.1.2.2.6.5. Acoustic Emission (AE)

Part of the fatigue failure study was accompanied by a computer based measurement of acoustic emissions which occured during fatigue testing. Prior to commencing a fatigue failure test a miniature quartz piezo-electric acoustic sensor (type MAC 300, Acoustic Emission Consultants, Sacramento, U.S.A.) was attached to the centre of a tablet face using a coupling agent, petroleum jelly. A block diagram of the acoustic emission system used in these experiments is shown in Fig. 29. During a fatigue test, data acquisition was achieved using a mini-computer (MINC-11, Digital Equipment Corp. U.S.A.) which received analogue signals from a pre-amplifier and an amplitude distribution unit (model 203, Acoustic Emission Technology Corp.,) which had a sorting range of 60db and 51 channels with fixed counting thresholds. Channel 0 had a threshold of 10mV and channel 50 a threshold of 10V. Channels 0-49 were each 1.2db wide and channel 50 registered all events with amplitudes greater than 10V.

Data were collected and written to the floppy discs as an unformatted binary file. The occurrence of an AE is designated by the recording of the amplitude channel number and this AE event of known amplitude is associated with a known time interval. After completion of a test, data was transferred by a telecommunications land line to a main frame computer (Prime 750, Prime Inc., U.S.A.) at Rutherford/Appleton Laboratory, Science and Engineering Research Council Central Computing Laboratory, Harwell, U.K. for data analysis. Transfer of one or more files between the Minc-11 and the Prime 750 computers could be scheduled from either computer and operated under control of the Prime at Rutherford/Appleton Laboratory. The Prime was also used to present data graphically for clearer analysis. Two different plots were obtained for each data set:

(1) AE events versus time in seconds,

(2) The number of events recorded in each of the 51 channels, plotted as a histogram.

2.1.2.2.7 Scanning Laser Acoustic Microscopy (SLAM).

Scanning Laser Acoustic Microscopy (type TM100, Sonomicroscope, Sonoscan Inc., Bensenville, U.S.A.) was used as a potential method of producing visual images of the internal structures of optically opaque tablet cores. A laser source scanned the specimen end directly opposite an ultrasonic source and changes in the reflected laser beam are detected by a photomultiplier and passed to a microcomputer for analysis. A schematic representation of the arrangement is shown in Fig. 30.

Ultrasound of wavelength 100 to 500MHz was produced by an acoustic transmitter and passed through a coupling agent such as water, which causes very low or zero attenuation of ultrasonic waves. However, due to the high aqueous solubility of some of the pharmaceutical tablets studied here, propan-1-ol also having low attenuation properties, was used as the coupling medium.

2.1.2.2.7.1 SLAM Specimen Preparation.

Tablet specimens were subjected to varying levels of mechanical stress by fatiguing tablets for 100 cycles, to represent the initial stages of crack propagation and 1000 cycles to represent the final stages of crack propagation prior to failure. The complete list of specimens prepared for SLAM analysis is shown in Table 3.

EXCIPIENT	COMPACTION FORCE	Level of mechanical stressing	
		LOW	HIGH
Emcompress	20kN	100	1000
Microtal	20	100	1000
Avicel	10	100	1000

Table 3. Specimens prepared for SLAM. Unstressed specimens were used as controls for all three excipients.

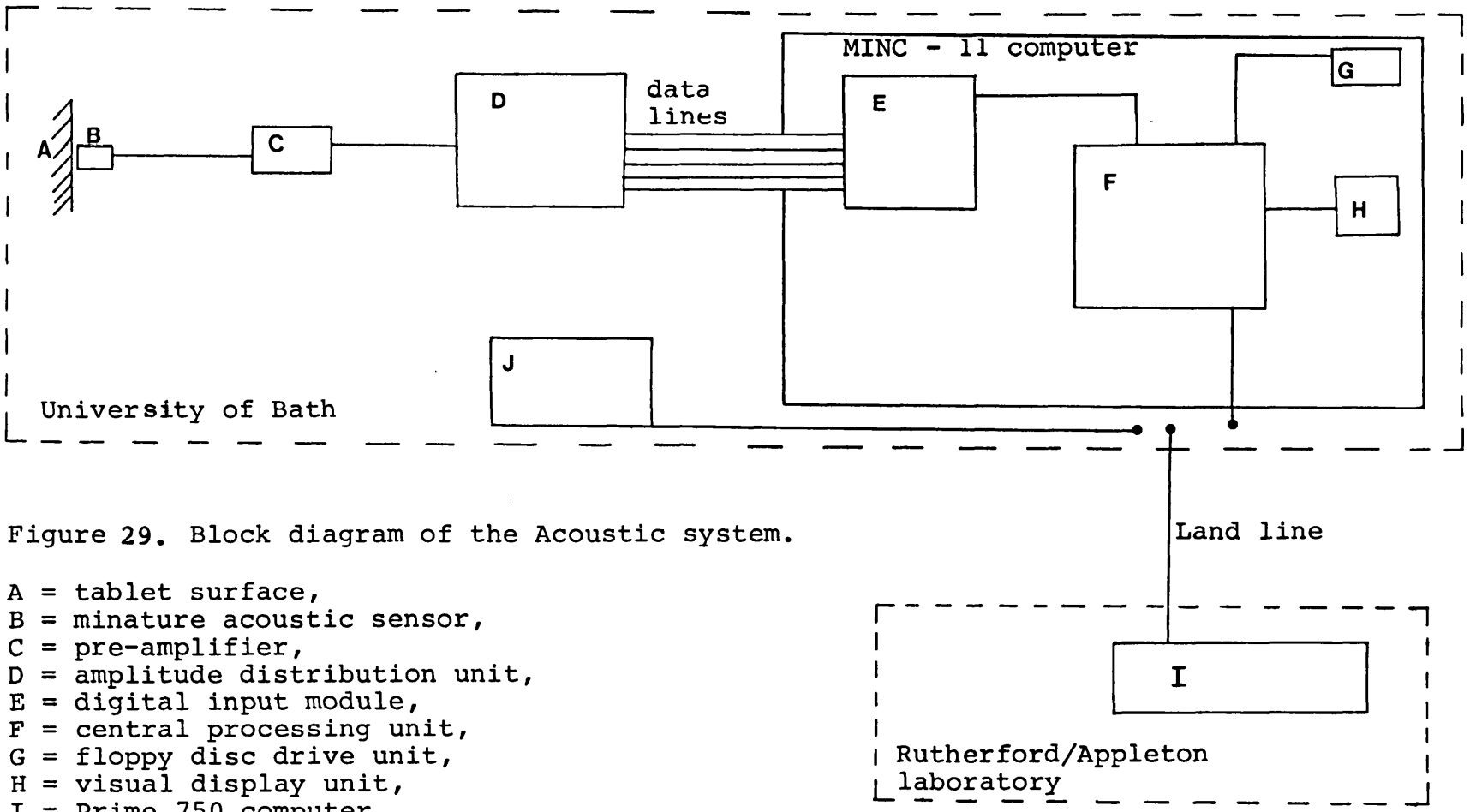

Figure 29. Block diagram of the Acoustic system.

A = tablet surface,
B = minature acoustic sensor,
C = pre-amplifier,
D = amplitude distribution unit,
E = digital input module,
F = central processing unit,
G = floppy disc drive unit,
H = visual display unit,
I = Prime 750 computer,
J = graphics terminal.

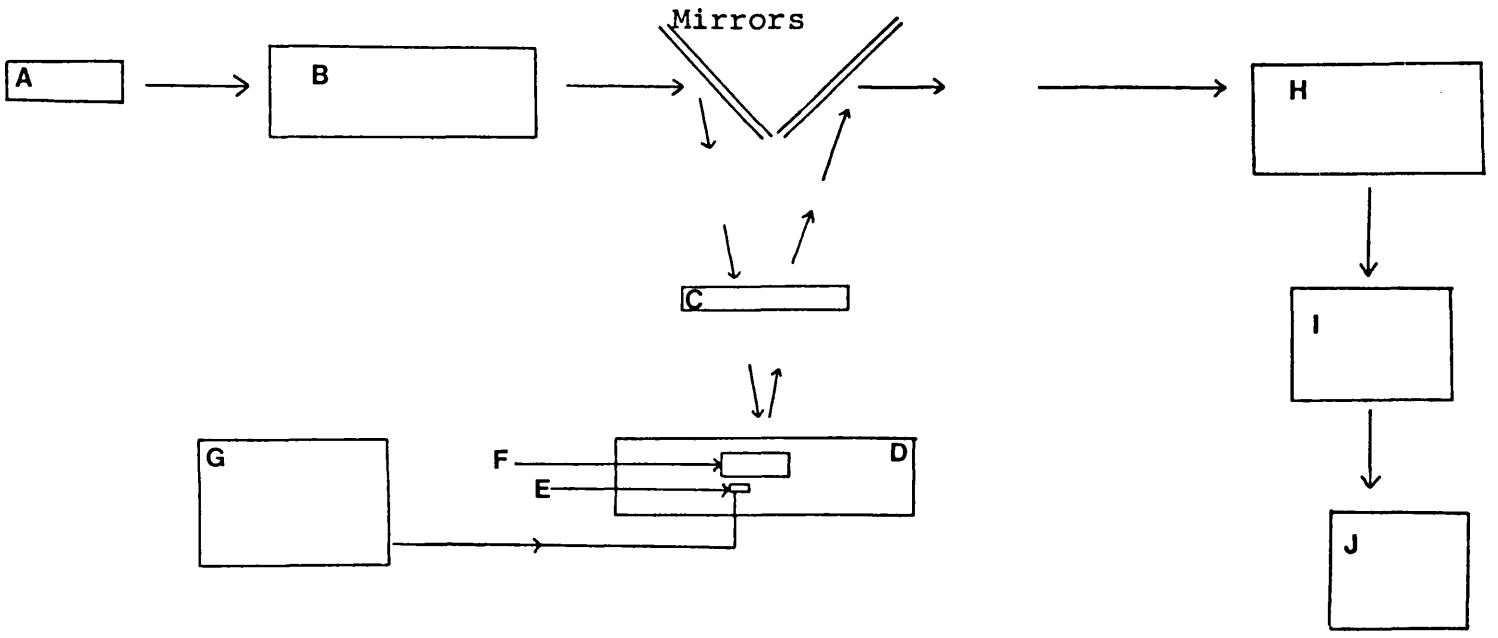

Figure 30. Block diagram of the Scanning Laser Acoustic Microscope.
A = laser gun,
B = beam scanners,
C = imaging optics,
D = stage with coupling medium,
E = ultrasconic transducer,
F = specimen,
G = acoustic frequency generator,
H = demodulator and photomultiplier,
I = acoustic signal processor,
J = acoustic image display unit.

2.1.2.3 Work of Compaction.

2.1.2.3.1 Tableting Machine.

A reciprocating tableting machine as described above in section 2.1.2.1.1 was used in this part of the study. A LVDT (type VAG 5.0mm, Sanagamo Instr., Bognor Regis, U.K.) was fitted onto the tableting machine such that the vertical displacement of the upper punch tip could be accurately determined (Fig. 32).

2.1.2.3.2 Tablet Mass and Compression.

The mass of powder to be examined was calculated as described above in section 2.1.2.2.6.1 and was manually transferred into the die. The powders to be examined were conditioned, as described below in section 2.2.6 and stored in air tight plastic containers prior to transferring into a pre-lubricated die. Punch and die lubrication was performed prior to every experiment by compressing a mixture of 50% w/w magnesium stearate in the powder to be examined. Tablet compression was performed under power and the rate of compression was controlled by the variable speed drive on the tableting machine, the rates available were from 35 to 80 tablets per minute. Due to the memory constraints of the microcomputer, each tablet was compressed, without ejection, a maximum of nineteen times.

In order to investigate multiple compressions of the same tablet, it was necessary for the tablet not be ejected from the die between successive compressions. There are two steel rings on the lower punch block: one is used to govern the position of the

lower punch and control tablet mass; the other steel ring is used to achieve control of the lower punch travel at ejection. Removal of the latter ring rendered the movement of the lower punch independent of the motion and position of the upper punch. Ejection of the tablet was performed manually by lifting the lower punch block after multiple compression of powders. Due to electrostatic disturbances caused by the three phase electric supply to the tableting machine when switched on and off, there was excessive interference at the start of data collection, thus data collection was commenced after the tableting machine was switched on, but before the start powder compression. The machine was started with the punches located in the end-of-cycle positions, so as ensure normal punch tip velocity at the point of compression.

2.1.2.3.3 Recalibration of Strain Gauges.

As small changes in the calibration value of the upper and lower punch strain gauges were observed to be taking place with time, the strain gauges were recalibrated before this part of the study was undertaken (Fig. 31). The method and interfacing used were identical to that described previously in section 2.1.2.1.3. Table 4 shows the recalibration data used in the study of work of compaction.

2.1.2.3.4 Linear Variable Displacement Transducer Fitting and Calibration.

A lever arm was fitted as close to the upper punch as

possible (Fig. 32), without any risk of damage to the upper punch strain gauges and in such a way that the precise displacement of the upper punch could be determined. The body of the 5.0mm LVDT was attached to the die plate as shown in Fig. 32 and then calibrated in situ using four hardened steel discs placed in the tablet die and subjected to compressive loading between the upper and lower punches. Each of the four discs was of known thickness. The LVDT was powered by a 15V d.c supply and interfaced as described above (section 2.1.2.2.4) using a card amplifer, the analogue signals were fed into the 8V channel of the ADC and then into a small microcomputer (BBC Model B) via the 1MHz BUS. A similar program to that described in 2.1.2.2.3 was used for LVDT calibration carried out here and the digital values acquired from the LVDT were plotted versus the disc thickness (Fig. 33). The slope, intercept and correlation coefficient values are shown in Table 5.

2.1.2.3.5 Data Acquisition.

The acquisition of data from the strain gauges after conditioning and amplifying was identical to that described above in sections 2.1.2.1.2/.3 . Data acquisition from the 5.0mm LVDT was identical to that described in section 2.1.2.2.3. During each compression cycle, 512 analogue values from each of the strain gauges and the LVDT were acquired and converted to the corresponding force and displacement values.

Data acquisition on the first compression cycle was triggered when the force deviated above a preset threshold level

(314N) but on subsequent compression cycles, data acquisition was displacement dependent. Due to insufficient random access memory (RAM) in the microcomputer, an additional side-ways RAM (SWR type 64, Solidisk Tech., Ltd., U.K.) was interfaced via a sideways ROM socket within the microcomputer, to provide additional memory. The SWR was used to store the analogue data as collected and after a maximum of nineteen compressions the data was recalled and manipulated. To allow fast processing, the data acquisition subroutine was written in 6502 Assembly code and the data manipulation element in BASIC, was also included, thus allowing immediate data analysis.

2.1.2.3.6 Data Manipulation.

A plot of force applied by the upper punch versus relative displacement was constructed (Fig. 34) and the area under the curve was calculated using equation 31.

$$\text{Total work} = \int_{Ds}^{Dm} F.dx \qquad \text{--------- Equation 31.}$$

where Ds = the displacement corresponding to the first force reading greater than the threshold value; Dm = the displacement corresponding to the maximum force applied by upper punch and F = the force applied by the upper punch.

The area under the force-displacement curves following subsequent compressions were calculated in the same way. Using the internal clock of the microcomputer, the time over which the force was applied and thus the time over which work was

performed during the first compression and subsequent re-compressions was determined. The data analysis subroutine was constructed such that the various measured and calculated parameters at each compression were printed for analysis and comparisons:

(1) total work performed at each compression according to equation 31,

(2) upper punch force,

(3) displacement at maximum force,

(4) time over which force was applied.

	slope	intercept	correlation coefficient
Upper punch	1.223	-184.3	0.9994
lower punch	0.873	187.5	0.9999

Table 4. Data obtained on recalibration of the strain gauges on the upper punch and lower punch holder and these calibration data were used in the study of work of compaction. Calibration plot is shown in figure 31.

	data
slope	-8485.5
intercept	9040
correlation coefficient	0.99995

Table 5. Calibration data of a LVDT used to monitor the upper punch displacement during the work of compaction study. Calibration plot is shown in figure 33.

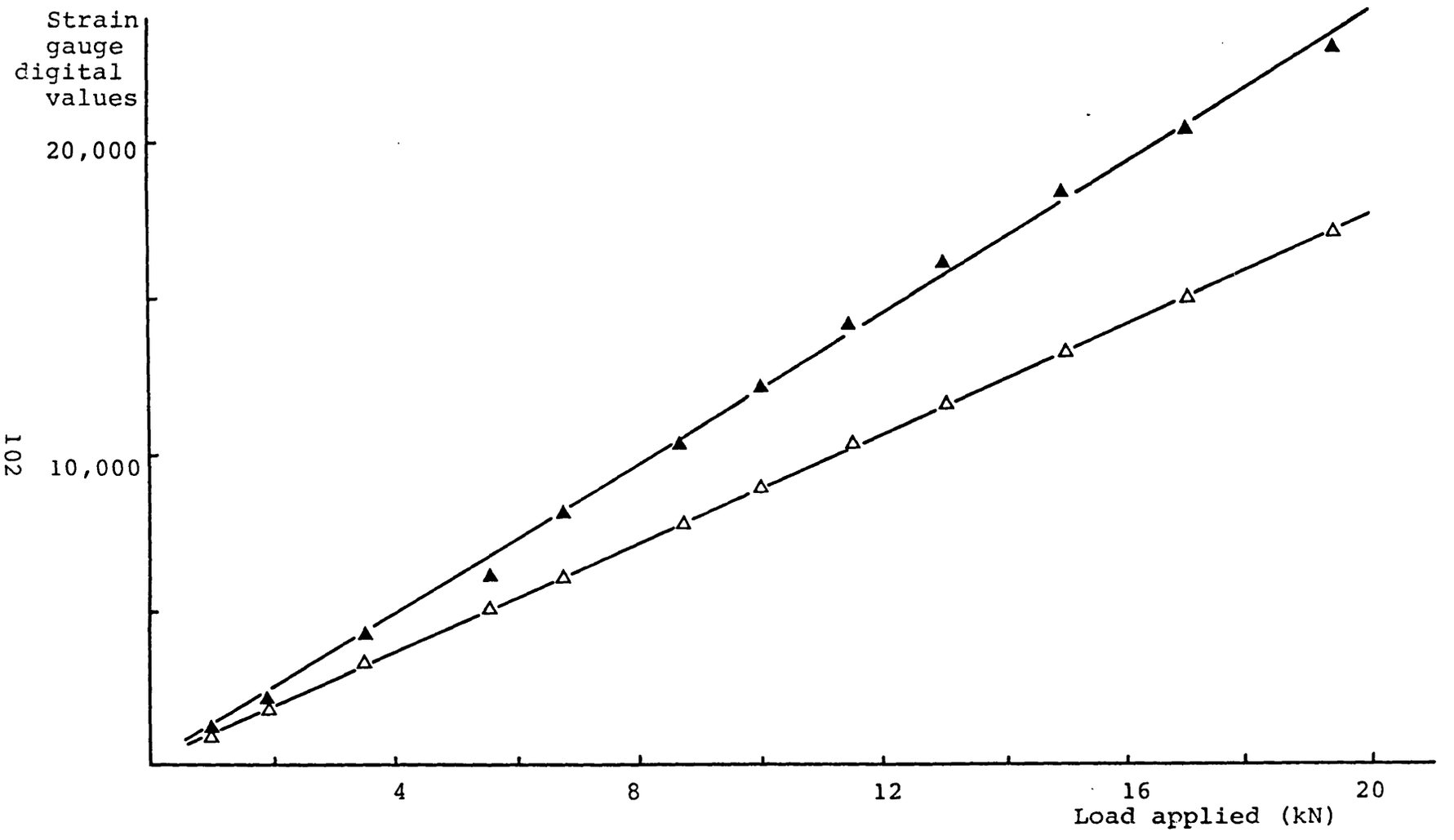

Figure 31. Recalibration of the strain gauges bonded on the upper punch (▲) and lower punch (△) using a precalibrated piezoelectric load cell with a load distribution washer. The slope, intercept and correlation coefficient values are shown in Table 4.

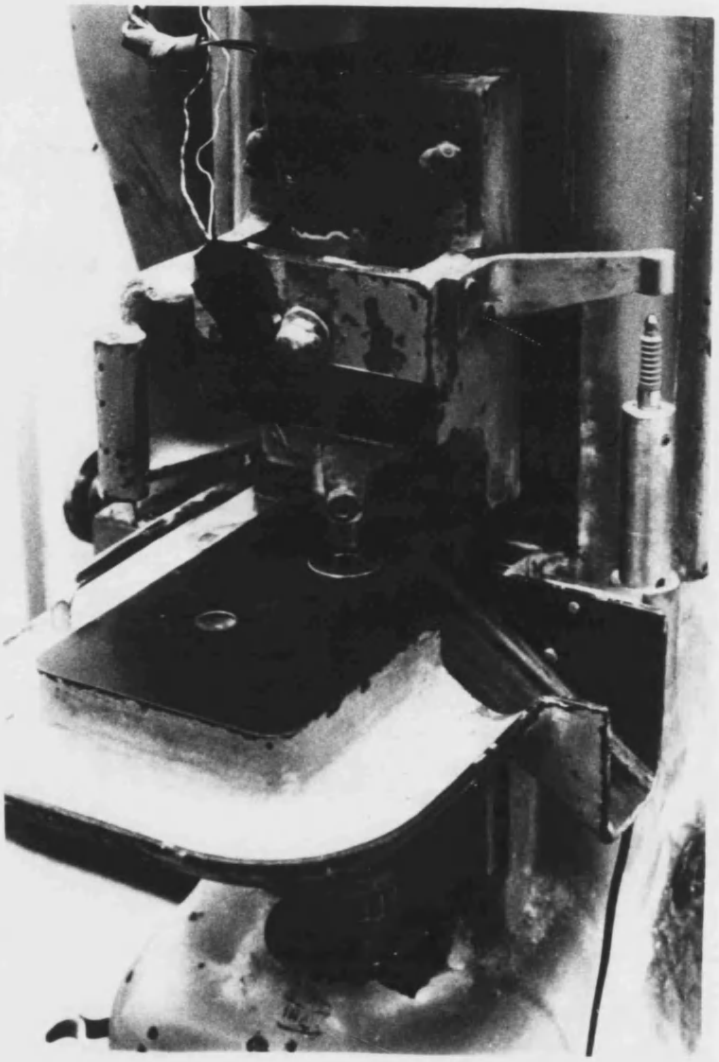

FIGURE 32 TABLETING MACHINE (E2) WITH LVDT TO MONITOR UPPER PUNCH DISPLACEMENT

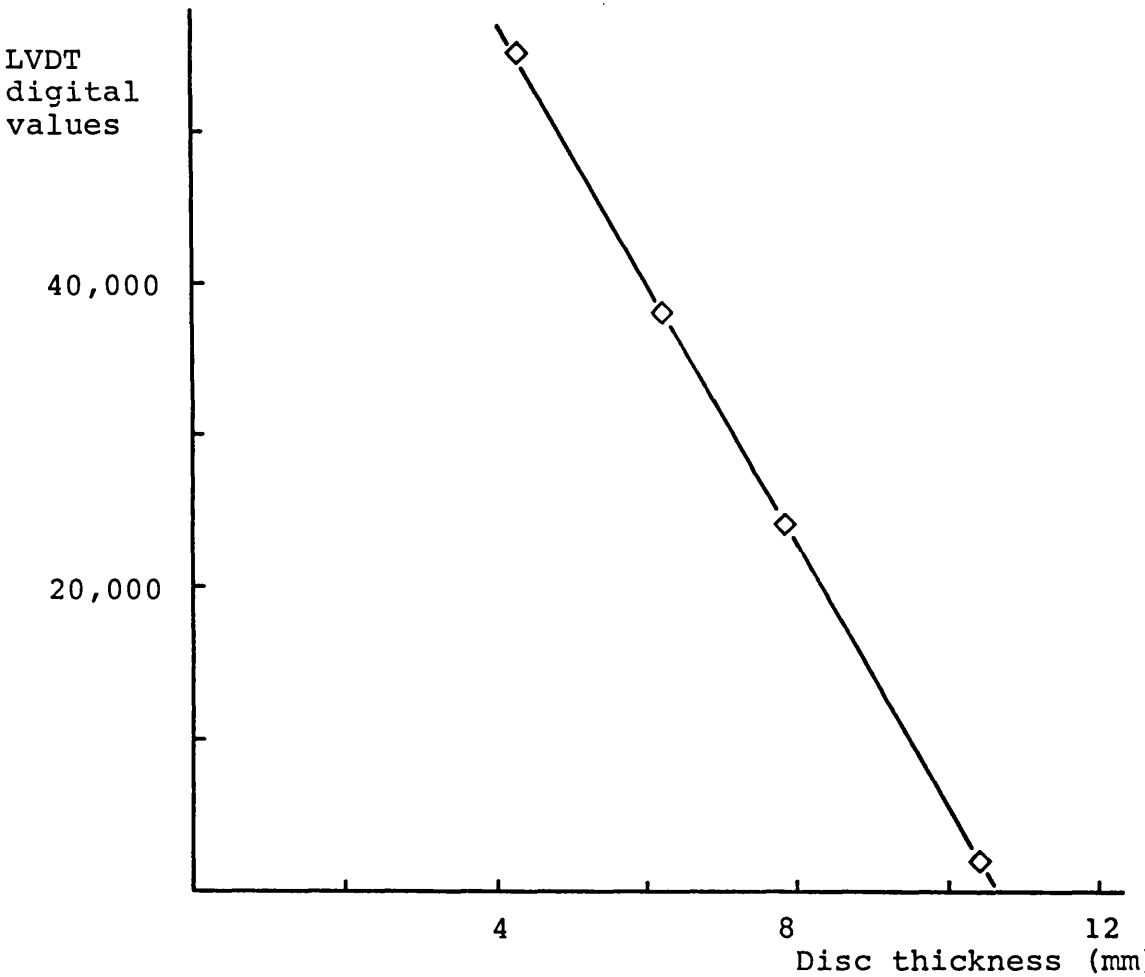

Figure 33. Calibration of the LVDT used to monitor upper punch displacement by plotting LVDT digital values versus the thickness of discs. The slope, intercept and correlation coefficient values are shown in Table 5.

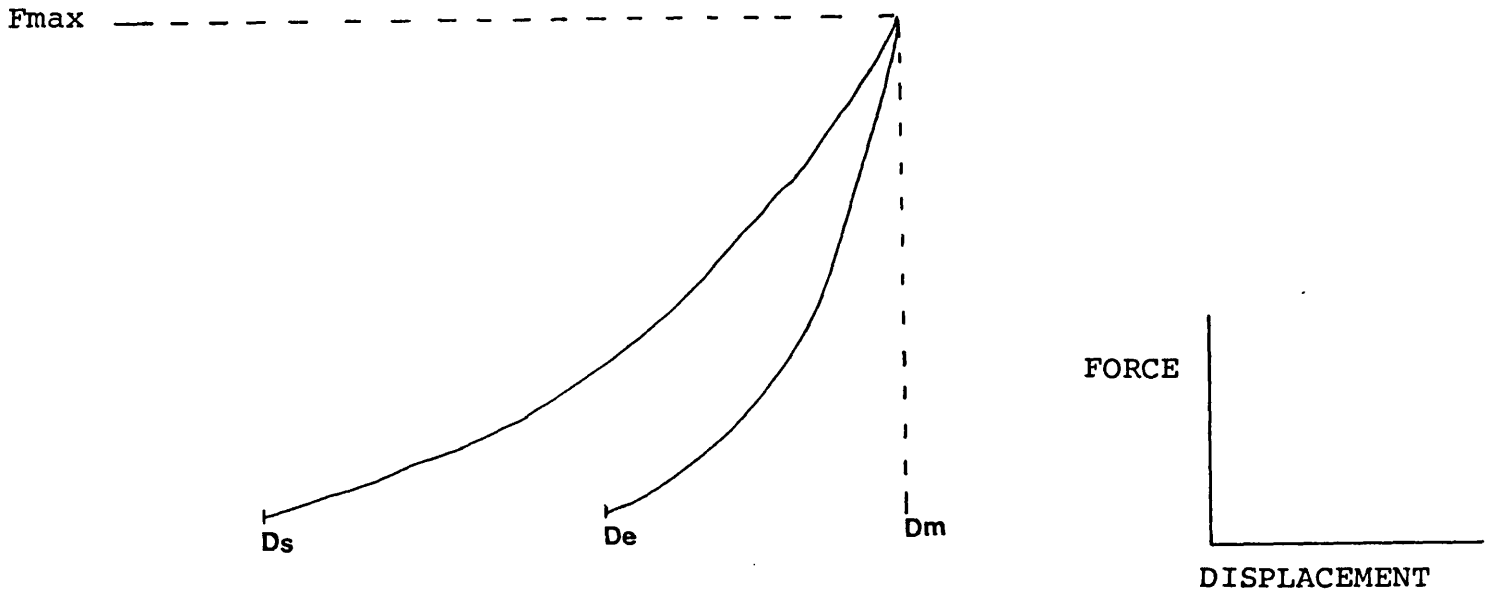

Figure 34. A typical force-displacement curve observed.
Ds = displacement corresponding to the first force reading deviating from the threshold,
De = displacement corresponding to the first force reading below the threshold,
Dm = displacement corresponding to the maximum force applied by upper punch,
Fmax = maximum force applied by the upper punch.

2.1.2.4 Creep Analysis.

2.1.2.4.1 Instrument Design.

A tensile tester (type T22K, JJ Lloyd, described above in section 2.1.2.2.2) was used to perform the creep analysis on different excipients. Due to the mechanical and structural limitations of the tensile tester forces greater than 1kN could only be applied in tension mode and for this reason a compression cage (type TG 27, heavy duty cage, JJ Lloyd Instr.,) which could withstand forces upto 20kN was used. A 20kN load cell (grade B, JJ Lloyd Instr.,) was used to monitor changes in load during testing. To allow precise, non-contacting, entry of upper punch into the 12.7mm diameter die the flat-faced punches were built into a rigid structure on the compression cage (Fig. 35). This arrangement also allowed periodical cleaning and lubrication of the die and punches without loss of alignment on re-assembly.

Two linear variable displacement transducers (LVDT) were attached such that the movement of the upper punch tip could be determined. A 5.0mm LVDT (type AG 5.0mm Sangamo Instr.,) was used to monitor coarse movement and to calculate tablet thickness at time zero. In addition a 2.5mm LVDT (type AG 2.5mm, Sangamo Instr.,) was used to monitor finer movements at constant stress. A constant stress module (type T510 JJ Lloyd Instr.,) was interfaced to the tensile tester thus allowing a constant stress to be maintained by triggering the electronic control driving mechanism of the tensile tester.

2.1.2.4.2 Determination of Creep Compliance.

The mass of powder required to produce a tablet of 2.5mm thickness at zero theoretical porosity was manually transferred into a pre-lubricated die. Powders to be examined were previously conditioned and sealed in an air-tight plastic container. The lubrication of punches and die was carried out prior to every creep compliance determination and was performed by the application of a 10% w/v suspension of magnesium stearate in acetone to the punches and die followed by removal of any excess fluid. Two rates of load application were used 3kN and 14kN per minute. The constant loads applied were 5, 10 and 15kN thus giving constant stress values equivalent to 39.5, 79 and 118.5MPa respectively.

2.1.2.4.3 Calibration of Instruments.

2.1.2.4.3.1 Load Cell Calibration.

The 20kN load cell was calibrated by JJ Lloyd Instr., Southampton, U.K. to give 2V full scale deflection at any magnification setting on the T22K.

2.1.2.4.3.2 Linear Variable Displacement Transducer Displacement.

(1) 2.5mm LVDT- see section 2.1.2.2.4

(2) 5.0mm LVDT- the punches in the compression cage were brought in contact to produce a force of approximately 10kN and a digital value of 54,800 units was obtained by adjusting the span and zero setting on the card amplifier of the LVDT (see

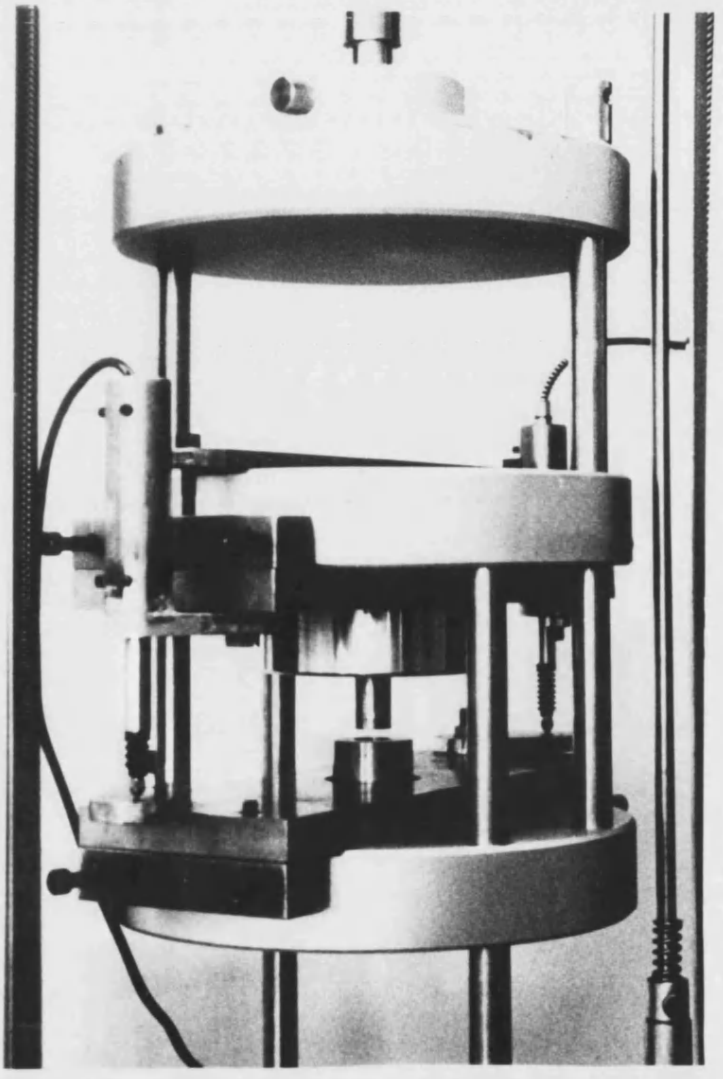

FIGURE 35. EXPERIMENTAL SET-UP TO MONITOR CREEP COMPLIANCE OF POWDERS

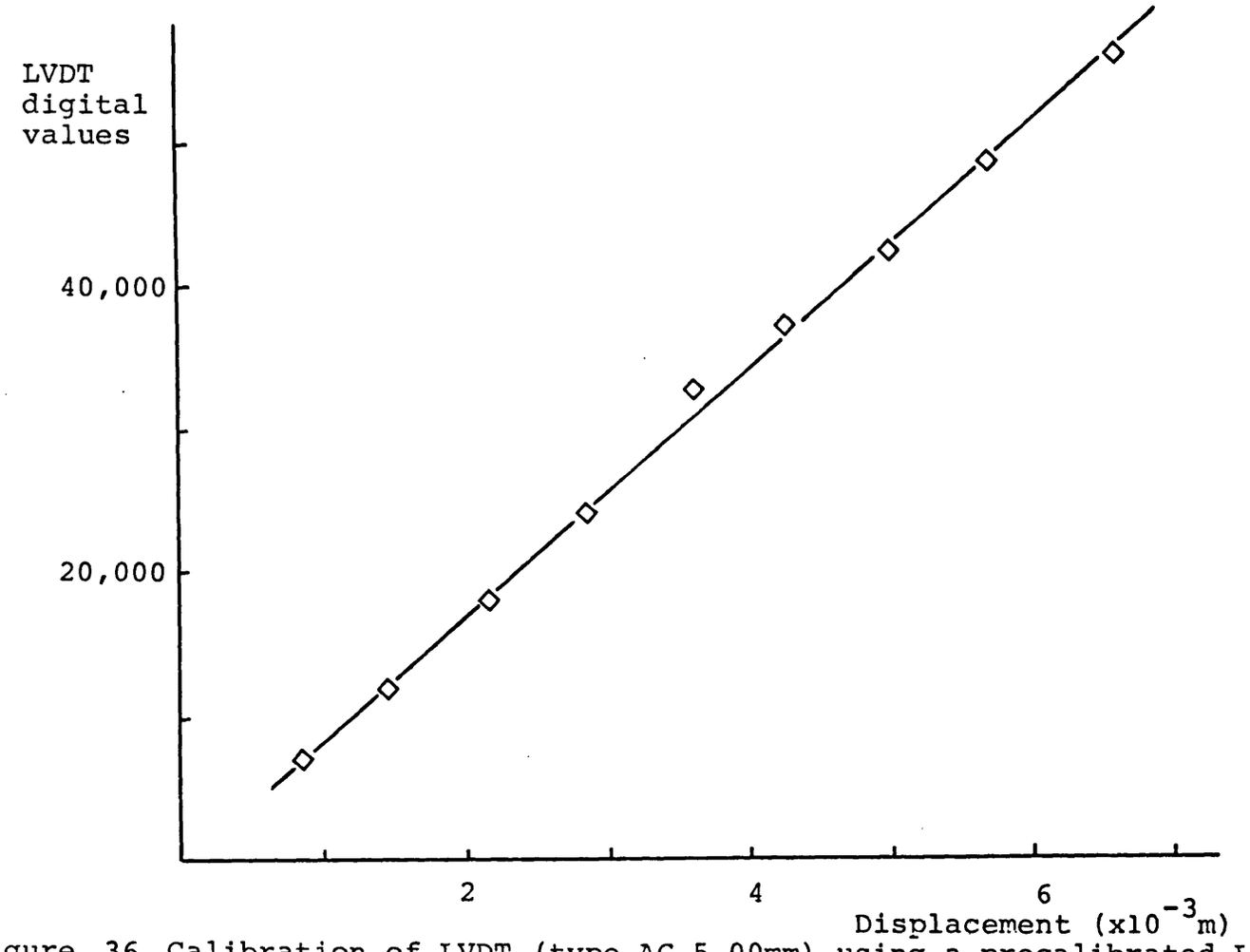

Figure 36. Calibration of LVDT (type AG 5.00mm) using a precalibrated LVDT. The slope, intercept and correlation coefficient values are shown in Table 6.

section 2.1.2.2.3). This LVDT was calibrated using a previously calibrated 5.0mm LVDT (type VAG 5.0, Sangamo Instr.,) which was described above in section 2.1.2.3.4. Both LVDTs were fitted into the compression cage and a short program in BASIC was constructed to allow means of 100 points from the AG 5.0mm plotted against means of 100 points (metricated) from the VAG 5.0mm LVDT (Fig. 36). The slope, intercept and correlation coefficient (Table 6) were obtained from data in Fig. 36.

	Data
Slope	8488
Intercept	212
Correlation coefficient	0.9998

Table 6. Calibration data of the LVDT attached to the creep compression cage, calculated from data in Fig. 36.

2.1.2.4.4 Data Acquisition.

Using two separate card amplifers (see 2.1.2.2.3), one for each of the LVDTs on the compression cage, allowed an easily usable digital output. Digital outputs corresponding to the force reading on the T22K were, together with the two separate outputs of the LVDTs fed into a fast analogue-digital converter. This converted the outputs sequentially to digital signals which were fed into a small microcomputer (BBC Model B) via the 1MHz BUS for data manipulation.

2.1.2.4.5 Data Manipulation.

The fast analogue digital converter was microcomputer controlled, thus allowing 260 points on each channel to be converted to the corresponding force and displacement values using the appropriate calibration factors in a menu-driven program. A plot of creep compliance against time was obtained and using a graphics dump routine, the plot was transferred on to a dot matrix printer (type FX-80, Epson, U.S.A.). Creep compliance was calculated according to equation 32.

$$\text{Creep compliance} = \frac{\text{strain}}{\text{stress}} \quad \text{---------- Equation 32.}$$

where stress = force applied divided by the area over which force is applied, and

$$\text{strain} = \frac{\Delta L}{L},$$

where ΔL change in compact thickness, L original compact thickness.

The original compact thickness was calculated from the knowledge of the difference in digital value of the AG 5.0mm LVDT when punches were in contact at about 10kN and that at the first constant stress reading. Thus creep compliance has the units 1/Pa.

2.1.2.4.6 Data Analysis.

Plots of creep compliance against time were obtained using a dot matrix printer, but due to memory constraints in the microcomputer, adequate graph scaling techniques could not be

applied. Hence data analysis was achieved by a regression analysis procedure in the menu-driven program.

A typical creep curve obtained in the present study is illustrated in Fig. 37. The plot can be divided into various sections according to theory (1.7).

The C-D portion is the linear viscous section (Fig. 37). Applying regression of creep compliance points with respect to time, the most linear portion as determined by the correlation coefficient values, was used to represent C-D.

The B-C portion is curvilinear (Fig. 37) and thus elucidatation of the intercept value was carried out by regression of data points between time zero and 20 seconds, giving five or more data points for each regression. Hence slopes calculated for the portion B-C represent the most linear section from the base of B-C curve and its associated intercept. All the calculated slopes, with the regression time limits together with the condition of the test were printed out for comparison.

The total time for the creep analysis was dependent on the C-D portion, the most linear portions were obtained when the time of analysis was 360 seconds, when the C-D portion formed at least 1/3 to a 1/2 of the total plot.

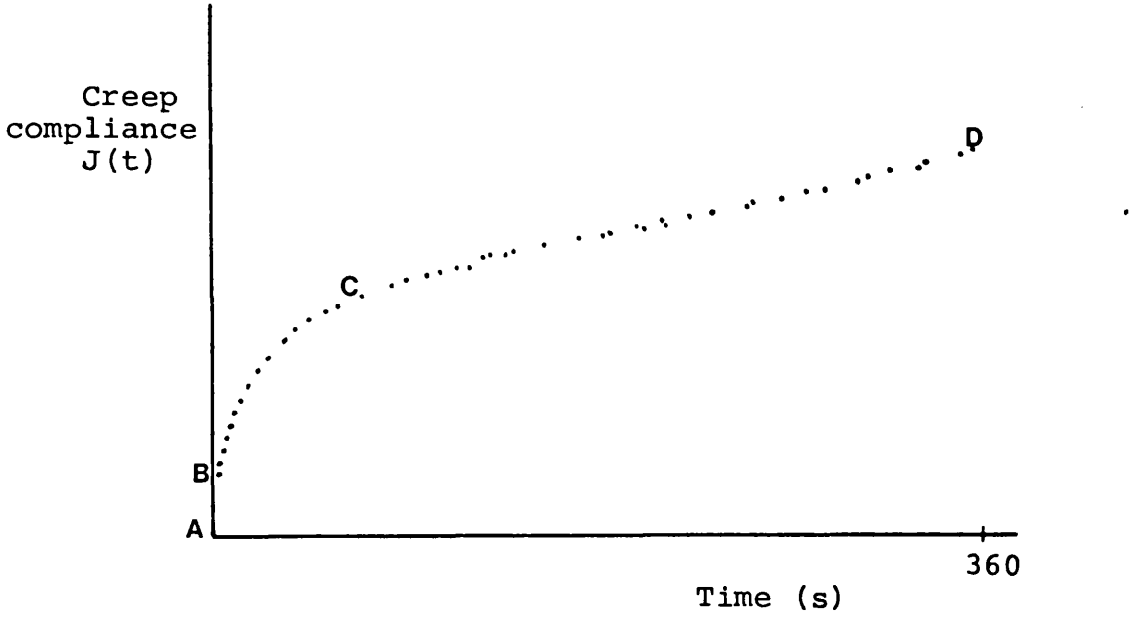

Figure 37. Creep curve observed over a 360 second time interval.
A-B = instantaneous elasticity,
B-C = $\hat{e}$ visco-elasticity,
C-D = linear viscous flow.

2.2 Physico-mechanical Properties of Sucrose and Sucrose-Based Tablets Produced by Direct Compression.

2.2.1 Materials.

Maltodextrin, "Snowflake" lot 01913, (type 20DE, CPC Products Ltd., Manchester, U.K.)

Gelatins of different viscosity grades characterized by Bloom Strength (B.S.) number, (Sigma Chemical Co., Poole, U.K.).

B.S.60 - from bovine skin , type IV, lot 23F 0414

B.S.175 - from porcine skin, type II, lot 13F 0146

B.S.225 - from bovine skin, type III, lot 63F 0670

B.S.300 - from porcine skin, type I, lot 72F 0657

Protein S (Relative molecular mass 15,000 D) high purity protein, (food grade type, Croda Food Ltd., Widnes, Cheshire, U.K.)

Cryogel, a cold-water soluble gelatin, lot 270, (food grade type, Croda Food Ltd.)

Dextrans (Sigma Chemical Co., Poole , U.K.) of various relative molecular mass (R.M.M):-

2,000,000 D lot 91F-0603

252,000 D lot 13F-0426

65,000 D lot 91F-0585

9,000 D lot 23F-0202

Alpha-cellulose (fibrous type) lot 92F-0243 (Sigma Chemical Co., Poole, U.K.)

Cellulose esters (Aldrich Chemical Co., Gillingham, U.K.) of various ester chain lengths:-

cellulose acetate lot 122177

cellulose triacetate lot 2014 PJ

Polyethylene glycol (BDH Chemicals Ltd., Poole U.K.), two different R.M.M. 4,000 D and 6,000 D.

Sucrose esters (DKS International Inc., Tokyo, Japan), three grades were used, with different proportions of esteric groupings. The ester in this product is a combination of 30% stearate and 70% palmitate. The grades are based on the different relative concentrations of mono- and a mixture of di-, tri-, and poly-ester units of the two esters.

Type F90 lot 0090103; 45% mono-ester and 55% a mixture of di-, tri-, and poly-ester (higher-esters).

Type F110 lot 0160106; 50% mono-ester and 50% a mixture of the mixture of the higher-esters.

Type F160 lot 0110104; 70% mono-ester and 30% a mixture of the mixture of the higher-esters.

Crystalline samples of sucrose obtained from Tate & Lyle Plc, London, U.K.

Granulated sucrose, (Domino Brown, Amstar Corp., American Sugar Division, New York, U.S.A.)

2.2.2 Preparation of Sucrose-based Materials for Direct Compression.

2.2.2.1 Transformation Process for Pure Sucrose.

A supersaturated solution of anhydrous cane sucrose was prepared by adding 100ml of deionised water to 200g of sucrose. The resulting mixture was gradually raised to a temperature of 130° C and then removed from heat. Shear was applied using a Silverson shear mixer (bench size type) to this mixture to initiate nucleation, at this point the mixture was observed to be turning opaque. Approximately 60 seconds, after initial application of shear, the final product was obtained and this was then spread on a large tray and allowed to cool. The process was repeated several times to provide sufficient final material for subsequent characterisation. The yield in all transformations was greater than 95%.

2.2.2.2 Co-transformation of Sucrose.

The method was similar to that described immediately above except that different proportions of polymeric material were added, in solid form, at the point in the transformation process where the heated supersaturated mixture of pure sucrose was observed just to be turning opaque. This point coincided with the initial stages of sucrose nucleation.

2.2.2.2.1 Polymeric Materials Co-transformed with Sucrose.

All the polymeric materials were used as received from the

Materials	Concentrations of polymeric material used as % w/w of sucrose.					
	1	3	5	10	20	30
Maltodextrin 20DE	1	3	5	10		
Gelatin:						
B.S. 60	1	3	5			
B.S. 175	1	3	5			
B.S. 225	1	3	5			
B.S. 300	1	3	5			
Protein S		3	5			
Cryogel		3	5			
Dextrans:						
R.M.M 2,000,000 D		3	5			
R.M.M 252,000 D		3	5			
R.M.M 65,000 D		3	5			
R.M.M 9,000 D		3	5			
Avicel	1	3	5	10	20	30
Alpha-cellulose		3		10		
Cellulose ester:						
cellulose acetate		3		10		
cellulose triacetate		3				
Sucrose ester:						
type DKF 90		3	5			
type DKF 110		3	5			
type DKF 160		3	5			

Table 7. Types of polymeric materials and concentrations used to prepare different direct compression materials based on sucrose.

suppliers and added to the heated supersaturated solution of pure sucrose at different concentrations of the polymeric material in sucrose. Table 7 shows the materials and concentrations used to prepare the co-transformed products.

2.2.2.3 Other Methods of Incorporating Polymeric Materials with Sucrose.

2.2.2.3.1 Admixes of Maltodextrin and Transformed Sucrose.

A transformed sucrose sample of standard particle size distribution (see 2.2.4) was mixed for 10 minutes in a tumbling cube blender fitted with intensifier bars, (2 litre capacity, Erweka, Frankfurt, F.R.G.) with each of seven different conentrations of maltodextrin: 1, 5, 10, 20, 40, 60 and 80 % w/w. The maltodextrin was used as received from the suppliers and mixes were conditioned as described in 2.2.6 prior to tablet compaction.

2.2.2.3.2 Admixes of Microcrystalline Cellulose (Avicel PH102) and Transformed Sucrose.

A transformed sucrose sample of standard particle size distribution (section 2.2.4) was mixed using the method described immediately above with six different percentages of Avicel PH102: 1, 5, 10, 20, 40, 80% w/w. The microcrystalline cellulose was used as received from the suppliers and mixes were conditioned as described in 2.2.6 prior to tablet compaction.

2.2.2.3.3 Maltodextrin Coat on Transformed Sucrose.

Approximately 485g of standard particle size transformed sucrose was coated in a fluidized bed spray granulator (STREA1, Aeromatic, Tadley, U.K.) using a solution prepared by dissolving 15g maltodextrin 20DE in 50ml hot distilled water. The solution was sprayed on to the fluidised transformed sucrose at a rate of approximately 5ml/minute using an inlet air temperature of 60°C. When all the solution had been added the coated powder was dried for 30 minutes at 60°C.

2.2.2.3.4 Polyethylene Glycol (PEG) Coat on Transformed Sucrose.

10g of PEG 4,000 or 6,000 in 80g of ethanol was slowly added to 200g of transformed sucrose in a heated rotary evaporator at 55°C. The mixture was rotated at 20 revolutions per minute for 30 mins. under vacuum. The product was further dried for two hours in a vacuum oven at 60° C and then passed through a 600μm aperture sieve to separate the coarser agglomerates.

2.2.2.3.5 Pure Agglomerated Sucrose.

Approximately 540g of standard particle size crystalline sucrose was placed in a fluidized bed spray granulator (STREA1, Aeromatic) and agglomerated by the addition of 250ml water sprayed at a rate of 9ml/minute using an inlet air temperature of 60°C. The agglomerates were then dried at 60°C for 30 mins. This sample was used as a control for the sample prepared in 2.2.2.3.6.

2.2.2.3.6 Impure Sucrose Crystals.

Approximately 490g of impure sucrose crystals recovered from the third re-crystallization stage of the refinery process and known as "third crop recovery" was agglomerated using 280ml of distilled water using the method described immediately above. "Third crop recovery" material was washed in 2 * 200g lots by adding 500ml of 0.01M hydrochloric acid (HCl) in methanol. The mixture was gently agitated for 5 mins. and the supernatant liquor was decanted from the solid material. This procedure was repeated twice, using fresh 0.01M HCl in methanol on each occasion. The purpose of carrying out a washing procedure was to remove fructose and glucose surface films from the sucrose crystals. The crystals were washed twice more, firstly using 500ml of methanol, in order to remove HCl from the crystal and then with 500ml diethyl ether. The latter was used to remove methanol from the crystals prior to drying overnight in a vacuum oven at 40°C.

2.2.3 Crystalline Brown Sugar.

A sample of this sugar was passed through a 500 μm test sieve to remove any coarse agglomerates prior to conditioning.

2.2.4 Particle Comminution.

All samples were first passed through a 500 μm aperture sieve to separate any coarser agglomerates. Such coarse agglomerates were then size reduced using a mill (End runner mill, Pascall Eng., Crawley, U.K.) and then remixed with the

particle size fraction below 500 μm. Sieve analysis by weight was carried out according to British Standards Method 1796 (1976). The sample was further reduced and continuously sampled and analysed by the above sieve method if necessary, in order to obtain a median diameter of 230 μm +/-20 μm, with an upper quartile point of 320 μm +/-20 μm and a lower quartile point of 140 μm +/-20 μm.

2.2.5 Scanning Electron Microscopy (SEM).

The powder to be analysed was thoroughly mixed in a polythene bag and a small representative sample removed. A smaller specimen of powder was removed using a spatula and placed on an aluminium planchette having a film of double-sided adhesive tape on its surface. The planchette with the powder specimen was placed in the chamber of a sputter coater (type S150B, Edwards High Vacuum, Crawley, U.K.) which was evacuated to less than 10 μm mercury pressure. The specimen was supported on an electrode below a gold film which formed a second electrode. A current of approximately 6-10 mA and voltage of 1.2kV was passed between the electrodes for 5 minutes during which time the specimen became coated with an ultra-thin film of gold, of approximately 30nm thickness.

The coated specimen planchettes were fixed to a mounting block using a colloidal silver adhesive. The block was then introduced into the column of the electron microscope through an evacuated air lock at a working distance of 39mm from the gun filament. Two microscopes were used, JEOL type 35C and T2000,

(JEOL Ltd., Tokyo, Japan).

2.2.6 Powder Conditioning.

All the co-transformed products prepared with the polymeric molecules and the binary powder mixes of transformed sucrose with either maltodextrin or Avicel PH102 were initially dried to constant weight in a hot air oven at 70°C (Baird & Tatlock Ltd., London, U.K.) and then stored prior to tablet compaction for 48 hours over a saturated solution of magnesium nitrate in an incubator (Size 2, Model 1M150, Gallenkamp Ltd., Loughborough, U.K.) at 25°C, to give a constant relative humidity (RH) of 55% +/- 3%. Other powders used in this study, where stated, were conditioned by storage for 48 hours in a RH of 55% +/- 3% at 25°C prior to tablet compaction. Samples which were not conditioned will be specifically identified in the results and discussion (Chapter 3).

2.2.7 Powder Flow Properties.

Powder flow properties of transformed sucrose, Avicel PH102 and six different mixes of these two powders have been determined (1%, 5%, 10%, 20%, 40% and 80% w/w of Avicel in transformed sucrose). Transformed sucrose used for the flow study was of the standard particle size distribution, as stated immediately above. Powder flow rate through a 0.25 inch diameter orfice was determined using an electronic recording balance (type 2200, Sartorius A.G., Switzerland), which was interfaced through the RS232 port to a small microcomputer (BBC model B, Acorn Computers

Ltd., Cambridge, U.K) and a dot matrix printer (type FX-80, Epson Ltd., U.K).

2.2.8 X-ray Diffraction Analysis.

A Philips PW1730 x-ray generator fitted with a copper target and a nickel filter was operated at 40kV and a current of 20mA. The copper radiation was detected using a xenon proportional counter (type PW1965) mounted on a diffractometer goniometer (type PW 1080) scanning between 5° - 45° corresponding to 2 θ. Pulses from the proportional counter were amplified and analysed using a Philips PW4620 ratemeter/channel analyser and plotted via a chart recorder. The Bragg angle and the degree of crystallinity were measured from the diffraction pattern.

3 RESULTS AND DISCUSSION.

3.1 Physico-mechanical Properties of Some Commercial Direct Compression Excipients.

The tensile strength of tablets was calculated according to the method of Newton and Fell (1968) and the results are illustrated in Fig. 38. Nutab tablets were found to possess the lowest tensile strength, where the increase in tensile strength with increase in compaction force was found to be lower in comparison with the other excipients studied, suggesting that there was relatively little influence of compaction force on the degree of inter-particle bonding for Nutab. Anhydrous lactose and Fast-Flo tablets were found to possess the highest tensile strength, but only slightly higher than that of Dipac tablets (Fig. 38). The results suggest that the strength of inter-particle bonding was greatest for anhydrous lactose and Fast-Flo, while a slightly lower strength of inter-particle bonding existed in Dipac tablets. Tablettose tablets were found to possess a tensile strength lower than that of Dipac. Inter-particle bonding is a function of the degree of elastic and plastic deformation undergone by the powder particles during the compression-decompression cycle of tablet production.

Schubert et al. (1975) stated that the tensile strength of materials may be identical despite the fact that the materials had different fracture strains. The deformation undergone by tablets prepared from various direct compression excipients during diametral tensile testing is shown in Fig. 39. There are 2

general types of behaviour which can be determined from the relationship shown in Fig. 39. Type 1 behaviour is found in specimens where little or no increase in tablet deformation occurs with increase in compaction force and where the "fracture strain" at the lowest compaction force (initial fracture strain), is small. Type 1 behaviour was observed with Nutab, Tablettose and Emcompress tablets. Type 2 behaviour is represented by an increase in tablet deformation with increase in compaction force and where initial tablet deformation is greater than that found in type 1 behaviour. Anhydrous lactose, Fast-Flo and Dipac were found to exhibit type 2 behaviour (Fig. 39). Avicel tablets were found to show type 2 behaviour with the greatest tablet deformation and "initial fracture strain" (Fig 41).

Rees and Rue (1978c) also observed such types of behaviour with some other excipients and because this difference was undetectable using tensile strength determinations, these workers derived a different parameter which was termed "work of failure". However, Rees and Rue did not take into account the dimensional changes which occurred after compaction and on storage. In the present study dimensional changes have been taken into consideration using a measurement called here "normalised work of failure" (NWF), calculated according to equation 29. Fig. 40 shows the relationship between NWF and compaction force for different excipients. Tablettose, Nutab and Emcompress were found to possess the lowest NWF; anhydrous lactose tablets were found to possess the largest NWF (Fig. 40), with Fast-Flo and Dipac tablets having intermediate values.

Whereas the tensile strengths of anhydrous lactose and Fast-Flo tablets were found to be very similar (Fig. 38), their NWF values were disparate (Fig. 40) exemplifying the concern expressed by Schubert et al. (1975) over the sole use of tensile strength data to characterise mechanical properties of materials.

The difference in tensile strength and NWF values results from differences in tablet deformation (Fig. 39). For example, although the increase in tablet deformation with increase in compaction force is of the same order, 2.0*E-5m for anhydrous lactose and Fast-Flo over the range of 6kN to 23kN compaction force, the initial mean tablet deformation is different. For anhydrous lactose the deformation is 8.6*E-5m while that for Fast-Flo is 7.5*E-5m. This difference is not measurable using tensile strength determinations. A much larger deformation was found for Avicel PH102 tablets (Fig. 41) than for other materials and the increase in deformation was found to be higher than for any of the other direct compression excipients studied.

According to Griffith (1920), the stress at a crack tip is given by equation 16. Using this relationship, the maximum stress at the crack tip is found to be inversely proportional to the radius of curvature at the crack tip. During a diametral test, one of the factors which influences the rate of crack propagation is the stress at the crack tip, if a material undergoes plastic deformation on application of load, the radius of curvature at the crack tip will increase (see Fig. 18), so that the stress will be distributed over a larger surface area and the rate of crack propagation will be slow (Orowan, 1955;

Irwin, 1960). This is thought to occur with Avicel PH102 tablets, which exhibit large tablet deformation (Fig. 41) and also for anhydrous lactose tablets which have been found to possess the next highest tablet deformation to Avicel PH102 in the group of excipients studied (Fig. 39). Avicel PH102 powder was found to exhibit poor flow which prevented reproducible volumetric filling under test conditions and consequently, the powder was compressed by manually turning the fly-wheel smoothly and reproducibly. Fig. 42 shows the influence of compaction force on the NWF values of Avicel tablets. Avicel PH102 tablets were found to possess the largest NWF values at any given compaction compared with the other excipients studied.

High NWF values are generally associated with powders in which plastic deformation is most prominent during compaction (Rees and Rue, 1978c). Avicel PH102 powder has been shown by Sixsmith (1982) to undergo extensive plastic flow during compaction.

An electron-micrograph (Fig. 100A, see Appendix I) of a fractured surface of Avicel PH102 (6kN compaction force) shows evidence of extensive plastic flow. Low NWF values are associated with powders in which particle fragmentation is more prominent than plastic flow during compaction. Emcompress tablets were found to possess low NWF values and supportive evidence of fragmentation taking place is shown in the electron-micrograph (Fig. 100B, see Appendix I) of a fractured surface of an Emcompress tablet compressed at 8kN compaction force. The NWF values for Avicel PH102 (Fig. 42) suggest that it is a much more

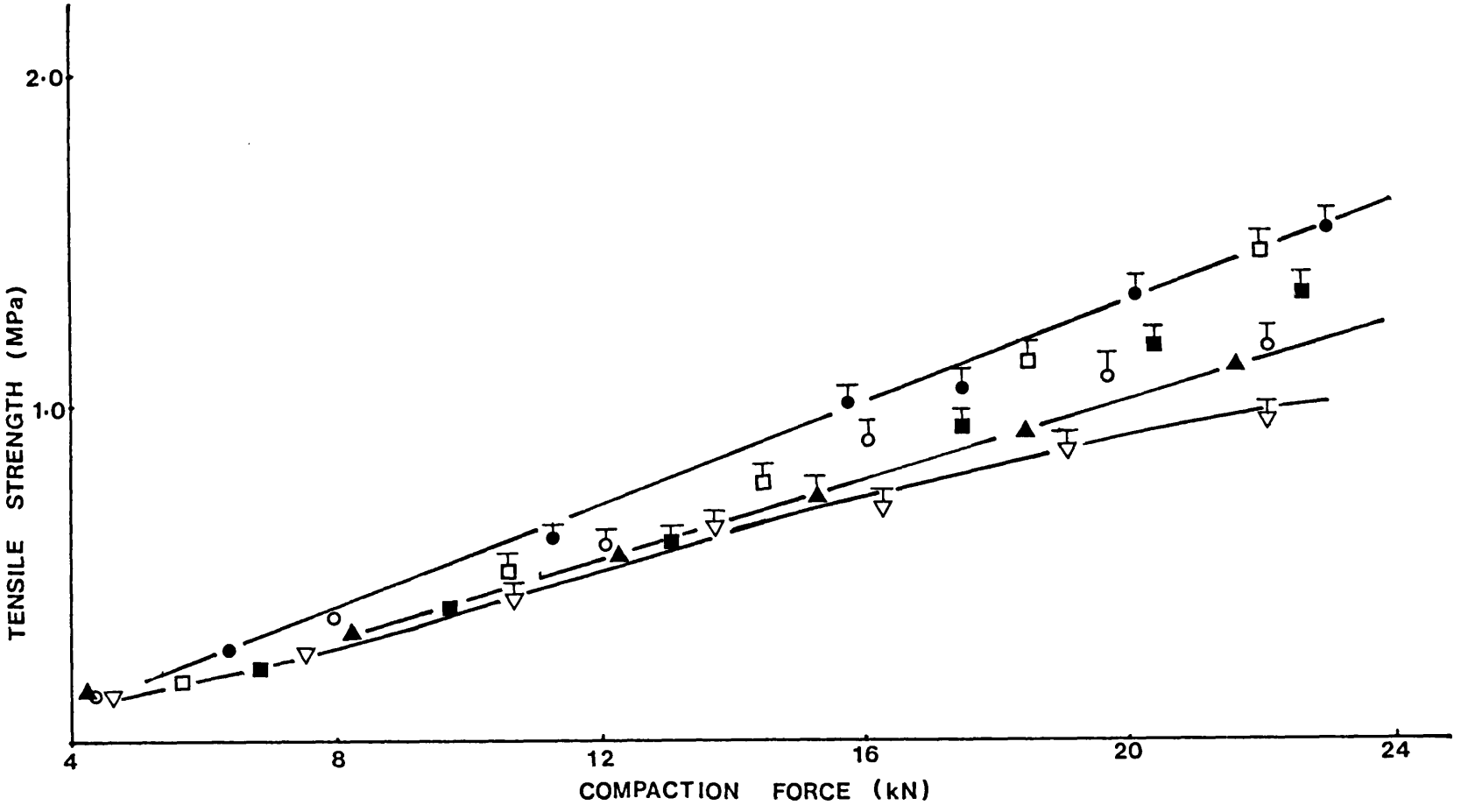

Figure 38. Relationship between tablet tensile strength and compaction force for some direct compression excipients: (●) Anhydrous lactose, (□) Fast-Flo, (■) Dipac, (▲) Emcompress, (o) Tablettose, (▽) Nutab. Tensile strength values plotted are the means of ten determinations and the corresponding confidence interval at 95%.

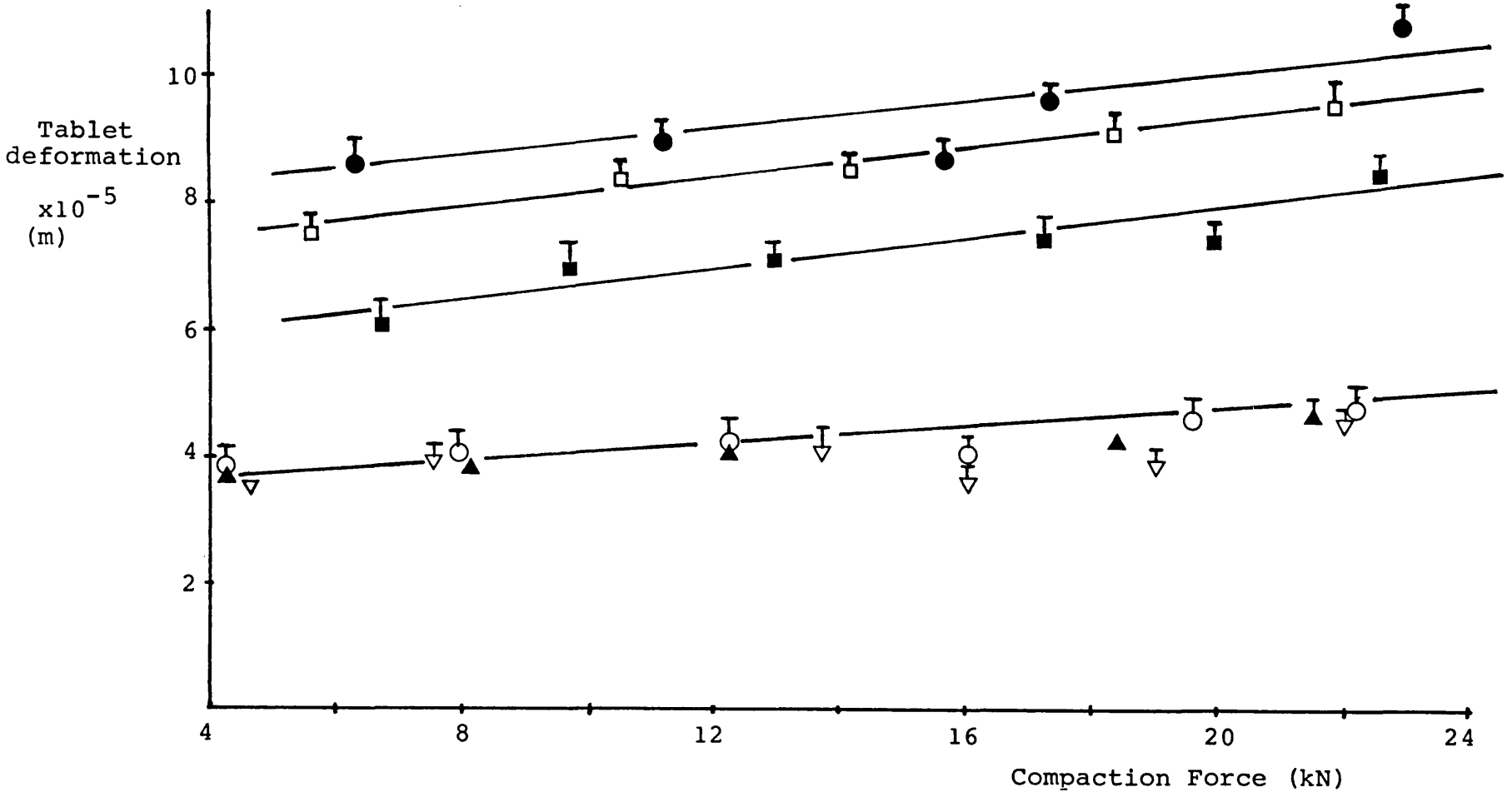

Figure 39. Relationship between tablet deformation during diametral testing and compaction force for some direct compression excipients: (●) Anhydrous lactose, (□) Fast-Flo, (■) Dipac, (▲) Emcompress, (○) Tablettose, (▽) Nutab.

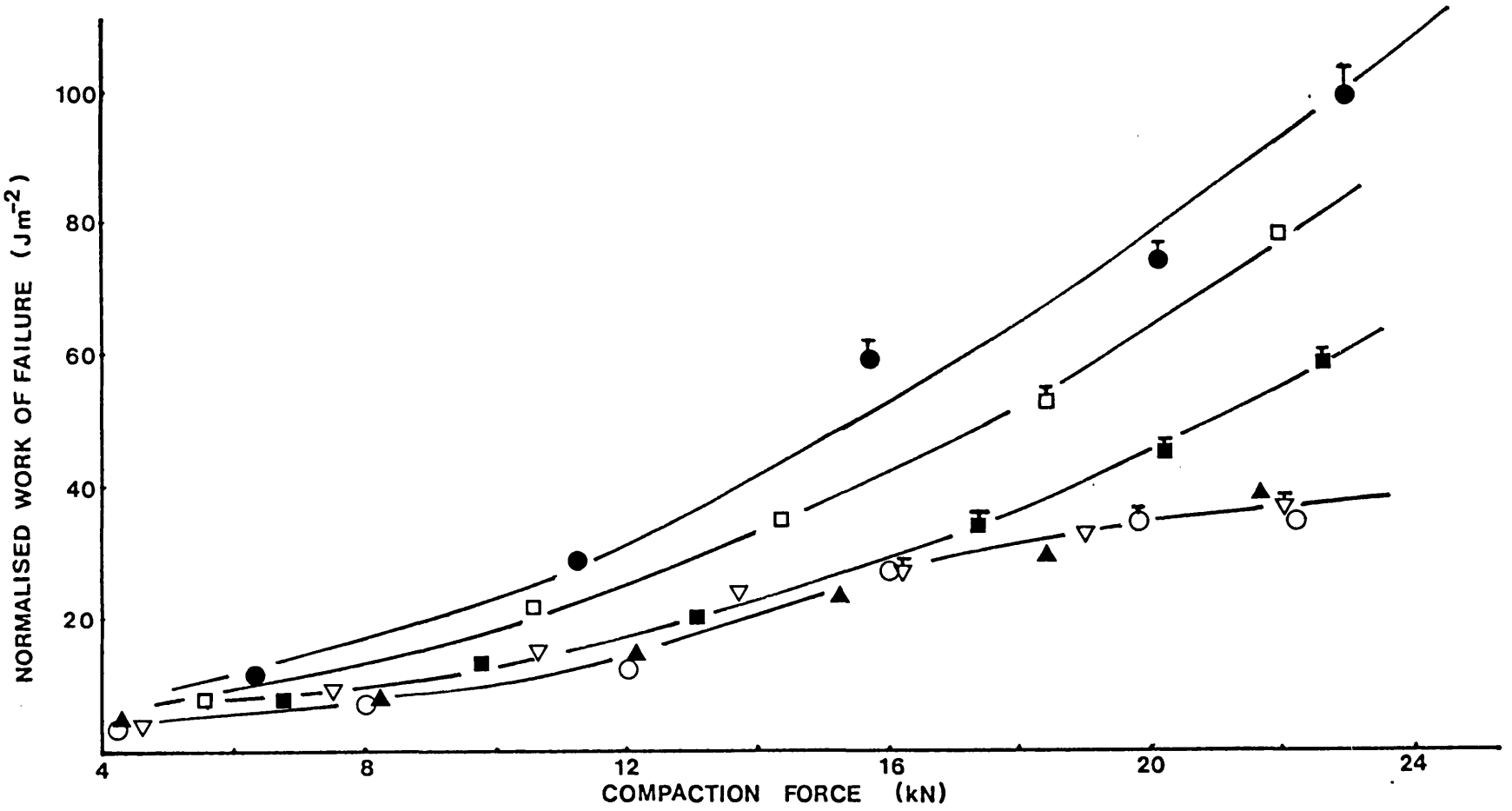

Figure 40. Relationship between normalised work of failure and compaction force for some direct compression excipients: (●) Anhydrous lactose, (□) Fast-Flo, (■) Dipac, (▲) Emcompress, (○) Tablettose, (▽) Nutab

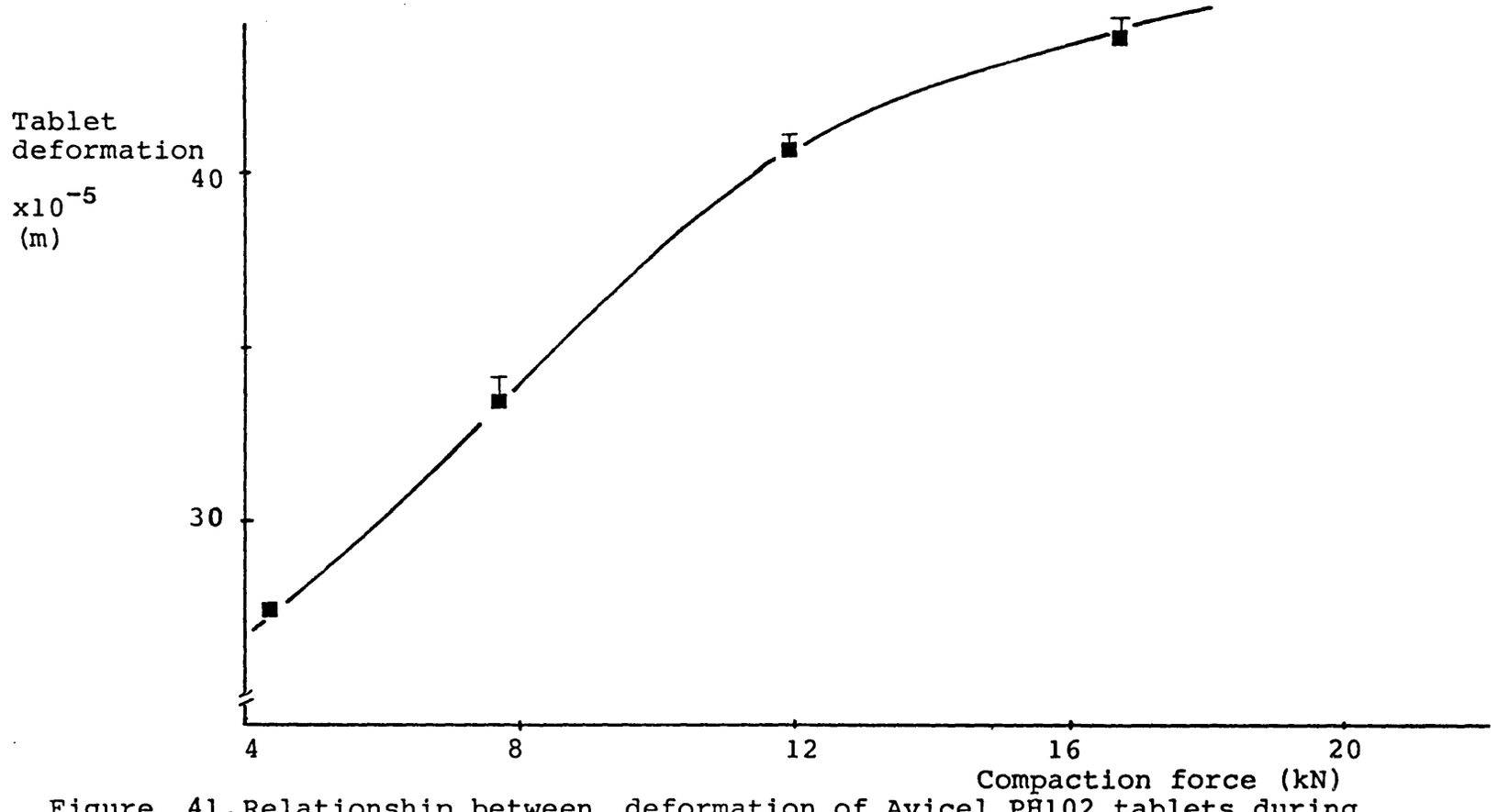

Figure 41. Relationship between deformation of Avicel PH102 tablets during diametral testing and compaction force.

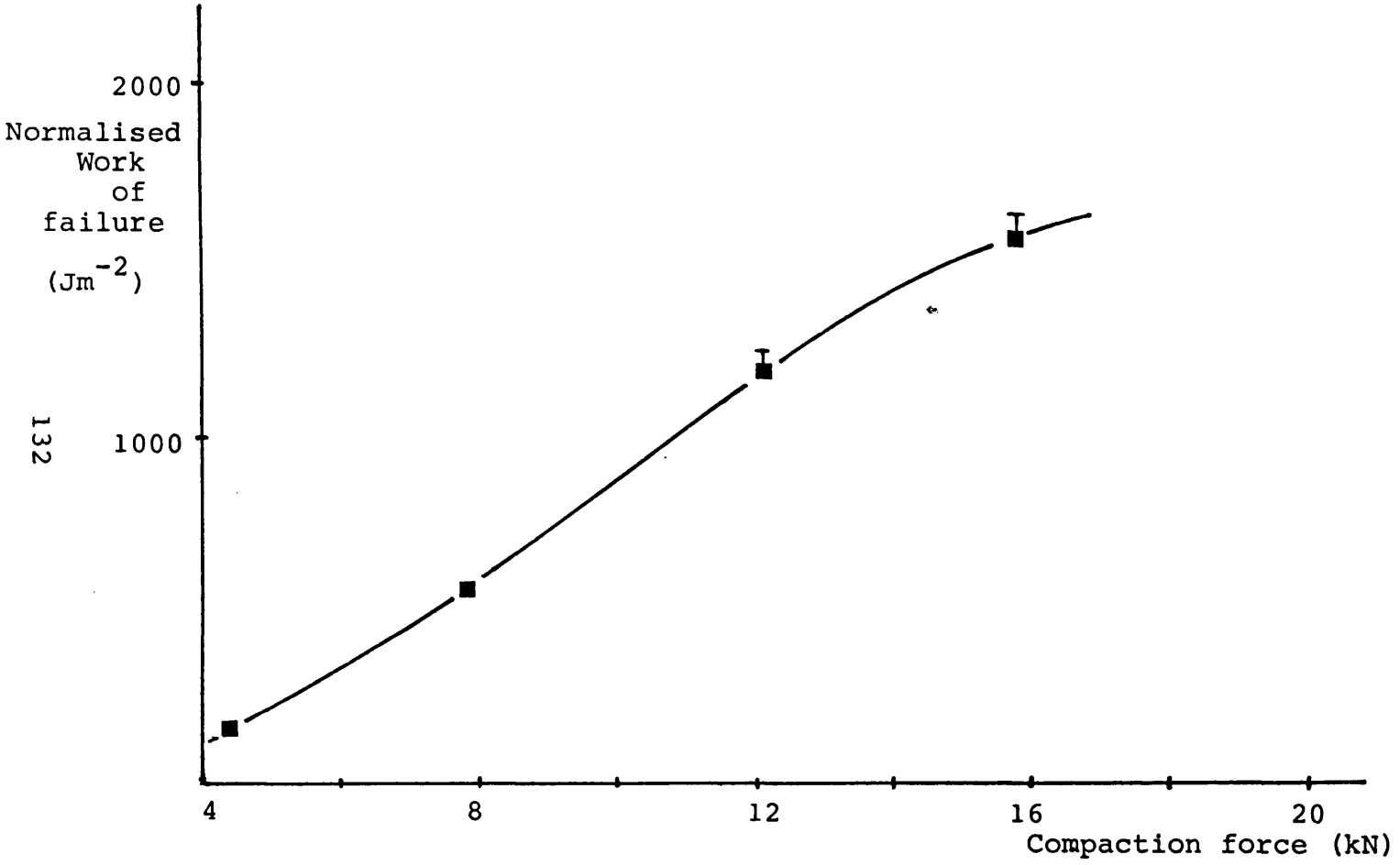

Figure 42. Relationship between normalised work of failure and compaction force for Avicel PH102 tablets.

plastic excipient than the other excipients studied. In relative terms, anhydrous lactose shows greater plasticity than the other excipients in Fig. 40.

Evidence supporting a correlation between plasticity of a powder during compaction and work of failure has been illustrated in a study carried out by Seager et al. (1980), who found that the addition of a plastic binder to a formulation using a spray-drying technique resulted in an increase in the work of failure values of the compressed tablets.

The relationship between NWF and compaction force was found to be useful in assessing the degree of particle deformation taking place during compaction. A parameter such as NWF can be measured more accurately than parameters measured during powder compaction due to greater instrument precision and more easily controllable experimental conditions. The chemical composition of the powders in a tablet will influence the rate of crack propagation, but the NWF parameter does not take into account the time elapsed during the tensile test.

Using the internal clock of the microcomputer, the time elapsed during a diametral tablet test was measured. Fig. 43 illustrates the relationship between time elapsed and compaction force used to prepare tablets from different direct compression excipients. Anhydrous lactose, Fast-Flo and Dipac showed an increase in time elapsed with increase in compaction force while time elapsed remained nearly constant for Emcompress, Nutab and Tablettose. Such behaviour could be predicted by studying the tablet deformation plots (Fig. 39), since the rate of platen

movement is constant in this study (2mm/minute).

A new parameter was postulated to account for the differences in elapsed time. This parameter was termed "Power of Failure" (units of J/s) and was calculated by dividing work of failure by the elapsed time, so as to provide a measure of the power expended in causing tensile failure of tablets. It was considered that such a parameter could be more sensitive to minor changes in plasticity of powders than NWF measurements.

The relationship between power of failure and compaction force for some direct compression excipients is illustrated in Fig. 44. The power of failure values show a distinct lack of sensitivity to powder plasticity especially for anhydrous lactose, Fast-Flo and Dipac, differences which were apparent in NWF-compaction force profile (Fig. 40). Hence the hypothesis that power of failure might be sensitive to minor changes in powder plasticity was found to be invalid for the direct compression excipients studied. The deformation which a tablet undergoes during a diametral test gives an indirect indication of the time taken for a tablet to fail, since the rate of strain the tablet is subjected to is constant. For example, anhydrous lactose tablet compressed at a compaction force 23kN undergoes approximately 10.35*E-5m deformation before failure, which indicates that failure will occur after approximately 3.1 seconds. Consequently, dividing WF, which takes into account tablet deformation, by the time elapsed during a diametral tablet test would obviously lead to a reduction in sensitivity. However, the introduction of a time component into the work term

may prove useful industrially as a means of rationalising tablet strength standards for quality assurance purposes between production facilities where test equipment is non-standard. Under such circumstances, tensile strength or NWF values differ due to tablets being subjected to different rates of strain in different equipment. A tablet subjected to a high strain rate may attain only a small NWF at failure whereas an identical tablet strained at slower rate would have a higher NWF. When the time to failure is considered, however, the first tablet's low NWF will be increased whereas the second tablet's NWF will be decreased - the two tablets could therefore have similar power of failure values, thus providing a standard test for different equipment.

Another parameter was derived in the present study by treating tablets as non-Newtonian plastic solids. "Failure Viscosity" (FV), with units of stress per strain rate (Pas). FV was calculated by dividing the tensile strength of the tablets by the tablet strain rate, where the deformation undergone by a tablet during the diametral tensile test, was divided by the tablet diameter to represent strain. This was further divided by the time elapsed during the diametral test to cause tensile failure of the tablet to give the tablet strain rate. The relationship between FV and compaction force for some direct compression excipients is shown in Fig. 45 and gave a similar classification of the excipients as the NWF-compaction force profile (Fig. 40). Nutab tablets were found to possess the lowest FV value, while anhydrous lactose tablets possessed the highest FV value. Failure viscosity is a measure of the

resistance to deformation offered by the tablet when subjected to diametral loading. The FV value will be large when the resistance to flow is high - a situation which arises as a result of formation of a large number of high strength inter-particle bonds. These conditions predominate when plastic deformation of the particles take place during compaction, thus the results suggest that other than Avicel PH102, anhydrous lactose possesses higher plasticity than any of the other direct compression excipients studied (Fig. 45). Both FV and NWF determinations were found to be useful parameters for predicting the plasticity of excipients. However, in order to examine the influence of polymeric additives on the plasticity of a sucrose excipient in later work, it was considered desirable to examine the sensitivity of alternative methods for characterisation of powder plasticity using conventional direct compression excipients.

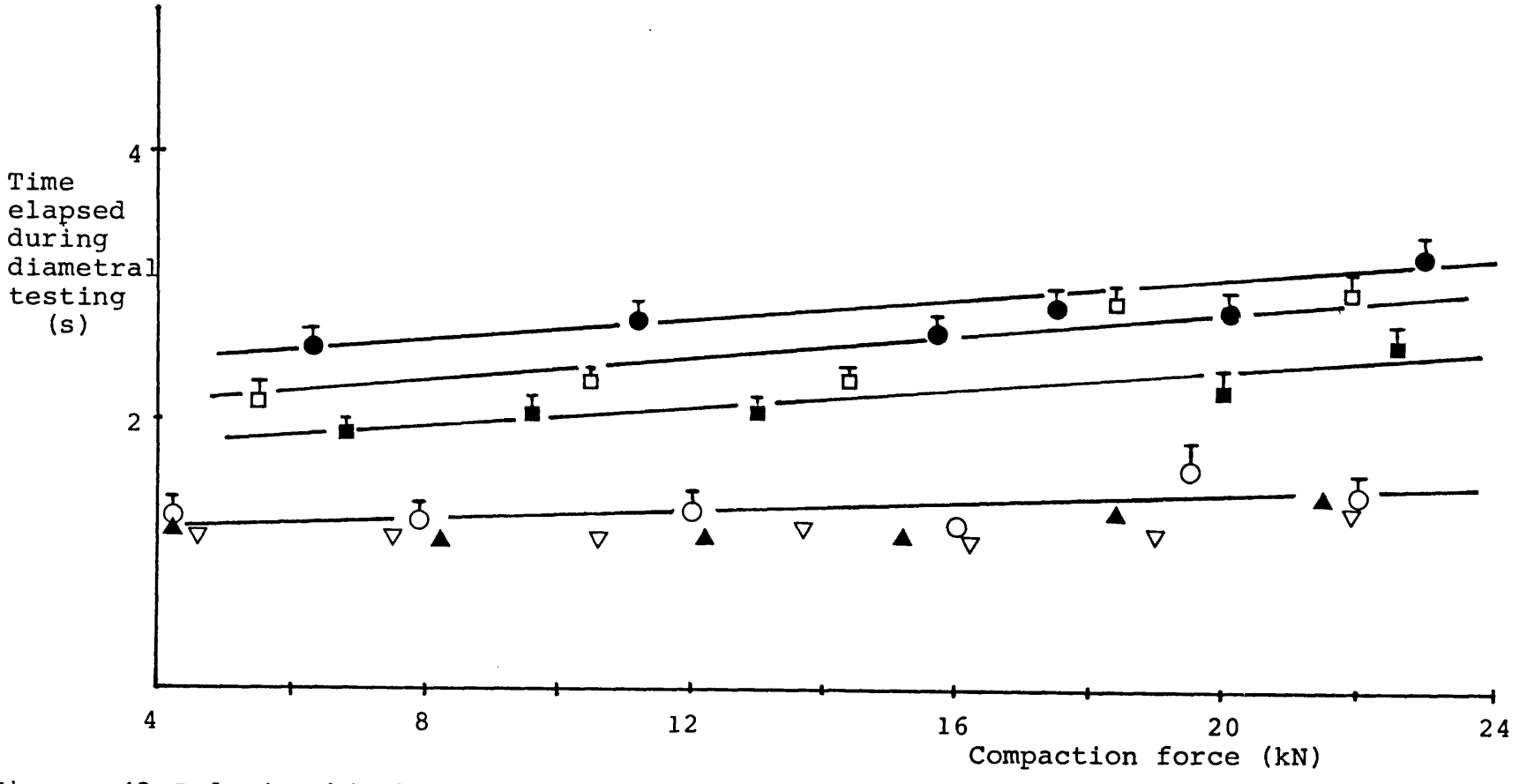

Figure 43. Relationship between the time elapsed during diametral testing of tablets and compaction force for some direct compression excipients: (●) Anhydrous lactose, (□) Fast-Flo, (■) Dipac, (▲) Emcompress, (o) Tablettose, (▽) Nutab.

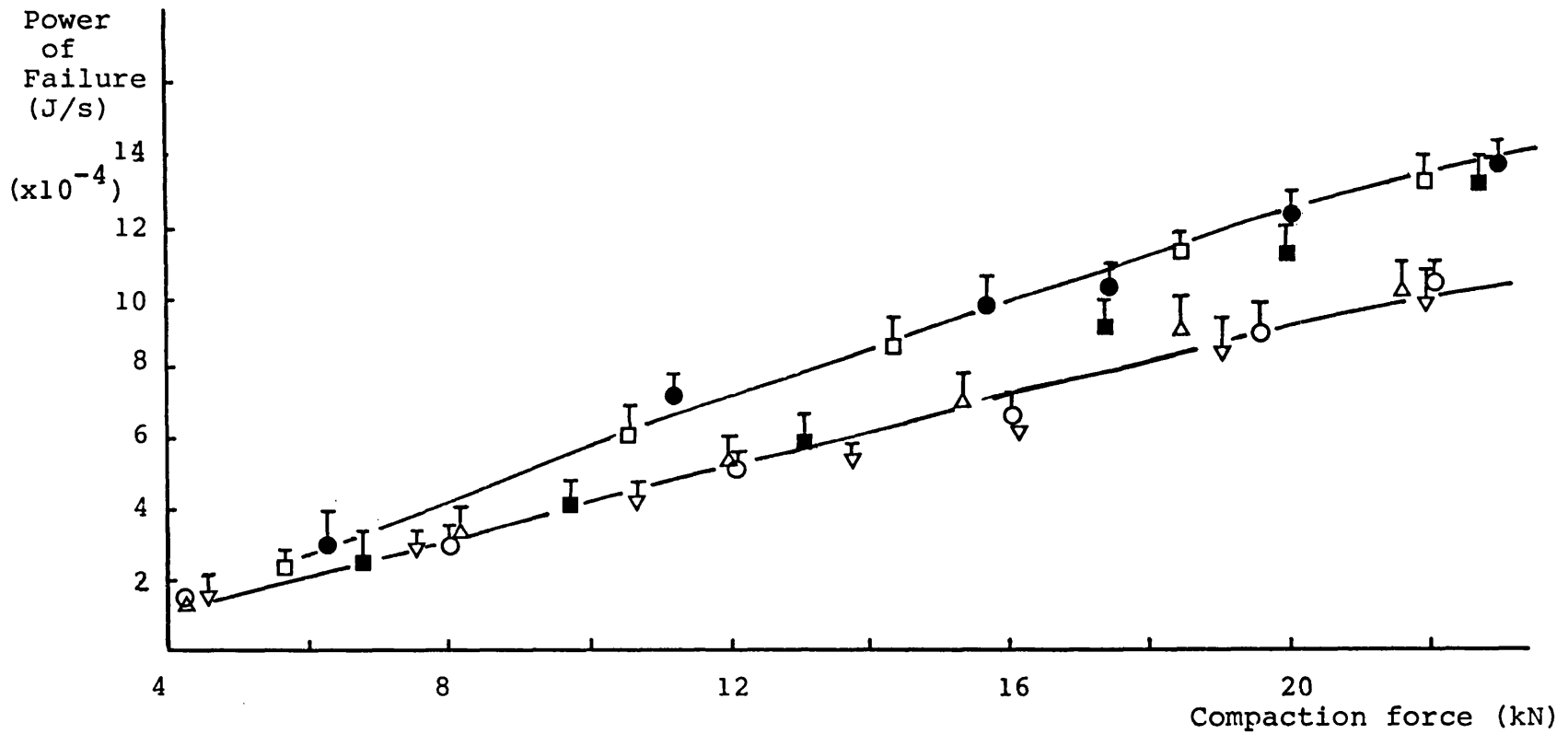

Figure 44. Relationship between the power of failure of tablets and compaction force for some direct compression excipients: (●) anhydrous lactose, (□) Fast-Flo, (■) Dipac, (△) Emcompress, (○) Tablettose and (▽) Nutab.

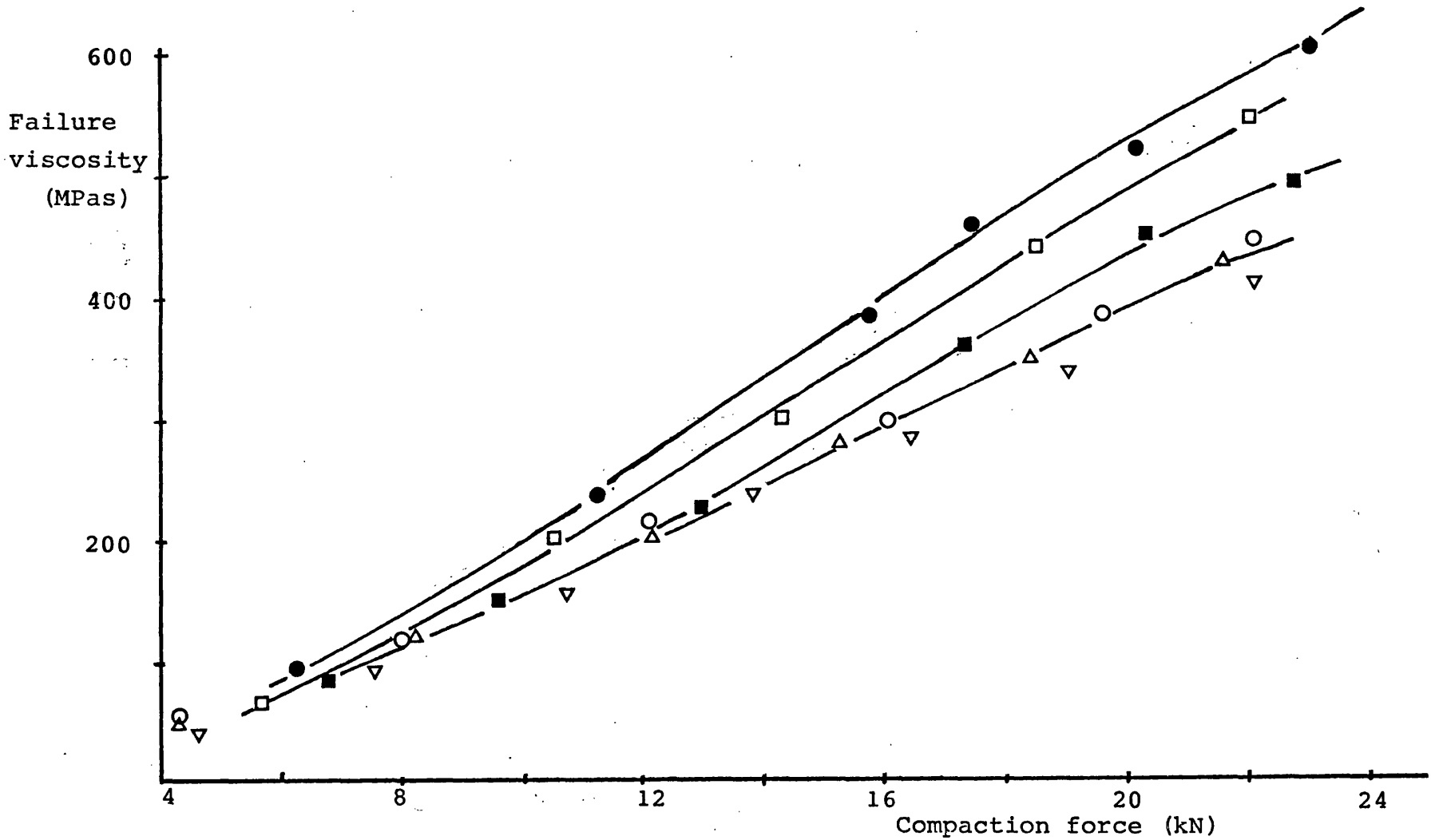

Figure 45. Relationship between failure viscosity and compaction force for some commercial direct compression excipients. Anhydrous lactose (●), Fast-Flo (□), Dipac (■), Tablettose (O), Emcompress (△) and Nutab (▽).

3.1.1 Fatigue Strength Determinations of Tablets.

The relationship between the number of cycles required for fatigue failure with increasing compaction force for some direct compression excipients is shown in Figs. 46 and 47. For Avicel PH102, Microtal and Dipac tablets, the number of cycles required for fatigue failure was found to increase with increase in compaction force (Fig. 46). This is the result of an obvious relationship: increase in compaction force results in an increase in the areas of intimate inter-particle contact, thus increasing the degree of inter-particle bonding and consequently the tablet possesses greater resistance to mechanical damage. Avicel PH102 tablets required the highest number of cycles for fatigue failure at any given compaction force (Fig. 46). No data for Avicel tablets compressed above 16kN compaction force was obtained, since these tablets were found not to undergo fatigue failure, even after 60,000 cycles (approximately 3 days). Fig. 47 shows that there was no influence of compaction force on the number of cycles required for fatigue failure for either Emcompress or Tablettose tablets. This behaviour was unexpected since the NWF value was previously found to increase with increase in compaction force for these tablets (Fig. 40), suggesting that the degree of inter-particle bonding increased with compaction force.

The different trends observed in Figs. 46 and 47 are a result of differences in the fatigue crack propagation (FCP) rates, since all variables, except those of a physico-chemical nature (material variables) of the powder in the Paris equation

(Equation 21) were maintained constant.

Irwin (1960) stated that the stress field at a crack tip increases rapidly as the radius of curvature at the crack tip decreases and the rate of crack propagation is rapid but, if plastic deformation were to take place in the crack tip zone, crack tip blunting would occur. It is thought that during fatiguing of Avicel tablets, these tablets undergo some degree of plastic deformation at the crack tip zone, consequently increasing the radius of curvature at the crack tip. According to Griffith (1920) and Irwin (1960), this would result in a reduction in the maximum stress at the crack tip and crack propagation would thus be retarded. Results for Microtal and Dipac tablets (Fig. 46) showed a similar trend to that of Avicel tablets, but were found to undergo fatigue failure at a lower number of cycles than Avicel, suggesting that the rate of FCP was much more rapid in Microtal and Dipac tablets and this is thought to be due to the lower degree of plastic deformation at the crack tip. This suggestion is supported by the fact that Avicel PH102 tablets (Fig. 41) underwent much larger deformation during the diametral test than Dipac (Fig. 39), indicating that Avicel is much more plastic than Dipac.

Ganderton and Shotton (1961) have cited two types of failure of tablets during a diametral test:

(i) Where the inter-particle bond is strong, fracture will take place across the particles, for example hexamine.

(ii) Where the inter-particle bond is weak, fracture will take place at points of contact between the particles, for example

aspirin.

For powders which can deform plastically on compaction, such as Avicel (Sixsmith, 1982), the inter-particle bonding will be extensive and strong, thus FCP in the tablet will be most likely to occur across the microcrystalline cellulose (mcc) particles rather than between the inter-particle points of contact (Ganderton and Shotton, 1961). However, mcc particles will undergo plastic deformation at the crack tip on loading, resulting in a reduction in the stress at the crack tip (Irwin, 1960) and consequently, a reduction in FCP rate.

A probable explanation for the observed trend in Fig. 47, is that once the fatigue crack is initiated, its subsequent propagation may be extremely rapid since there may not exist mechanisms to reduce the radius of curvature at the crack tip. The deformation undergone during the diametral test by Emcompress and Tablettose was found to be very small (Fig. 39), thus supporting the suggestion that very little plastic deformation is likely to take place at the crack tip. Consequently, the maximum stress at the crack tip will be large and the crack propagation will be rapid. Compaction force was found to have no influence on the number of cycles required for fatigue failure of Emcompress and Tablettose tablets. Between 8 and 16kN compaction force, the number of cycles required to cause fatigue failure of Dipac and Microtal tablets (Fig. 46) was lower than either Emcompress or Tablettose (Fig. 47), despite the fact that both Microtal and Dipac tablets apparently have a higher degree of inter-particle bonding (c.f. Figs. 40 and 81, in section 3.2.2.1). One possible

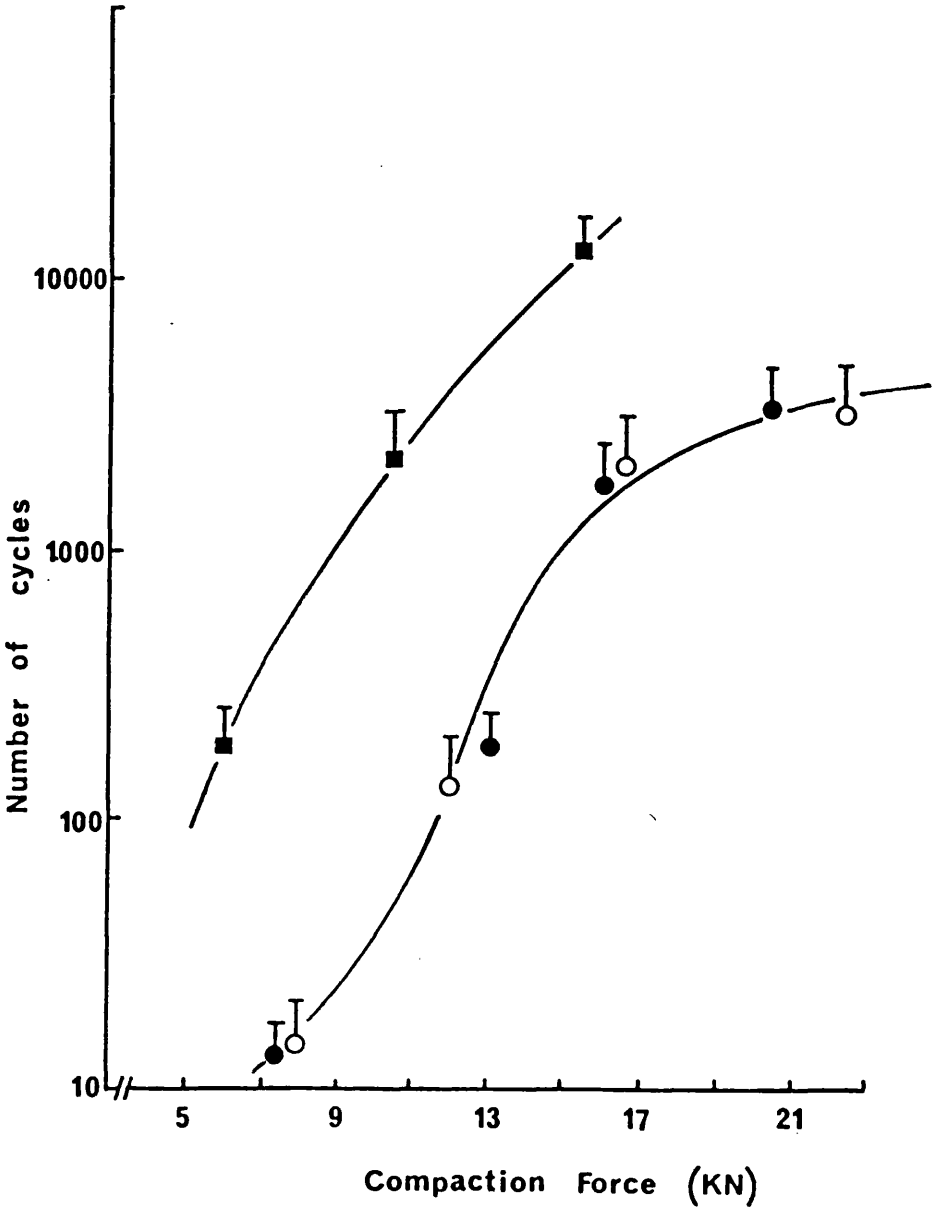

Figure 46. Influence of compaction force on the number of cycles required for fatigue failure of (■) Avicel PH102, (●) Microtal, (O) Dipac tablets. The points plotted are the mean of a minimum of five determinations and corresponding standard deviations.

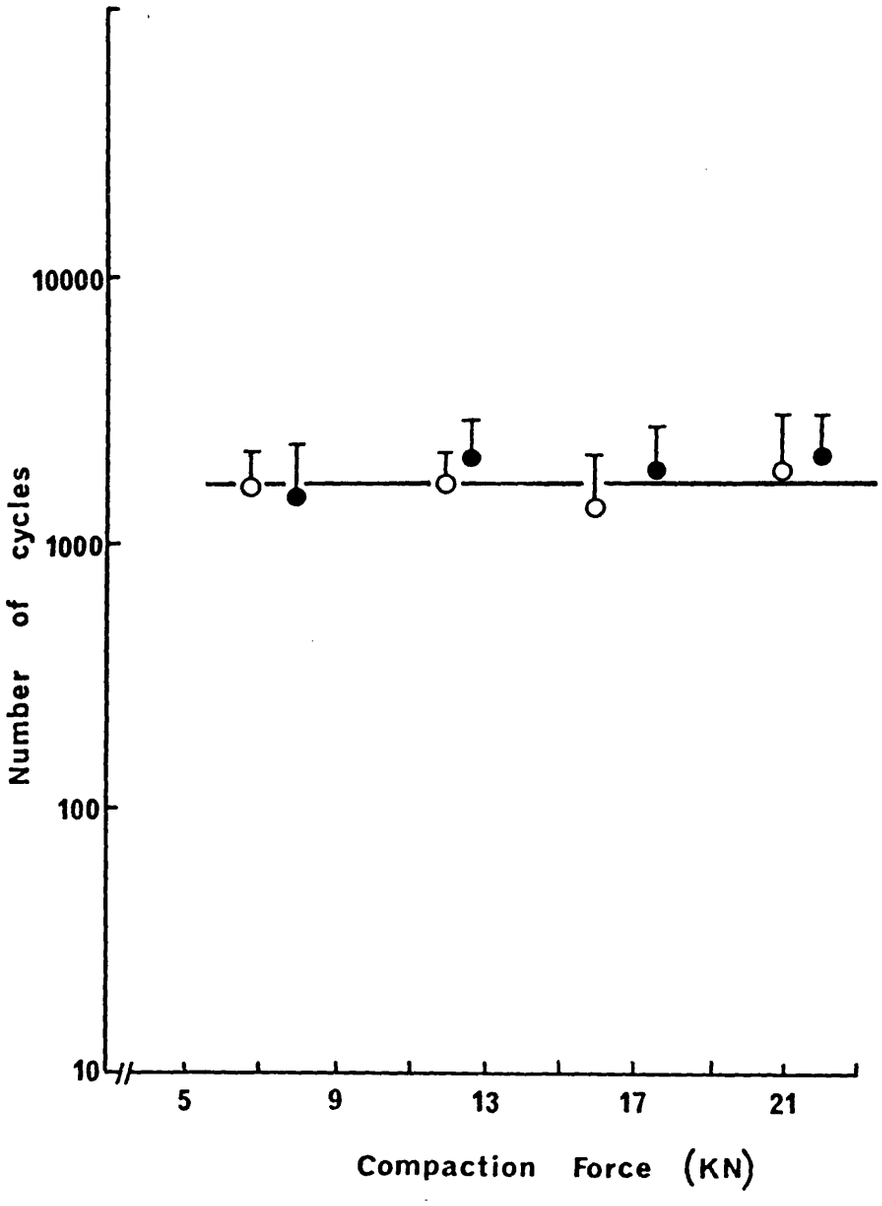

Figure 47. Influence of compaction force on the number of cycles required for fatigue failure of (●) Emcompress, (O) Tablettose tablets.

reason for this observation is that the crack initiation in Emcompress and Tablettose tablets is the FCP rate-determining step and after initiation the FCP rate will be rapid, as explained above. In the case of Microtal and Dipac tablets it is thought that the FCP rate-determining steps are most likely to be the radius of curvature of the crack tip and the degree of inter-particle bonding. This will also be true for Avicel tablets.

Above 16kN compaction force, all tablets, except Avicel, undergo fatigue failure after a similar number of cycles (Figs. 46, 47), despite the fact that Microtal has higher NWF than Dipac which in turn has higher values than Emcompress or Tablettose tablets (Figs. 40 and 81). The fatigue results of Microtal and Dipac tablets showed similar profiles. It can be concluded that fatigue testing can differentiate between brittle and ductile fracture, for example Emcompress and Microtal and even between coarse differences in the degree of plasticity, for example Avicel and Microtal. But small differences in the plasticity cannot be elucidated, for example, Microtal and Dipac.

3.1.1.1 Acoustic Emission During Fatigue Testing of Tablets.

Acoustic emission (AE) monitoring provides a means of following the damage in a component, especially crack propagation (Engle and Dunegan, 1969). The formation of a crack and its subsequent propagation are associated with release of elastic energy, which can be detected by placing a sensitive piezo-electric acoustic sensor on the surface of the component.

Fig. 48a and 49a show the AE data acquired during the fatigue test of a Microtal tablet compressed at 8 and 12kN compaction force respectively. Not surprisingly, AE for a 12kN Microtal tablet was found to be much greater than that for an 8kN tablet, since the degree of inter-particle bonding would be greater at 12kN than at 8kN. This is clearly shown on the histogram of the number of events versus channel number (Figs. 48b and 49b). The channel number represents a classification of the AE based on its energy level, the higher the energy level of the AE, the higher will be the channel number in which the acoustic event is recorded. Between channels 0 and 10, a 12kN Microtal tablet showed greater AE than an 8kN tablet, indicating that the fracture (debonding) in a 12kN tablet occurred with larger release of elastic energy. In both cases (Figs. 48a and 49a) after the point of loading (L), which caused a burst of AE suggesting some fracture had taken place, there was a gradual increase in the AE up to the point of fatigue failure (X).

The AE of a Microtal tablet compressed at 20kN (Fig. 50a) was found to show a similar profile to that observed in Figs. 48a and 49a. Due to the time scale it would seem that the AE was instantaneous from the point of loading, but it is most likely to increase gradually up to the point of failure. The profile of the energy levels of the AE (Fig. 50b) showed that the greatest number of events occurred between channels 0 to 10, with no higher energy levels associated with a 20kN tablet. This profile was similar for a Microtal tablet compressed at a compaction force of 12kN (Fig. 49b) despite the fact that the

number of cycles required for fatigue failure is much higher for a Microtal tablet compressed at 20kN compaction force.

The AE data for Avicel PH102 compressed at 6kN is shown in Fig. 51a. Again, at the point of loading, L, there was a burst of AE followed by a gradual increase until the point of fatigue failure of the tablet (X, Fig. 51a). The profile was similar to that observed for Microtal tablets, suggesting the FCP was gradual up to the point of fatigue failure. Fig. 51b shows the distribution of the energy levels of the AE from an Avicel tablet compressed at 6kN compaction force. One would anticipate during fracture of an Avicel tablet, that AE would be large since the inter-particle bonding is extensive and strong, but Fig. 51b shows a similar energy profile to that for a Microtal tablet (Fig. 48b).

Fig. 52a shows the AE data for an Emcompress tablet compressed at a compaction force of 12kN. After the point of loading (L), there was an increase in AE accompanied by sudden bursts of AE, which were observed to increase until the point of fatigue failure (X). Fig. 53a shows the cumulative number of AE with time for an Emcompress tablet compressed at a compaction force of 20kN and the profile shows that the step-wise increase in AE is similar to that observed for a 12kN Emcompress tablet (Fig. 52a). These profiles are different from those obtained for Avicel and Microtal tablets. The sudden bursts of AE in Emcompress tablets suggest that once a crack was initiated the FCP was rapid. This supports the hypothesis postulated earlier, that due to absence of mechanisms which would cause blunting of

the crack tip, stress at the crack tip would be large. However, these bursts were short-lived, indicating that the path of the crack was short (Figs. 52a and 53a). During compaction of Emcompress powder, the principle consolidation mechanism is by brittle fragmentaion. This view is supported by the fact that the NWF values of Emcompress tablets were low (Fig. 40) and Fig. 100B, see Appendix I, shows the large number of fines and fractured particles. Consolidation by brittle fragmentation will increase the number of smaller particles (Armstrong and Haines-Nutt, 1970) thereby decreasing the number of voids in a tablet. It is thought that the FCP in Emcompress tablets will be arrested when the crack intercepts a void. The void effectively increases the radius of curvature of the crack tip, temporarily arresting crack propagation. This explains the short-lived AE burts and the high number of cycles required to cause fatigue failure for Emcompress.

It was considered unsurprising that Emcompress tablets compressed at 20kN showed a higher AE than at 12kN compaction force, but it was surprising to observe that there was no apparent influence of compaction force on the number of cycles required for fatigue failure. These results indicated that after the initiation of a crack in Emcompress tablets, at the loading levels used in the present study, its rate was not influenced by the degree of inter-particle bonding whereas in Microtal and Avicel tablets, the FCP rates were influenced by inter-particle bonding. The profiles obtained for Microtal, Avicel and Emcompress tablets indicated that cumulative AE increased with

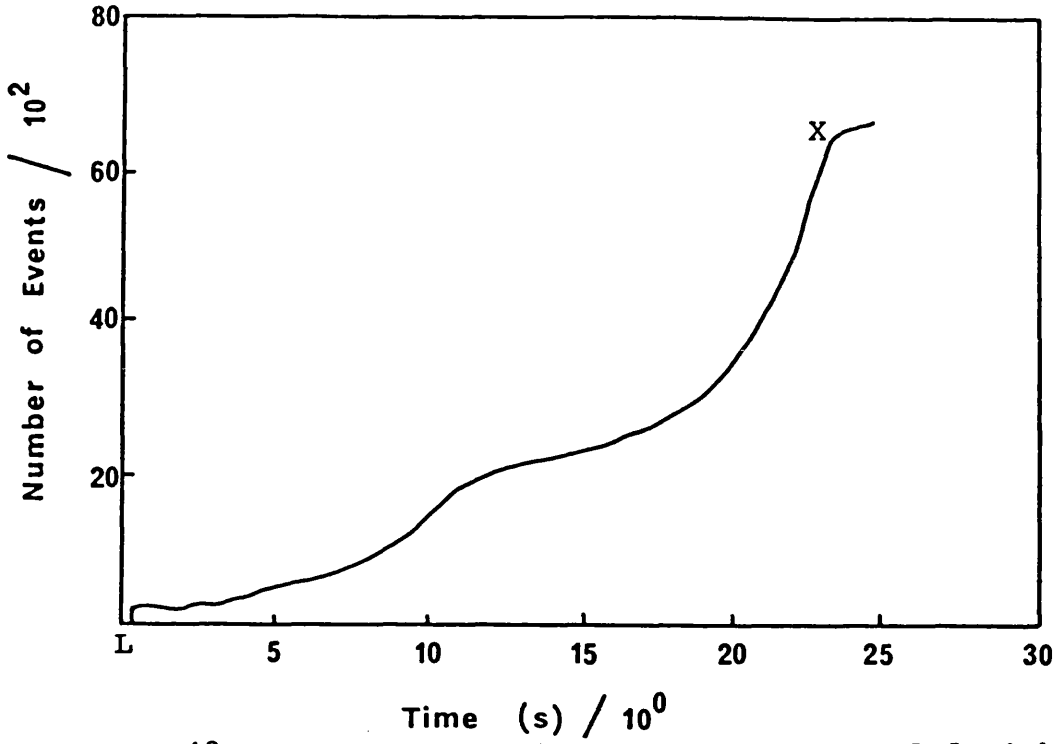

Figure 48a. Cumulative number of events recorded with time during fatigue testing a Microtal tablet compressed at a compaction force of 8kN. "L" is the point of loading and "X" is the point of fatigue failure.

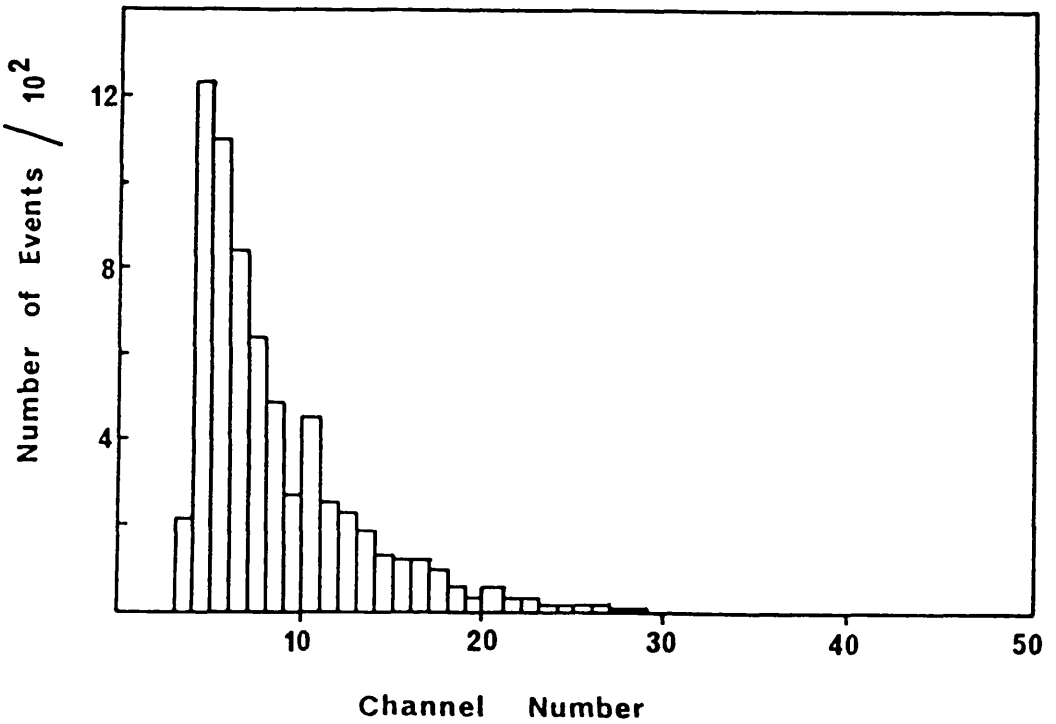

Figure 48b. The distribution of energy levels of the acoustic emission during fatigue testing of a Microtal tablet compressed at a compaction force of 8kN.

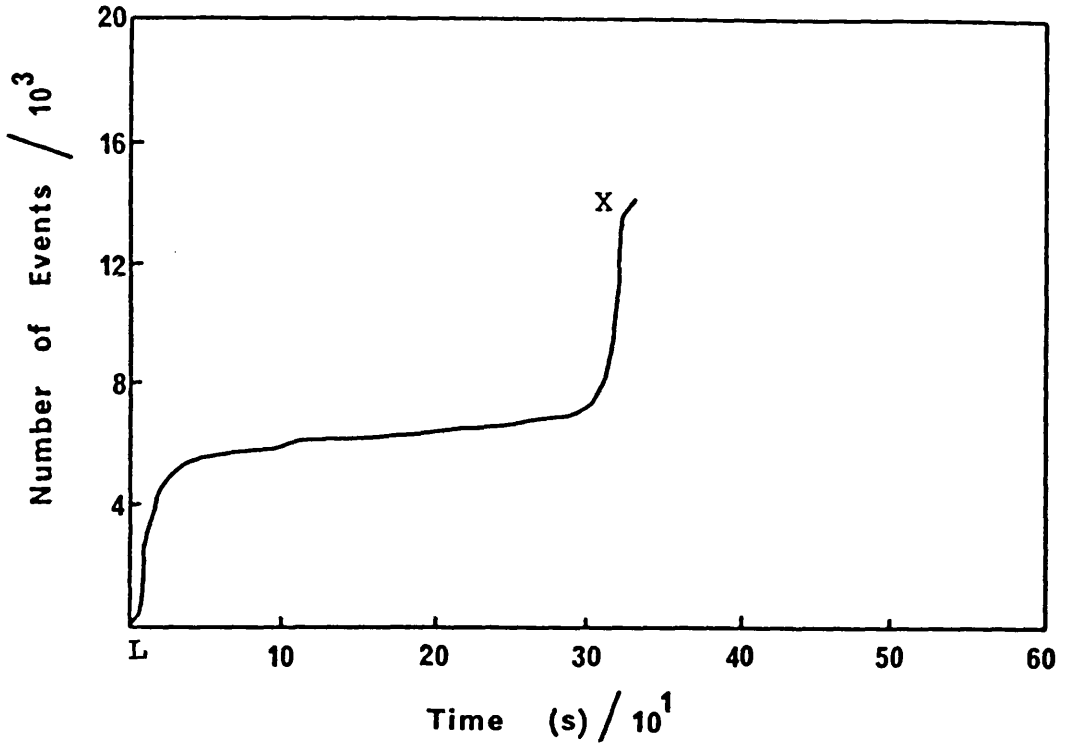

Figure 49a. Cumulative number of acoustic events recorded with time during fatigue testing of a Microtal tablet compressed at a compaction force of 12kN. "L" is the point of loading and "X" is the point of fatigue failure.

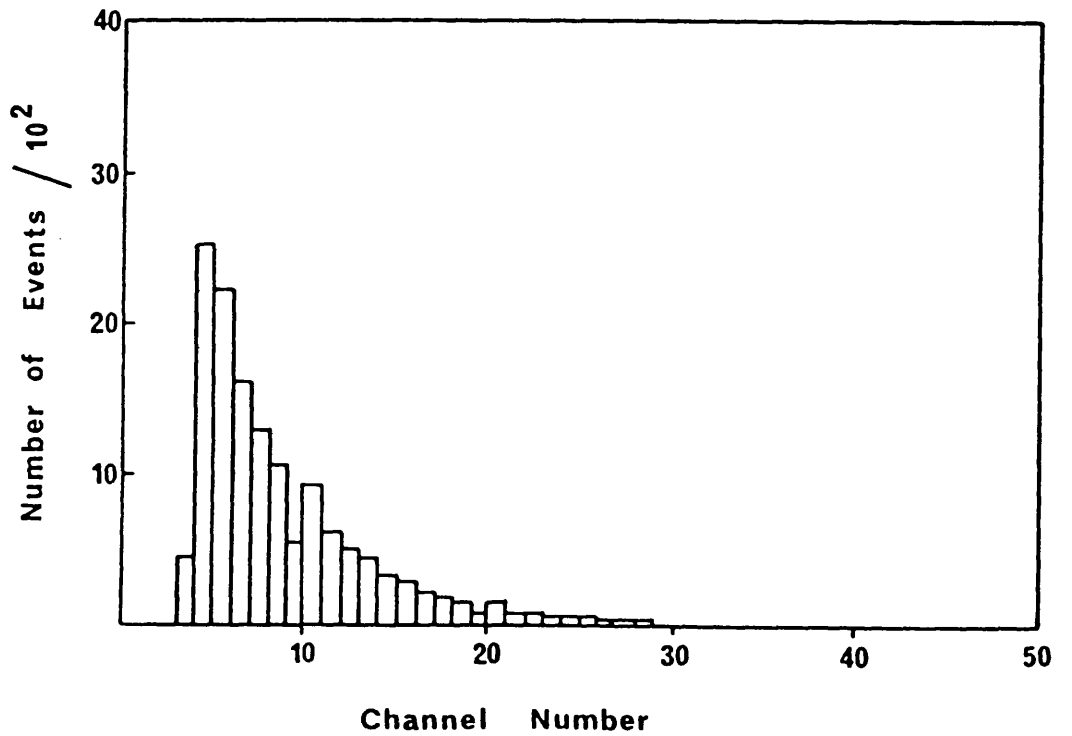

Figure 49b. The distribution of energy levels of the acoustic emission during fatigue testing of a Microtal tablet compressed at a compaction force of 12kN.

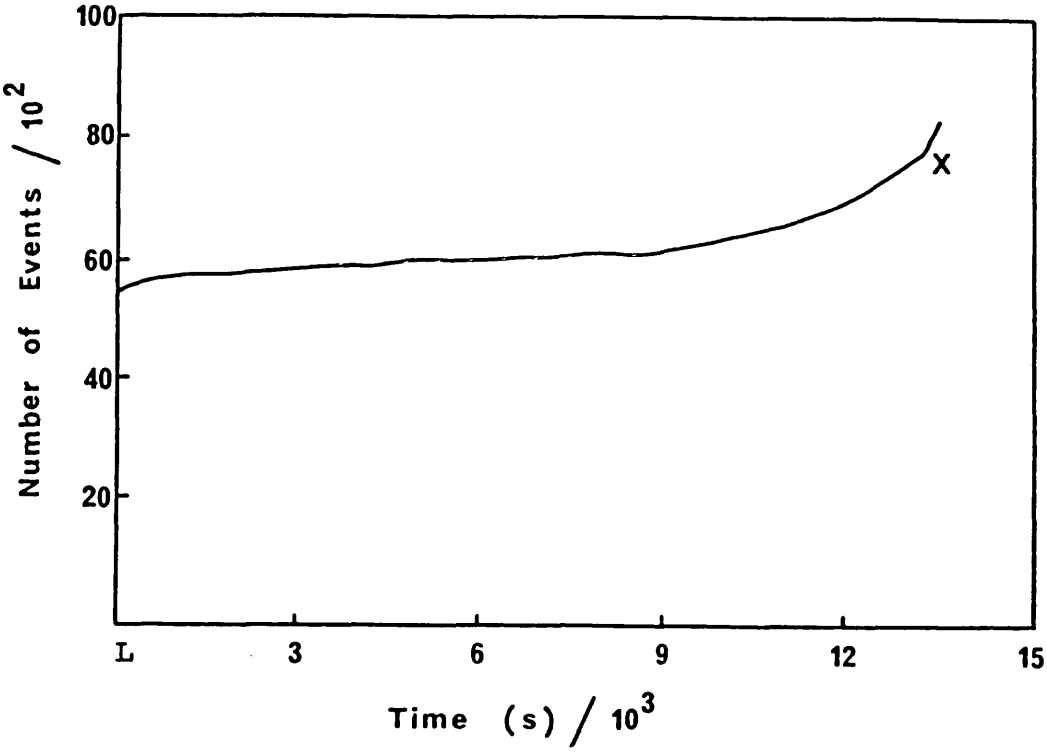

Figure 50a. Cumulative number of acoustic events recorded with time during fatigue testing of a Microtal tablet compressed at a compaction force of 20kN. "L" is the point of loading and "X" is the point of fatigue failure.

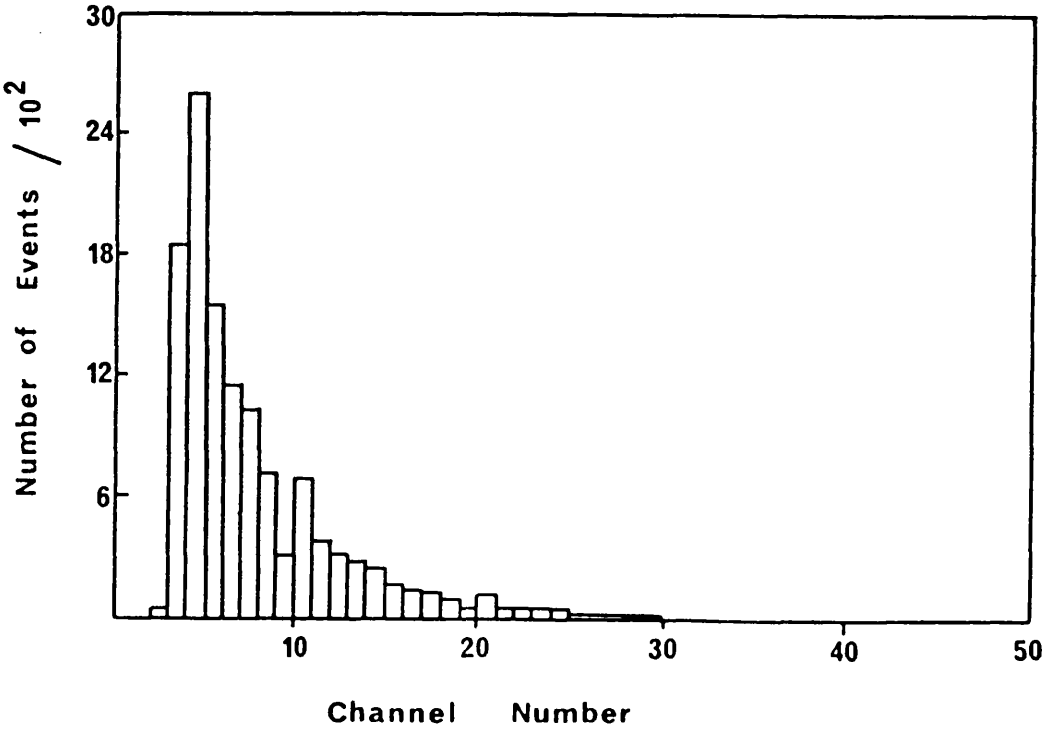

Figure 50b. The distribution of energy levels of the acoustic emission during fatigue testing of a Microtal tablet compressed at a compaction force of 20kN.

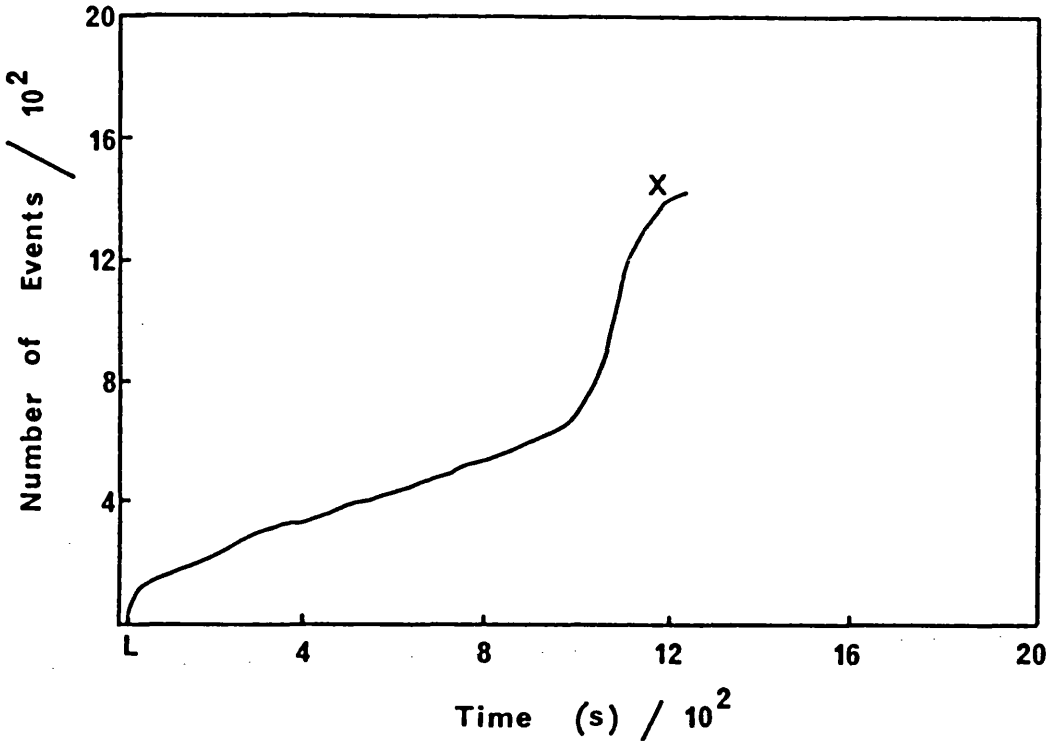

Figure 51a. Cumulative number of acoustic events recorded with time during fatigue testing of an Avicel PH102 tablet compressed at a compaction force of 6kN. "L" is the point of loading and "X" is the point of fatigue failure.

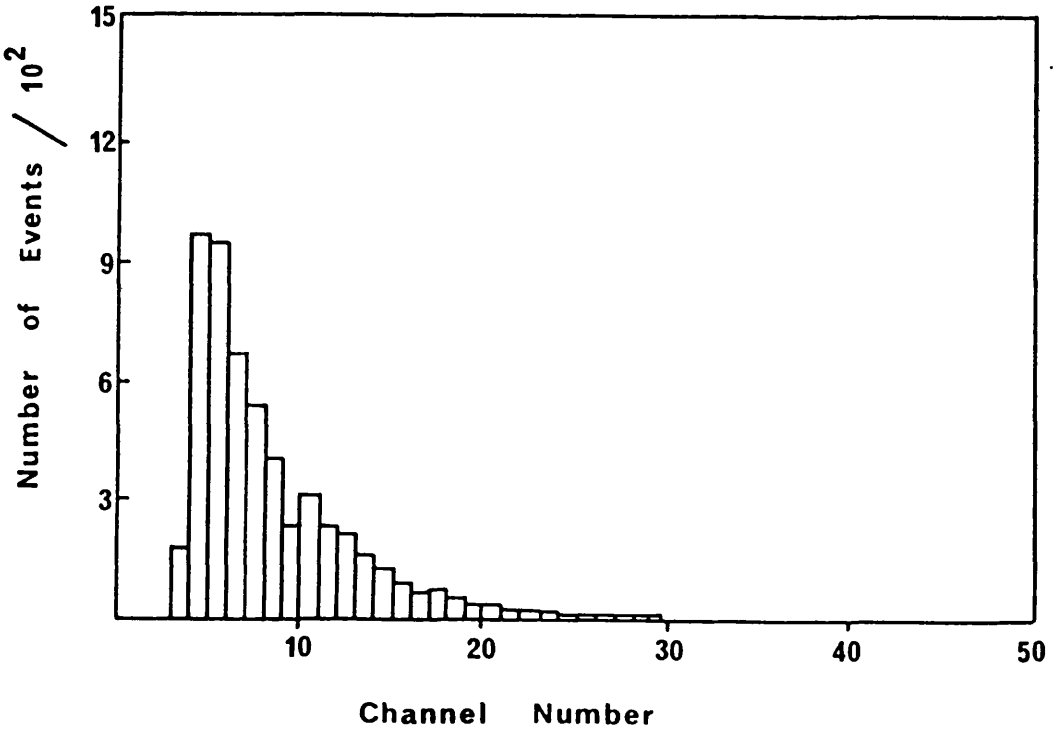

Figure 51b. The distribution of energy levels of the acoustic emission during fatigue testing of an Avicel PH102 tablet compressed at a compaction force of 6kN.

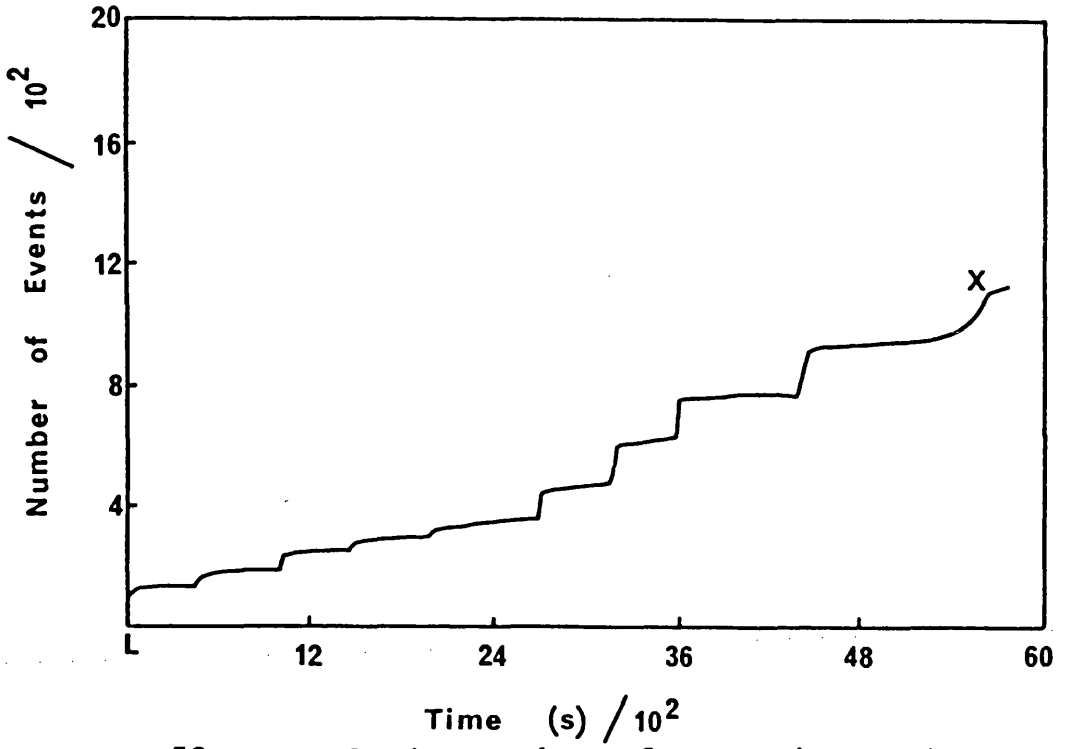

Figure 52a. Cumulative number of acoustic events recorded with time during fatigue testing of an Emcompress tablet compressed at a compaction force of 8kN. "L" is the point of loading and "X" is the point of fatigue failure.

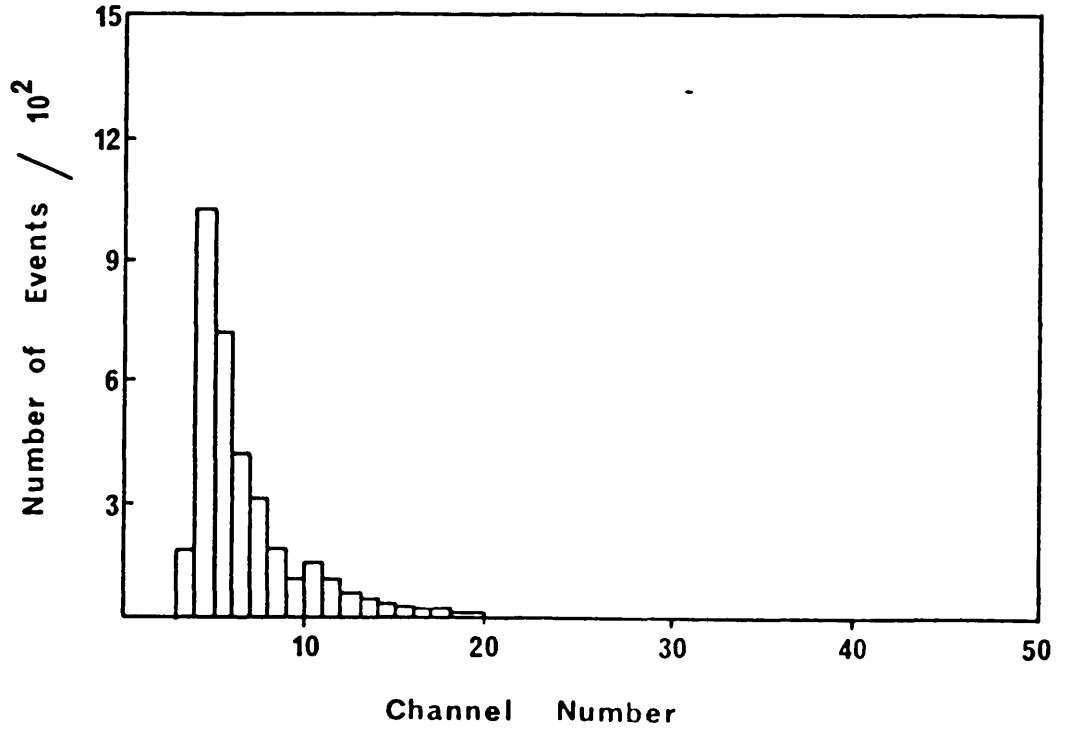

Figure 52b. The distribution of energy levels of the acoustic emission during fatigue testing of an Emcompress tablet compressed at a compaction force of 8kN.

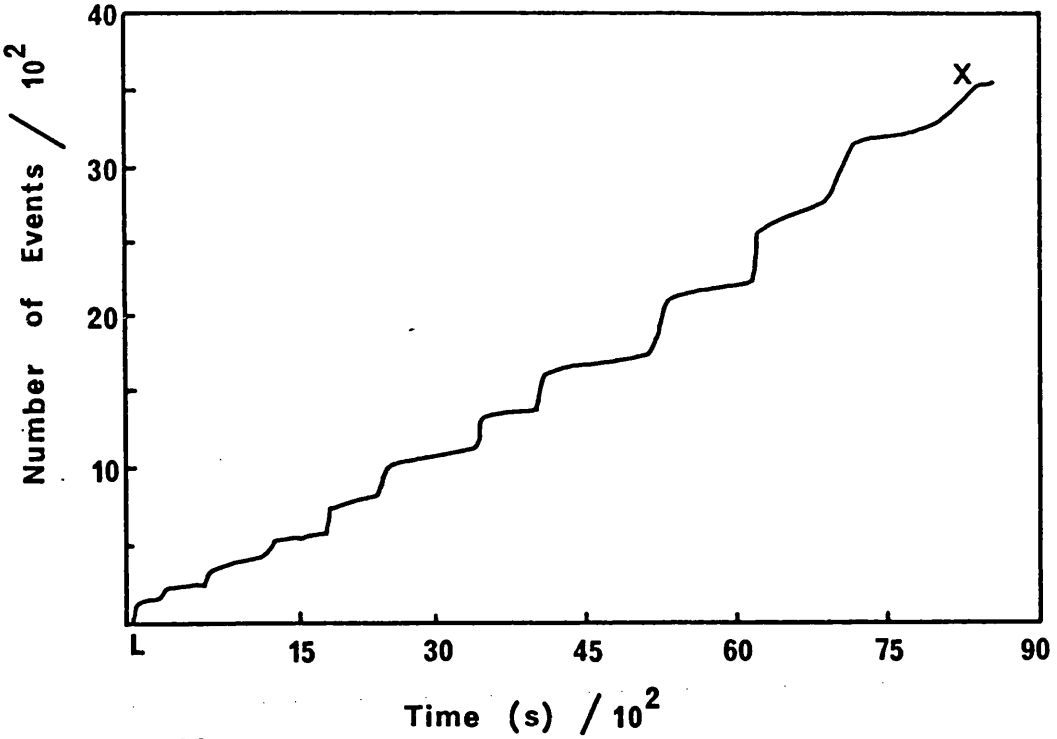

Figure 53a. Cumulative number of acoustic events recorded with time during fatigue testing of an Emcompress tablet compressed at a compaction force of 20kN. "L" is the point of loading and "X" is the point of fatigue failure.

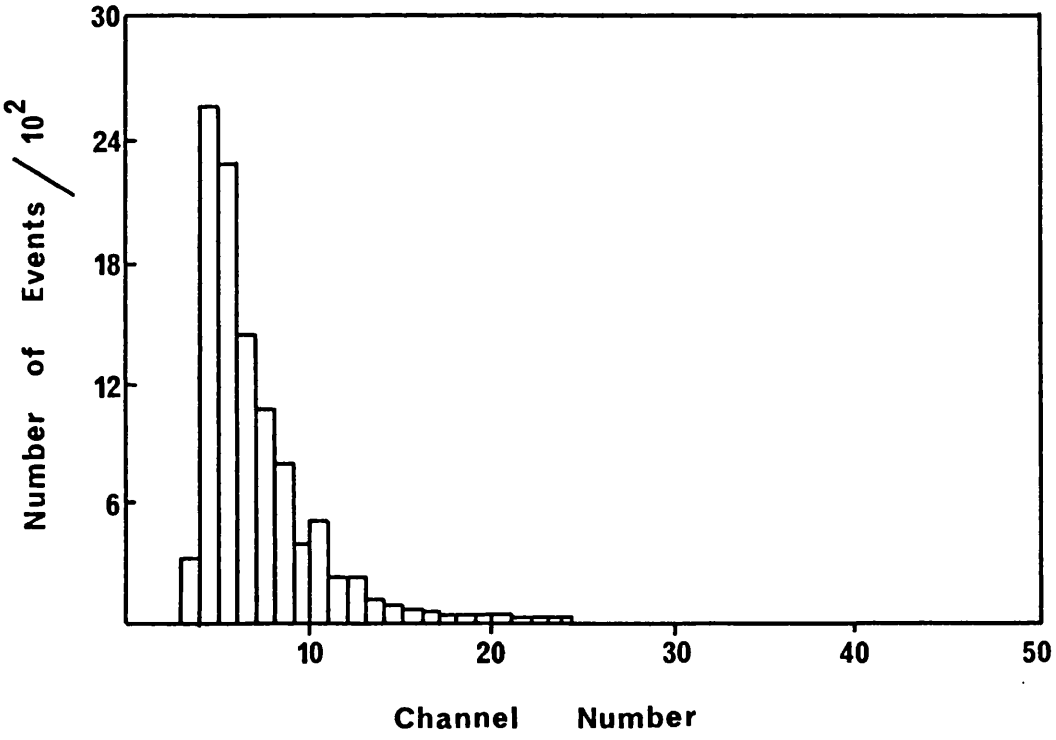

Figure 53b. The distribution of energy levels of the acoustic emission during fatigue testing of an Emcompress tablet compressed at a compaction force of 20kN.

number of cycles probably because damage continues to occur during successive cycles. Similar results have been reported by Fuwa et al. (1974) and Williams and Reifsnider (1974) for reinforced plastic composites.

The AE profiles appear to indicate that two types of fracture are taking place during fatigue testing of tablets:

- Type 1 behaviour was that associated with Avicel and Microtal tablets, where the AE increased gradually with time, suggesting the FCP was retarded, presumably by plastic flow;

- Type 2 behaviour was that found in Emcompress tablets, where the AE increased in sudden bursts.

AE can be used for detecting damage and damage growth, however there appears to be no difference in FCP for Avicel and Microtal tablets. A difference might have been expected since NWF values for Avicel were much greater than for Microtal (Figs. 42 and 81, in section 3.2.2.1), suggesting that Avicel undergoes plastic deformation during compaction to a much larger degree than Microtal. The latter explains the large difference in the number of cycles required for fatigue failure for Avicel compared to Microtal, at all compaction forces. In order to examine the progress of a crack or cracks in tablets, a non-destructive method of testing samples was employed.

3.1.1.2 Non-destructive Testing of Tablets.

Scanning Laser Acoustic Microscopy (SLAM) was used as a potential method for producing visual images of the internal structures of optically opaque tablets.

In order to observe the progress of a crack or cracks in tablets, preliminary studies of stressed tablets (at two levels of stressing, below the point of fatigue) were performed. Two levels of stressing (damage) were chosen, firstly following 100 cycles fatiguing to represent the initial phase of crack initiation and propagation and secondly, after 1000 cycles to represent the final stages of crack propagation in a tablet prior to fatigue failure. However experiments using SLAM indicated that the acoustic waves with a frequency of 10MHz to 500MHz could not penetrate the tablets. It was considered that there were several possible explanations for the failure of these experiments.

(i) large tablet thickness (approximately 3.0mm),

(ii) the porosity of tablet structure, entrapped air within the tablet may act as a barrier to the acoustic waves.

For these reasons the mass used in compression was reduced to that required to produce a 1.75mm thick tablet at zero theoretical porosity. This was found to reduce the tablet thickness to approximately 2.25mm and to allow the fatigue test to be conducted up to a maximum of 1000 cycles of stressing. These tablets were embedded in an epoxy resin in order to reduce the air voidage of the tablet prior to examination using SLAM: tablets, after stressing, were soaked in epoxy resin at room temperature under high vacuum for two hours and then the surface was carefully wiped clean so as to remove excess resin. The tablets were then placed in an oven at 65 ^{o}C for 48 hours to complete polymerisation of the resin.

Emcompress (20kN), Microtal (20kN) and Avicel (10kN) tablets were compressed and embedded as described immediately above and examined by SLAM. Unfortunately, no images of the internal core of the tablets were obtained. In order to elucidate the reason(s), an absorbtion-echo profile of these tablets was carried out. Using a 1MHz acoustic transmitter, various metal structures and pharmaceutical tablets were subjected to acoustic waves and the echoes produced were plotted with time. Fig. 54a shows an absorbtion-echo profile for a metal bar. It shows that metal does absorb acoustic waves but emits them as an echo, such characteristics are desirable for specimens to be examined using SLAM. Fig 54b shows the absorbtion-echo profile for pharmaceutical tablets examined, including tablets without the epoxy resin. There was an absence of an echo for all tablets and suggesting that porosity of the tablets had no influence on the absorbtion pattern. Materials which completely absorb acoustic waves are referred to as possessing high attenuation (Blitz, 1967) and are therefore impossible to examine by acoustic techniques (Reiter, 1984).

Increasing the temperature can affect the degree of attenuation (Reiter, 1984). Emcompress tablets, in 60° C water, were found to show some degree of echo (Fig. 54c), however, the working acoustic frequency could not be increased above 4MHz and was found to be of little value in SLAM. It was concluded that the SLAM technique could not be used for the formation of visual images of the internal structures of pharmaceutical tablets.

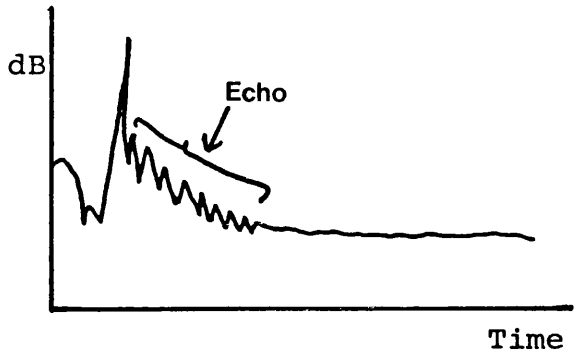

a. Metal bar at ambient temperature.

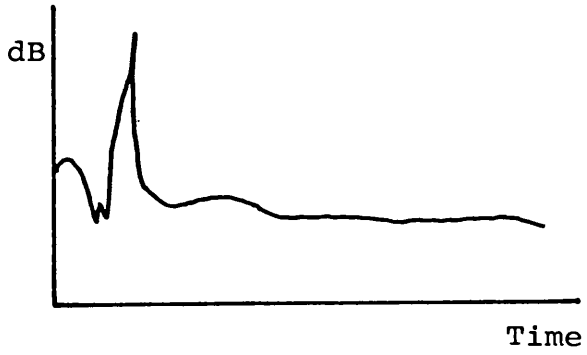

b. Pharmaceutical tablets, including tablets embedded with epoxy resin to reduce voidage (at ambient temperature).

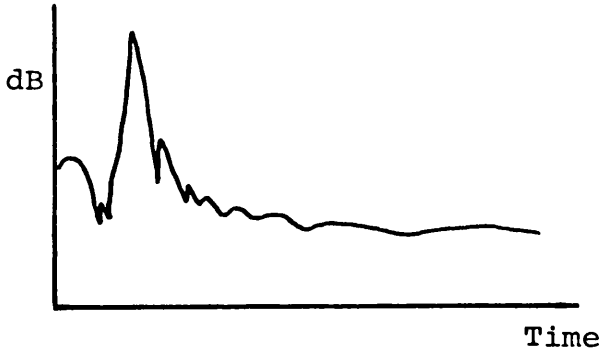

c. Emcompress tablet at 60°C.

Figure 54. Absorbtion-echo profiles for different specimens using a 1MHz acoustic transmitter.

3.1.2 Determination of True Work of Compaction.

In order to determine the true work of compaction, work performed for elastic deformation is subtracted from the total work (Polderman and de Blaey, 1970). In the literature, workers have restricted their studies to performing only two compressions, thus making an assumption that the work performed during the second compression is purely elastic (for example, Polderman and de Blaey, 1970, 1971a, 1971b; Krycer et al., 1982; Ragnarsson and Sjogren, 1983, 1984a,b, 1985). Probable reasons for restricting their studies to only two compressions may be due to the impractical nature of multiple compression or perhaps the lack of data storage facilities. An important consequence is that the assumption remains questionable, since no supportive evidence has been presented. Armstrong et al. (1982) have been able to acquire force-displacement (FD) data from a maximum of thirteen compressions, without ejection and store data rapidly without reducing data acquisition rate. However, they did not determine the work performed on compression or re-compression. In the present study, FD data has been acquired from a maximum of 19 compressions, without ejection and the work of compaction at every compression was determined. The data acquisition system developed in this study allowed FD data to be acquired even at the fastest compaction rate (approximately 80 tablets per minute). Details of the system have been described above in section 2.1.2.3.

In order to check the validity of the assumption made by all previous workers, that the work performed during the second

compression is purely that required to overcome elastic deformation, the total work performed at every compression was plotted versus the number of re-compressions. In this study, the rate of compaction and compaction force were altered in order to investigate their influence on true work of compaction. Unlike other workers (Polderman and de Blaey, 1971a, 1971b, 1971c; Krycer et al., 1982; Ragnarsson and Sjogren, 1983, 1984a,b, 1985), the frictional work has been included in the true work of compaction since the frictional properties are a function of the inherent chemical and physico-mechanical properties of the excipients.

3.1.2.1 True Work of Compaction for Avicel PH102.

Figs. 55(a, b) show the relationship between the work of compaction after the first compression with increasing number of re-compressions, without ejection, for Avicel PH102 (mcc) at a compaction force of 8kN and different compaction rates. The work of compaction values are the means of a minimum of five determinations and corresponding standard deviations have been plotted. Fig. 55a shows the results when the compaction rate was approximately 35 and 65 tablets per minute, giving contact times of 0.1504 and 0.107 seconds respectively. There was decay in the work performed to a constant value of approximately 0.96 J after the 10th compression. While Fig. 55b shows the results when the compaction rate was approximately 55 and 80 tablets per minute, giving contact times of 0.1152 and 0.0917 seconds respectively. Again, the work of compaction was found to decay, from

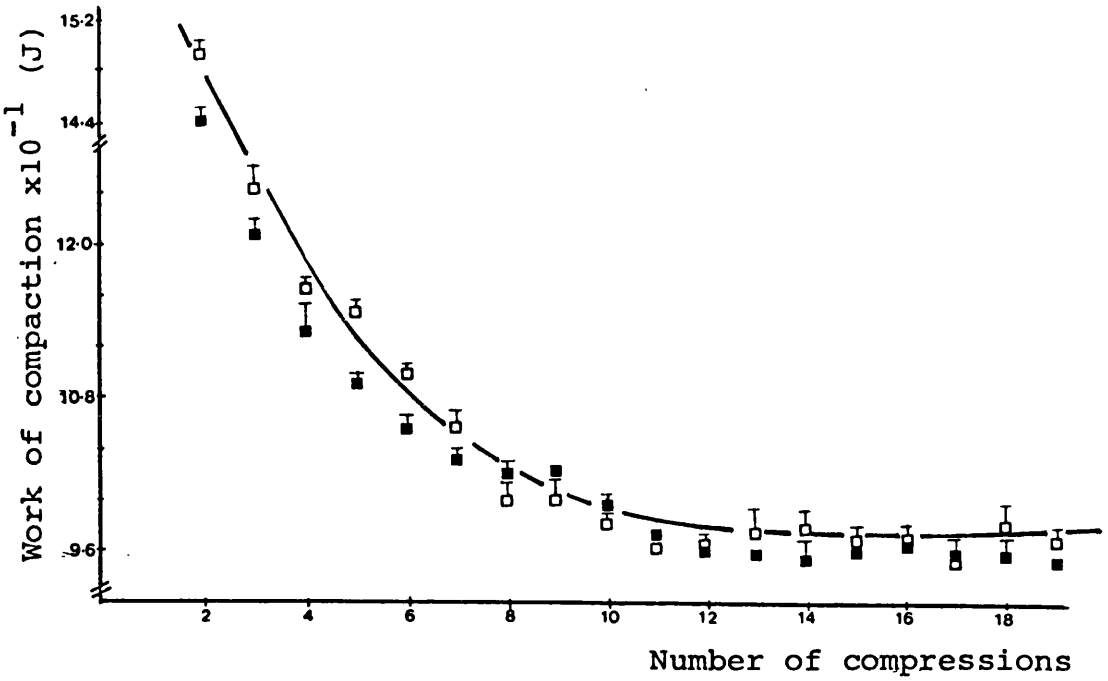

a. Contact time (□) 15.04 and (■) 10.70 seconds x10^{-2}.

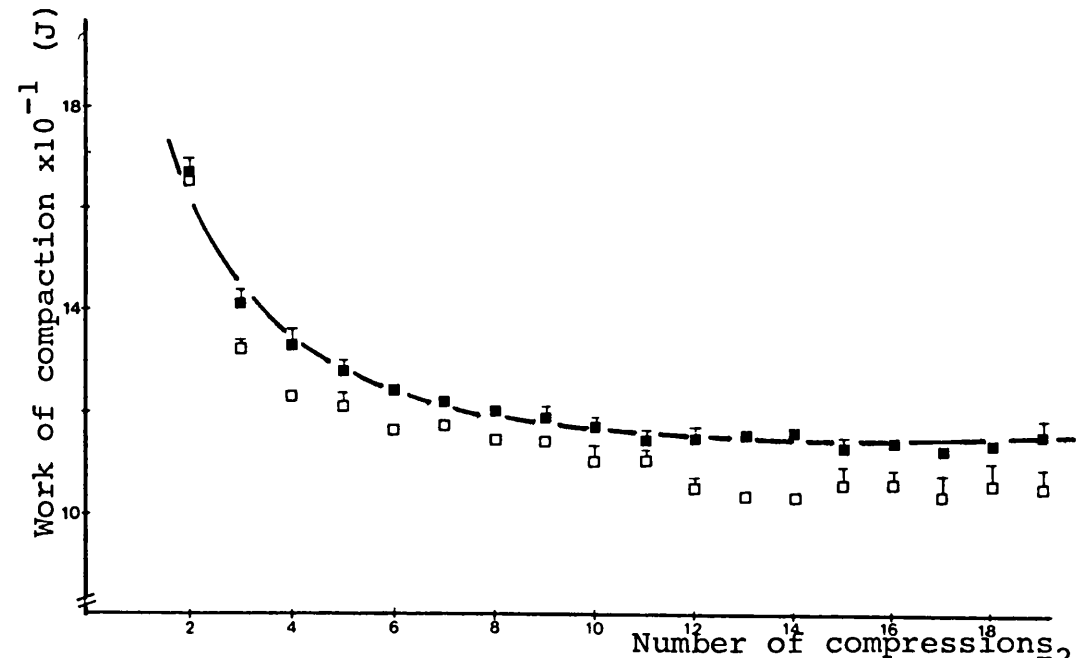

b. Contact time (□) 11.52 and (■) 9.17 seconds x 10^{-2}.

Figure 55 (a &b). Relationship between the work of compaction and number of compressions for Avicel PH102 compressed at 8kN. Compaction rate is effectively represented by contact time, lower the contact time, higher is the compaction rate.

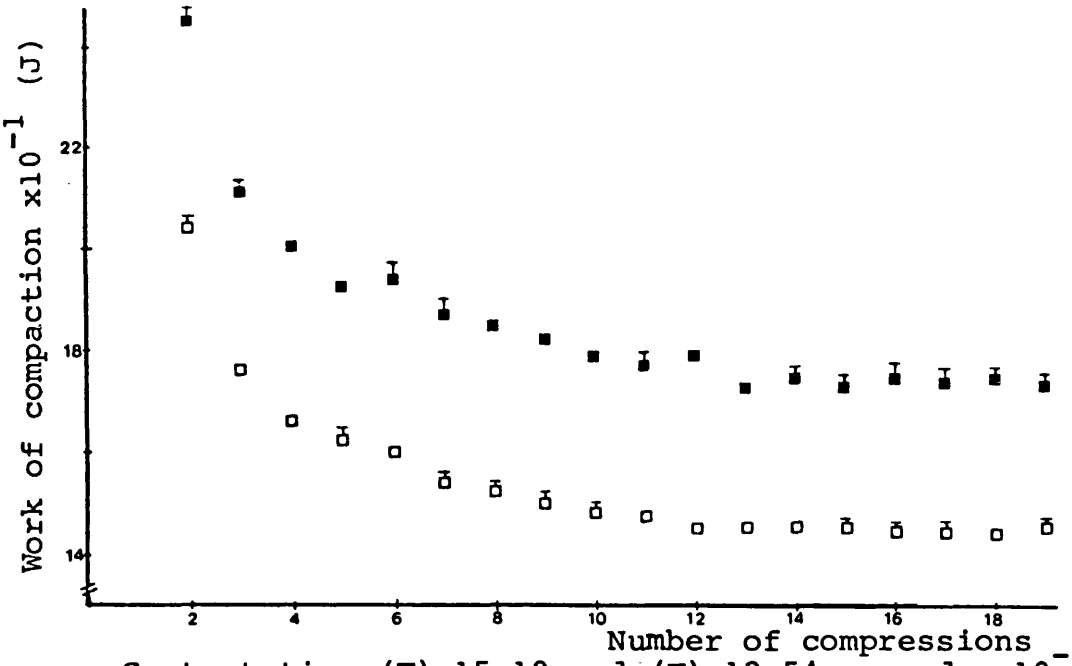

a. Contact time (□) 15.19 and (■) 12.54 seconds x10^{-2}.

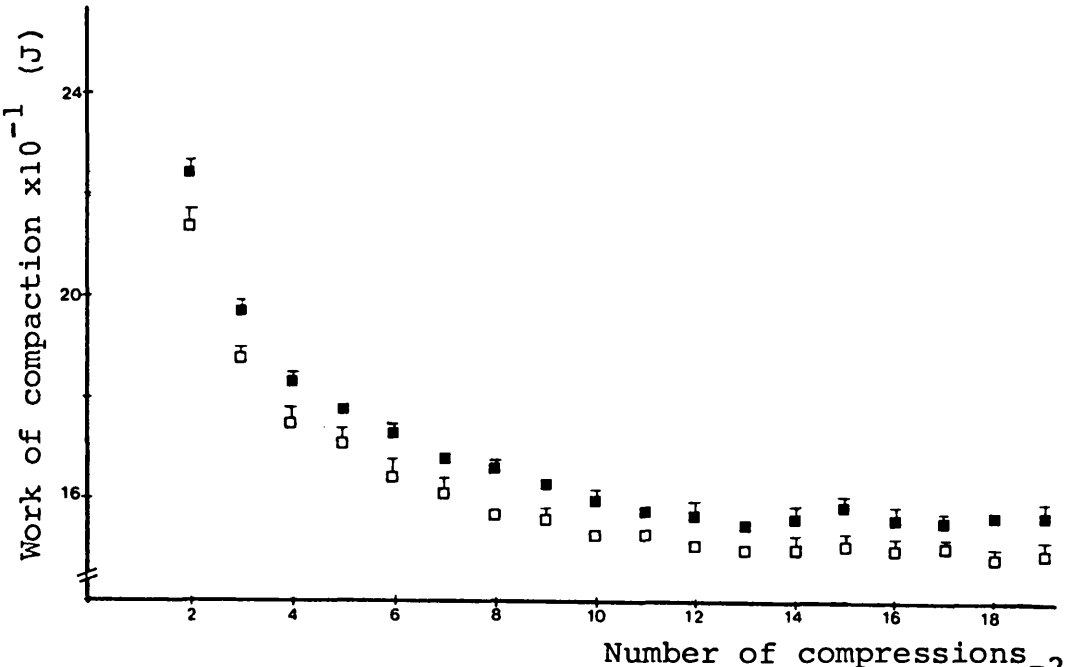

b. Contact time (□) 11.46 and (■) 9.73 seconds x 10^{-2}.

Figure 56 (a & b). Relationship between the work of compaction and number of compressions for Avicel PH102 compressed at 12kN. Compaction rate effectively represents rate of compaction, lower contact time represents high compaction rates.

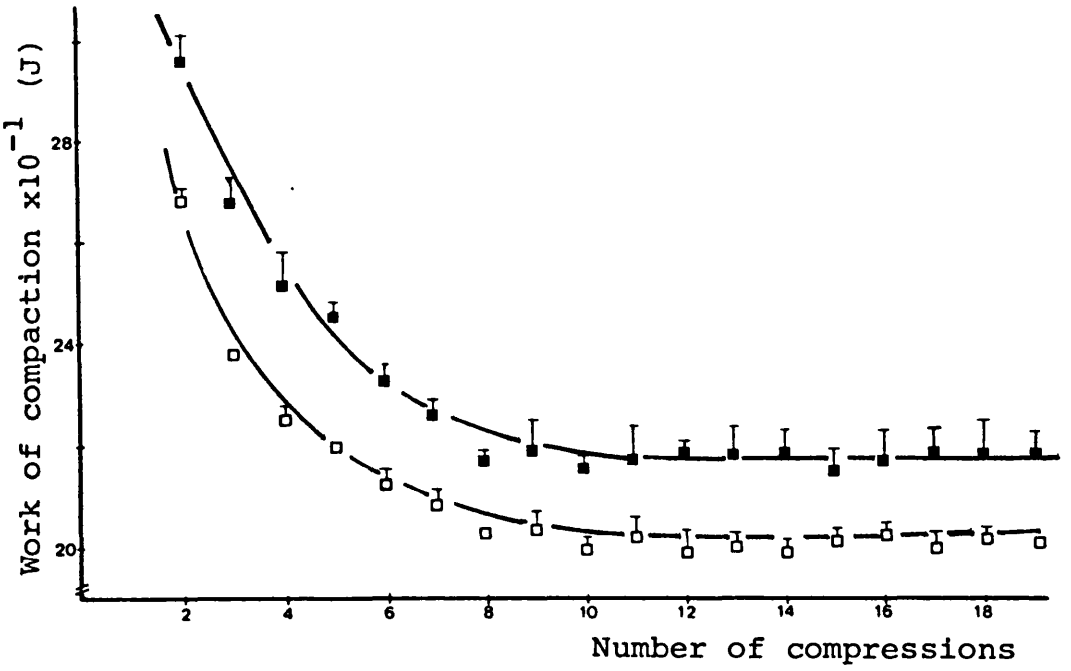

a. Contact time (□) 16.72 and (■) 12.97 seconds x10^{-2}.

b. Contact time (□) 11.75 and (■) 9.9 seconds x10^{-2}.

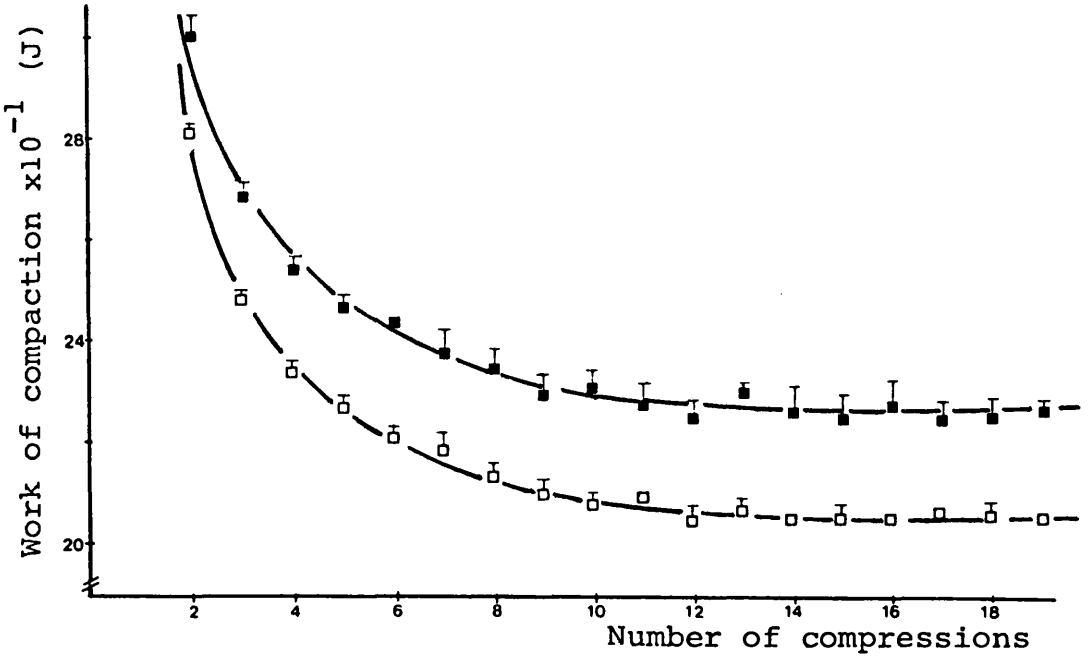

Figure 57(a & b). Relationship between the work of compaction and number of compressions for Avicel PH102 compressed at 16kN. Compaction rate is effectively represented by contact time, lower the contact time, higher the compaction rate.

approximately 1.65 J to a constant value of approximately 1.1 J after the 10th compression.

Figs. 56 (a, b) and 57 (a, b) show similar decay curves when the compaction force was increased to 12kN and 16kN respectively. The decay curves suggest that the work carried out on the second compression was not purely elastic, but a combination of elastic and plastic. One would anticipate that at the lowest compaction rate, the upper punch will induce greater plastic flow since it is in contact with the powder for the longest time, consequently, constant work would be attained more rapidly. However, the results show that altering the rate of compaction had no measurable influence on the decay in work for Avicel and constant work was always attained after 10 compressions. One possible explanation is that the change in contact time was too small to show any measurable change in the degree of plastic flow in such a plot.

Results for Avicel PH102 (Figs. 55, 56 and 57) showed that the work carried out on second compression was not purely elastic work, but a combination of elastic and plastic. It was not until the 10th compression that all possible plastic deformation was complete and since a constant value of work was obtained on subsequent compressions, it most accurately represented the work required for elastic deformation rather than the work performed during the second compression.

Fig. 58a shows the relationship between the maximum force applied on re-compression with increasing number of compressions for Avicel PH102. The force applied at first compression decayed

from approximately 8200 N to a constant value of approximately 7400 N after the 8th compression when the contact time was 0.0917 seconds (or a compaction rate of 80 tablets per minute). A similar drop in the maximum force applied was observed when the compaction rate was 35 tablets per minute (Fig. 58a). Fig. 58b shows the relationship between the maximum deformation undergone by the above tablets on re-compression. The tablet deformation decays from 28.7*E-4m to a constant value of 20.0*E-4 m, which was attained after the 11th compression when the compaction rate was 80 tablets per minute. When the compaction rate is reduced to approximately 35 tablets per minute, a similar decay profile for tablet deformation was obtained (Fig. 58b). On increasing the compaction force to 16kN, similar decay profiles of force and tablet deformation were obtained (Figs. 59a, b).

These profiles suggest that decay in the work of compaction (Figs. 55, 56 and 57) was due to decay of both the maximum force applied and the deformation which the tablet undergoes on re-compression. Tablet porosity will decrease on re-compression, which will be accompanied by a reduction in tablet volume, an assumption which is supported by the fact that the deformation undergone by the tablet decreased on re-compression (Figs. 58b and 59b). Since the upper punch displacement was constant, on re-compression the upper punch would encounter a structure of reduced volume, which resulted in a decrease in force applied. However when a constant force and tablet deformation were obtained this indicated that the tablet had attained its ultimate minimum porosity at that specific compaction force. This would

indicate that all possible plastic deformation was complete and any deformation occurring on subsequent compressions was purely elastic.

Travers and Merriman (1970) have measured the temperature rise on compression, relaxation and re-compression of pharmaceutical powders. The rise could be separated into two components: firstly, that associated with the heat of formation of the compact which is probably due to irreversible deformation and bonding and secondly, that associated with elastic deformation of the compressed compact. They state that the rise in temperature on re-compression, followed by a fall in the relaxation could be reproduced "many times" on the same compact, however, they do not state the number of re-compressions performed. These workers also stated that on re-compression, the rise in temperature was to a value lower than the initial rise. Their results would imply that after the first compression, all possible irreversible deformation was complete and the second compression represents work performed for elastic deformation of the compact since a constant rise in temperature was attained. The present study shows that this interpretation is incorrect.

Armstrong et al. (1982) reported that at a compaction rate of 46 tablets per minute, the "Frel" values of Avicel tablets decreased on re-compression, a constant value was attained as early as after 5 compressions, where "Frel" is given as the ratio of force applied at nth compression to that applied at the first compression. The results in the present study show that a minimum of 10 compressions are necessary in order to attain a constant

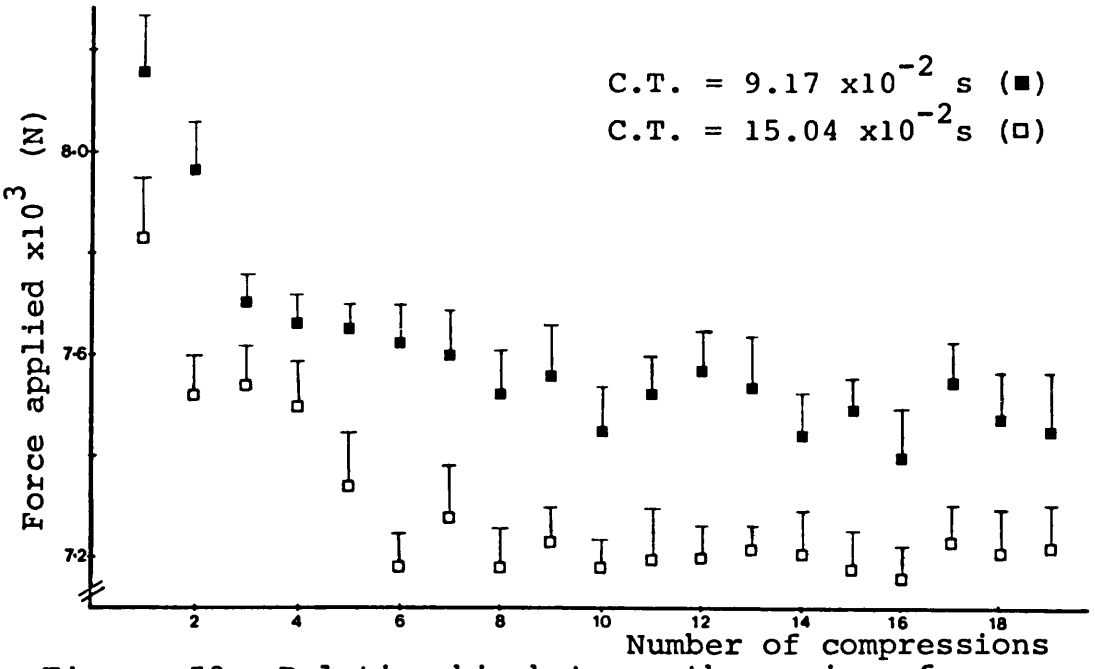

Figure 58a. Relationship between the maximum force applied and the number of compressions for Avicel PH102 at an initial force of approximately 8kN. C.T. refers to contact time.

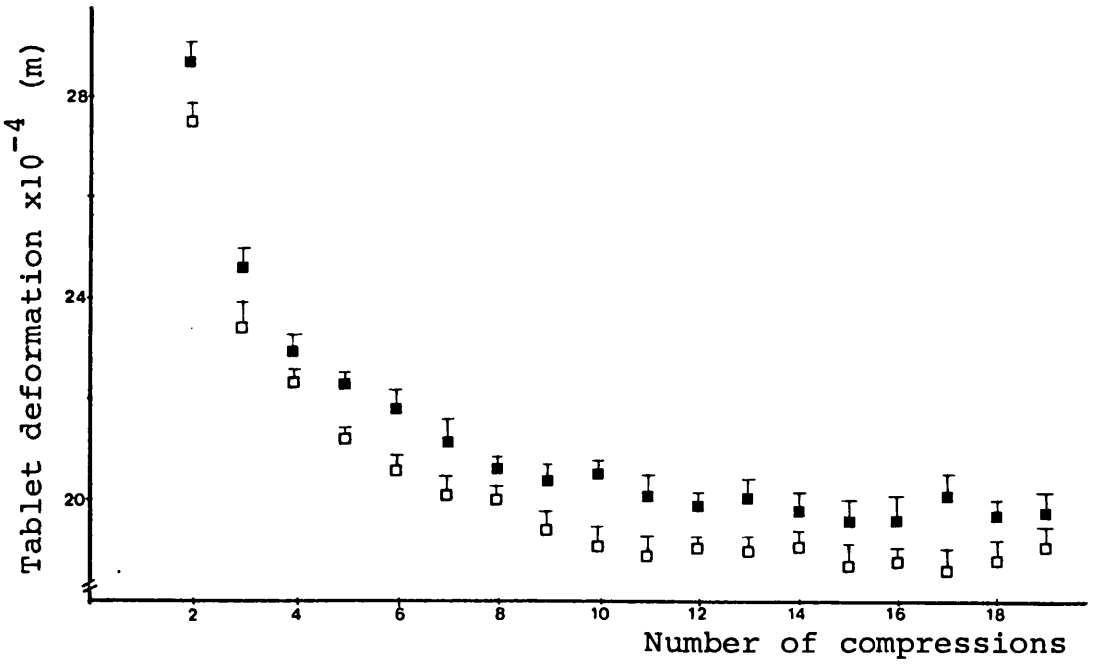

Figure 58b. Relationship between the tablet deformation and number of compressions for Avicel PH102 compressed at a compaction force of approximately 8kN at two compaction rates. Symbols as above.

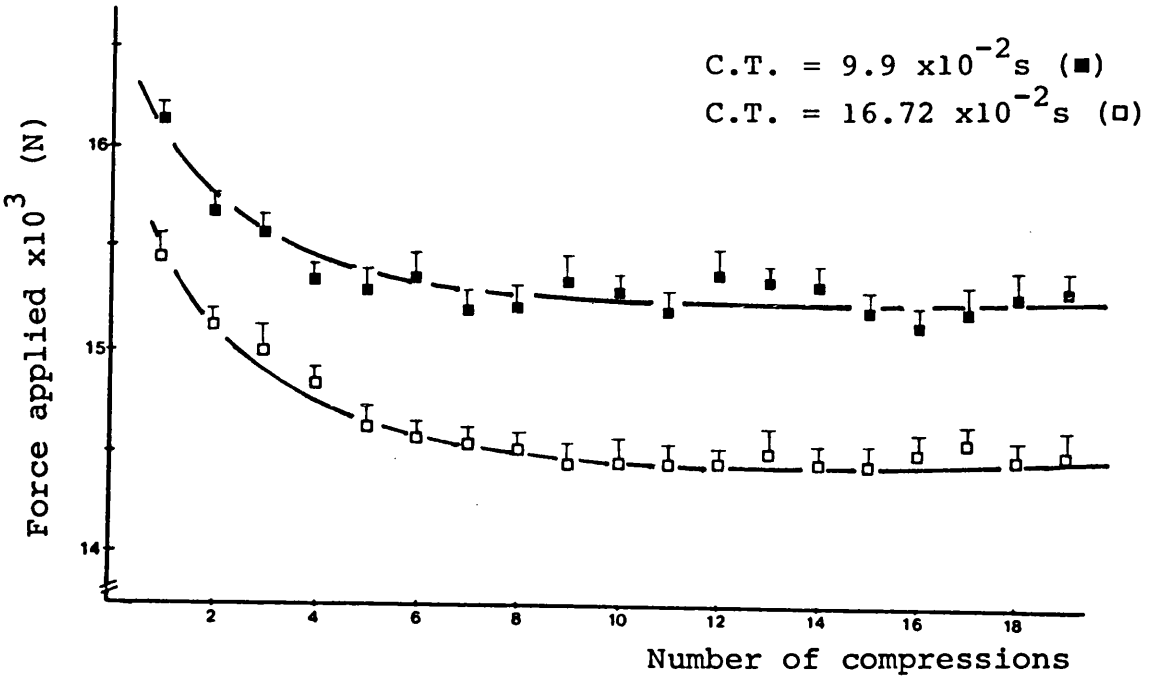

Figure 59a. Relationship between the maximum force applied and the number of compressions for Avicel PH102 compressed at an initial force of approximately 16kN. C.T. refers to contact time.

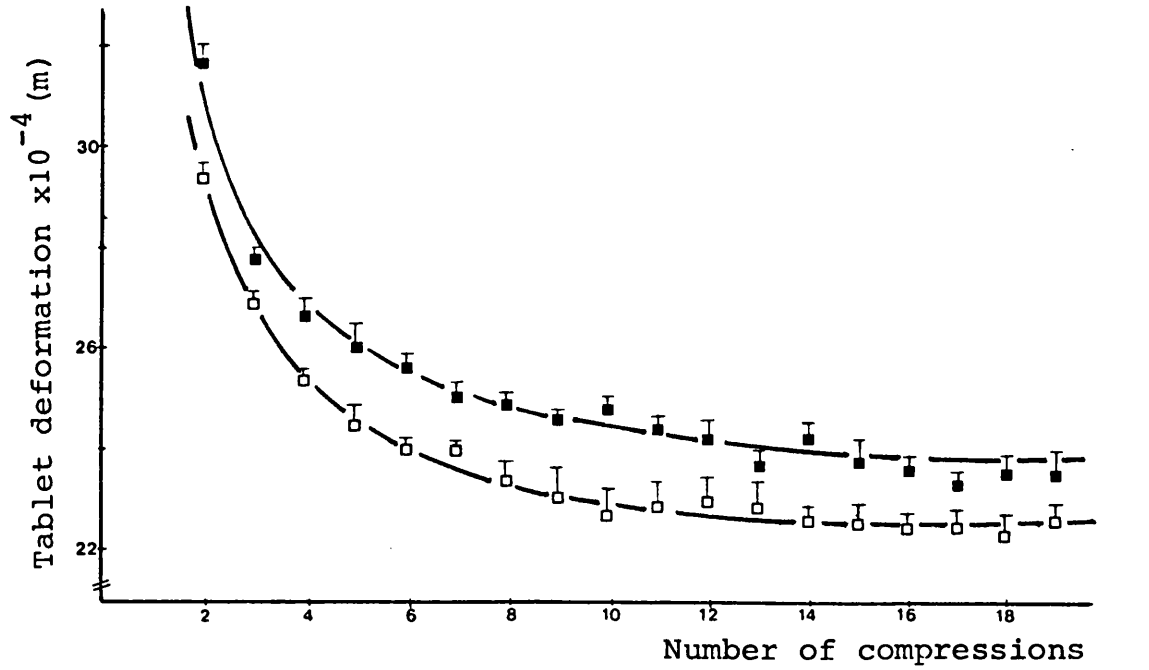

Figure 59b. Relationship between the tablet deformation and number of compressions for Avicel PH102 compressed at a compaction force of approximately 16kN. Symbols as above.

Comp. force kN	Contact time 1*E-2 s	Total work J	Constant Elastic work J	2nd comp. work J	True work of comp. J
8	15.04	9.77	0.95	1.44	8.82
	11.52	9.75	1.05	1.65	8.70
	10.70	10.36	0.97	1.50	9.39
	9.17	10.73	1.14	1.66	9.59
12	15.91	13.26	1.43	2.04	11.83
	12.54	12.58	1.73	2.45	10.85
	11.46	13.78	1.50	2.14	12.28
	9.74	13.70	1.55	2.25	12.15
16	16.72	15.63	2.00	2.68	13.63
	12.97	14.53	2.16	2.96	11.57
	11.75	16.36	2.03	2.81	14.33
	9.90	16.65	2.25	3.01	14.40

Table 8. Summary of work of compaction data for Avicel PH102 at three different compaction forces and four different compaction rates (contact times). Total work is the area under the first FD curve and true of compaction is calculated by subtracting the constant elastic work from the total work.

maximum force and hence a constant "Frel" value.

Table 8 summarises the results for Avicel PH102. Increasing the compaction force from 8kN to 16kN caused an increase in the work carried out for elastic deformation from approximately 1.0 J to 2.0 J. In order to determine the true work of compaction (Table 8) the work performed for elastic deformation, a constant value after the 10th compression, was subtracted from the total work. Thus in the case of Avicel PH102, the results indicated that the assumption made by all workers in the literature was invalid. It is clear from the data presented, that using the area under the second FD curve leads to an over-estimation of the work performed for elastic deformation and consequently an under-estimation of true work of compaction for Avicel PH102 at all the compaction forces and rates of compaction studied (Table 8).

3.1.2.2 True Work of Compaction for Microtal.

Figs. 60 (a, b) show the relationship between the work of compaction and number of compressions, without ejection, for Microtal at a compaction force of approximately 8kN and at four different compaction rates. At all compaction rates, there was a decay in the work carried out after the first compression and a constant value, which was obtained after approximately 13 compressions. No difference in the decay profile was observed when the compaction rate was altered. These profiles were similar to those obtained for Avicel PH102 (Figs. 55, 56 and 57), suggesting that the work performed on second compression was not purely that required to cause elastic deformation, but a

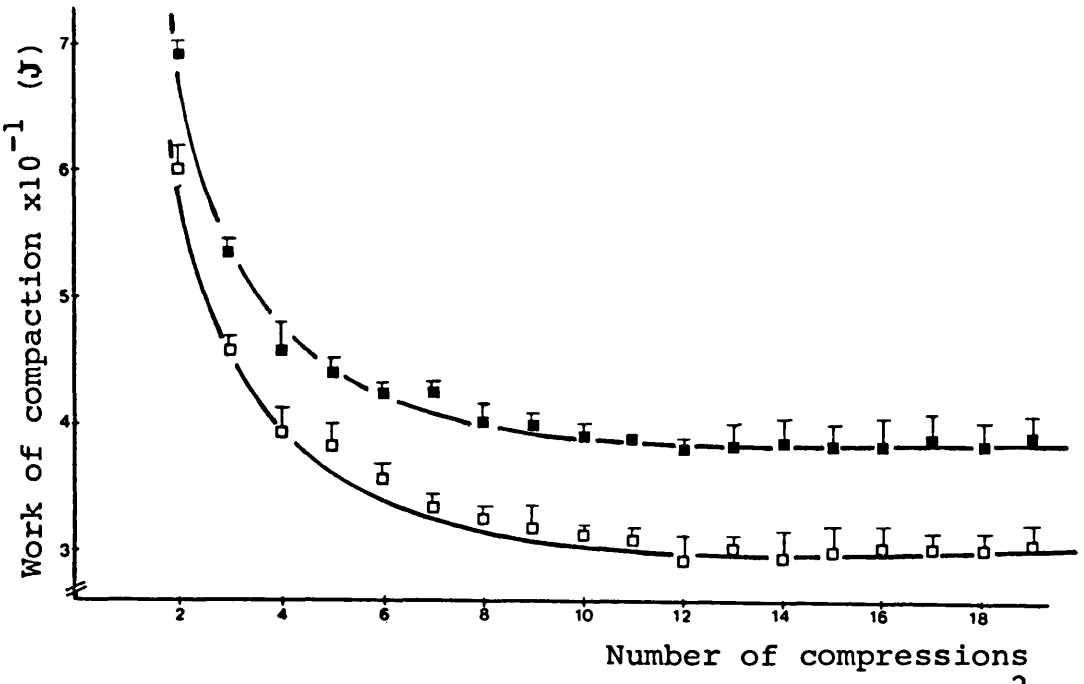

a. Contact time (■) 11.65 and (□) 7.68 seconds x10^{-2}.

b. Contact time (■) 10.11 and 6.77 seconds x10^{-2}.□

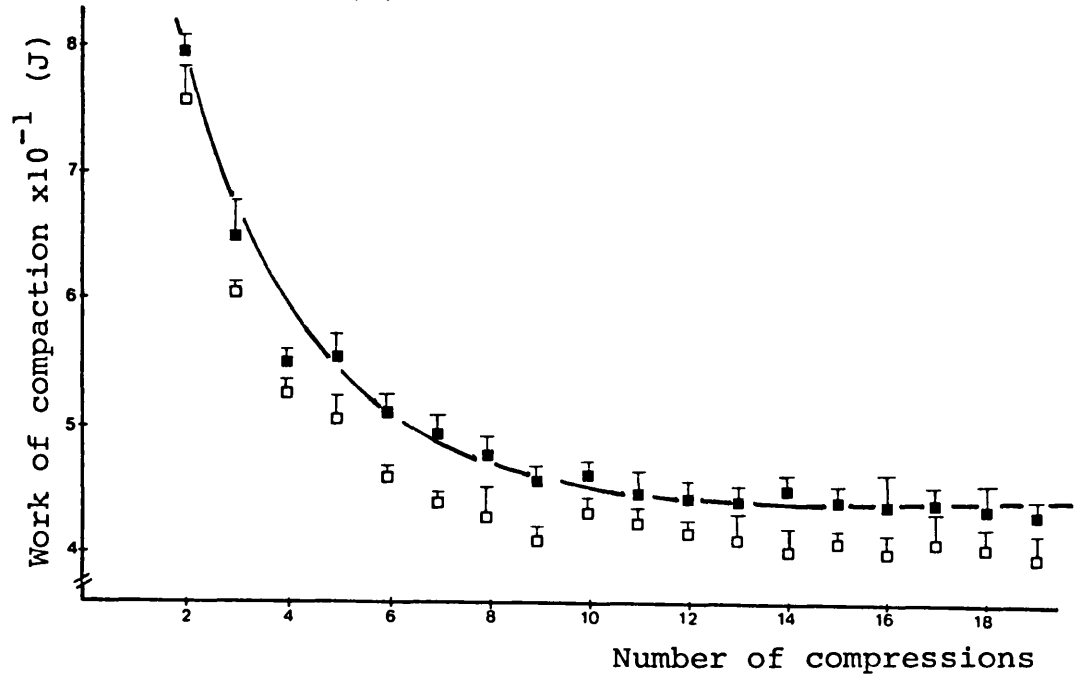

Figure 60(a &b), Relationship between the work of compaction and number of compressions for Microtal compressed at 8kN and four different compaction rates. Compaction rate is effectively represented by contact time, lower the contact time, higher the compaction rate.

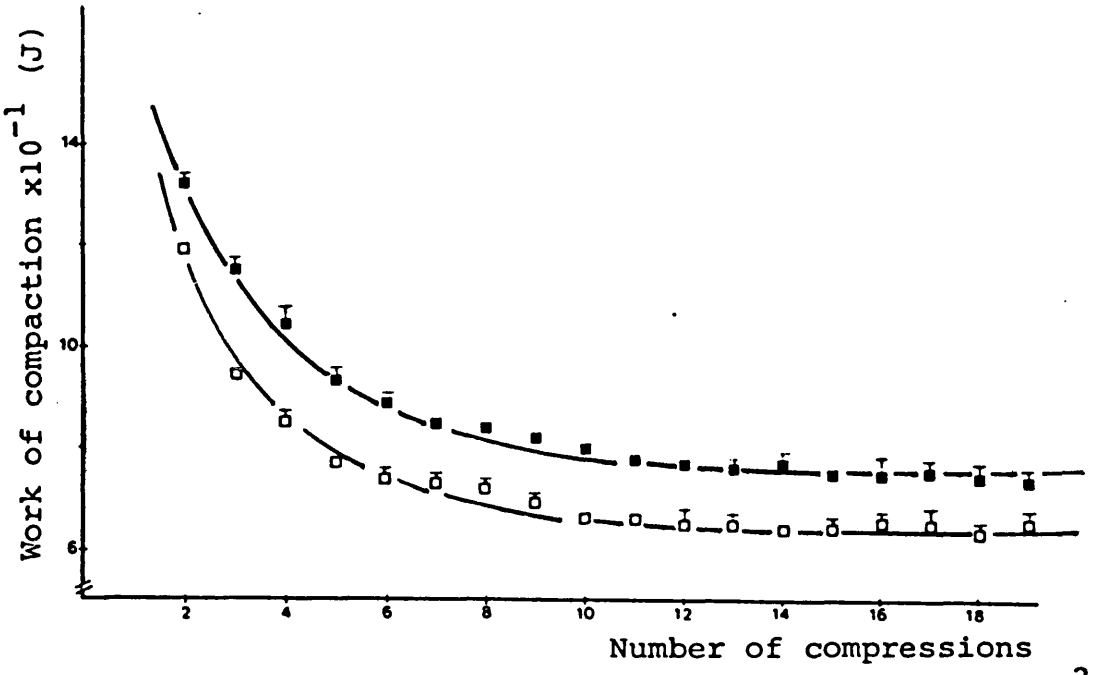

a. Contact time (□) 12.34 and (■) 10.96 seconds x10^{-2}.

b. Contact time (□) 8.6 and (■) 7.56 seconds x10^{-2}.

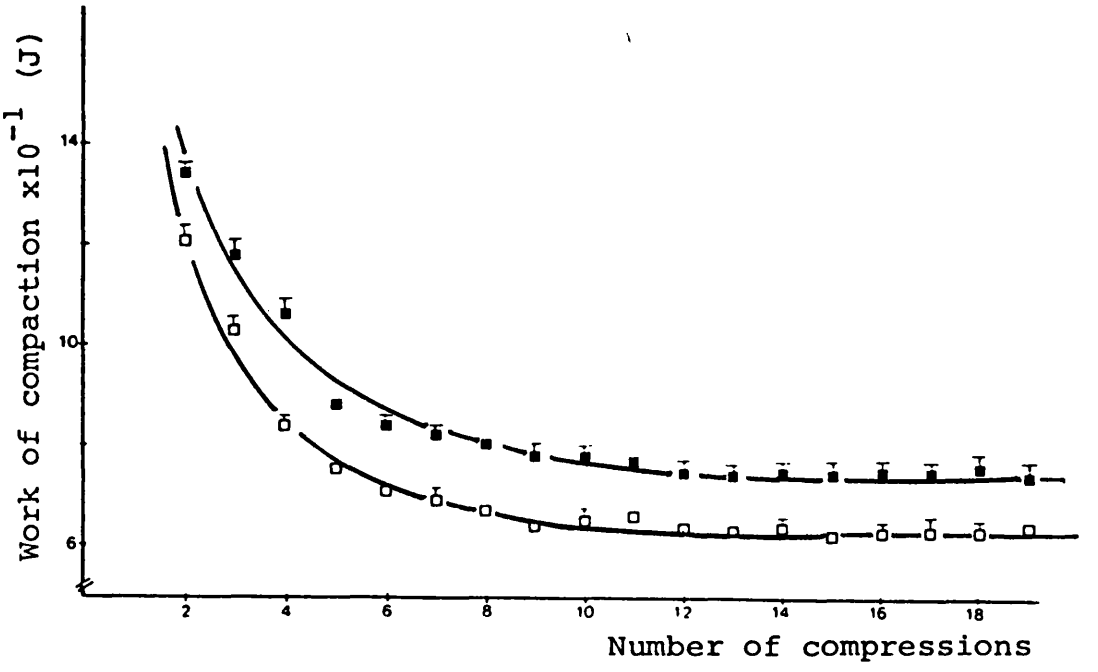

Figure 61(a & b). Relationship between the work of compaction and number of compressions for Microtal compressed at 12kN and four different compaction rates. Compaction rate is effectively represented by contact time, lower the contact time, higher the compaction rate.

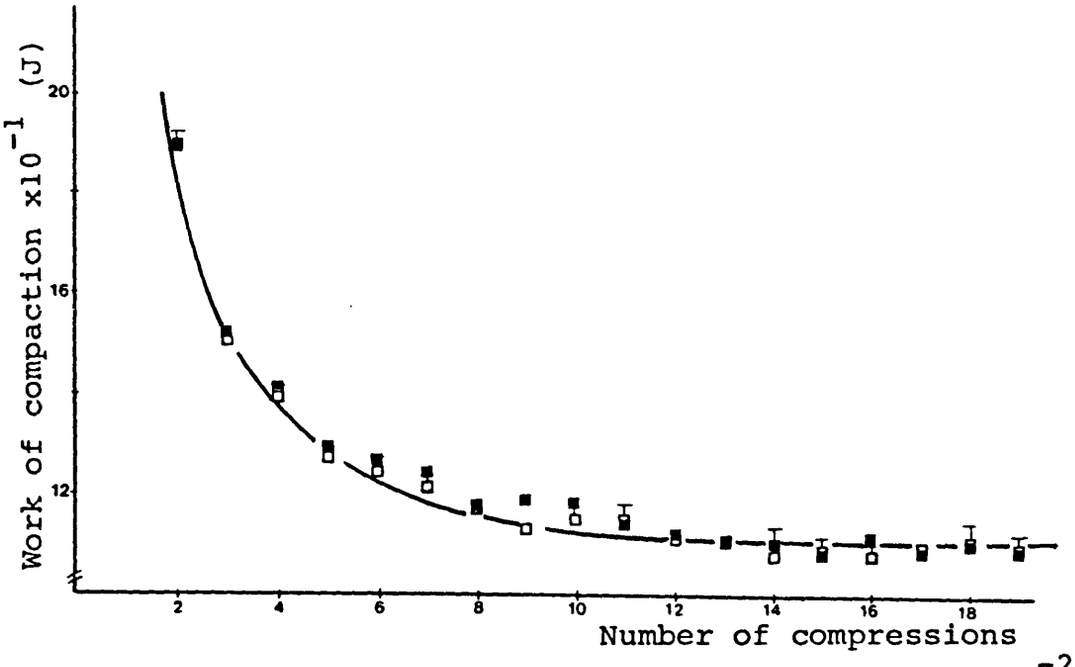

a. Contact time (□) 13.43 and (■) 11.81 seconds x10^{-2}.

b. Contact time (□) 8.94 and (■) 7.89 seconds x10^{-2}.

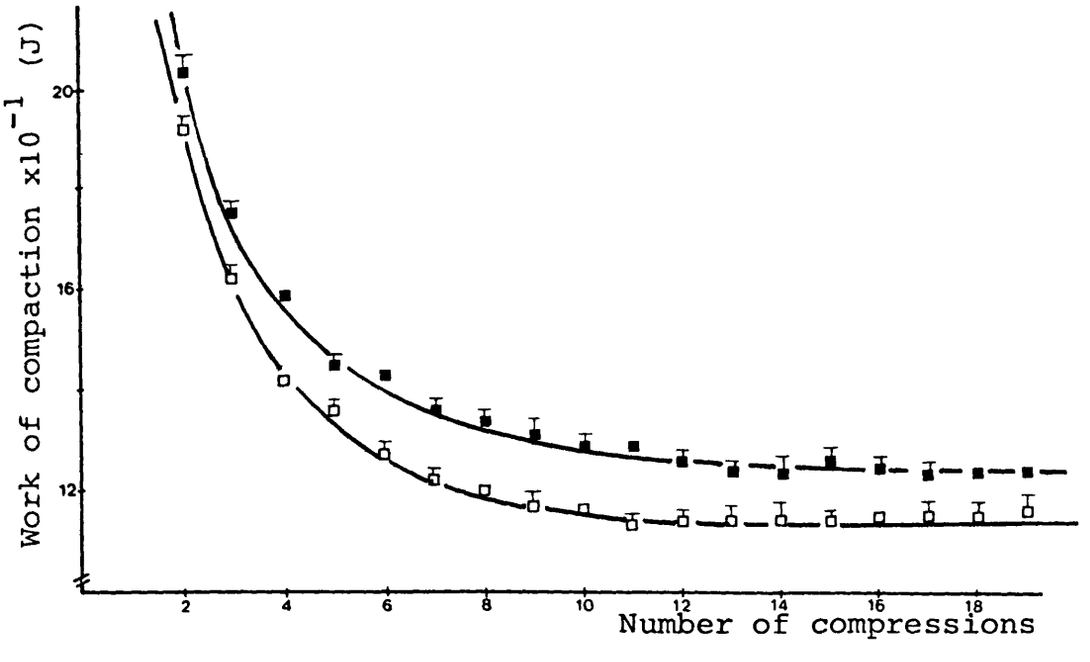

Figure 62(a & b). Relationship between the work of compaction and number of compressions for Microtal compressed at 16kN and four different compaction rates. Compaction rate is effectively represented by contact time, lower the contact time, higher the compaction rate.

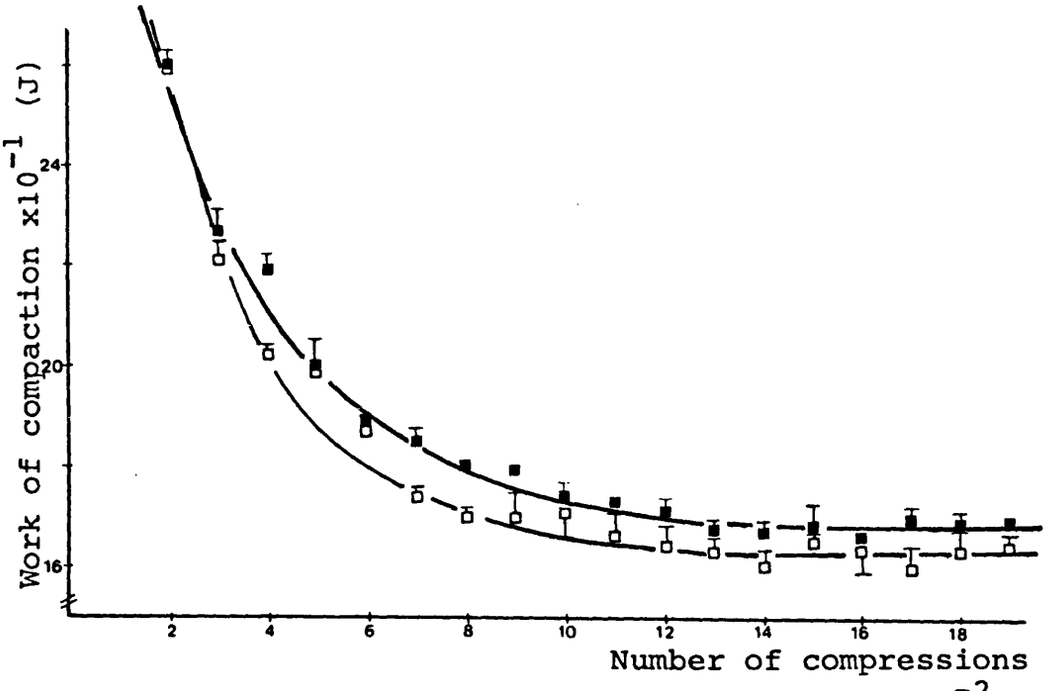

a. Contact time (□) 9.18 and (■) 8.31 seconds x10^{-2}.

b. Contact time (■) 13.95 and (□) 12.47 seconds x10^{-2}.

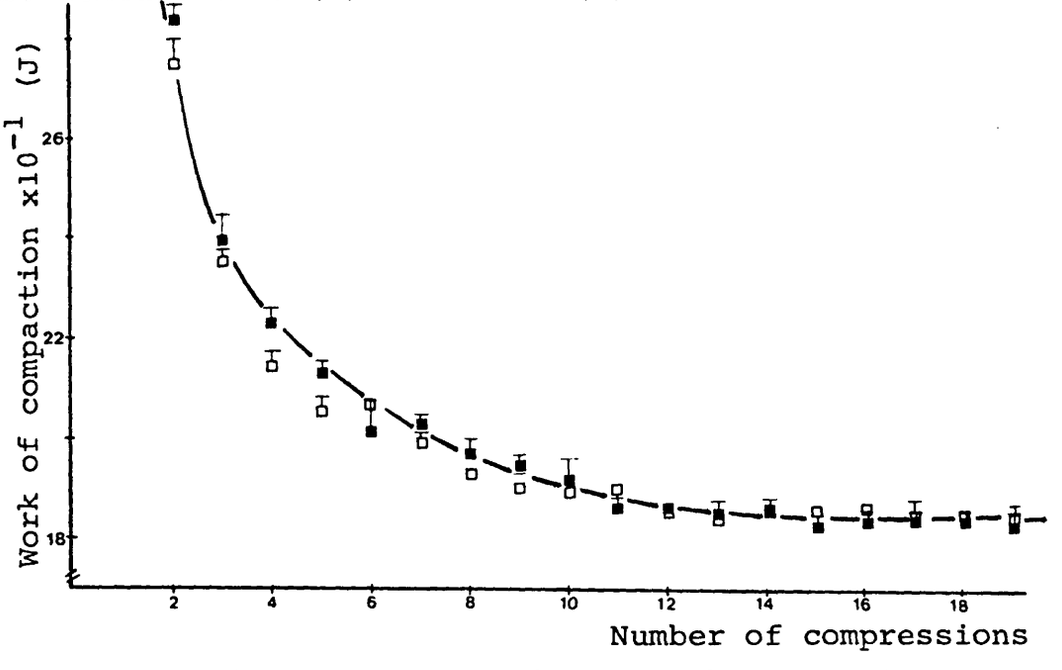

Figure 63(a & b). Relationship between the work of compaction and number of compressions for Microtal compressed at 20kN and four different compaction rates. Compaction rate is effectively represented by contact time, lower the contact time, higher the compaction rate.

combination of elastic and that required for irreversible deformation. These results correspond with those for Avicel,i.e. the work performed during the second compression is an over-estimation of work required for elastic deformation, consequently resulting in an under-estimation of true work of compaction.

Figs. 61, 62 and 63 (a, b) show similar decay profiles when the compaction force was increased to 12kN, 16kN and 20kN respectively, further confirmation that true work of compaction can only be obtained using constant values of elastic work, which were obtained long after the second compression.

The measured decay in work of compaction was due to a composite of the decay of applied force and tablet deformation on re-compression. This is shown in Figs. 64 (a and b) and 65 (a and b), at compaction forces of approximately 8kN and 20kN respectively. Similar profiles were also obtained at 12 and 16kN compaction force. These profiles are similar to those for Avicel (Figs. 58 and 59). However, the degree of force decay was greater for Microtal than for Avicel tablets at all compaction forces and rates of compaction. For example, Microtal compressed at approximately 8kN compaction force (Fig. 64a), the force applied decreased from 8500 N to a constant value of 5200 N after the 11th compression. In the case of Avicel (Fig. 58a), the decrease was from 8200 N to a constant value of 7400 N, after the 8th compression. This would suggest that a more resistant structure was produced by Avicel on re-compression, probably due to rapid achievement of a structure with ultimate minimal porosity. Table 9 summarises the results for Microtal and indicates once again

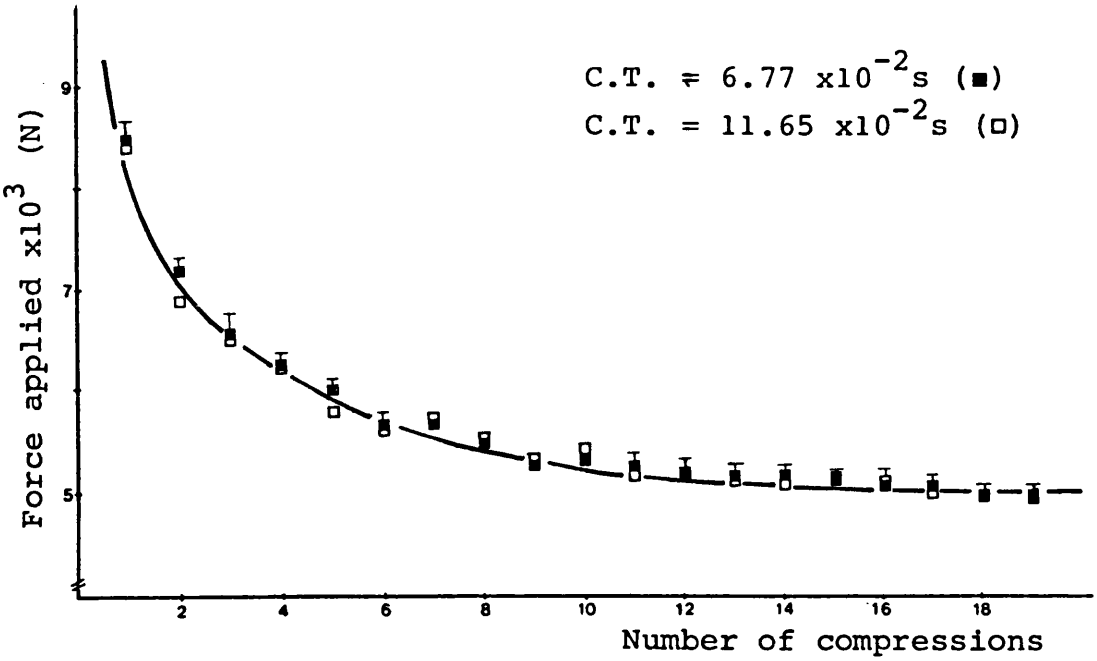

Figure 64a. Relationship between the maximum force applied and the number of compressions for Microtal compressed at an initial force of approximately 8kN. C.T. refers to contact time.

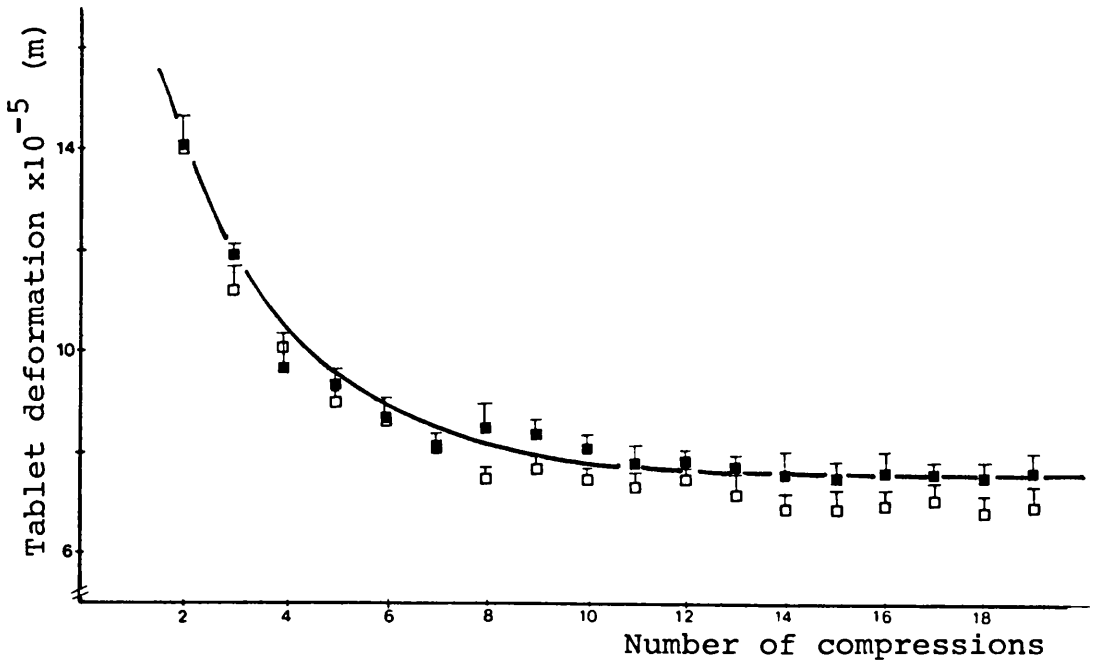

Figure 64b. Relationship between the tablet deformation and number of compressions for Microtal compressed at a compaction force of approximately 8kN. Symbols as above.

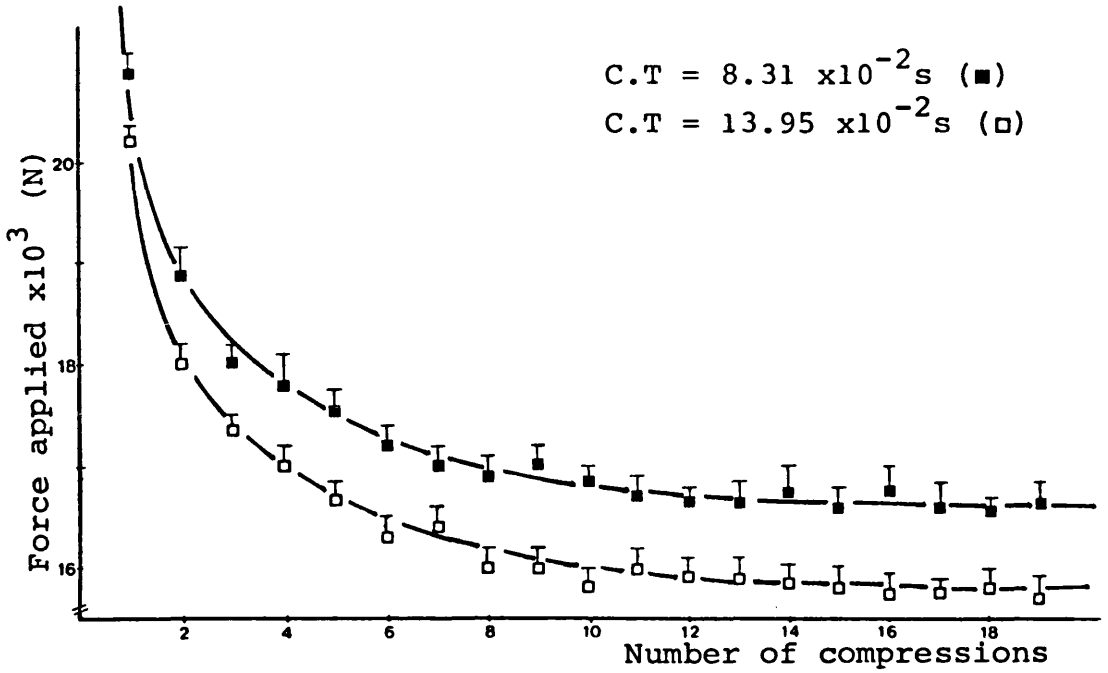

Figure 65a. Relationship between the maximum force applied and the number of compressions for Microtal compressed at an initial force of approximately 20kN. C.T. refers to contact time.

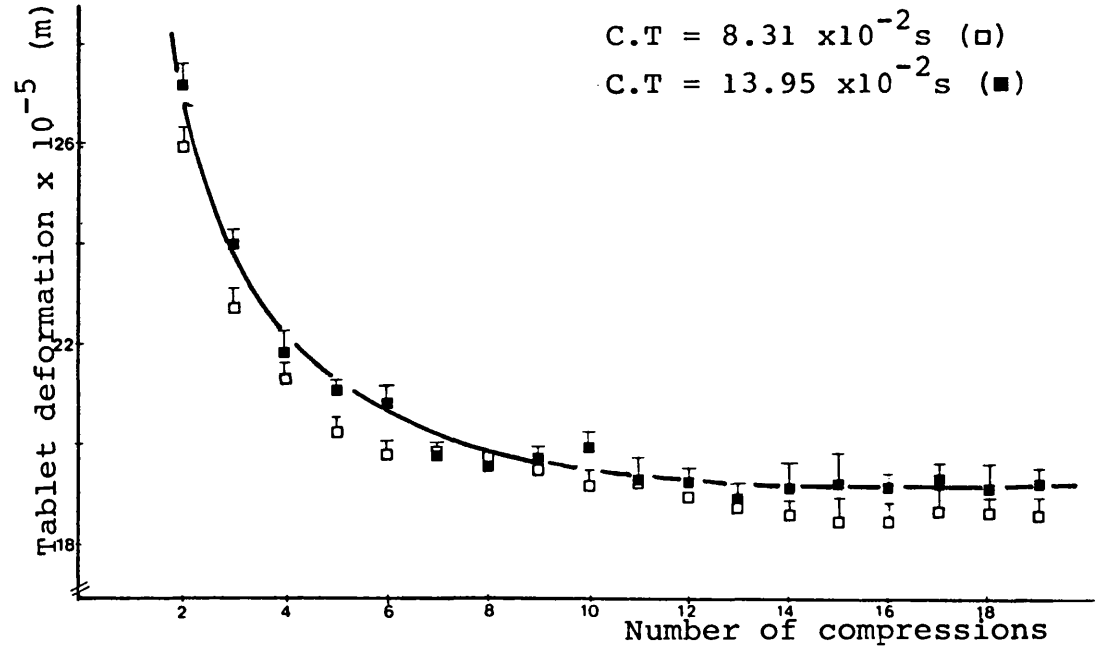

Figure 65b. Relationship between the tablet deformation and number of compressions for Microtal compressed at a compaction force of approximately 20kN.

Comp. force kN	Contact time 1*E-2 s	Total work J	Constant elastic work J	2nd Comp. work J	True work of Comp. J
8	11.65	5.63	0.38	0.70	5.25
	10.11	5.24	0.43	0.79	4.81
	7.68	4.92	0.30	0.60	4.62
	6.77	5.31	0.40	0.76	4.91
12	12.34	7.97	0.64	1.20	7.33
	10.96	7.87	0.75	1.33	7.12
	8.60	8.10	0.63	1.21	7.47
	7.56	8.25	0.73	1.31	7.52
16	13.43	10.98	1.14	1.92	9.84
	11.81	10.65	1.24	2.03	9.41
	8.94	10.93	1.09	1.88	9.84
	7.89	10.64	1.10	1.89	9.54
20	13.95	13.74	1.84	2.85	11.90
	12.47	12.98	1.85	2.75	11.13
	9.18	12.92	1.60	2.59	11.32
	8.32	13.34	1.67	2.60	11.67

Table 9. Summary of the work of compaction data for Microtal at four compaction forces and rates of compaction (effectively represented by contact times). True work of compaction was calculated by subtracting the constant value of elastic work from the total work.

that the assumption that work performed during the second compression is purely that required to cause elastic deformation is invalid and would lead to an over-estimation of the work required for elastic deformation. Consequently, this would lead to an under-estimation of the true work of compaction for Microtal. The true works of compaction in Table 9 were calculated by subtracting the constant work of compaction from the total work.

3.1.2.3 True Work of Compaction for Emcompress

Figs. 66, 67, 68 and 69 (a and b) show the relationship between the work performed after the first compression with increasing number of compressions for Emcompress at approximately 8, 12, 16 and 20kN compaction force respectively and four different compaction rates. The decay profiles in all these figures were similar and show a drop in the work performed at the second compression to a constant value after approximately the 13th compression. Hence these profiles were very similar to those for Microtal (Figs. 60, 61, 62 and 63) and show again that the work performed at the second compression was not purely that required for elastic deformation, but a combination of that required for elastic and irreversible deformations and it was not until the 13th compression, that all possible irreversible deformation was complete at that particular compaction force.

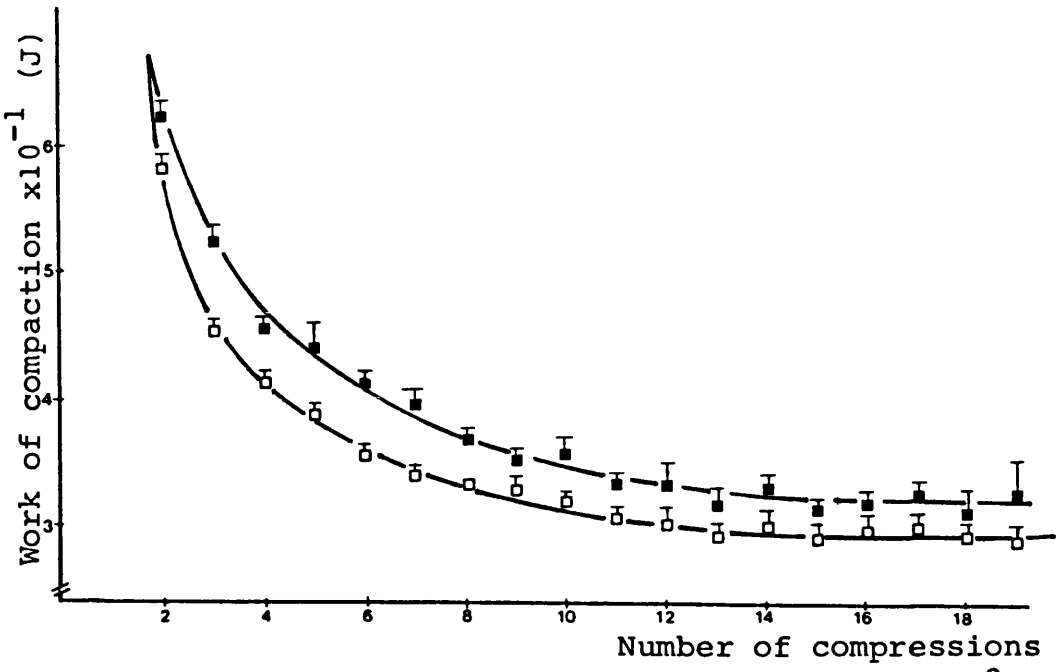

a. Contact time (□) 12.36 and (■) 8.35 seconds x10^{-2}.

b. Contact time (■) 10.57 and (□) 7.20 seconds x10^{-2}.

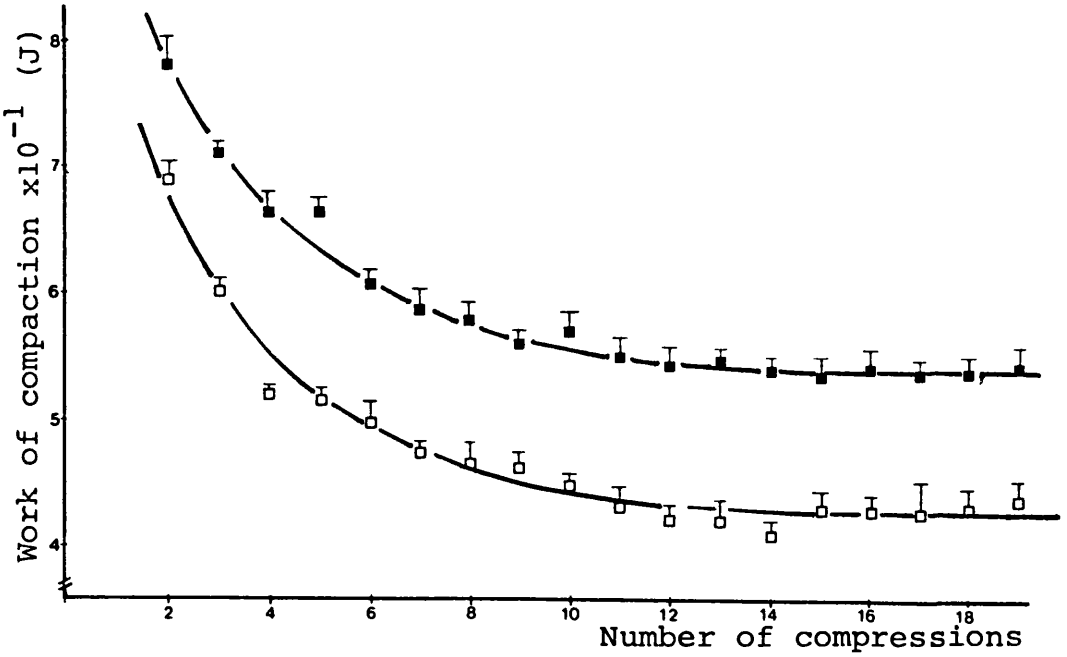

Figure 66(a & b). Relationship between the work of compaction and number of compressions for Emcompress compressed at 8kN and four different compaction rates. Compaction rate is effectively represented by contact time, lower the contact time, higher the compaction rate.

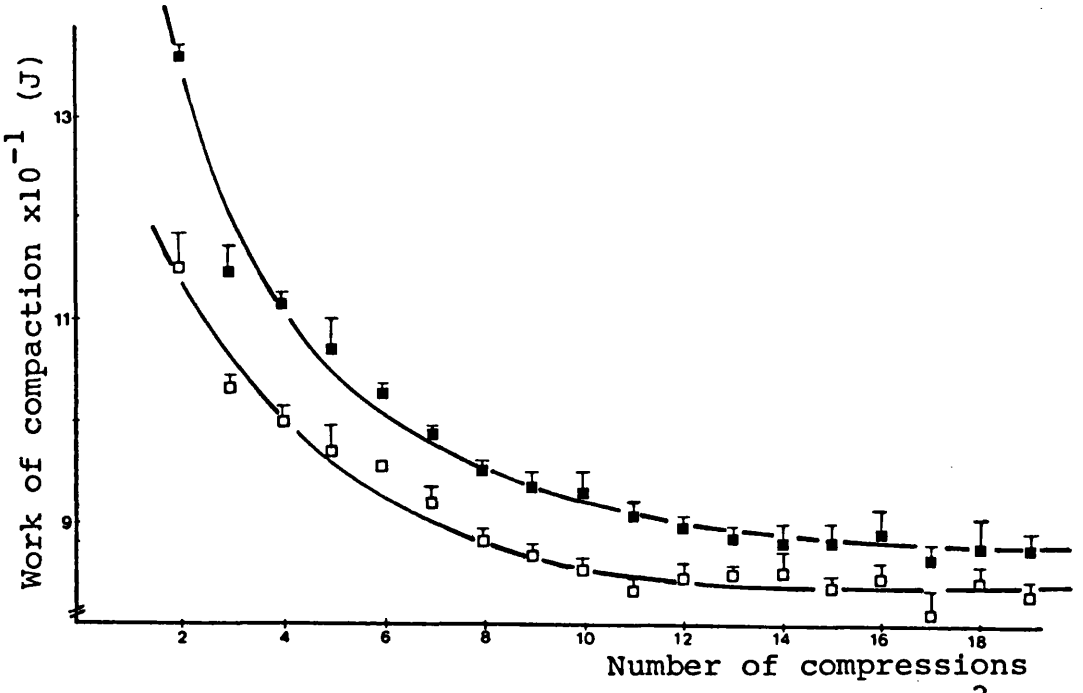

a. Contact time (■) 11.35 and (□) 7.44 seconds x10^{-2}.

b. Contact time (□) 13.78 and (■) 8.84 seconds x10^{-2}.

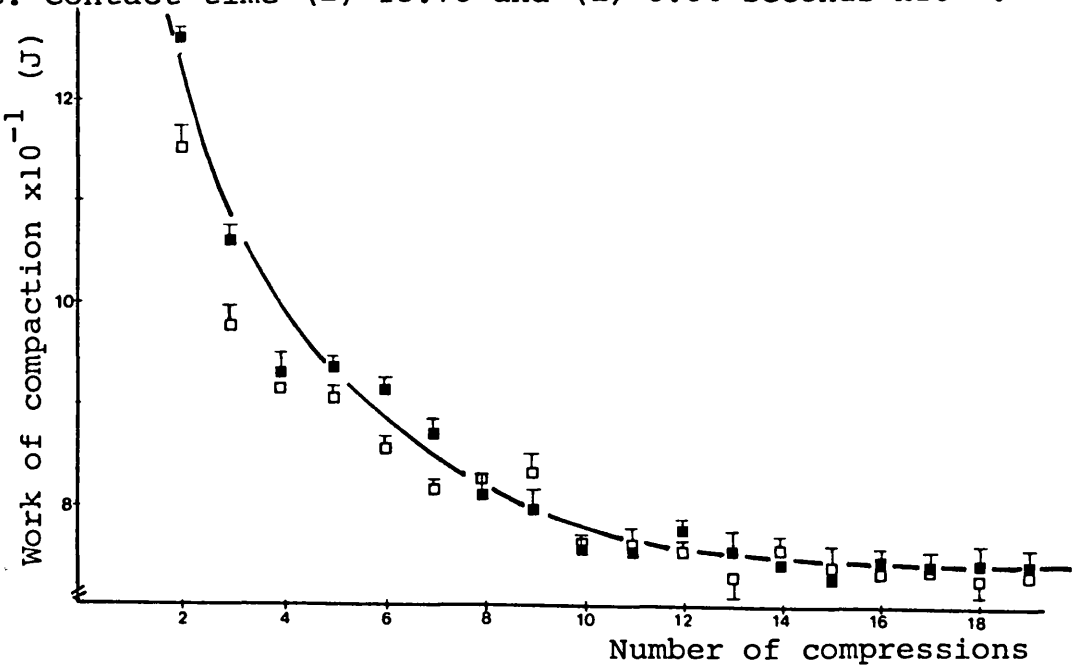

Figure 67 (a & b). Relationship between the work of compaction and number of compressions for Emcompress compressed at 12kN and four different compaction rates. Compaction rate is effectively represented by the contact time, lower the contact time, higher the compaction rate.

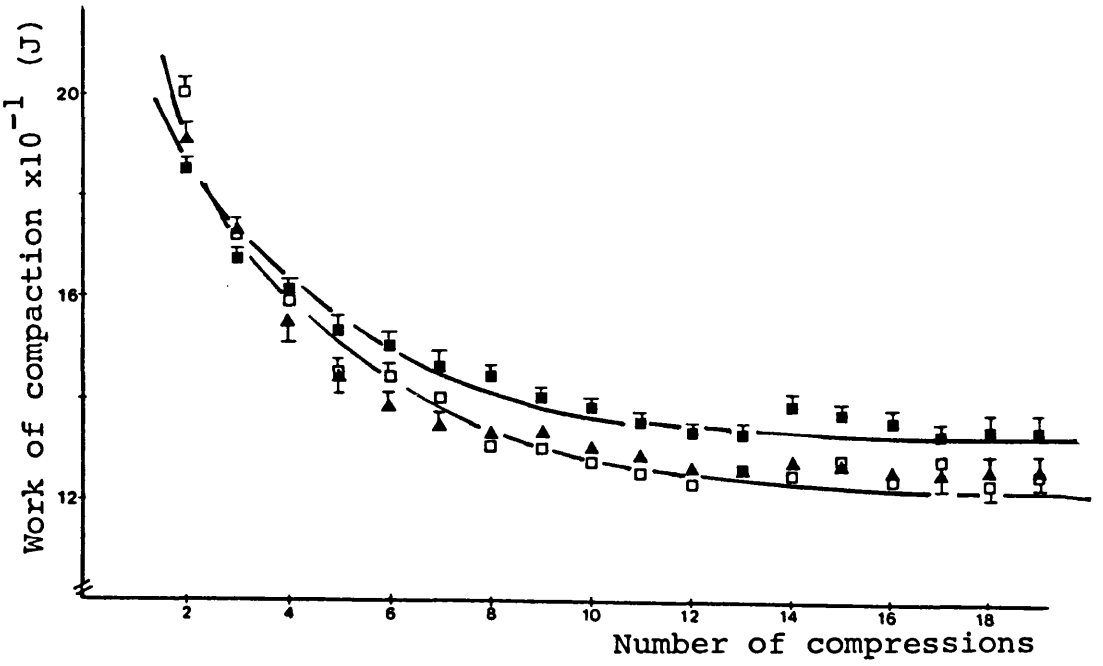

a. Contact time (□) 14.00, (▲) 9.30 and (■) 8.26 seconds x10^{-2}.

b. Contact time (■) 11.89 seconds x10^{-2}.

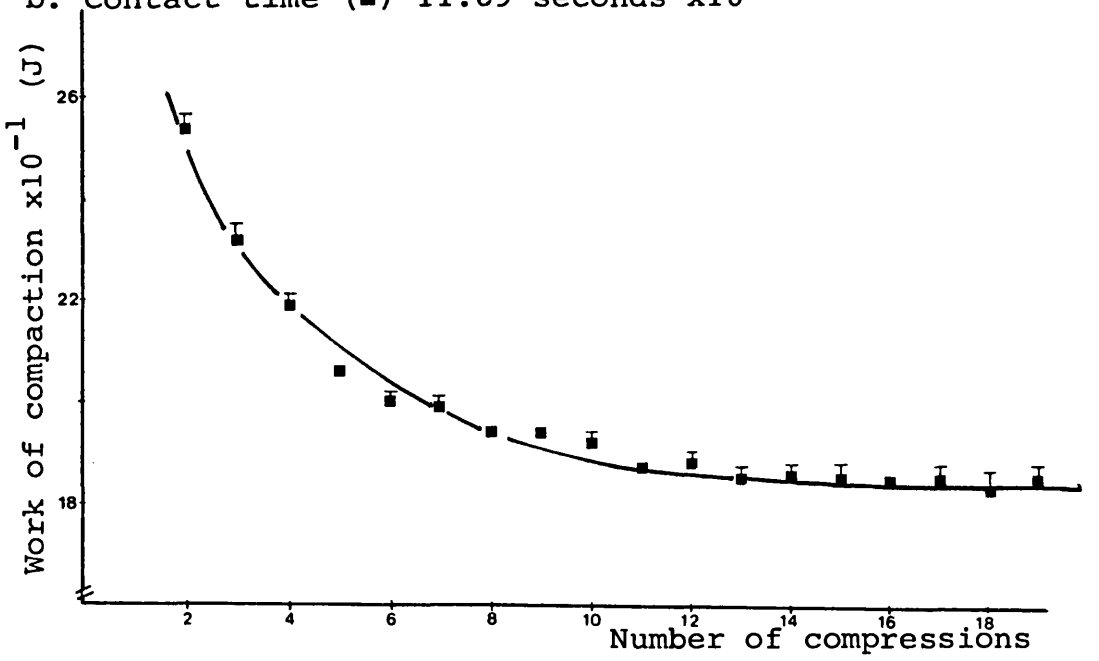

Figure 68 (a & b). Relationship between the work of compaction and number of compressions for Emcompress compressed at 16kN and four different compaction rates. Compaction rate is effectively represented by the contact time, lower the contact time, higher the compaction rate.

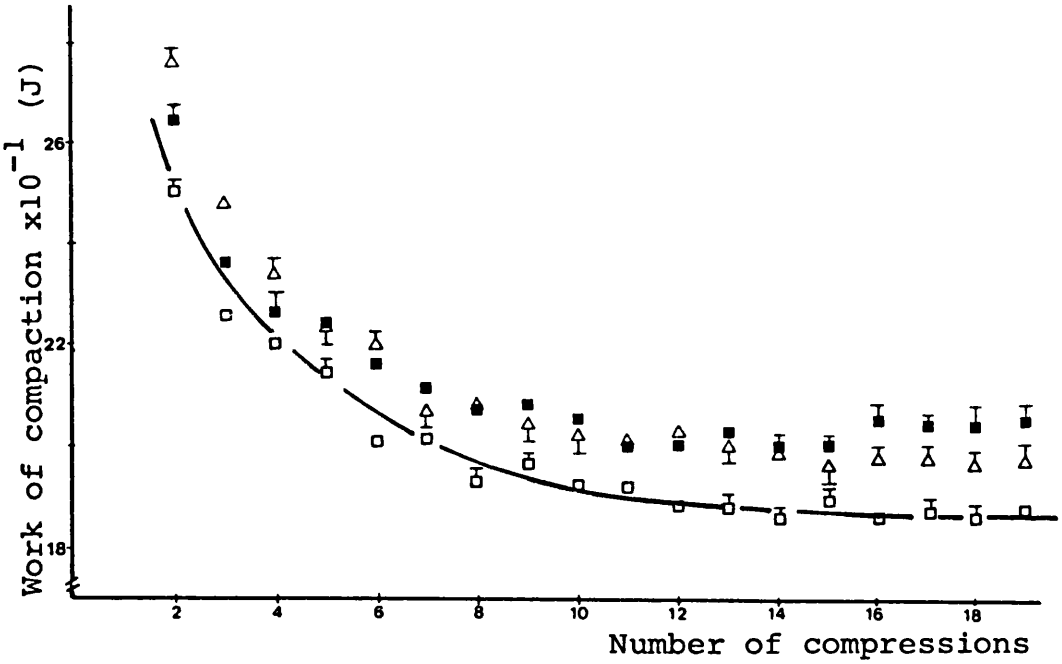

a. Contact time (□) 14.41, (△) 10.10 and (■) 8.25 seconds x10^{-2}.

b. Contact time (■) 12.76 seconds x10^{-2}.

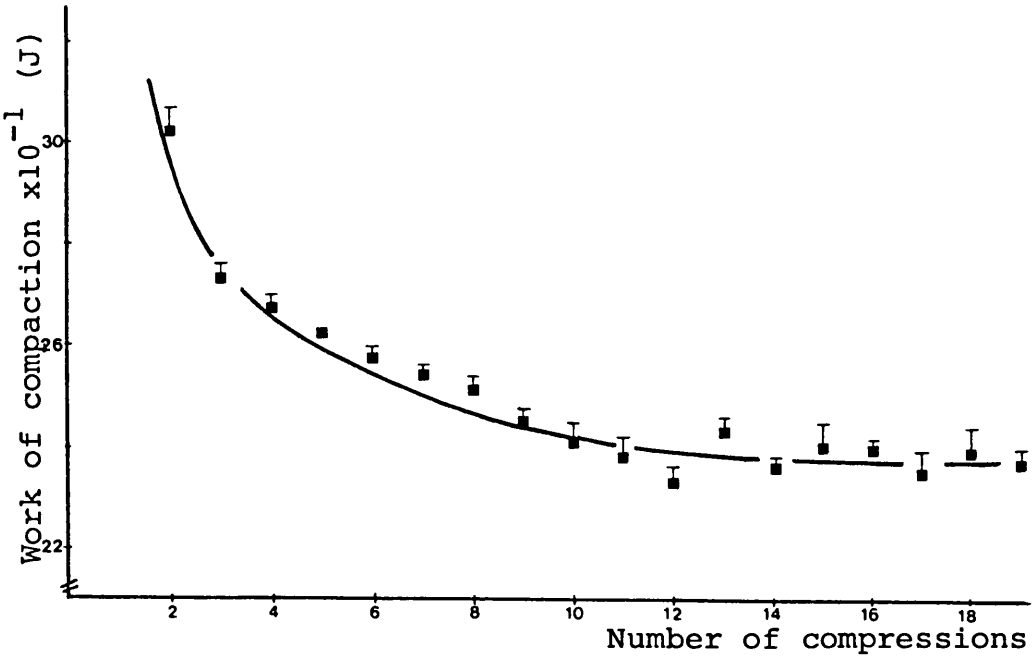

Figure 69(a & b). Relationship between the work of compaction and number of compressions for Emcompress compressed at 20kN and four different compaction rates. Compaction rate is effectively represented by the contact time, lower the contact time, higher the compaction rate.

Comp. force kN	Contact time 1*E-2 s	Total work J	Constant elastic work J	2nd Comp. work J	True work J
8	12.36	5.51	0.29	0.58	5.22
	10.57	5.21	0.54	0.78	4.67
	8.35	5.36	0.34	0.62	5.02
	7.20	5.49	0.43	0.69	5.06
12	13.78	8.26	0.74	1.15	7.52
	11.35	7.22	0.87	1.36	6.35
	8.84	7.75	0.74	1.26	7.01
	7.44	7.66	0.84	1.15	6.82
16	14.00	10.20	1.25	2.00	8.95
	11.89	11.05	1.85	2.53	9.20
	9.30	10.10	1.25	1.91	8.85
	8.26	10.00	1.32	1.85	8.68
20	14.41	12.04	1.85	2.50	10.19
	12.76	12.04	2.37	3.02	9.67
	10.10	12.84	1.96	2.76	10.88
	8.25	11.91	2.10	2.64	9.81

Table 10. Summary of work of compaction data for Emcompress at four different compaction forces and compaction rates, the latter represented by contact time, faster compaction rates will give shorter contact times.

The reason for the decay in the work of compaction from the second compression to a constant value after the 13th compression was inferred from the relationship between the force applied and tablet deformation with number of compressions (Figs. 70 and 71). Again, these profiles show a similar decay curve to those obtained for Microtal (Figs. 64 and 65). Table 10 summarises the results for Emcompress and shows the values of true work of compaction.

The results for all three direct compression excipients studied show that use of the work performed during the second compression resulted in an over-estimation of the work required for elastic deformation. Hence, in true work determinations it is imperative that a constant value of work be established before subtracting it from the total work and where a constant value is not established, it was found that an error of approximately 6-10% could be experienced in accepting the work performed in second compression as purely elastic (Tables 8, 9 and 10). The true work for Avicel PH102 was found to be higher than that for either Microtal or Emcompress, at all compaction forces studied, suggesting that the greatest amount of irreversible work was performed in the compaction of Avicel (Tables 8, 9 and 10). The values for Microtal and Emcompress were similar, suggesting that the irreversible deformation for these two direct compression excipients was similar. This appears to contradict results described in sections 3.2.2.1 and 3.1 where Microtal tablets were found to possess much higher NWF values than Emcompress (Figs. 40 and 81) indicating that the degree of

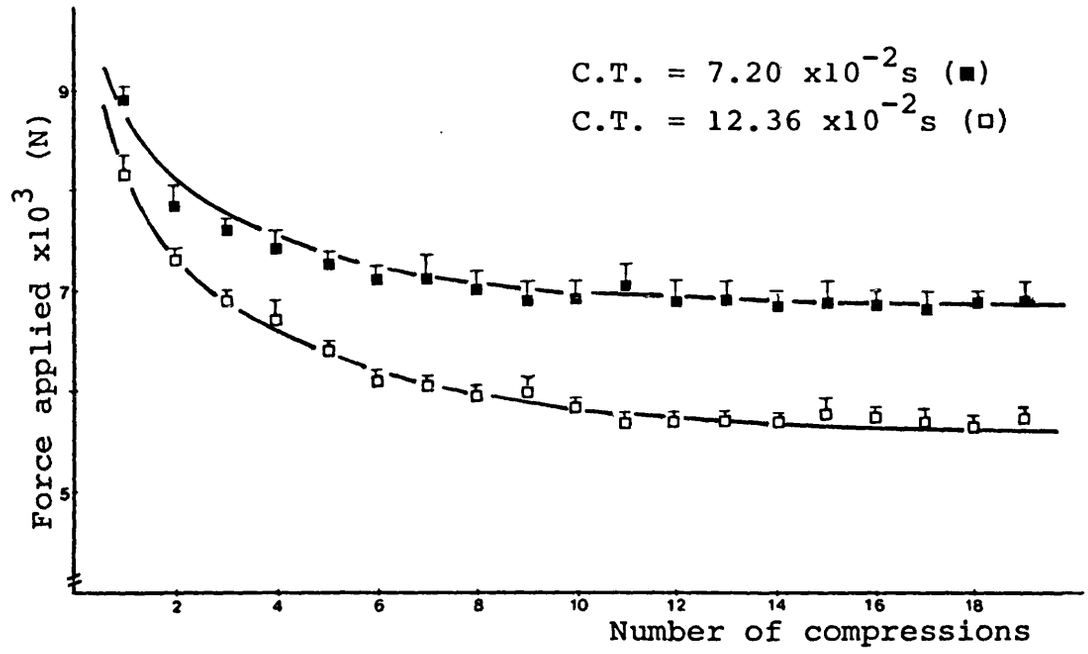

Figure 70a. Relationship between the maximum force applied and the number of compressions for Emcompress compressed at an initial force of approximately 8kN. C.T. refers to contact time.

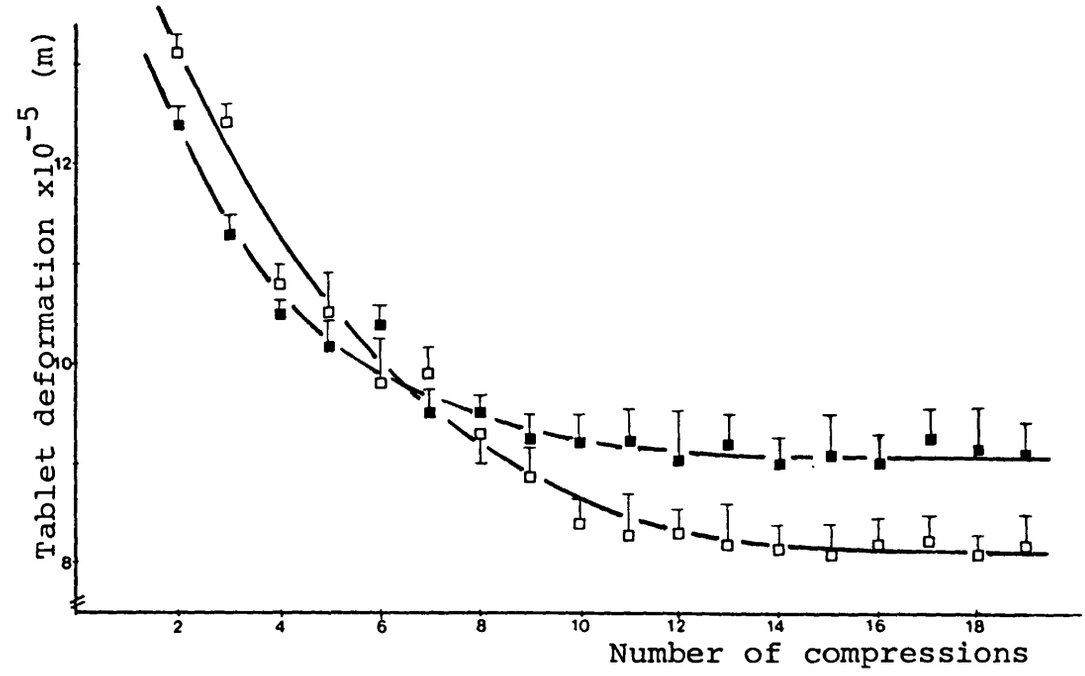

Figure 70b. Relationship between the tablet deformation and number of compressions for Emcompress compressed at a compaction force of approximately 8kN. Symbols as above.

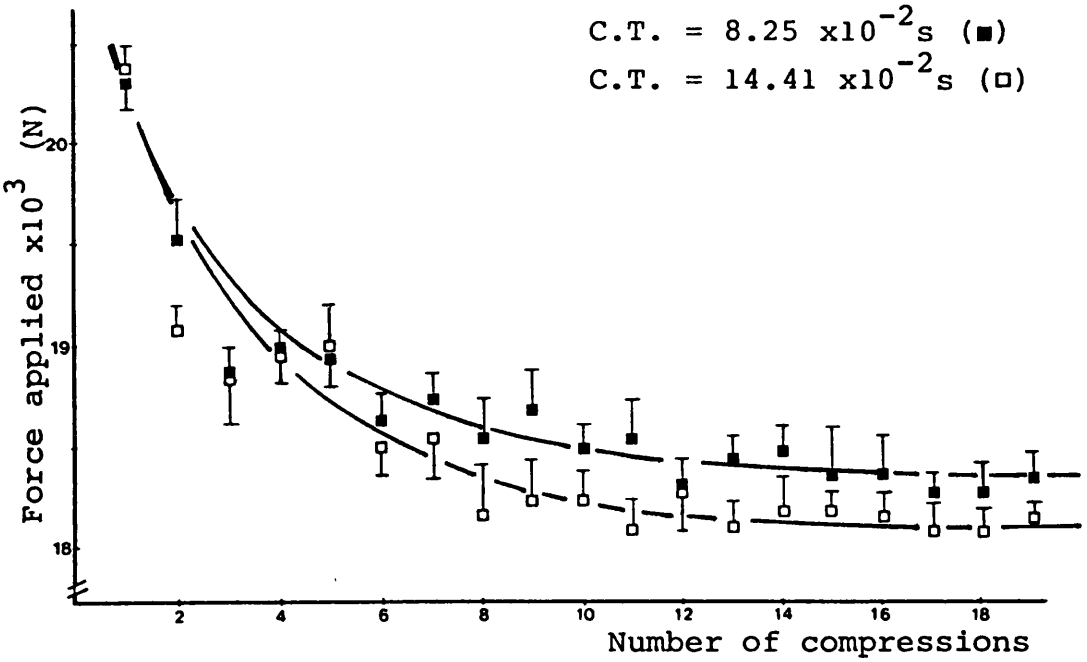

Figure 71a. Relationship between the maximum force applied and the number of compressions for Emcompress compressed at an initial force of approximately 20kN. C.T. refers to contact time.

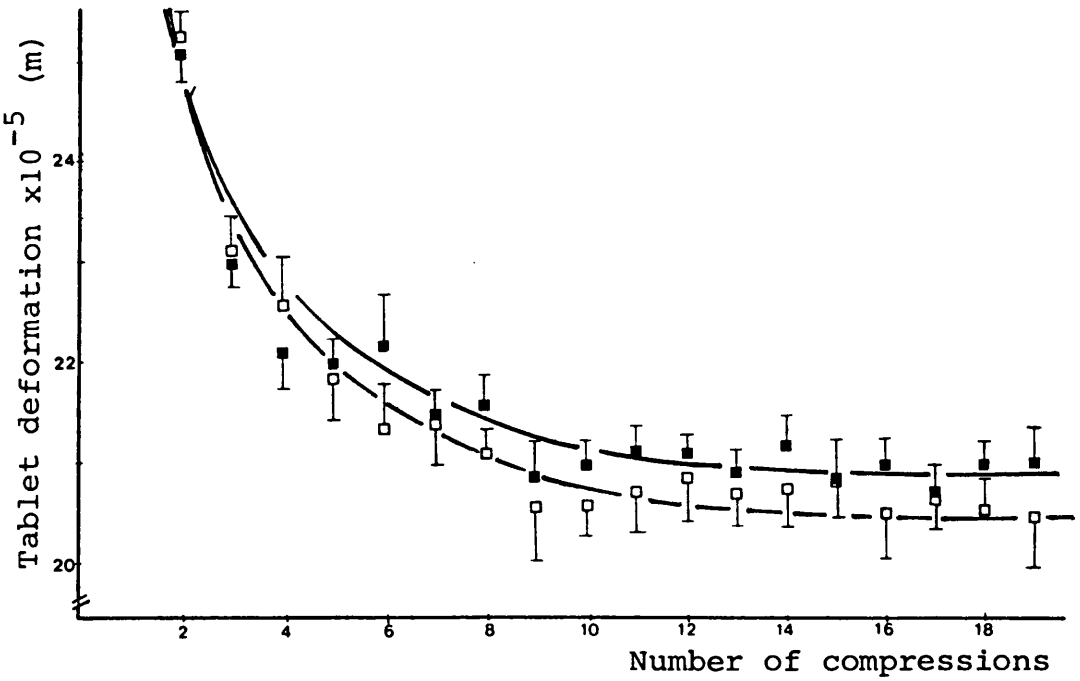

Figure 71b. Relationship between the tablet deformation and number of compressions for Emcompress compressed at a compaction force of approximately 20kN. Symbols as above.

inter-particle bonding was greater in Microtal than for Emcompress. Thus it was concluded that true work of compaction does not always give an indication of the degree of irreversible deformation possible in excipients and this is in agreement with the results recently reported by Ragnarsson and Sjogren (1985), who have stated true work of compaction "to be a poor measure of the plastic properties of a substance". However, these workers found it useful as a test of inter-batch variations in compaction behaviour of materials because true work was influenced by particle interaction.

3.1.3. Power of Compaction.

Force-displacement curves do not take into account the time over which the force has been applied, but it is frequently reported and well documented that time-dependent effects do occur on compaction (David and Augsberger, 1977; Rees and Rue, 1978b). Consequently, Armstrong et al. (1983) proposed a measure of the power expended during compression obtained by dividing the area under the FD curve by the time over which the force is applied. However, no data has been presented by these workers. Power of compaction was calculated according to equation 33 in order to avoid error in power of compaction determinations.

$$\text{Power of compaction} = \frac{\text{True work}}{\text{time}} \quad \text{-------- Equation 33.}$$

where true work was determined according to equation 34.

$$\text{True work} = (\text{Total work} - \text{elastic work}) \quad \text{-------- Equation 34.}$$

where elastic work is represented by the constant value of work

Comp. force	Contact time 1*E-2 s	Power(1) J/s	Power(2) J/s	% Error
8kN	15.10	58.7 (0.3)	57.7 (0.5)	5.4
	11.52	75.5 (0.7)	70.4 (1.2)	6.8
	10.70	87.8 (0.2)	86.5 (0.5)	5.3
	9.17	109.1 (0.9)	103.2 (0.3)	5.4
16kN	16.72	81.5 (1.1)	77.5 (0.8)	4.9
	12.97	95.4 (0.5)	89.2 (0.9)	6.5
	11.75	122.0 (1.4)	115.3 (1.1)	5.5
	9.90	145.4 (1.7)	137.7 (1.5)	5.3

Table 11. Influence of the method used for calculating power of compaction for Avicel PH102. Power(1) refers to the determinations according to equation 33, while Power(2) is based on determinations using the 2nd compression work to represent true work of compaction. The percentage error experienced in using the latter method of calculating power of compaction is also tabulated. The power values are the means of five determinations and corresponding standard deviations are given in parentheses.

Comp. force	Contact time 1*E-2 s	Power(1) J/s	Power(2) J/s	% Error
8kN	11.65	46.0 (0.5)	44.0 (0.3)	5.3
	10.10	49.0 (1.1)	47.0 (0.2)	4.1
	7.68	61.5 (0.7)	58.1 (0.3)	5.1
	6.77	74.3 (0.8)	70.4 (1.5)	5.3
20kN	13.95	85.3 (1.9)	78.1 (0.4)	6.3
	12.47	89.3 (0.7)	82.0 (1.1)	8.2
	9.18	123.3 (1.8)	112.5 (0.9)	8.8
	8.32	140.4 (2.3)	129.2 (0.7)	8.0

Table 12. Influence of the method used for calculating power of compaction for Microtal tablets. Power(1) refers to the determination according to equation 33, while Power(2) is based on determinations using the second compression to calculate true work of compaction. The percentage error experienced in accepting the latter method is also tabulated. Power values are the mean of five determinations with corresponding standard deviations in parentheses.

obtained after 10 compressions in the case of Avicel and 13 compressions in the case of Microtal and Emcompress.

Tables 11, 12 and 13 show the error in power of compaction determinations if the work performed during the second compression was used in the true work determinations. For all three direct compression excipients studied, error in power of compaction determinations was between 5-8%. Similar error levels were also found at intermediate compaction forces.

Comp. force	Contact time 1*E-2 s	Power(1) J/s	Power(2) J/s	% Error
8kN	12.36	42.2 (0.4)	39.9 (0.6)	5.5
	10.57	44.2 (0.3)	41.9 (0.8)	5.2
	8.35	60.1 (1.4)	56.8 (0.5)	5.5
	7.20	70.3 (1.5)	66.7 (0.3)	5.1
20kN	14.41	70.7 (0.8)	66.3 (1.4)	6.2
	12.76	75.8 (0.9)	70.7 (0.6)	6.7
	10.10	107.7 (2.2)	99.8 (0.5)	7.3
	8.25	118.9 (1.7)	112.4 (0.8)	5.5

Table 13. Influence of the method of calculating power of compaction for Emcompress. Power(1) was determined according to equation 33, while Power(2) is based on determinations using the work performed during the second compression to calculate true work of compaction. The percentage error experienced in accepting the latter method is tabulated. The power values are the mean of five determinations and corresponding standard deviations are given in parentheses.

The measurement, power of compaction, takes into account the time during which work was performed and this is also known to be an important factor when transferring formulations from slow to high speed tableting machines. The contact time effectively represents the rate of compaction, higher compaction rates giving shorter contact times. Predictably, power of compaction values increased when the compaction rate was increased, since true work was carried out in a shorter time interval. Fig. 72 shows the relationship between power of compaction and contact time for Avicel, Microtal and Emcompress at a compaction force of approximately 8kN. Due to the limitations of the motor in the tableting machine used in this study, the fastest compaction rate was approximately 80 tablets per minute and the slowest was 35 tablets per minute, thus power of compaction was determined for just four points. These points suggest that the relationship between power and contact time can represented by a curve (Fig. 72). Such a plot could be used to elucidate power of compaction values at higher compaction rates, if the plot was extrapolated to contact times corresponding to those experienced on a faster tableting machine. For example Microtal, if compressed on a faster machine producing a contact time of, say, 6.0*E-2 seconds, would be predicted to have corresponding power of compaction value of approximately 90 J/s (or Watt).

Fig. 73 shows the relationship between tensile strength of Microtal and Emcompress tablets at 8kN compaction force with power of compaction. It is proposed that by extrapolating such a

plot, the tensile strengths could be estimated at higher or lower power of compaction values. Using the previous example, for Microtal (Fig. 72) compressed on a faster machine with a power of compaction value of 90 J/s and using Fig. 73, the tensile strength of these tablets could be predicted to be approximately 0.55 MPa. These plots (Figs. 72 and 73) would be useful in relating probable tensile strength of tablets compressed on a faster machine using data obtained from a slower machine. Such information, if accurate, would be invaluable to formulators, when transferring formulations from a slow to a high speed tableting machine.

Fig. 73 shows that as power of compaction increased, (implying an increase in compaction rate) a fall in the tensile strength of Microtal tablets was observed. This was due to the fact that the time over which the force was applied was reduced. David and Augsberger (1977) have reported that reducing the time over which the force was applied results in a decrease in the tensile strength of tablets due to a reduction in the time dependent deformation. This suggests that Microtal possesses some degree of time dependent deformation. This observation supports the findings in section 3.2.2.1 (Fig. 81), which show that Microtal possesses high NWF values. No change in tensile strength was observed for Emcompress (Fig. 73), indicating that Emcompress probably does not undergo time dependent deformation.

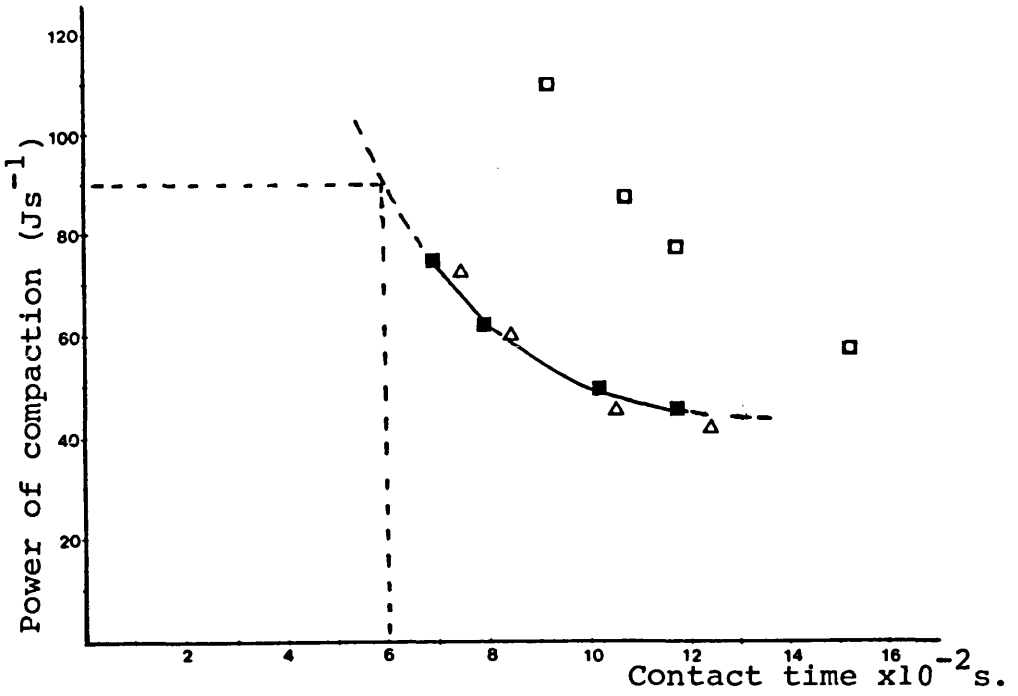

Figure 72. Relationship between power of compaction and contact time, at a compaction force of 8kN, for (□) Avicel PH102, (■) Microtal and (△) Emcompress.

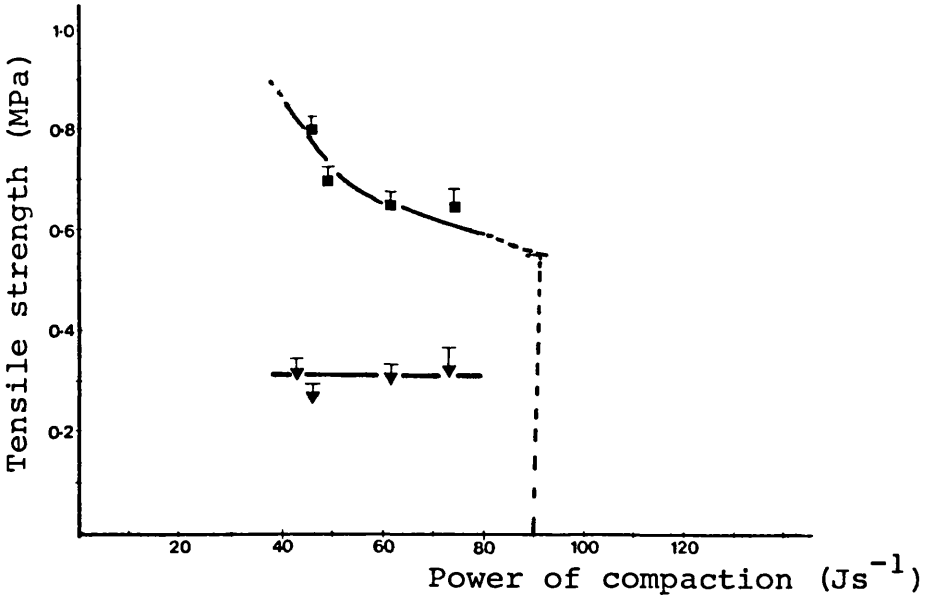

Figure 73. Relationship between tensile strength of (■) Microtal and (▼) Emcompress tablets compressed at a compaction force of 8kN and power of compaction.

3.1.4 Creep Analysis of Some Direct Compression Excipients.

The rheological phenomenon known as creep may be defined as slow and progressive deformation of a material under constant stress. Creep is different from stress relaxation, which is a time dependent reduction in stress under constant strain. However, the mechanisms involved in these two processes are closely related, however creep analysis provides information about the elastic, visco-elastic and visco-plastic properties of a material. Creep tests carried out by metallurgists involve determining the strain, known as "creep strain" and plotting it versus time (Seitz, 1943). Such plots (creep curves) are characteristic of the material at that particular load and temperature (Hult, 1966).

Examination of the rheological characteristics of semi-solid material is carried out by performing creep tests as discussed above in section 1.7. In this study, powders studied were treated as analogous to semi-solids, thus the theory of creep measurement was applied (Equation 25). The behaviour of a semi-solid may be divided into three regions: elastic, visco-elastic and visco-plastic or viscous behaviour. Of these only viscous behaviour does not truly exist in solids, but can be envisaged to be similar to irreversible deformation (plastic or brittle deformation). Formation of a tablet with adequate mechanical properties is dependent on inter-particle bonding. The areas of true contact are both formed and destroyed during the compression and decompression stages of tableting and the stages are largely dependent on the rheological properties of the

powders compressed. Knowledge of these rheological properties, especially for direct compression excipients, may give information regarding the compactibility of powders.

Preliminary investigations showed that creep curves for all direct compression excipients were similar in profile to the theoretical curve (Fig. 20). These curves were also similar to those obtained for semi-solids, for example for white soft paraffin (Barry and Grace, 1971c). The direct compression excipients examined differ in their compactibility and were selected to provide for a sensitivity evaluation of the creep test and to determine differences in the rheological characteristics of these excipients. The hypothesis tested was that the linear portion (C-D, Fig. 20) provides a measure of the degree of plastic deformation in powders.

Two further parameters were determined from creep curves, the slope of the linear portion of the B-C region (Fig. 20) and its corresponding intercept on the compliance axis. Creep curves were determined at three stress levels (39.5, 79 and 118.5 MPa) and two load rates (3 and 14kN/minute). Tables 14-16 (a and b) show the three rheological parameters determined from the creep curves.

The intercept on the ordinate was used to indicate the degree of elastic behaviour of a material. In terms of a canonical model, this represented the instantaneous stretching of the spring of one Maxwell unit when a load is applied (Fig. 21). The largest intercept value was obtained with Starch 1500, suggesting that this material undergoes the greatest degree of

Material	C-D 1*E-10	B-C 1*E-8	Intercept 1*E-7
Emcompress	0.31 (0.05)	----	0.48 (0.06)
Emcompress(A)	3.50 (0.36)	2.14 (0.37)	1.68 (0.32)
Microtal	4.20 (0.16)	1.90 (0.30)	1.38 (0.28)
Avicel PH102	6.25 (0.18)	3.62 (0.54)	3.50 (0.23)
Starch 1500	8.71 (0.27)	3.50 (0.42)	5.60 (0.23)

Table 14a. Slopes of two regions of the creep curve and the intercept when subjected to a constant stress of 39.5MPa and load rate of 3kN/minute. The figures are the means of five determinations and figures in parentheses are corresponding standard deviations. Emcompress(A) refers to a binary mixture of 50% w/w Avicel PH102 in Emcompress.

Material	C-D 1*E-10	B-C 1*E-8	Intercept 1*E-7
Emcompress	0.49 (0.04)	----	0.38 (0.09)
Emcompress(A)	4.07 (0.30)	2.34 (0.16)	3.10 (0.46)
Microtal	4.30 (0.38)	2.20 (0.11)	2.80 (0.47)
Avicel PH102	6.10 (0.69)	3.10 (0.28)	6.20 (0.25)
Starch 1500	9.20 (1.02)	2.13 (0.61)	8.51 (1.00)

Table 14b. Slopes of two regions of the creep curve and the intercept when the materials were subjected to a constant stress of 39.5MPa and load rate of 14kN/minute. Figures in parentheses are corresponding standard deviation of the mean, where n = 5. Emcompress(A) refers to a binary mix of 50% w/w Avicel PH102 in Emcompress.

Material	C-D 1*E-10	B-C 1*E-9	Intercept 1*E-8
Emcompress	0.28 (0.10)	----	0.20 (0.03)
Emcompress(A)	1.70 (0.15)	8.66 (0.80)	2.50 (0.26)
Microtal	2.00 (0.17)	7.72 (0.22)	1.63 (0.13)
Avicel PH102	3.00 (0.14)	12.00 (0.49)	2.40 (0.22)
Starch 1500	3.42 (0.25)	15.20 (0.54)	3.84 (0.31)

Table 15a. Slopes of two regions of the creep curve and the intercept when the powders were subjected to a constant stress of 79MPa at a load rate of 3kN/minute. The mean of five determinations and corresponding standard deviations in parentheses have been tabulated. Emcompress(A) refers to a binary mix of 50% w/w of Avicel PH102 in Emcompress.

Material	C-D 1*E-10	B-C 1*E-8	Intercept 1*E-7
Emcompress	0.28 (0.04)	----	2.70 (0.60)
Emcompress(A)	1.67 (0.20)	6.90 (0.72)	11.00 (0.50)
Microtal	2.31 (0.07)	8.50 (0.60)	8.00 (0.19)
Avicel PH102	2.78 (0.11)	10.30 (0.10)	15.30 (0.30)
Starch 1500	3.30 (0.17)	19.00 (2.60)	19.40 (0.76)

Table 15b. Slopes of two regions of the creep curve and the intercept when powders have been subjected to a constant stress of 79MPa at a load rate of 14kN/minute. Emcompress(A) as before. Mean of five determinations with corresponding standard deviations are given in parentheses.

Material	C-D 1*E-11	B-C 1*E-9	Intercept 1*E-9
Emcompress	2.11 (0.50)	----	0.27 (0.06)
Emcompress(A)	12.10 (1.70)	4.90 (0.20)	1.22 (0.20)
Microtal	13.00 (0.50)	3.50 (0.20)	3.30 (0.40)
Avicel PH102	15.00 (0.30)	5.50 (0.60)	9.90 (0.70)
Starch 1500	17.70 (1.20)	5.30 (0.90)	14.30 (0.90)

Table 16a. Slopes of two regions of the creep curve and the intercept when the powders were subjected to a constant stress of 118.5MPa and load rate of 3kN/minute. Mean of five determinations are tabulated and figures in parentheses are corresponding standard deviations. Emcompress(A) refers to binary mix of 50% w/w Avicel PH102 in Emcompress.

Material	C-D 1*E-11	B-C 1*E-9	Intercept 1*E-9
Emcompress	2.45 (0.50)	----	1.73 (0.41)
Emcompress(A)	12.10 (1.30)	5.70 (1.20)	3.00 (0.50)
Microtal	12.75 (0.55)	5.65 (0.18)	2.64 (0.43)
Avicel PH102	14.84 (0.40)	6.79 (0.30)	5.10 (0.60)
Starch 1500	16.50 (1.54)	8.50 (1.40)	7.23 (0.72)

Table 16b. Slopes of two regions of the creep curve and the intercept when the powders were subjected to constant stress of 118.5MPa at load rate of 14kN/minute. The slope and intercepts are the mean of five determinations and figures in parentheses are corresponding standard deviations. Emcompress(A) refers to a binary mix of 50% w/w Avicel PH102 in Emcompress.

elastic deformation and this was true for all stress levels and rates of loading (Tables 14-16). This was followed by Avicel PH102 which in turn was followed by Microtal and 50% w/w Avicel in Emcompress having approximately equal amounts of elastic properties. The lowest elasticity was exhibited by Emcompress. Hence a rank order of degree of elasticity was obtained: Starch 1500 > Avicel > Microtal = 50% Avicel in Emcompress > Emcompress. This is in agreement with the results of Rees and Rue (1978b) using stress relaxation, who stated that Starch 1500 undergoes a high degree of elastic recovery. It is therefore likely that during the decompression phase of tablet production, destruction of inter-particle bonding by elastic recovery was responsible for the low mechanical strength of Starch 1500 tablets reported by Rees and Rue (1978b).

The results showed no sensitivity to rate of strain, but this was perhaps due to the small range of strain rates used in this study. The constraints on range of strain rates are those imposed by the feed-back and servo-mechanisms of the constant stress module and the tester.

In the creep curve C-D (Fig. 20) is a linear region of Newtonian compliance in semi-solids and can be envisaged to be analogous to the irreversible deformation of a material. In terms of a canonical model, when load has been applied for a sufficient time, ensuring that all Voigt units are fully extended, the deformation is analogous to viscous flow and is irreversible. It represents the viscous nature of the liquid in the dash-pot of a Maxwell unit (Fig. 21). A measure of the viscosity (residual

shear viscosity) is obtained by determining the slope of the C-D portion.

In tables 14-16 (a and b) the slopes of the C-D portion for some direct compression excipients are tabulated. A rank order of decreasing value of the slope was obtained at all stress levels and rates of loading: Starch 1500 > Avicel PH102 > Microtal = 50% w/w Avicel PH102 in Emcompress > Emcompress. The relationship between plastic deformation and the slope C-D is that when a powder undergoes a considerable amount of strain the slope will have a large numerical value. High strains are only possible when there exist mechanisms within a compact to reduce the applied load and such reduction can be attained through plastic flow. The results indicate that Starch 1500 had the greatest plastic deformation. The slope for Emcompress was very much lower than for the other direct compression excipients, suggesting that Emcompress had minimal plastic properties. This view is supported by the fact that there was no time dependent deformation taking place when the rate of compaction was altered (Fig. 73) and by data reported by David and Augsburger (1977). Thus, the C-D portion was used to give an indication of the plastic deformation capacity of a powder.

Morri et al. (1973) have reported the use of creep curves in order to analyse rheological properties of powders. However, these workers used compressive strain (creep strain) instead of creep compliance versus time and since strain determinations were made during dynamic compression (i.e not constant stress), their plots are not true creep curves. Unlike the results reported in

this present study, Morri et al. (1973) were unable to show distinction between plastic, visco-elastic and elastic deformation.

The reason why Starch 1500 forms tablets of low mechanical strength (Rees and Rue, 1978b) despite the fact that it undergoes the largest plastic deformation, is because of the high elastic characteristics as shown in Tables 14-16. It is most likely that during the decompression phase, the elastic recovery of Starch 1500 particles will lead to destruction of inter-particle bonds. Avicel PH102 undergoes plastic deformation to a slightly lower degree than Starch 1500, but since Avicel undergoes much smaller elastic deformation compared with Starch 1500, Avicel tablets will have higher mechanical strength. Results reported by David and Augsburger (1977) and Rees and Rue (1978b) support this hypothesis.

The visco-elastic characteristics were derived from the B-C region (Table 14-16). The value of Starch 1500 and Avicel PH102 were approximately similar and those of Microtal and 50% w/w Avicel in Emcompress were also similar. The B-C region was absent for data obtained for Emcompress, indicating that Emcompress exhibits negligible visco-elastic behaviour. Visco-elasticity can be represented in the canonical model by Voigt units (Fig. 21) which produce retarded elastic deformation of the powder.

The occurrence of capping and lamination during the compression of tablets depends on the rheological characteristics of the powder(s) compressed (Shotton and Obiorah, 1975; Hiestand et al., 1977). Pilpel et al. (1984) have determined the plasto-

elasticity of mixtures of paracetamol and Avicel powders and the tensile strengths of their tablets. They state that the logarithms of tensile strength were inversely proportional to the ratios of the samples' elastic recovery:plastic compression. Table 17 shows the ratio of elastic :plastic deformation for the direct compression excipients in the present study. Avicel has the largest value at a constant stress of 39.5 MPa, suggesting, according to Pilpel et al. (1984), that it should possess the lowest tensile strength. This would suggest that the degree of inter-particle bonding was less for Avicel PH102 than for example Emcompress. This contradicts earlier results (Figs. 40 and 42) for Emcompress and Avicel tablets. However, at a constant stress of 79 MPa, Emcompress possessed a much higher ratio than Avicel PH102, thus the relationship stated by Pilpel et al. would be valid. Microtal possessed the lowest ratio at all three stress levels (Table 17) suggesting that Microtal tablets would have the highest degree of inter-particle bonding and highest tensile strengths, which is probably incorrect since all other results obtained above in section 3.1, 3.1.1 and below in section 3.2.2.1 indicate that Avicel had a higher degree of inter-particle bonding than either Emcompress or Microtal. At a constant stress of 118.5 MPa, according to the scheme proposed by Pilpel et al. (1984), 50% w/w Avicel in Emcompress would have a higher degree of inter-particle bonding than tablets compressed purely for Avicel. This is highly unlikely, since the degree of plastic deformation is going to be greater in Avicel than in a binary mix of Avicel and Emcompress, because Emcompress

consolidates purely by brittle fragmentation processes. A probable reason for lack of agreement between the data reported by Pilpel et al. (1984) and those in Table 17 is the difference in the methods used to determine the elastic and plastic parameters. Pilpel et al. have used equations suggested by Armstrong and Haines-Nutt (1972), where plastic compression (PC) and elastic recovery (ER) are calculated according to equations 35 and 36.

$$PC = (Ho - HL/Ho)*100\% \quad \text{---------- Equation 35.}$$

$$ER = (Hr - HL/Hr)*100\% \quad \text{---------- Equation 36.}$$

where Ho = tablet thickness when tablet is first formed, HL = tablet thickness at the end of loading and Hr = tablet thickness after tablet ejection.

Hence, PC calculated by Pilpel et al. (1984) is a combination of elastic, visco-elastic and plastic deformation of the powders and not purely plastic deformation. Thus, the elastic:plastic ratio was found not to predict correctly the probable compaction behaviour of powders, but examination of the three parameters derived from the creep curves were found to predict the compactibility of powders.

The results reported in this study showed that the rheological characteristics of powders could be determined by creep curves in quantitative terms, giving useful information, especially for preformulation studies.

Material	Ratio of elastic:plastic deformation at three stress levels		
	39.5 MPa	79.0 MPa	118.5 MPa
Emcompress	775.6	964.0	70.6
Emcompress(A)	762.0	659.0	24.8
Microtal	651.0	346.0	18.3
Avicel PH102	1016.0	550.0	34.4
Starch 1500	925.0	589.0	43.8

Table 17. Ratio of elastic:plastic deformation (as determined from creep curves at a load rate of 14kN/minute) for various direct compression excipients. Emcompress(A) refers to binary mix of 50% w/w Avicel in Emcompress.

3.2 Influence of Polymeric Additives on the Physico-mechanical Properties of Sucrose Crystals.

3.2.1 Effect of Crystallization Method on the Physico-mechanical Properties of Sucrose Tablets.

A method of sucrose crystallization, termed transformation was used in this study, as described above in section 1.4.2. The product of conventional sucrose crystallization (commercial cane sucrose) is shown in Fig. 101A (see Appendix I), while the detailed habit of a single coarse sucrose crystal is illustrated in Fig. 101B. The product of sucrose transformation is illustrated in Fig. 101C (see Appendix I) and a detailed surface view of an agglomerate is illustrated in Fig. 101D. Both products are anhydrous forms of sucrose, but show a large degree of morphological differentiation with the agglomerated product being composed of sucrose microcrystals. Scanning electron photomicrography showed that the agglomerates have a rough surface texture with surface asperities and pores suggesting the possibility of formation of stable ordered units between drug particles and the agglomerate in a drug-excipient powder mix which could be beneficial in reducing segregation tendencies (Staniforth, 1982).

X-ray diffraction patterns obtained for both the sucrose polytypes are shown in Fig. 74. Quantitative assessment of the pattern has been carried out by measuring the peak positions, according to Bragg angle, and diffraction intensity (peak height) and such data for the two forms of sucrose is shown in Table 18.

Peak number 1 corresponding to a Bragg angle of 4.25° for commercial sucrose had a larger peak height than that for transformed sucrose. It was also observed that the peak for transformed sucrose possessed a wider base. The peak height of peak number 16, for commercial sucrose, was much larger than that for transformed sucrose. This would suggest that commerical sucrose is more crystalline than transformed sucrose. However, in both these cases there was no shift in the peak position as observed for example when morphic changes occur. Other minor peak height differences can also be observed (Table 18). It was considered that the data obtained showed that both forms of sucrose were highly crystalline in nature, with relatively small differences in crystallinity.

In order to carry out meaningful comparisons between the two types of sucrose products (Fig. 101 A-D), the particle size distributions were standardized and the moisture content was controlled by subjecting a previously dried product having a constant weight to a relative humidity of 55% for 48 hours.

Determination of NWF of sucrose and sucrose-based tablets were used to characterize changes in consolidation behaviour, particularly changes in plasticity. NWF determinations were used in preference to other measures partly because of the simplicity of testing and partly because data interpretation and comparison is reasonable well established.

The relationship between the NWF of tablets produced from commercial and transformed sucrose and increasing compaction force is illustrated in Fig. 75. The results showed that

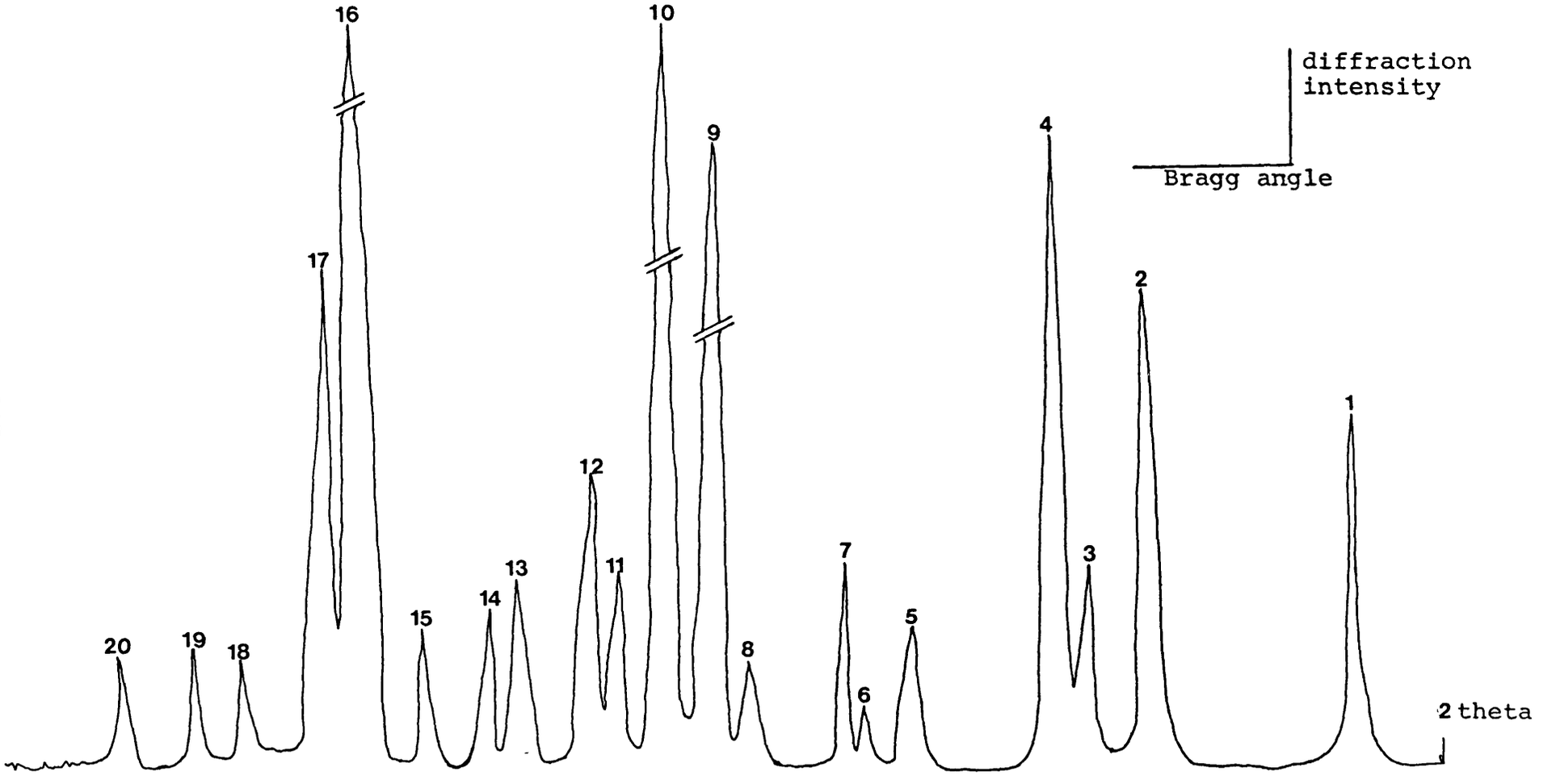

Figure 74. X-ray diffraction pattern for sucrose. The first 20 clear peaks have been used in the quantitative assessment of powders by measuring the Bragg angle and diffraction intensity (peak height).

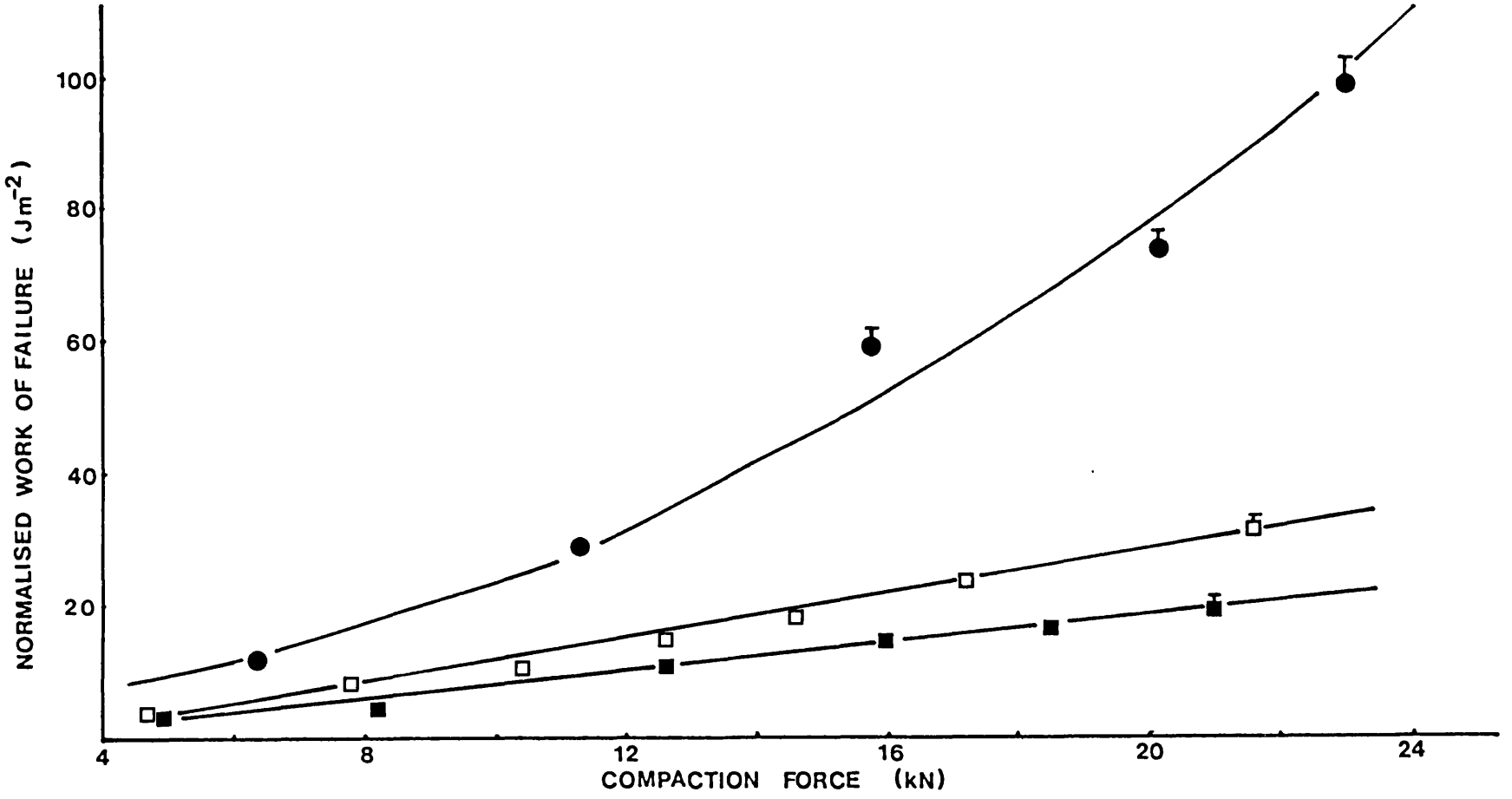

Figure 75. Relationship between normalised work of failure and compaction force for (□) transformed sucrose, (■) commercial sucrose and (●) anhydrous lactose tablets.

Peak No.	SUCROSE		TRANSFORMED SUCROSE	
	Bragg angle (deg.)	Peak height	Bragg angle (deg.)	Peak height
1	4.25°	59.0mm	4.20°	13.5mm
2	5.88	85.0	5.85	80.5
3	6.35	30.0	6.38	51.0
4	6.60	110.0	6.57	97.0
5	7.75	23.0	7.80	45.0
6	8.20	10.0	8.18	13.5
7	8.38	32.0	8.40	19.0
8	9.10	15.0	9.10	12.0
9	9.43	148.0	9.40	160.0
10	9.80	142.0	9.80	124.0
11	10.20	30.0	10.20	39.0
12	10.45	46.5	10.43	45.5
13	11.05	81.0	11.05	44.0
14	11.25	26.0	11.28	16.5
15	11.80	17.5	11.80	24.0
16	12.35	227.0	12.40	145.0
17	12.60	82.5	12.63	58.5
18	13.30	18.5	13.25	14.0
19	13.68	19.0	13.73	15.5
20	14.30	15.5	14.35	15.0

Table 18. Data derived from x-ray diffraction patterns of commercial and transformed sucrose, the peak height gives an indication of degree of crystallinity.

Ratio of Avicel PH102 to Transformed sucrose % w/w		Flow rate kg/s E*-3
0	100	4.34 +/- 0.05
1	99	4.32 +/- 0.04
5	95	4.34 +/- 0.03
10	90	4.32 +/- 0.05
20	80	3.90 +/- 0.04
40	60	2.50 +/- 0.08
80	20	0.90 +/- 0.10 *
100	0	0.51 +/- 0.12 *

Table 19. Influence of powder composition on measured flow rate. Note * indicates flow induced by mechanical agitation.

transformed sucrose tablets had slightly higher NWF values than tablets of commercial sucrose at all the compaction forces studied.

A possible explanation for the higher NWF values for transformed sucrose is that the product consists of agglomerates made up of sucrose microcrystals which can be considered to be inherently weaker than a single sucrose crystal. Microcrystal agglomeration probably facilitates irreversible deformation resulting in an increased degree of inter-particle bonding. It is known that single sucrose crystals possess higher Vickers hardness values (63.6 kg/m*E-3), than equivalent sodium chloride crystals (21.2) and aspirin (8.7) (Ridgway et al., 1970). This indicates that sucrose crystals are robust and would require very high loads in order to cause fracture through irreversible deformation, reducing the possibility of creation of clean new surfaces available for inter-particle bonding. However, transformed sucrose, which is composed of agglomerates of sucrose microcrystals held together by solid sucrose bridges will fracture much more readily than a single sucrose crystal, thereby promoting inter-particle bonding and producing tablets with higher NWF than commercial sucrose tablets. The NWF of anhydrous lactose tablets have also been plotted in Fig. 75 for comparison purposes.

A comparison of the inherent plasticity of transformed sucrose and Avicel PH102 was obtained by compressing binary mixes containing different concentrations of transformed sucrose and Avicel PH102. As expected, pure Avicel tablets showed higher NWF

values than pure transformed sucrose (Fig. 76). However, a marked rise in the NWF of transformed sucrose tablets was found as the percentage of Avicel PH102 was increased from 20% w/w to 80% w/w. In contrast, lower concentrations of 1, 5 or 10% w/w of Avicel in transformed sucrose were found to have no influence on NWF compared with that of pure transformed sucrose (Fig. 76).

Sheikh-Salem and Fell (1981) demonstrated the existence of a minimum tensile strength of tablets prepared from mixtures of two powders which exhibit different consolidation behaviour, such as lactose and sodium chloride. These workers suggested that when bonding between lactose and sodium chloride predominated, over the bonding between lactose-lactose particles or sodium chloride-sodium chloride particles, the tensile strength of the tablets was lower than those of either of the individual components alone. The tensile strength of tablets prepared from mixtures of transformed sucrose and Avicel PH102 is shown in Fig. 77. The points plotted in Fig. 77 are the means of ten determinations with corresponding confidence intervals at 95% level, showing that there was no significant alteration in tensile strength of transformed sucrose when 1%, 5% and 10% w/w Avicel PH102 was mixed with it. A probable explanation for the absence of a minimum tensile strength in the mixtures of Avicel and transformed sucrose is that the two powders studied, sucrose and Avicel PH102 are examples of powders which consolidate by two extremely different processes: sucrose by brittle fragmentation (Hardman and Lilley, 1970) and Avicel PH102 predominatly by ductile flow (Sixsmith, 1982). The influence of the plastic flow

of Avicel PH102 above a concentration of 20% w/w in sucrose was found to be profound, whereas below this percentage fragmentation of sucrose predominated. This concept will be discussed further in a latter part of this section.

High fluidity or flowability is one of the requirements listed by Kanig (1970) for an ideal direct compression excipient. The influence of powder composition on bulk flow rate is shown in Table 19. Transformed sucrose was found to exhibit high flow rates, alone and caused an increase in the flow rate of Avicel PH102 as the concentration of transformed sucrose in Avicel increased. The inherent flow pattern of transformed sucrose is shown in Fig. 78a. Flow of pure Avicel PH102 was only possible after mechanical agitation of the powder bed and even then flow was irregular (Fig. 78b). The increase in measured flow rates (Table 19), with increase in percentage of transformed sucrose is considered to be due to a reduction in inter-particle friction reducing bridging.

In general, for direct compression processing, material specifications may need to be more closely controlled than for wet granulations, where alteration in process conditions can be used to compensate for differences in powder properties. The inherent plasticity of a diluent excipient is a property which could be specified, especially in formulations where the drug or other excipients lack inherent plasticity. Indeed, one of the reasons for the tendency to consider direct compression as a technique for use only with low-dose drugs is that most of the presently available direct compression excipients lack

acceptable inherent plasticity.

Inter-particle bonding can be considered to result from intimate contact areas established during the compaction process. Both types of irreversible deformation, plastic flow and brittle fragmentation, of the powder particles lead to the establishment of such contact areas. During fragmentation, particle size reduction is thought to occur (Higuchi et al., 1953; Armstrong and Haines-Nutt, 1970) and is accompanied by the creation of clean surfaces. When these clean surfaces come into close proximity, the degree of van der Waals bonding will be extensive, giving a compact of high mechanical resistance possessing high tensile strength and NWF.

In practice, the NWF of compacts of powders which undergo brittle fragmentation is low. A probable explanation for this is that with reduction in the particle size of powder such as occurs in brittle fragmentation, the number of contact points between particles increases so that the distribution of stress at each contact point is reduced also reducing the possibility for other clean surfaces to form intimate contacts. However, powders which undergo ductile flow, have stresses at contact points which are comparatively large leading to plastic flow which increases inter-particle contact areas and consequently, the degree of van der Waals bonding. A consequence of ductile flow is that such powders generally produce tablets with larger NWF values and have a higher drug carrying capacity than comparable powders which undergo brittle fracture.

Microcrystalline cellulose (mcc) is a direct compression

excipient which possesses a large degree of inherent plasticity, however it has poor inherent fluidity. In order to overcome such poor flow properties and take advantage of the high plasticity, numerous workers including Wells and Langridge (1981); Chilamkurti et al. (1983); Armstrong and Lowndes (1984), have used combinations of mcc and other excipients to formulate acceptable tablets using the direct compression technique.

In the present studies work was carried out to characterize the inherent plasticity of sucrose, with the objective of producing a direct compression excipient, using the principles of particle engineering outlined by Staniforth (1984). The objective of the study was to produce a direct compression excipient with improved plasticity, high fluidity, physiological inertness and chemical stability. Co-crystallization of sucrose with polymeric materials was used as a method of improving plasticity. There were four main reasons for using a co-transformation process in preference to other particle engineering methods:

a. subjecting a supersaturated sucrose syrup to high shear induced catastrophic nucleation, giving rise to crash crystallization which increased the heat of crystallization to a level where not only could new crystal polytypes be produced, but the crystals could also be dried without the need for external heating.

b. incorporation of polymeric materials could be performed with greater practical ease than compared with conventional sucrose co-crystallization techniques;

c. the yields of the transformation process were high,

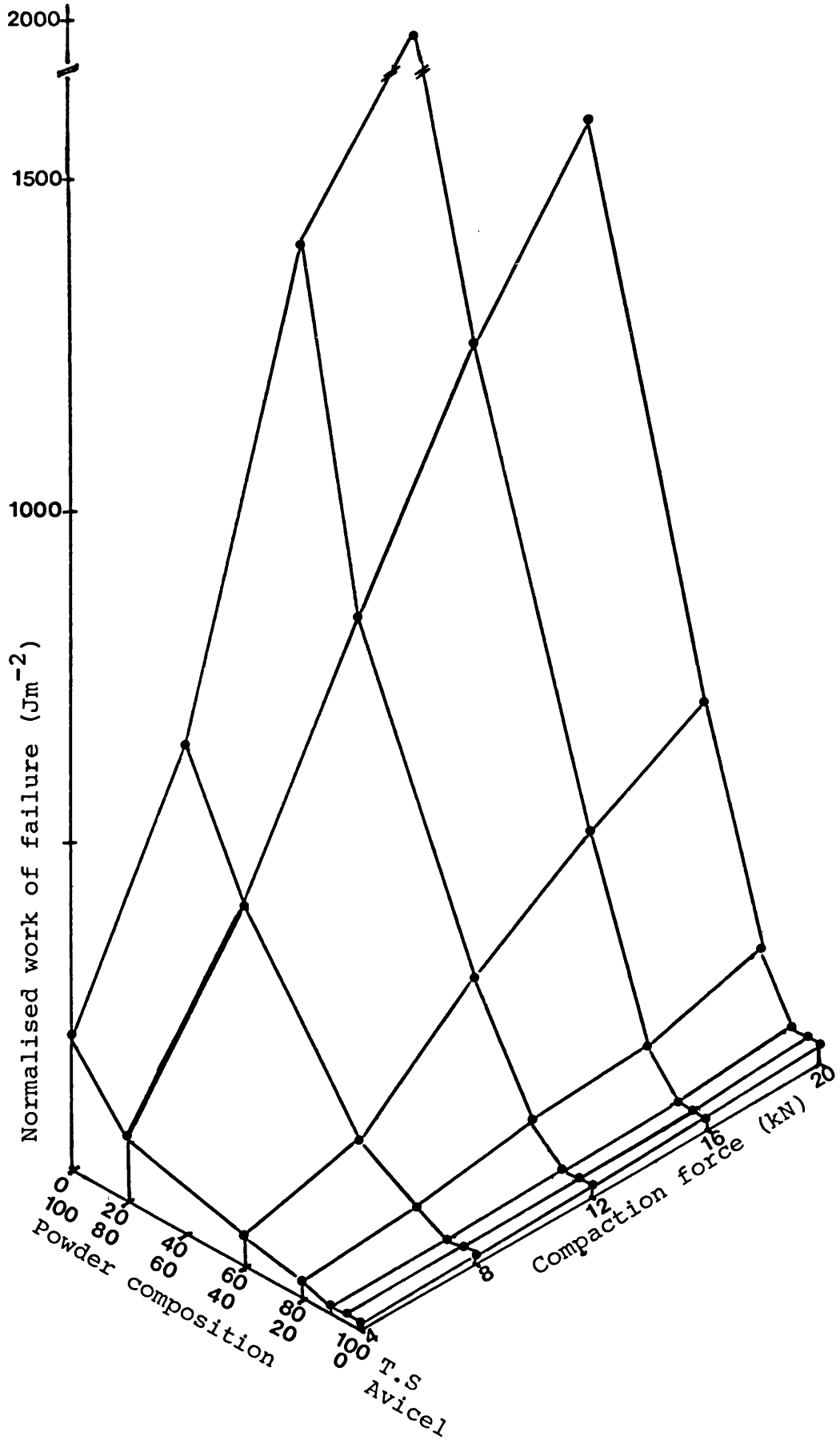

Figure 76. Influence of powder composition and compaction force on the NWF of the tablets. T.S is transformed sucrose.

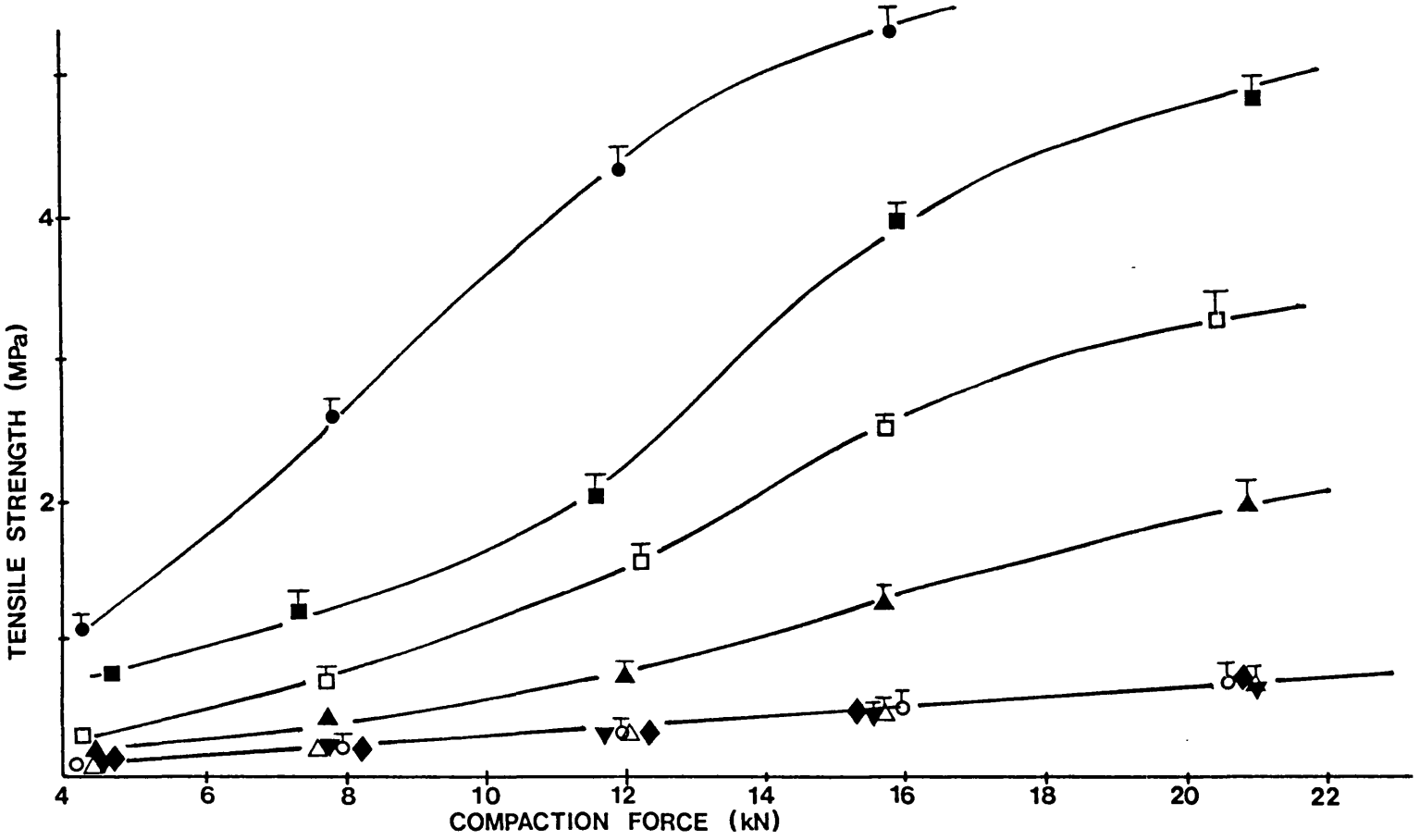

Figure 77. Influence of powder composition and compaction force on the tensile strength of tablets: (Δ) pure transformed sucrose, (o) 1% w/w Avicel, (▼) 5% w/w Avicel, (◆) 10% w/w Avicel, (▲) 20% w/w Avicel, (□) 40% w/w Avicel, (■) 80% w/w Avicel and (●) pure Avicel PH102. The tensile strength are the mean of ten determinations and the confidence interval at 95% are also plotted.

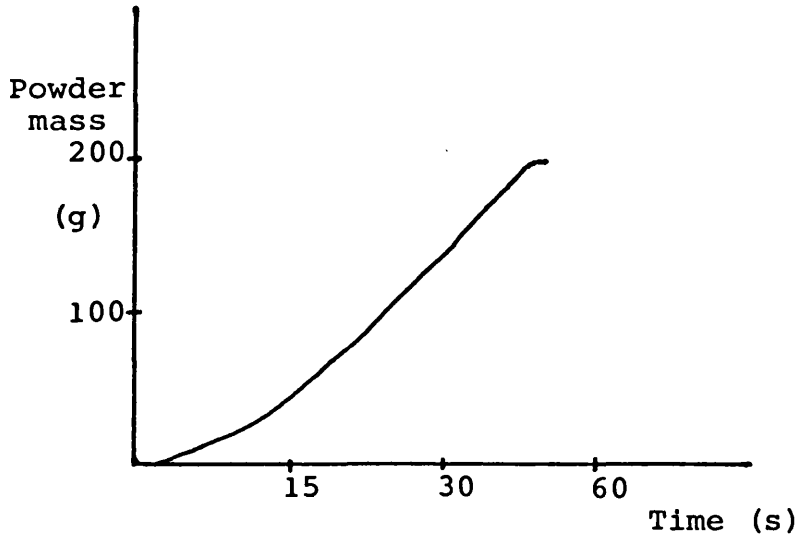

a. Flow exhibited by pure transformed sucrose (regular flow).

b. Flow exhibited by pure Avicel PH102 (irregular flow) after mechanical agitation.

Figure 78(a & b). Flow patterns exhibited by transformed sucrose and Avicel PH102 powders.

often approaching 100%;

d. crystallization of sucrose by a transformation process produced agglomerates with a large number of surface pores which could be useful for the formation of non-segregrating mixes. Additionally, the product showed inherent flowability which was also highly desirable for use in direct compression systems.

3.2.2 Influence of Co-transformation of Sucrose with Polymeric Materials on the Normalised Work of Failure.

It was hypothesised that the addition of polymeric materials to sucrose could be used as a method of increasing the inherent plasticity of sucrose. Polymeric materials were chosen in preference to other additives because of their known plasticizing effect, for example when used as binding agents in granulation processes.

3.2.2.1 Sucrose-based Direct Compression Excipients Co-transformed with Maltodextrin

Maltodextrin is a general term used to describe the product of starch hydrolysis and is composed of oligosaccharides, usually having a degree of polymerisation of between 10 and 30 glucose units.

The physico-mechanical influence of the concentration of maltodextrin incorporated during transformation of sucrose was investigated. Fig. 100C (see Appendix I) shows a typical agglomerate of sucrose transformed with 3% maltodextrin but

there was no difference in crystallite or agglomerate structure between sucrose transformed with either 1% or 3% maltodextrin nor was any significant change in the agglomerate morphology found previously for transformed sucrose (Fig. 101D, see Appendix I) which showed that the microcrystalline habit was retained when sucrose was co-transformed in the presence of maltodextrin.

Fig. 79 shows the relationship between NWF and compaction force for maltodextrin co-transformed powder. The incorporation of maltodextrin, at all concentrations was observed to increase the NWF of the transformed sucrose tablets, the increase suggesting that maltodextrin was exerting a plasticizing effect on the co-transformed product. It is considered that the increased plasticity seen in sucrose transformed with 1% w/w of maltodextrin may be due to relaxation of the sucrose lattice by small concentrations of maltodextrin. Further increases in concentration have a lower plasticizing effect and although the reason for this is not clear it may be due to the reduced influence of maltodextrin as a mixture component in comparison with its action as a crystal poison. The influence of maltodextrin as a component of sucrose mixtures is discussed in more detail below.

X-ray diffraction studies showed that maltodextrin had no significant effect on the polymorphic form of sucrose crystals. Table 20 shows the influence of co-transformation with different concentrations of maltodextrin on Bragg angle (peak position) and crystallinity (peak height) for sucrose. The x-ray data showed only small differences in crystallinity between the co-

transformed powders prepared with 1% maltodextrin and those with either 3% or 10% maltodextrin; for example, the peak height was reduced for a sample co-transformed with 1% maltodextrin relative to the corresponding peak for either 3% or 10% maltodextrin co-transformed material for peaks at Bragg angle approximately 5.8° . No differences in the x-ray diffraction patterns were observed between the 3% and 10% maltodextrin powders, despite the fact that a difference in plasticity was found for these powders (Fig. 79).

The mechanical properties of co-transformed sucrose containing 3% w/w maltodextrin, prepared by Tate and Lyle Plc., on a continuous production scale (Microtal D.C.E.) were compared with those for the same maltodextrin concentration in sucrose prepared on a small scale in the laboratory. In the latter case, maltodextrin was incorporated in a powder form at the point of nucleation, whereas in the former, the maltodextrin was present in solution form in the heated supersaturated sucrose syrup. The results (Fig. 80) showed that the co-transformed product prepared on a laboratory scale exhibited a very similar NWF profile to the production scale product suggesting that the maltodextrin in both products had a similar influence on plasticity and was not influenced by the initial phyiscal form of maltodextrin.

When the concentration of maltodextrin incorporated with sucrose was 1% w/w, the NWF profile was found to be comparable to that for anhydrous lactose (Fig. 40, section 3.1). However, the moisture level of the co-transformed sucrose at the point of compression was only 0.2% of total dry powder mass, compared to

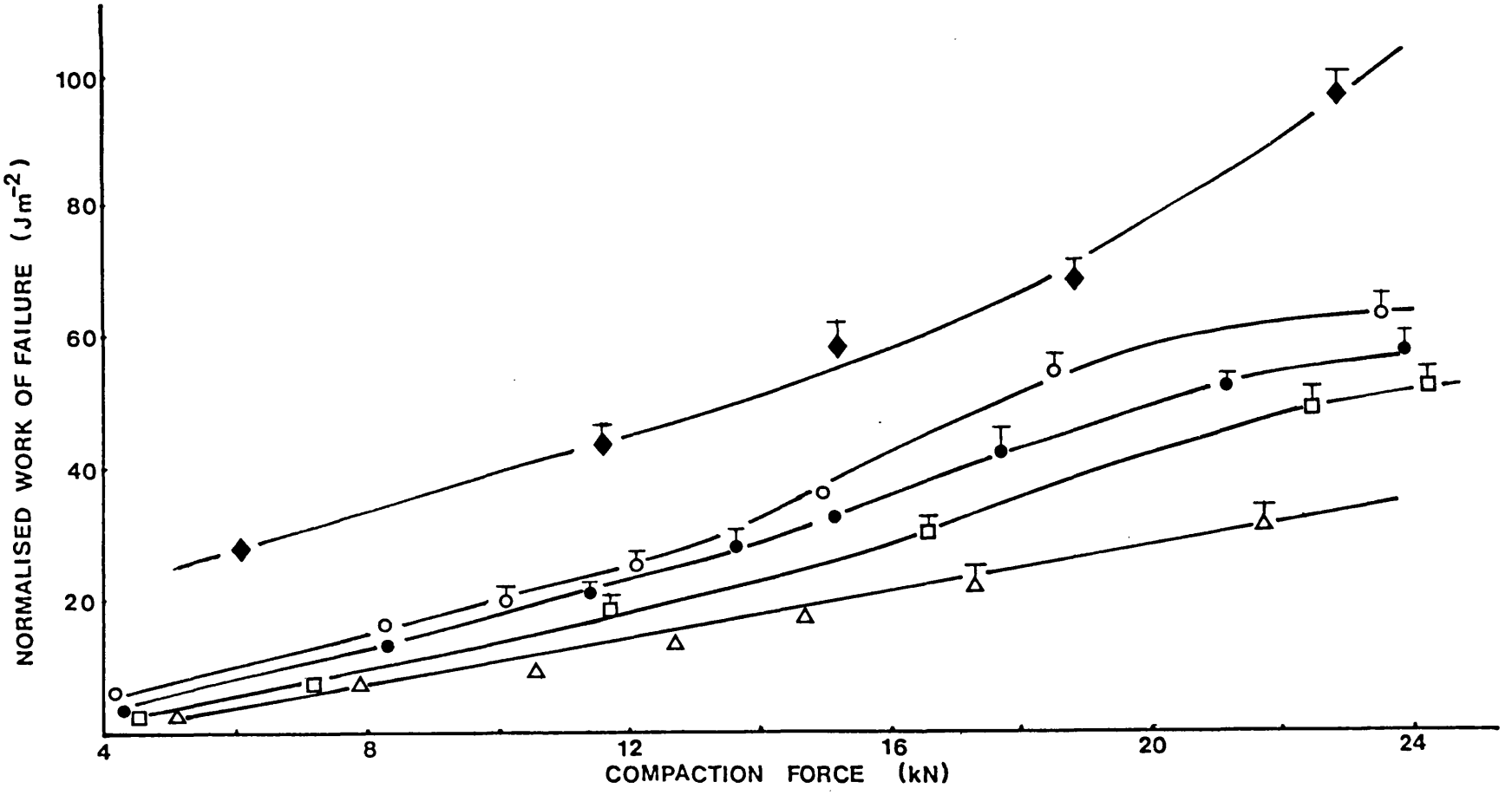

Figure 79. Relationship between normalised work of failure and compaction force for sucrose co-transformed with (◆) 1% maltodextrin, (o) 3% maltodextrin, (●) 5% maltodextrin and (□) 10% w/w maltodextrin. Pure transformed sucrose is denoted by (△).

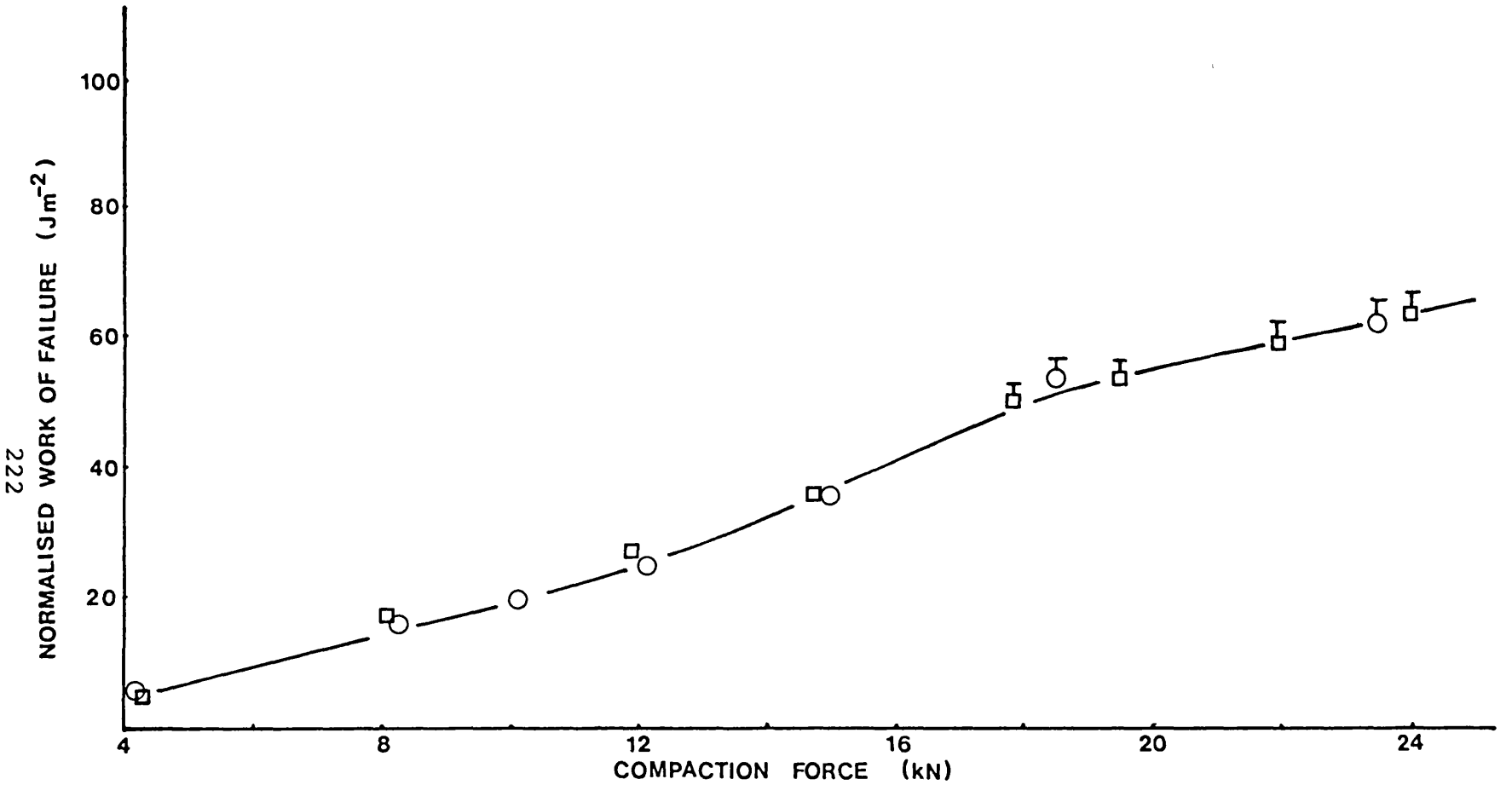

Figure 80. Influence of the method of preparing co-transformed sucrose with maltodextrin on the normalised work of failure of the tablets with increasing compaction force. (□) Pilot plant sample, (○) laboratory scale sample.

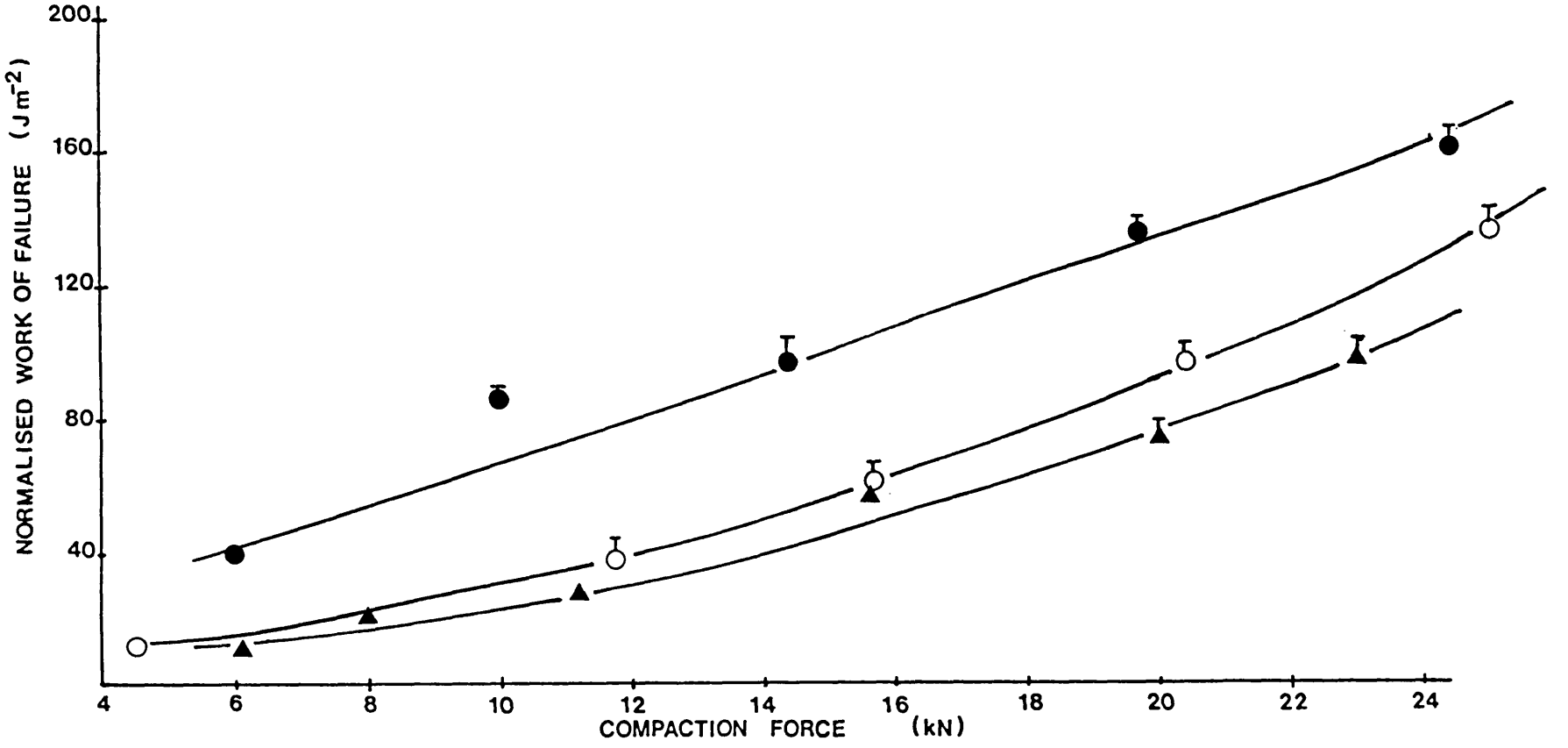

Figure 81. Relationship between the normalised work of failure and compaction force for tablets compressed of powders of approximately similar moisture content. (▲) anhydrous lactose , (●) and (O) are sample of sucrose co-transformed with 1% and 3% w/w maltodextrin respectively.

approximately 0.8% for anhydrous lactose. It is therefore possible that the water content of anhydrous lactose provided the plasticizing effect obtained by addition of maltodextrin with sucrose.

To test this hypothesis, samples of co-transformed sucrose with 1% and 3% maltodextrin at moisture levels of 0.5% and 0.65% respectively were compressed. These were the inherent moisture levels in the powders at the end of the co-transformation process. The relationship between NWF and compaction force for these powders is shown in Fig. 81. Both, 1% and 3% maltodextrin based powders with included moisture showed greater plasticity than anhydrous lactose. However anhydrous lactose was previously shown (Fig. 40) to possess higher NWF than Fast-Flo, Dipac, Emcompress, Nutab, and Tablettose all of which had comparable moisture contents. The effect of moisture on NWF suggests that such a parameter is a reflection of the bulk powder plasticity, which is influenced by particle interaction rather than inherent plasticity of individual powder particles, which would not be dependent on particle interaction. The moisture appears to be acting as a plasticizier and it has been hypothesised by Khan et al. (1981) that moisture affects the compaction properties of powders due to internal lubrication, which facilitates slippage and flow within the individual microcrystals.

Fig. 82 shows the relationship between sucrose excipient composition, compaction force and NWF. In this case the sucrose excipient was produced by dry mixing pure transformed sucrose with seven different concentrations of maltodextrin. In order to

minimise the effect of moisture, all the binary mixes of transformed sucrose and maltodextrin had a moisture content at the point of compaction of approximately 0.25% expressed as a percentage of total dry powder mass. 100% maltodextrin was found to produce tablets which had large NWF values, especially when compressed at forces larger than 14kN. The addition of 1% w/w maltodextrin did not alter the NWF values of transformed sucrose and even the addition of 5%, 10%, 20% and 40% w/w of maltodextrin to pure transformed sucrose did not result in an increase in NWF compared with values obtained for pure transformed sucrose. Conversely, over the range 10kN to 20kN compaction force, the addition of 5%, 10%, 20% and 40% w/w maltodextrin altered the NWF, where values were found to be lower than those for pure transformed sucrose or 100% maltodextrin alone, i.e. a minimal NWF value was obtained. The explanation for such behaviour is unclear, but it is considered possible that bonding between particles of the same component could be greater than that between particles of different composition, when the mechanism of bonding is only slightly different. However, this explanation does not seem to hold for binary mixes of transformed sucrose and Avicel PH102, where no minimal NWF or tensile strength were obtained (Figs. 76 and 77 respectively).

Sheikh-Salem and Fell (1981) have reported that the addition of sodium chloride to lactose powder resulted in a fall in the tensile strength of the tablets to a level below that of either of the individual components alone.

It is postulated that a minimal NWF or tensile strength of

tablets is not obtained when the powders possess extremely different modes of irreversible deformation during compaction. For example, consider powder A, which undergoes purely plastic deformation and powder B, which undergoes extensive particle fragmentation during compaction. As a result, tablets of powder A will possess a larger NWF than tablets of powder B. In binary mixes of powders A and B, when the concentration of powder B is low, the consolidation mechanism of powder A will remain unaffected. This is also true for a powder mix of a low concentration of A in B. In a powder mix of 40% w/w of A in B, the plastic flow of powder A will predominate but the NWF values of the tablets will be lower than for tablets compressed purely from powder A, since the concentration of powder A is reduced. The NWF values for tablets of such a binary mix will be larger than for tablets compressed purely from powder B. This is the case for Avicel PH102 and transformed sucrose. However a minimal NWF or tensile strength will be obtained when the powder(s) possess closely related or combinations of irreversible deformation modes, for example transformed sucrose and maltodextrin and the powders used by Sheikh-Salem and Fell (1981).

An increase in NWF was only observed for tablets containing 60% w/w maltodextrin with transformed sucrose. The results represented in Fig. 79 and 82 indicate that co-transformation of low concentrations of maltodextrin with sucrose imparts greater plasticity than binary mixes of maltodextrin with transformed sucrose. The plasticizing action of maltodextrin in co-

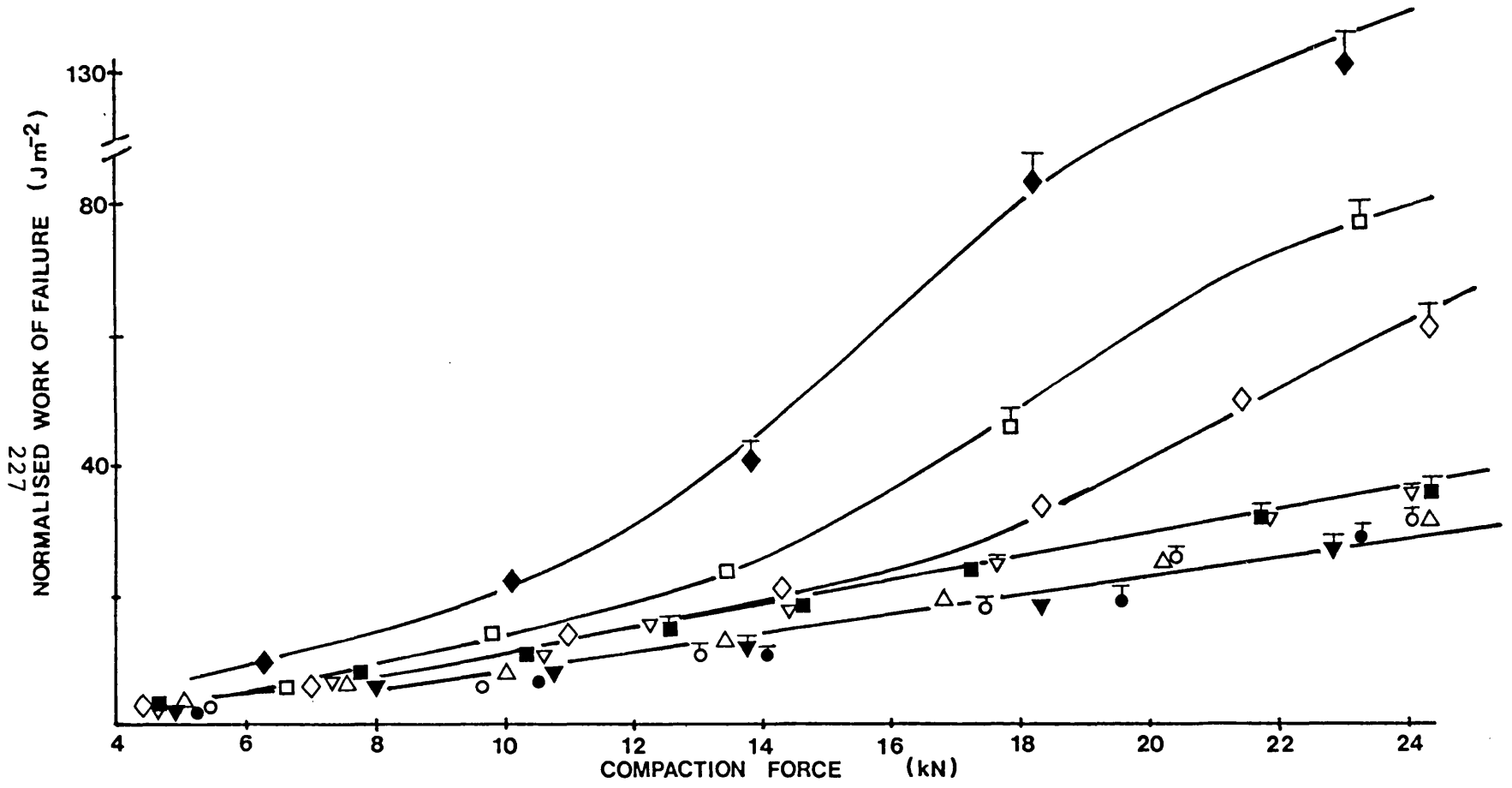

Figure 82. Influence of powder composition and compaction force on the normalised work of failure of the tablets, where (■) is pure transformed sucrose and (◆) is pure maltodextrin. (□) is 80% w/w maltodextrin in transformed sucrose, (◇) is 60%, (▼) is 40%, (●) is 20%, (o) is 10%, (△) is 5% and (▽) is 1%.

Peak No.	% Maltodextrin co-transformed with sucrose 1% p1	1% p2	3% p1	3% p2	10% p1	10% p2
1	4.13°	13.0mm	4.15°	14.0mm	4.13°	15.0mm
2	5.78	14.5	5.80	100.0	5.80	96.0
3	6.25	42.0	6.35	60.0	6.35	56.0
4	6.40	65.5	6.60	94.0	6.55	97.0
5	7.70	26.5	7.75	50.0	7.68	52.0
6	8.13	9.5	8.10	17.0	8.10	17.5
7	8.33	12.0	8.38	19.0	8.33	19.0
8	9.05	8.0	9.05	16.0	9.05	13.0
9	9.38	146.0	9.40	194.0	9.40	181.0
10	9.75	97.5	9.78	131.0	9.80	124.0
11	10.28	39.0	10.18	46.5	10.18	52.0
12	10.38	43.0	10.40	59.0	10.40	59.0
13	10.95	48.0	11.05	60.0	11.00	54.0
14	11.20	18.0	11.25	20.0	11.23	18.5
15	11.75	31.0	11.78	32.0	11.78	31.0
16	12.35	152.0	12.35	165.0	12.33	159.0
17	12.55	57.0	12.60	67.5	12.63	65.0
18	13.20	17.5	12.25	20.0	13.23	16.0
19	13.68	21.0	13.70	18.0	13.68	20.0
20	14.28	17.0	14.32	17.0	14.30	19.0

Table 20. Data derived from x-ray diffraction patterns for sucrose co-transformed with 1%, 3% and 10% w/w maltodextrin. p1 and p2 refer to the Bragg angle and diffraction intensity (peak height) respectively.

transformed sucrose is considered to be due to a weakening of the bonding between sucrose microcrystals. Consequently, during compaction, fracture of the agglomerate will take place more readily, creating more clean surfaces which can be involved in subsequent bonding. It is considered that at concentrations greater than 1% the internal agglomerate structure may still be weakened but that bonding between dissimilar particles predominates thereby reducing the NWF values of tablets (Fig. 79). However, in dry binary mixes containing concentrations of maltodextrin greater than 40%, the concentration was considered high enough to establish a large number of maltodextrin -maltodextrin particle bonds, leading to an increase in the NWF above that for transformed sucrose tablets (Fig. 82).

3.2.2.2 Gelatin.

The first two workers to study the mechanical properties of gelatin gels were Rankine (1906) and Hatschek (1921). These workers found that a gelatin gel will deform at a constant strain when a load is applied, resulting in permanent deformation. Later, Ueno (1963) studied the creep behaviour of gelatin gels and found that under constant stress, the gels exhibited visco-elastic properties. Gelatins are widely used in both confectionary and pharmaceutical tableting, for their favourable binding/adhesive properties. A fundamental property of gelatin which affects its commercial use is the rigidity of the gels it can form. A parameter was developed by Bloom (1925) to measure the rigidity of gels, subsequently called Bloom strength (B.S.).

A linear relationship between Bloom strength and modulus of ridigity has since been shown by Saunders and Ward (1954).

Because gelatin possesses binding/adhesive properties, it is widely used as a constituent of granulating fluids where it can impart plasticity to a formulation (Seager et al., 1980) and for this reason it has been used here as an additive in the co-transformation of sucrose. Several gelatins with a range of different B.S. were used to study the influence of gel rigidity or viscosity on their plasticizing effect on transformed sucrose.

3.2.2.2.1 Sucrose-based Direct Compression Excipients Produced Using Gelatins of Different Bloom Strengths.

The influence of gelatin Bloom strength on NWF of co-transformed sucrose was studied. The agglomerate structure and morphology of pure transformed sucrose was found to be retained when sucrose was co-transformed with gelatin. Fig. 100D (see Appendix I) show the agglomerate type present in all the gelatin co-transformed products.

Fig. 83 shows the relationship between NWF and compaction force for tablets compressed from co-transformed powders prepared using various percentages of a gelatin with a B.S. of 60. Increasing the percentage of this gelatin from 1% w/w to 3% and 5% w/w was found to reduce the plasticity of the co-transformed product. However, at 3% and 5% w/w concentration of gelatin, the co-transformed products exhibited only a small plasticizing influence on transformed sucrose (Fig. 83). The incorporation of 1% gelatin was found to have a larger plasticizing effect on

transformed sucrose than 1% maltodextrin when judged according to NWF profiles (Fig. 79). It is probable that gelatin possesses a greater inherent plasticity than maltodextrin possibly because gelatin has a more coiled molecular shape with greater molecular space than maltodextrin, allowing gelatin to deform much more than maltodextrin. It might be expected that the plasticity of tablets compressed from co-transformed product would increase as the concentration of gelatin incorporated was increased. However, the results shown in figure 83 do not follow this relationship, rather there was a decrease in NWF at concentrations of 3% and 5% w/w gelatin similar to that found previously for incorporation of maltodextrin.

The effect of moisture content at the time of compression was shown to affect the NWF of tablets containing maltodextrin. Moisture levels of co-transformed sucrose with gelatin powders are given in Table 21, all three co-transformed powders compressed showed comparable moisture levels. It therefore appears that the increase in plasticity found in tablets containing 1% w/w gelatin was produced by an effect other than that of moisture acting as a plasticizing binder.

The influence of incorporating a gelatin with a Bloom strength of 175 on NWF is shown in Fig. 84. A trend similar to that observed with maltodextrin and gelatin B.S. 60, was also observed for gelatin B.S. 175, i.e. a reduction in the concentration of polymeric material incorporated in sucrose during co-transformation was found to cause an increased plasticizing effect on transformed sucrose. The incorporation of

3% and 5% w/w of gelatin B.S. 175 resulted in only a small increase in the plasticity of transformed sucrose (Fig. 84). However, powder co-transformed with 1% gelatin B.S. 175 showed plasticity comparable to that of anhydrous lactose and Fast-Flo although lower than that found with gelatin B.S. 60. The difference between the plasticity of co-transformed powders with 1% B.S. 60 (Fig. 83) and 1% B.S. 175 (Fig. 84) gelatin was not due to moisture differences in the powders, since the moisture levels at the time of compression, (Table 21), were similar for both powders.

Fig. 85 shows the relationship between NWF and compaction force for sucrose co-transformed with gelatin having a B.S. of 225. The results have been plotted on the same scale as figures 83 and 84 for ease of comparison. The inclusion of 3% w/w B.S. 225 gelatin in the co-transformed powder was found to slightly increase the plasticity of transformed sucrose whereas inclusion of 5% w/w of B.S. 225 gelatin caused a reduction in the plasticity of transformed sucrose. As previously, incorporation of 1% gelatin resulted in an increase in plasticity. The results in Table 21 show that the moisture level at the time of compression for these powders was similar to that for powders prepared using B.S. 60 and B.S. 175 gelatin, and it therefore appears that the influence of moisture can again be disregarded.

The effect of co-transforming sucrose in the presence of gelatin with a B.S. of 300 on NWF profile of compressed tablets is shown in Fig. 86. The presence of a 3% and 5% w/w concentration of gelatin with a B.S. 300 were found to increase

the NWF of transformed sucrose by a small amount, but as in previous experiments, 1% gelatin was found to increase the plasticity of transformed sucrose markedly.

Fig. 87 shows the relationship between peak NWF value between 22-24kN compaction force and Bloom strength at various concentrations of gelatin. It was noted that the incorporation of 1% w/w of gelatin of any Bloom strength introduced greater plasticity to transformed sucrose than either a 3% or 5% w/w concentration of the same B.S. gelatin. This trend was similar to that observed for co-transformed powders containing maltodextrin (Fig. 79) and the explanation is thought to be the same for both these polymeric materials. The reason for this behaviour is not yet known. Quantitative assessment of the x-ray diffraction patterns of 1% and 5% gelatin B.S. 300 was carried out and the data is shown in Table 22. It was found that concentration had no effect on either the Bragg angle (peak position) or crystallinity (peak height). Further, no variation in the number of peaks was found (Fig. 74) and it can therefore be assumed that change in concentration had no effect on either morphic form or crystallinity of sucrose co-transformed with gelatin.

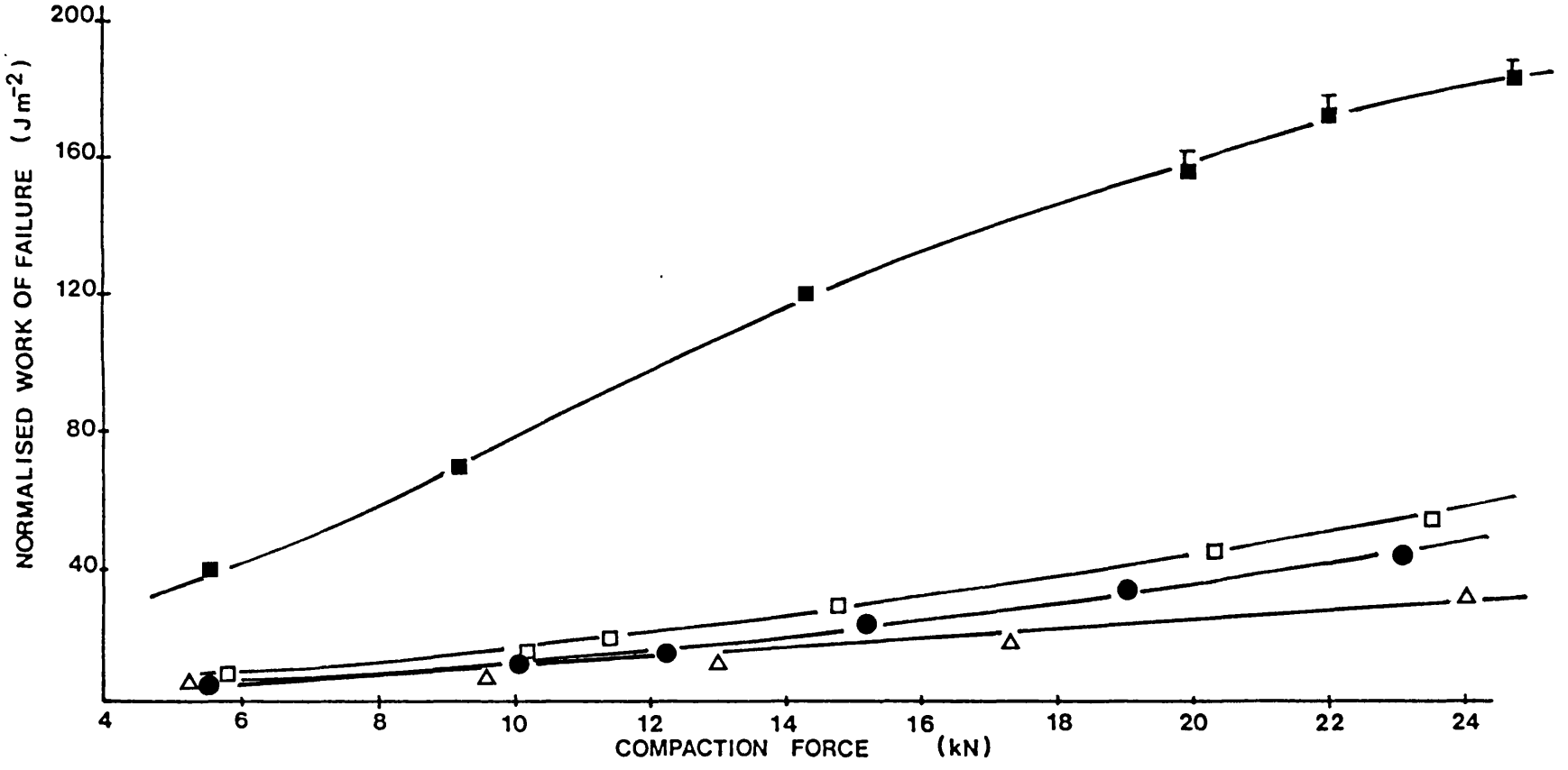

Figure 83. Influence of the concentration of gelatin B.S. 60 and compaction force on the normalised work of failure of tablets. (■) 1%, (□) 3% and (●) 5% w/w gelatin co-transformed with sucrose. (Δ) pure transformed sucrose.

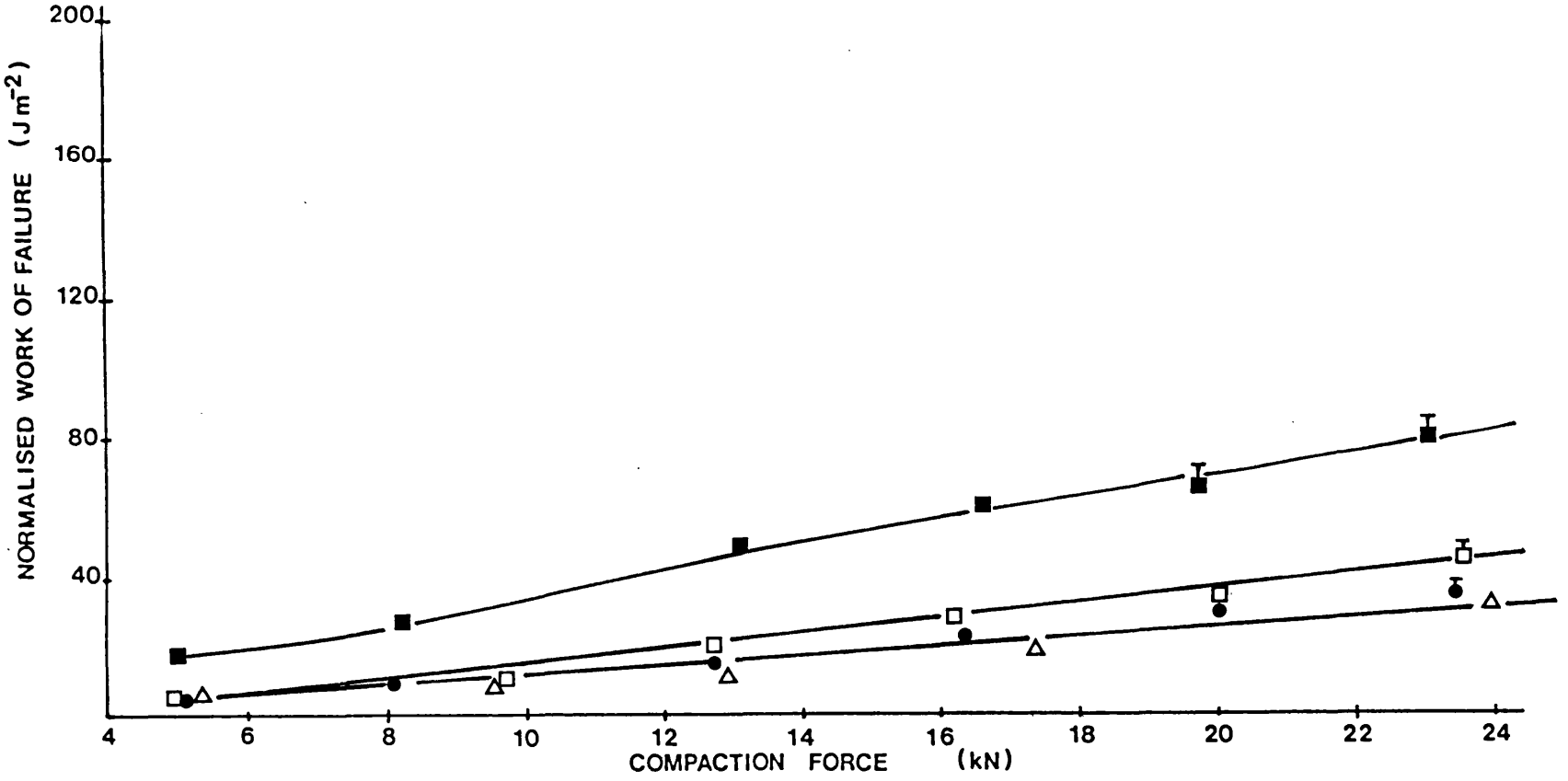

Figure 84. Influence of the concentration of gelatin B.S. 175 co-transformed with sucrose and compaction force on the normalised work of failure of the tablets. (■) 1%, (□) 3% and (●) 5% w/w gelatin co-transformed with sucrose. (△) pure transformed sucrose.

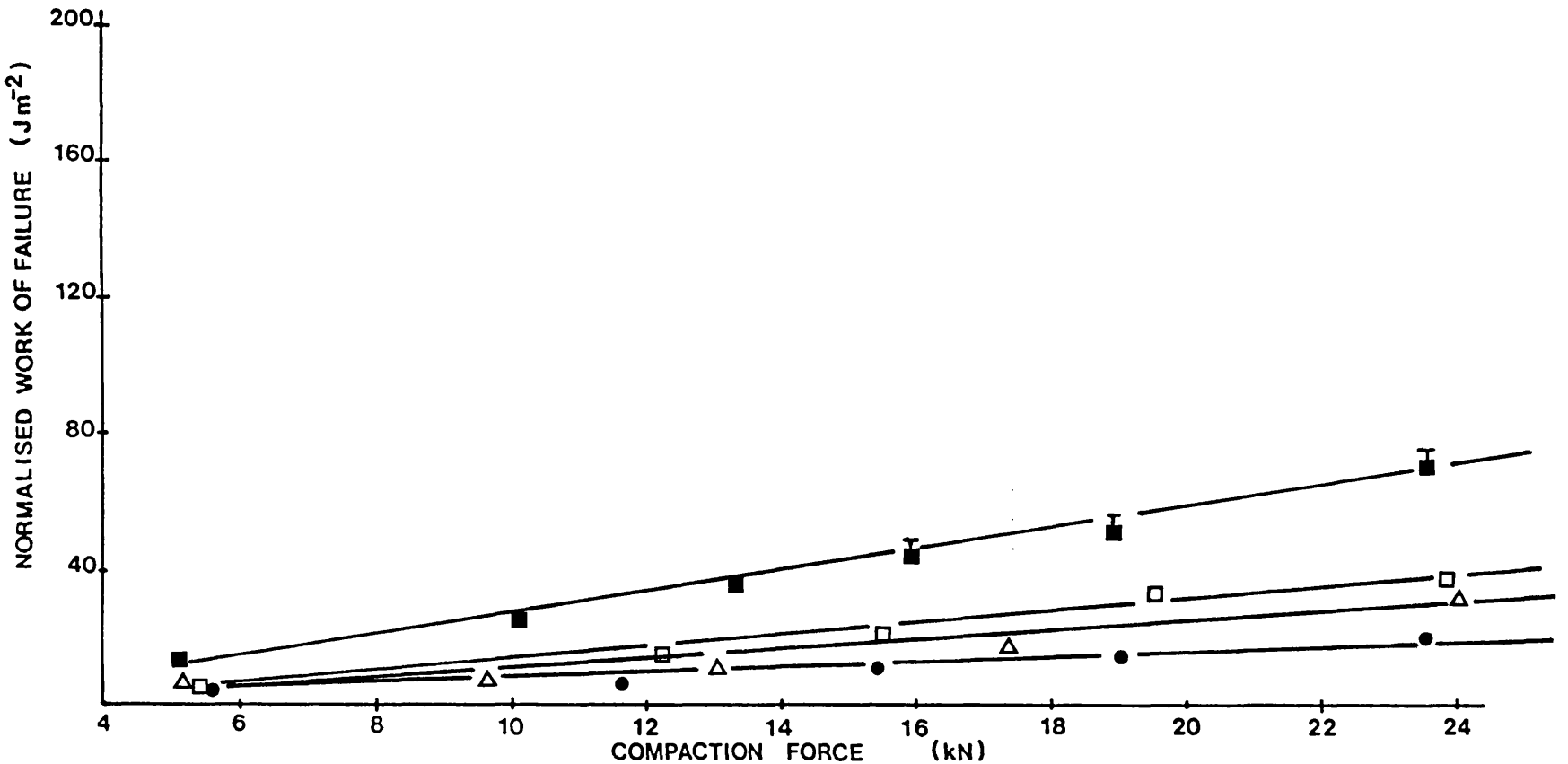

Figure 85. Influence of the concentration of gelatin B.S. 225 co-transformed with sucrose and compaction force on the normalised work of failure of the tablets. (■) 1%, (□) 3% and (●) 5% w/w gelatin co-transformed with sucrose. (Δ) pure transformed sucrose.

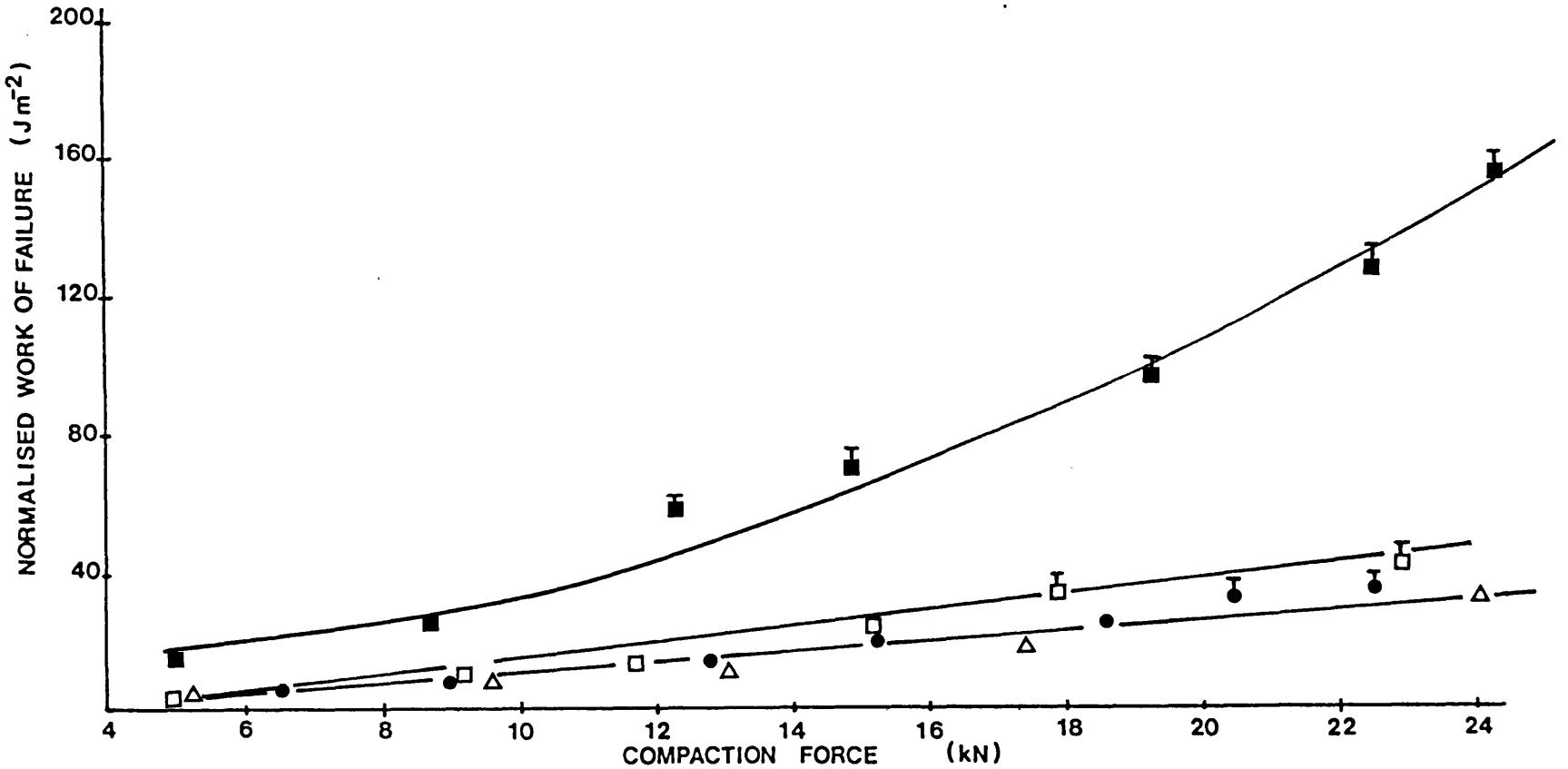

Figure 86. Influence of the concentration of gelatin B.S. 300 co-transformed with sucrose and compaction force on the normalised work of failure of the tablets. (■) 1%, (□) 3% and (●) 5% gelatin co-transformed with sucrose. (△) pure transformed sucrose.

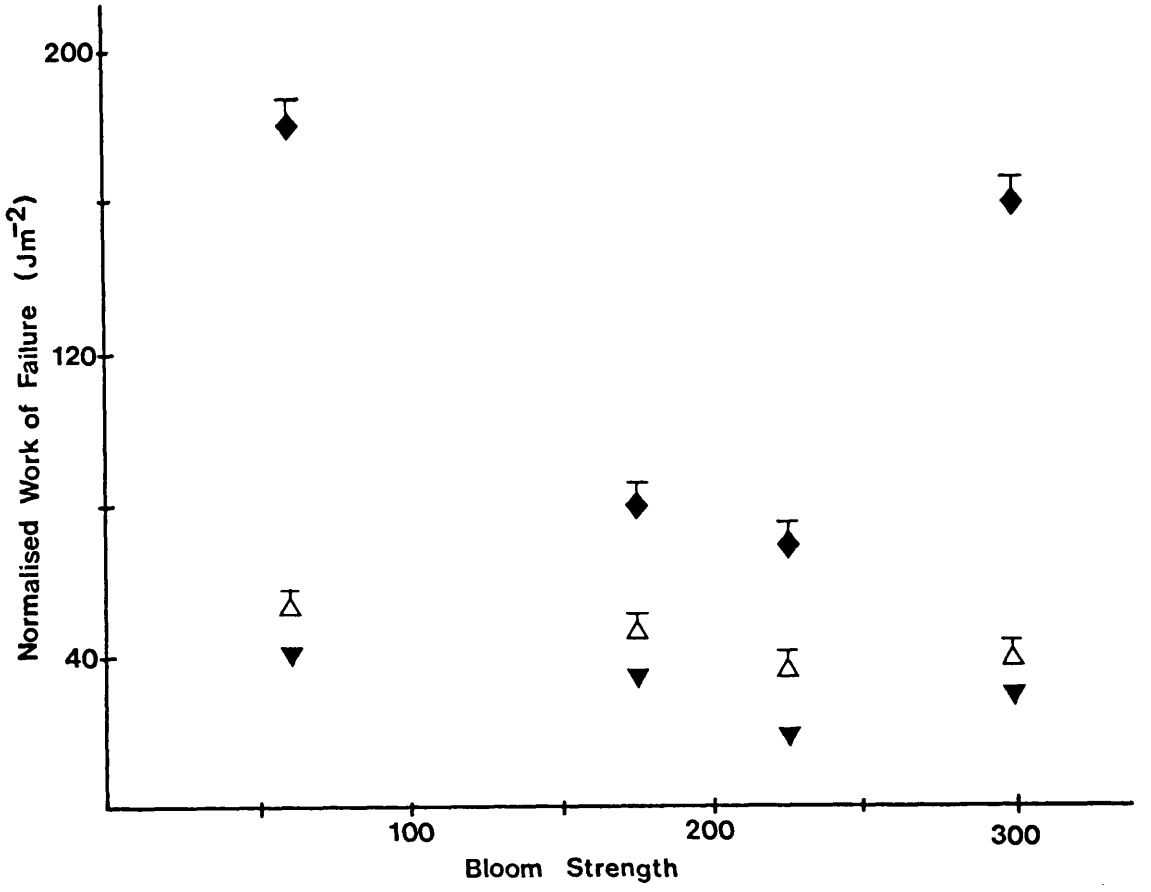

Figure 87. Influence of Bloom strength and concentration of gelatin co-transformed with sucrose on the peak normalised work of failure (between 22-24kN compaction force). (◆) 1%, (Δ) 3% and (▼) 5%w/w of gelatin co-transformed with sucrose.

Gelatin conc.%w/w	Moisture level at point of compression (%w/w). Bloom strength of the gelatin incorporated			
	60	175	225	300
1	0.26%	0.24	0.28	0.25
3	0.20	0.22	0.27	0.20
5	0.24	0.30	0.21	0.26

Table 21. Moisture levels, expressed as a percentage of total dry mass, at the time of compression for co-transformed powders prepared using different gelatin B.S and concentrations.

Peak Number	% gelatin co-transformed with sucrose 1%		5%	
	p1	p2	p1	p2
1	4.15°	15.0mm	4.18°	12.0mm
2	5.80	11.5	5.78	14.0
3	6.30	57.0	6.30	63.0
4	6.55	84.0	6.58	79.5
5	7.75	48.0	7.78	51.0
6	8.10	15.0	8.10	20.0
7	8.30	17.0	8.33	23.0
8	9.05	18.0	9.08	23.0
9	9.40	207.0	9.40	192.0
10	9.78	110.0	9.82	127.0
11	10.15	45.0	10.13	57.0
12	10.40	52.0	10.40	43.0
13	10.95	55.0	10.95	60.5
14	11.32	14.0	11.37	20.0
15	11.75	26.5	11.78	22.0
16	12.30	142.0	12.25	160.0
17	12.58	58.0	12.55	67.5
18	13.20	20.0	13.20	14.0
19	13.68	18.5	13.65	22.0
20	14.35	18.0	14.38	14.5

Table 22. Data derived from x-ray diffraction patterns, for co-transformed powder containing 1% and 5% w/w gelatin B.S. 300. p1 and p2 refer to the Bragg angle and to the degree of crystallinity respectively.

3.2.2.2.2 Sucrose-based Direct Compression Excipient Co-transformed with Protein S and Cryogel

Unlike gelatin, which swells in water at room temperature but is insoluble except at elevated temperature, Protein S and Cryogel are high purity gelatins which are soluble in both cold and hot water. In a study conducted by Seager et al. (1980), Protein S was used as a binder in order to impart plasticity to a paracetamol tablet formulation. These workers reported that Protein S showed considerable and rapid stress relaxation and tablets compressed using pure Protein S were found to possess crushing forces in excess of 20 "Schleuniger units", indicating that large areas of high strength bonds were formed during compaction. To take advantage of these properties, Protein S and Cryogel were used in this study to prepare co-transformed powders.

Fig. 88 shows the relationship between the NWF and compaction force for two concentrations of Protein S and Cryogel. There was a very small increase in the plasticity of the powder with 5% w/w of Protein S compared to transformed sucrose alone, 3% w/w Protein S showing no influence. Cryogel, at a concentration of 3% and 5% w/w caused a slight reduction in the plasticity of transformed sucrose (Fig. 88).

Moisture levels measured at the time of compression for all the co-transformed powders shown in Fig. 88 are tabulated in Table 23. All the samples were observed to have a slightly higher moisture level than transformed sucrose (c.f Table 18) and although the moisture level between these co-transformed powders

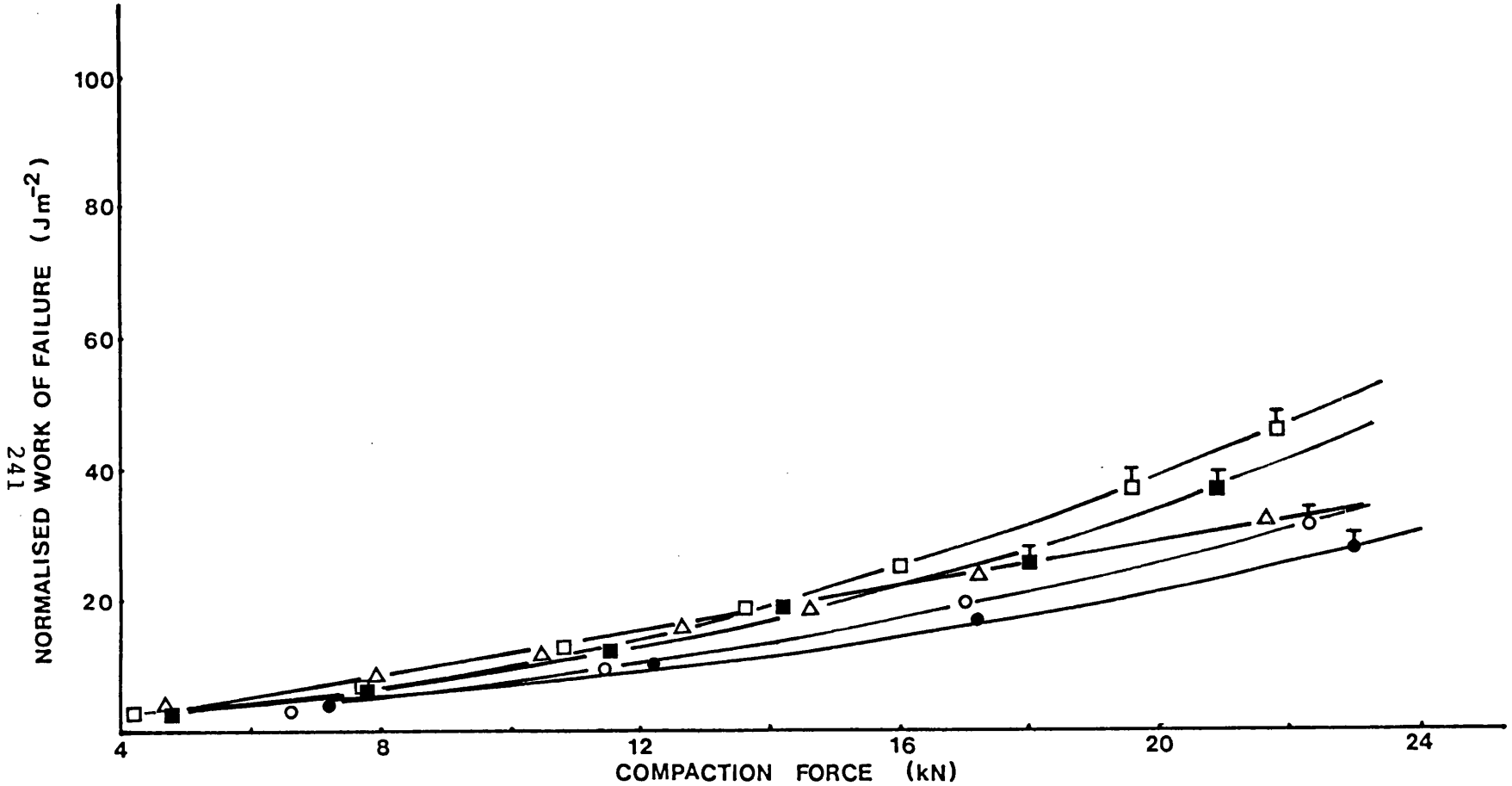

Figure 88. Influence of co-transformation of 5% (□), 3% w/w Protein S (■) and 5% (●), 3% w/w (o) Cryogel with sucrose and compaction force on the normalised work of failure of tablets. (△) Transformed sucrose

varied considerably, there was no significant influence on the plasticity of the powders.

Gelatin concentration (% w/w).	Moisture level at point of compression (% w/w).	
	Protein S	Cryogel
3	0.38	0.33
5	0.27	0.20

Table 23. Moisture content, expressed as a percentage of total powder dry mass, at the time of compression for co-transformed powders prepared using two different concentrations of Protein S and Cryogel.

3.2.2.3 Sucrose-based Direct Compression Excipients Co-transformed with Dextrans of Different Molecular Weights.

Dextrans are polysaccharides, usually synthesized by micro-organsims. It is known that the presence of dextrans during sucrose crystallization alters sucrose crystal habit. Various workers (Sutherland and Paton, 1969; Chou and Wnukowski, 1980; VanHook, 1980; and Vaccari et al., 1981) have shown that dextran causes elongation of sucrose crystals to an extent which has been found to block centrifuges used in purification of sucrose and that the presence of dextran during crystallization reduces the yield of sucrose. Dextran is used in the present study because of its reported influence on sucrose crystal habit: it is hypothesised that such habit modification may result in changes in the compressional behaviour of transformed sucrose through relaxation of the sucrose crystal lattice.

Fig. 102A (see Appendix I) shows the detailed surface morphology of agglomerates present in all samples co-transformed with dextran. If the surface morphology of this co-transformed specimen is compared with that of transformed sucrose (Fig. 101D) and other co-transformed powders (Figs. 100C and 100D), it appears that dextran has had little influence on either individual crystallite morphology or on agglomerates produced by the co-transformation process.

Powers (1978) has exmained the mode of action of non-sucrose compounds in the modification of sucrose habit. When a sucrose crystal is growing from its supersaturated solution which contains some non-sucrose (NS) molecules, occasionally a molecule

of NS material will approach sufficiently close to one of the crystal faces to be weakly attracted. If NS material has some similarity of structure to the sucrose on at least one face, there is a statistical chance that the NS molecule may adhere to the surface for a finite period of time. Depending on the affinity of the NS material either a layer or a few molecules or even a single NS molecule may be held on to the face. Consequently, any subsequent sucrose attachment to that face is impeded and the growth rate slowed, and this may result in habit modification evidenced on a macroscopic level. Study of the x-ray diffraction pattern for sucrose co-transformed with dextran with a molecular weight of 252,000 D showed no alteration in the Bragg angle or crystallinity when the concentration of the dextran was 3% or 5% w/w (Table 24).

Fig. 89 shows the influence of dextran molecular weight on NWF-compaction force profile at 3% w/w concentration of dextran in co-transformed sucrose. The co-transformed powders prepared using dextrans with molecular weights 9,000 D and 65,000 D show similar NWF values to those for transformed sucrose. When dextran with a molecular weight 252,000 D and 2,000,000 D were incorporated the NWF values were higher than those for transformed sucrose. Thus, increasing the molecular weight of dextran included in the co-transformed powder was found to increase NWF values. The moisture levels for co-transformed sucrose using different molecular weight dextrans are tabulated in Table 25. It would appear that whatever differences in plasticity were observed for the various powders these were due

to an effect of dextran incorporation and not to moisture levels. The NWF results obtained for sucrose co-transformed with dextran were directly comparable with those for pure transformed sucrose and the moisture levels of both sets of material were very similar (Tables 18 and 25).

Fig. 90 shows the influence of dextran molecular weight on the NWF of tablets compressed from sucrose co-transformed with 5% w/w dextran. The incorporation of 5% dextran caused a reduction in NWF when compared with pure transformed sucrose. The results appear to indicate that at a concentration of 5%, dextran reduces the inherent plasticity of transformed sucrose. The influence of moisture on the performance of these samples can be disregarded since the moisture levels in Table 25 show that the values were comparable with those of other dextran co-transformed products, which did not show this effect. It is thought that dextran may introduce flaws in sucrose microcrystals which probably remain intact during compaction, however, during the diametral test, their coalescence with the main fracture crack would give low tensile strength and NWF values which could lead to misinterpretation as due to low inter-particle bonding. A probable reason for the absence of habit modification of sucrose by dextran is that due to the massive crystallization pressure at the point of transformation and thus crash crystallization, dextran may have been unable to adhere long enough to any of the sucrose faces.

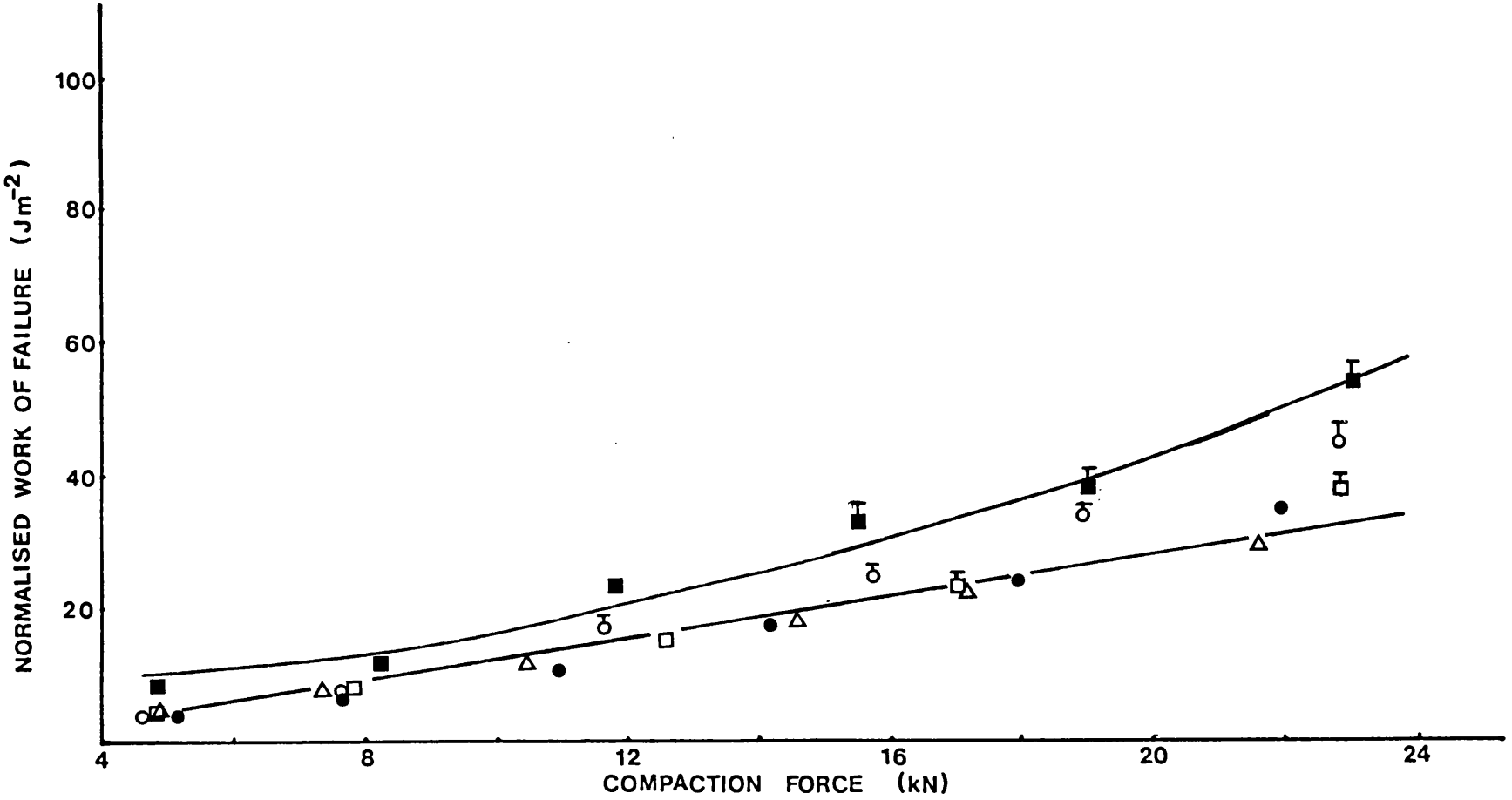

Figure 89. Influence of co-transformation of 3% w/w dextran of different molecular weight with sucrose and compaction force on the normalised work of failure of tablets. (■) 2,000,000 D, (o) 252,000 D, (□) 65,000 D, (●) 9,000 D and (△) pure transformed sucrose.

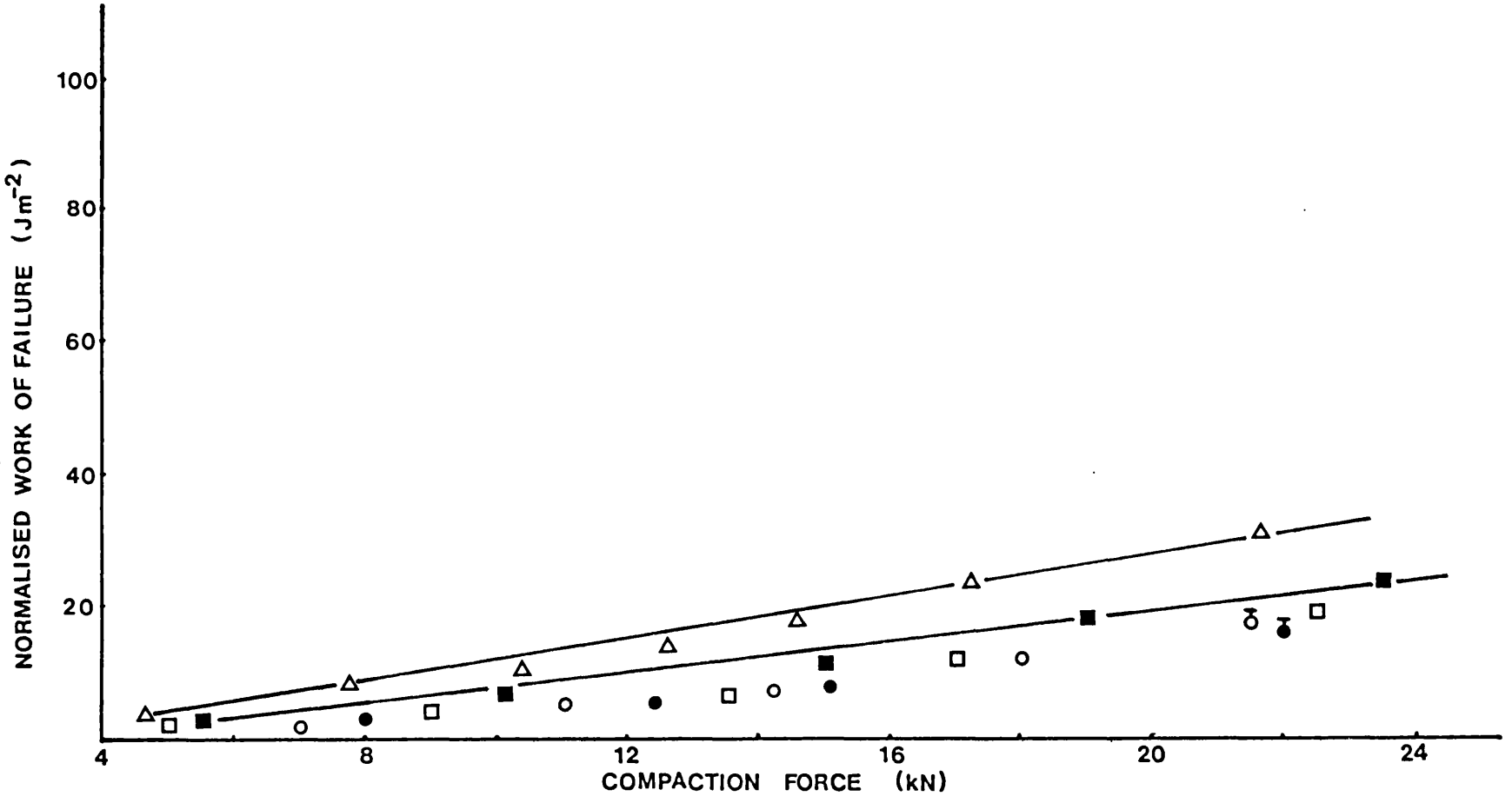

Figure 90. Influence of co-transformation of 5% w/w dextran of different molecular weight with sucrose and compaction force on the normalised work of failure of tablets. (■) 2,000,000 D, (o) 252,000 D, (□) 65,000, (●) 9,000 D and (Δ) pure transformed sucrose.

Peak No.	3% w/w DEXTRAN Bragg angle	Peak height	5% w/w DEXTRAN Bragg angle	Peak height
1	4.00°	9.0mm	4.05°	10.0mm
2	5.65	68.0	5.65	54.0
3	6.25	43.0	6.25	50.0
4	6.35	63.0	6.40	65.5
5	7.60	34.0	7.60	39.0
6	8.00	15.0	8.05	12.5
7	8.20	17.0	8.20	17.5
8	8.90	13.0	8.85	12.0
9	9.25	136.0	9.25	139.0
10	9.65	100.5	9.70	98.0
11	10.05	40.0	10.00	36.0
12	10.30	45.5	10.30	43.0
13	10.90	47.0	10.90	45.5
14	11.10	17.0	11.10	18.0
15	11.65	29.0	11.70	30.5
16	12.25	160.0	12.30	148.0
17	12.45	68.0	12.45	60.0
18	13.10	22.0	13.15	25.0
19	13.55	22.0	13.60	21.0
20	14.20	19.0	14.25	21.5

Table 24. Data derived from x-ray diffraction patterns for sucrose co-transformed with 3% and 5% w/w dextran with a molecular weight of 252,000 D.

Molecular weight of dextran (D)	% moisture content 3% w/w dextran	5% w/w dextran
2,000,000	0.24	0.21
252,000	0.19	0.22
65,000	0.26	0.20
9,000	0.25	0.23

Table 25. Moisture content, expressed as a percentage of total dry powder mass, in co-transformed powders with 3% and 5% w/w dextran of different molecular weights.

3.2.2.4 Sucrose-based Direct Compression Excipients Co-transformed with Microcrystalline Cellulose.

Microcrystalline cellulose products with different particle size (Avicel PH101, PH102, PH103 & PH105) have received great attention in the literature. Reier et al. (1966) suggested that permanent deformation by plastic flow takes place during the compaction of mcc. In the present study, our results showed that Avicel PH102 (mcc) possessed the largest NWF and hence largest plasticity when compared with other commercial direct compression excipients (Figs. 42 and 40). Wells and Langridge (1981) used mcc to impart plasticity to dicalcium phosphate dihydrate powder to enable a direct compression technique to be employed. A similar method has been used by Chilamkurti et al. (1983) to provide plasticity in a specific formulation. Armstrong and Lowndes (1984) have suggested the use of binary mixtures of mcc with a spray dried lactose (Zeparox) as a potential direct compression excipient.

In the present study, sucrose was transformed in the presence of mcc particles with the objective of entrappment of mcc in the sucrose crystal agglomerates thereby increasing the plasticity of the final powder.

The influence of mcc on NWF-compaction force profile is shown in Fig. 91. All powders co-transformed with mcc were found to have higher NWF values than pure transformed sucrose (Fig. 91). Increasing the percentage of mcc in the co-transformed powder caused an increase in the NWF values. This behaviour was expected since mcc deforms by plastic flow, consequently

facilitating intimate contact between mcc particles and increasing the number of bonding points. When the concentration of mcc co-transformed with sucrose was increased above 30% w/w of mcc, the transformation process was found to be inhibited. In the co-transformed product containing 30% w/w mcc, it was considered that the presence of a larger concentration of mcc particles resulted in increased NWF values due to the increased plasticity of the co-transformed product.

Fig. 76 shows the influence of a binary dry mix of mcc and pure transformed sucrose on NWF; below a concentration of 20% w/w mcc mixed with transformed sucrose there was no significant increase in NWF of tablets. Thus, when 10% w/w mcc was mixed with pure transformed sucrose, at a compaction force of approximately 20kN, a NWF value of 30 J/m2 was obtained, whereas when the mcc concentration was increased to 20% w/w, the NWF was increased four fold to 120 J/m2 at the same compaction force. However, when the percentage of mcc co-transformed with sucrose was increased from 10% to 20% w/w, the NWF increased only from approximately 53 to 61 J/m2 and, when sucrose was co-transformed with 30% w/w mcc, the NWF increased to only 68 J/m2 (Fig. 91).

Table 26 shows the moisture levels, at the time of compression for the co-transformed products in Fig. 91. The influence of moisture on the performance of these products can be disregarded since the moisture levels in Table 26 show that the values for all the co-transformed products with mcc are comparable. Thus a probable explanation for the trend shown in Fig. 91 is that during the co-transformation process, some

fraction of the mcc molecules get entrapped within the sucrose agglomerate, as suggested by the microscopic examination of this product, consequently reducing the effective concentration of mcc in the product. This explains the lack of difference in NWF between the four co-transformed products at lower compaction forces (4-8kN in Fig. 91), since at lower compaction forces only a very small fraction of the agglomerates undergo fracture thus releasing only a small number of mcc particles so that mcc is unable to exert its full potential effect on sucrose compactibility and consequently, the degree of inter-particle bonding is similar for all these powders.

The trend obtained when sucrose was co-transformed with mcc was different from that for other polymeric materials such as, maltodextrin and gelatin, where a reduction in the concentration of maltodextrin and gelatin incorporated, increased the plasticity of transformed sucrose. This difference in behaviour of mcc and either maltodextrin or gelatin suggests that the mechanism by which plasticity was altered using mcc was different from that for maltodextrin or gelatin. Unlike maltodextrin and gelatin, mcc is insoluble in aqueous media, and consequently, mcc is unlikely to be able to influence the sucrose lattice or the agglomerate structure during the transformation process. The mcc may have a dry binder plasticizing effect, so that an increase in mcc concentration simply increases the plasticity of the mixed product rather than having any effect on the sucrose per se.

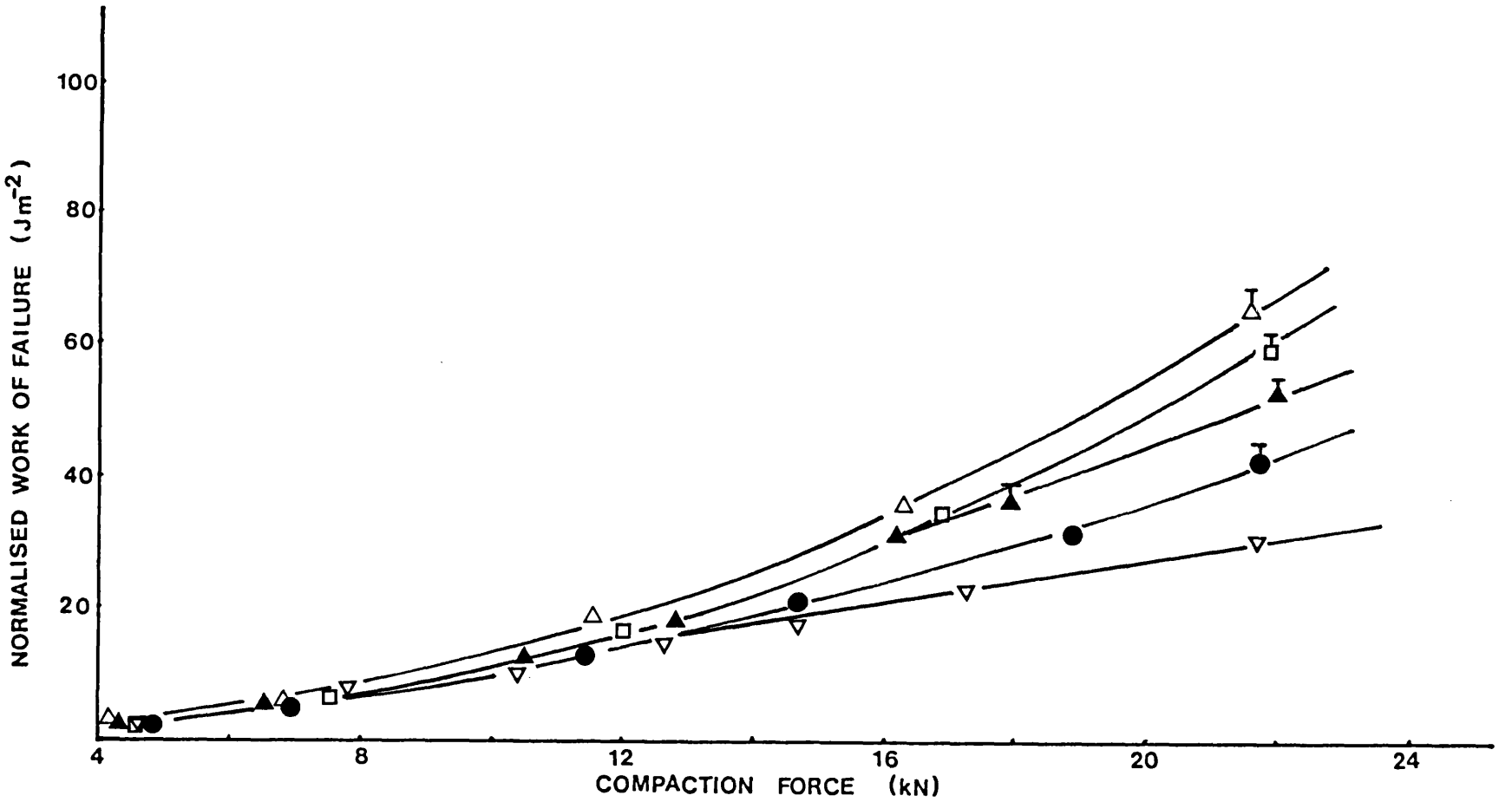

Figure 91. Influence of co-transformation of increasing concentrations of microcrystalline cellulose with sucrose and compaction force on the normalised work of failure of tablets. (●) 3%, (▲) 10%, (□) 20% and (△) 30% w/w microcrystalline cellulose co-transformed with sucrose. (▽) pure transformed sucrose.

Concentration of mcc in sucrose (% w/w)	Concentration of moisture at time of compression (%).
3	0.20
10	0.25
20	0.24
30	0.27

Table 26. Moisture levels, expressed as a percentage of total dry powder mass at the time of compression for co-transformed powders with mcc (Avicel PH102).

Concentration of cellulose ester in co-transformed powder	Concentration of moisture at the time of compression (%)
3% cellulose acetate	0.26
10% cellulose acetate	0.23
3% cellulose triacetate	0.21

Table 27. Moisture level, expressed as a percentage of total dry powder mass, in various co-transformed powders with cellulose esters, at the point of compression.

3.2.2.5 Sucrose-based Direct Compression Excipients Co-transformed with Other Types of Celluloses.

3.2.2.5.1 Fibrous Alpha Cellulose (fc).

Unlike mcc, fibrous alpha cellulose is inexpensive. Sucrose was co-transformed with 3% and 10% w/w of fc. Fig. 102B shows an agglomerate present in a co-transformed product with 10% w/w of fc. The cellulose fibres have been partially enclosed in the agglomerate.

Fig. 92 shows the relationship between NWF and compaction force for a 3% w/w fc co-transformed powder. The powder with 10% w/w was found to exhibit poor flow which prevented reproducible volumetric filling under test conditions, even after the addition of 5% w/w colloidal silicon dioxide as a glidant (Aerosil). Sucrose co-transformed with 3% w/w fc possessed larger NWF values than pure transformed sucrose and the NWF values of the former were similar to sucrose co-transformed powder with 10% mcc. The moisture content at the point of compression was approximately 0.25% of the total dry powder mass for sucrose co-transformed with 3% w/w fc. It was considered that fc is less entrapped at 3% than mcc at 10%, therefore fc was exerting a greater inter-agglomerate binding effect than mcc.

3.2.2.5.2 Cellulose Esters.

To investigate the influence of side chains on the cellulose unit, two types of cellulose esters - cellulose acetate and triacetate - were co-transformed with sucrose. Fig. 102C

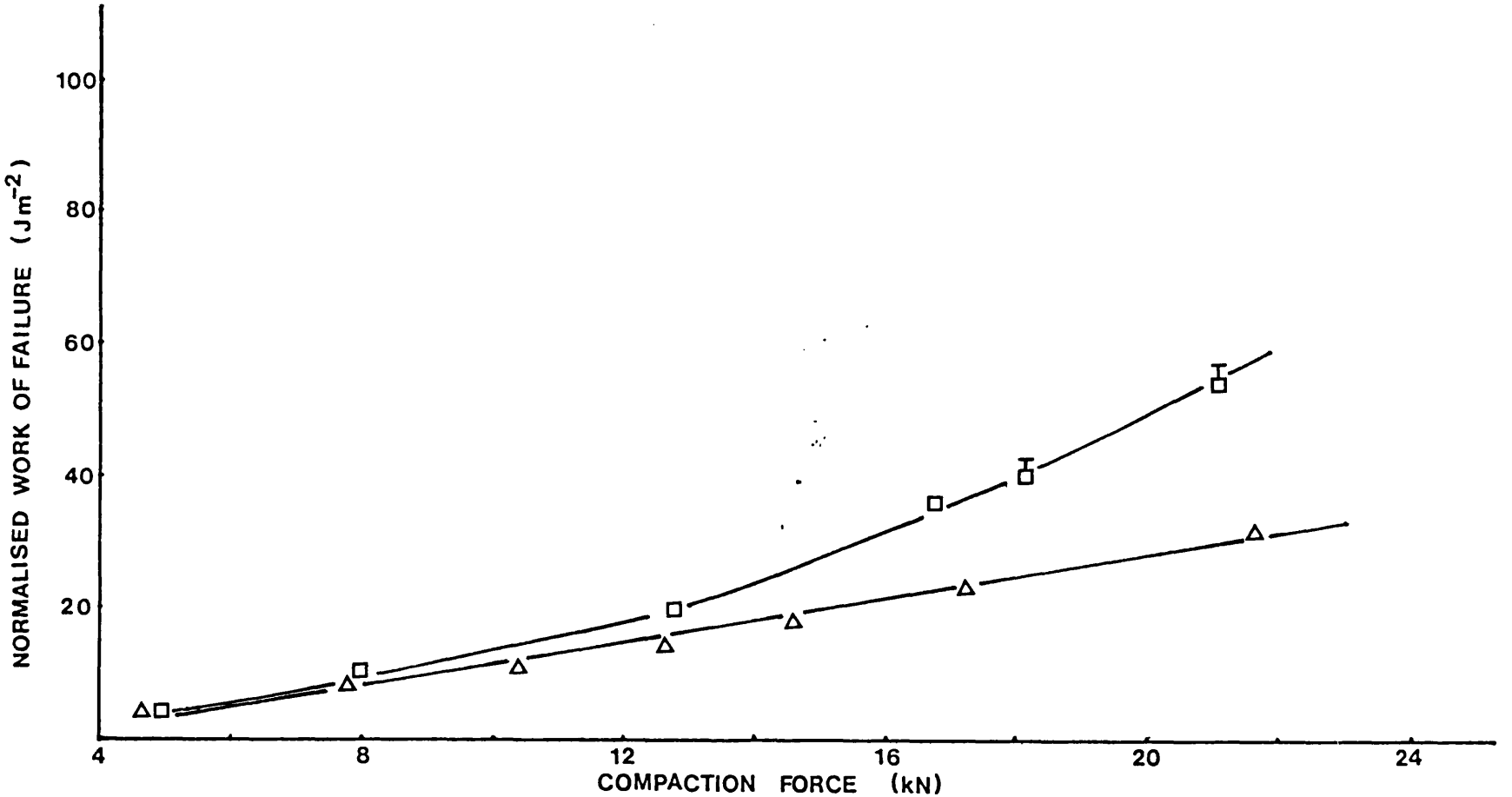

Figure 92. Influence of co-transforming 3% w/w fibrous cellulose with sucrose and compaction force on the normalised work of failure of tablets. (□) 3% fibrous cellulose and (△) pure transformed sucrose.

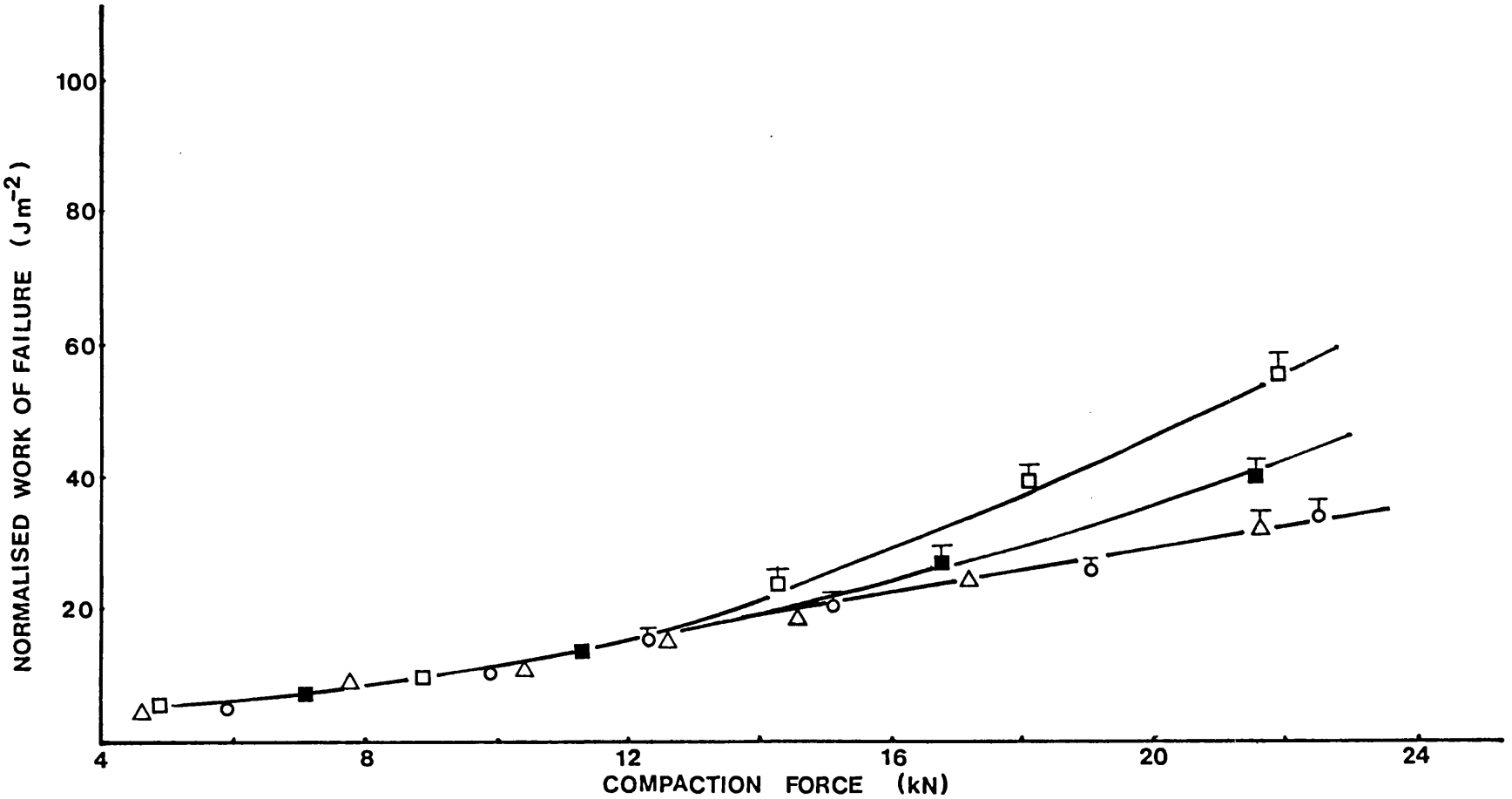

Figure 93. Influence of co-transforming different types of cellulose esters with sucrose and compaction force on the normalised work of failure of tablets. (□) 10%, (■) 3% w/w cellulose acetate and (o) 3% w/w cellulose triacetate co-transformed with sucrose. (△) pure transformed sucrose.

(see Appendix I) shows a typical agglomerate present in a powder sample of sucrose co-transformed with 10% w/w cellulose acetate (ca). Similar agglomerates were also present in samples of sucrose co-transformed with 3% ca and with cellulose triacetate. The influence of 3% and 10% w/w of ca on NWF of co-transformed sucrose tablets is shown in Fig 93. The co-transformation of sucrose with 3% w/w ca resulted in an increase in the NWF compared to pure transformed sucrose and the NWF was further increased for 10% w/w ca co-transformed product. However, when sucrose was co-transformed with 3% w/w cellulose triaceate. NWF values were similar to those for pure transformed sucrose, These results indicate that the plasticity of transformed sucrose was not improved by increasing the number of acetate groups in the cellulose unit. The moisture levels at the time of compression for the cellulose ester-based powders are shown in Table 27. These values are similar to those for other co-transformed powders and it is therefore considered that the influence of moisture content can be disregarded.

3.2.2.6 Sucrose-based Direct Compression Excipients Co-transformed with Sucrose Esters.

Sucrose was co-transformed with three types of sucrose esters having different ester chain lengths. It was considered that some of the sucrose ester could co-crystallize with sucrose, thus providing a method of incorporating long chain fatty acids during sucrose transformation with the objective of plasticizing the transformed sucrose. Three grades of sucrose esters; type F90

contains 45% mono-esters of stearate and palmitate (ratio of 3:7) and 55% a mixture of di-, tri-, and poly-esteric groupings of the same ratio of esters, while type F110 consists of 50% mono-ester and 50% di-, tri-, and poly-esters. Type F160 contains 70% mono-ester and 30% is higher poly-esters.

5% w/w sucrose ester was found to be the maximum percentage of sucrose ester which could be co-transformed with sucrose. Fig. 102D (see Appendix I) shows a typical agglomerate present in all the sucrose ester co-transformed powders which was similar to those present in sucrose transformed with other polymeric materials (c.f Figs. 100C, 100D and 101D, see Appendix I). Examination of the crystal structure by x-ray diffraction showed that no change in crystal lattice structure occurred during co-transformation of sucrose with 3% w/w of type F90 or F160 and the x-ray diffraction pattern was comparable to that for pure transformed sucrose (Table 28). Fig 94 shows the influence of the grade of sucrose ester on the NWF-compaction force profile when the concentration of sucrose ester co-transformed was 3% w/w. Both F90 and F110 types of sucrose esters were found to slightly increase the plasticity of transformed sucrose.

Fig. 95 shows the influence of different types of sucrose esters on the NWF-compaction force profile when the concentration of sucrose ester co-transformed with sucrose was 5% w/w. The results indicate that the inclusion of 5% w/w sucrose esters produced very little change in the behaviour of transformed sucrose tablets, with a reduction in plasticity compared with that found at 3% for F90 and F110. A general trend also suggested

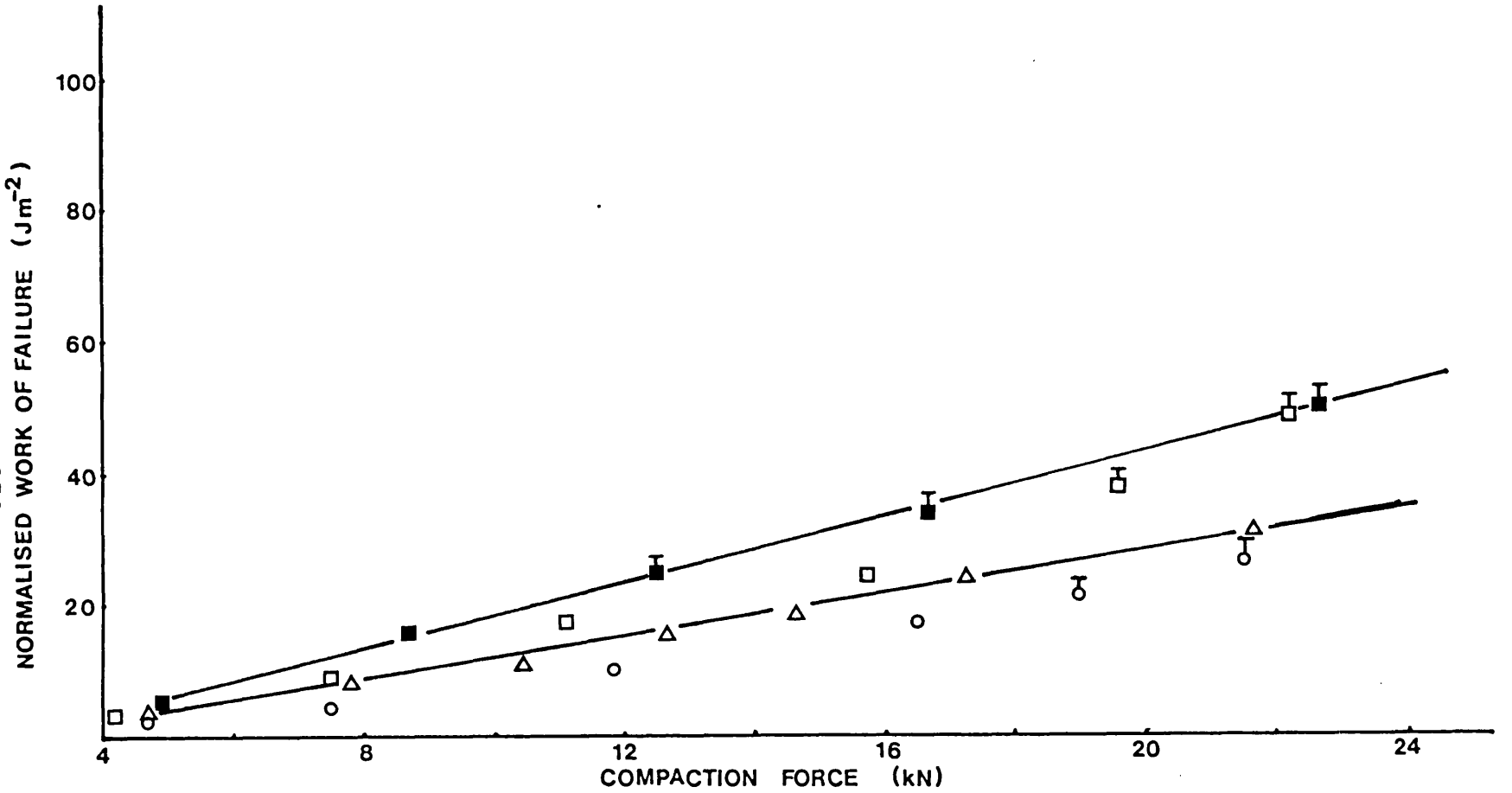

Figure 94. Influence of co-transforming different types of sucrose esters at a concentration of 3% w/w with sucrose and compaction force on the normalised work of failure of tablets. (■) F90, (□) F110, (o) F160 and (Δ) pure transformed sucrose.

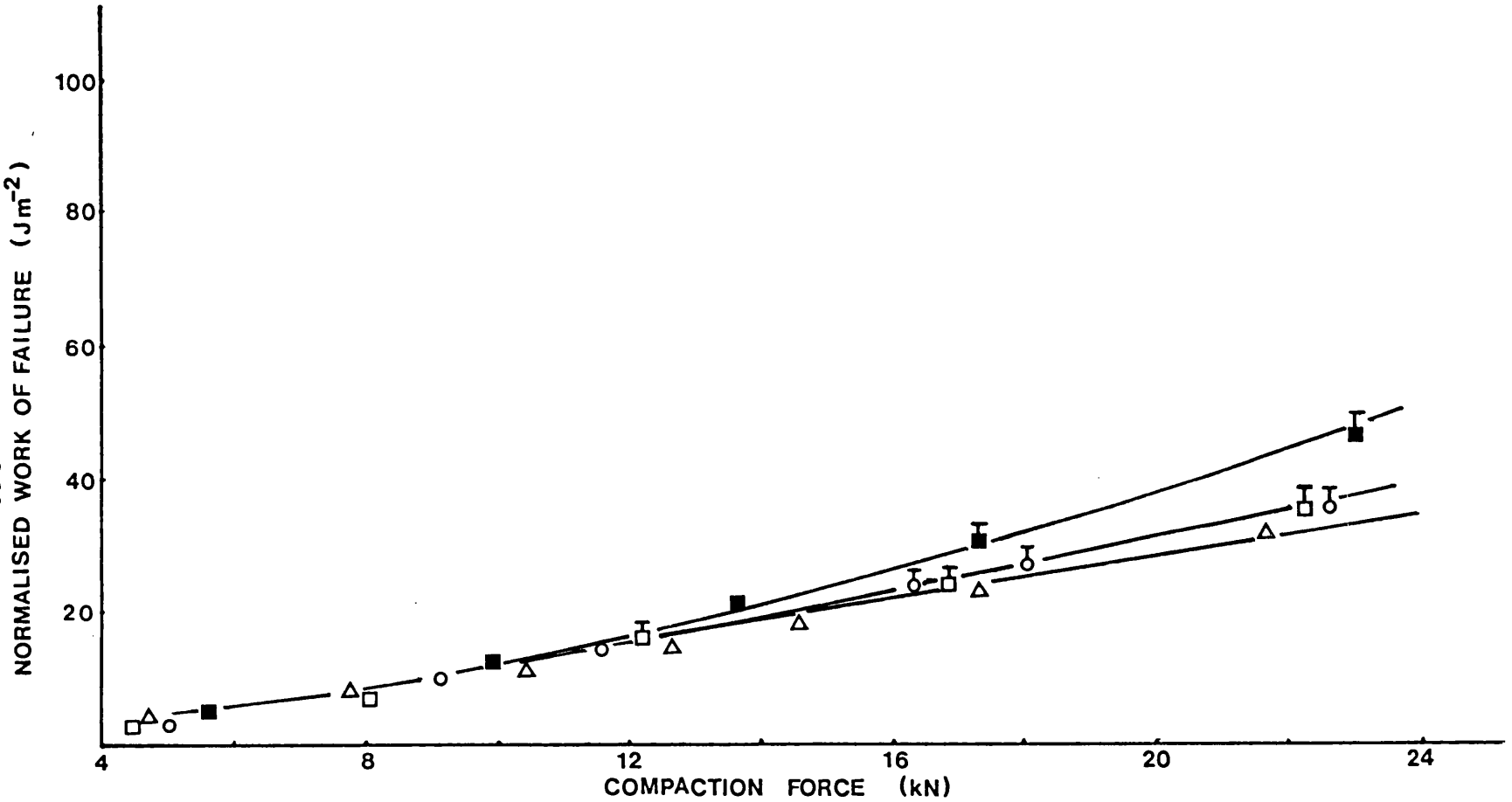

Figure 95. Influence of co-transforming different types of sucrose esters at a concentration of 5% w/w with sucrose and compaction force on the normalised work of failure of tablets. (■) F90, (□) F110, (o) F160 and (Δ) pure transformed sucrose.

Peak No.	Sucrose co-transformed with 3% sucrose ester F90 p1	F90 p2	F160 p1	F160 p2
1	4.05°	12.0mm	4.00°	16.0mm
2	5.20	50.0	5.20	62.0
3	6.25	33.5	6.25	45.0
4	6.45	49.0	6.50	40.0
5	7.65	36.0	7.65	34.0
6	8.05	13.0	8.00	17.0
7	8.15	20.0	8.15	25.0
8	8.90	18.0	8.95	15.0
9	9.30	120.0	9.35	137.0
10	9.60	103.0	9.60	94.0
11	10.10	50.0	10.15	47.0
12	10.35	60.0	10.35	67.0
13	10.85	58.0	10.80	54.0
14	11.05	24.0	11.05	30.0
15	11.60	25.0	11.55	22.0
16	12.25	157.0	12.30	169.0
17	12.45	74.0	12.40	67.0
18	13.20	24.0	13.20	24.0
19	13.60	20.0	13.55	15.0
20	14.20	16.0	14.25	17.0

Table 28. Data derived from x-ray diffraction patterns of sucrose co-transformed with 3% sucrose ester types F90 and F160. The Bragg angle is represented by p1, while the degree of crystallinity (peak height) is represented by p2.

Sucrose ester grade	Ester conc. (% w/w).	moisture level at time of compression (%).
F90	3	0.20
F90	5	0.20
F110	3	0.23
F110	5	0.27
F160	3	0.30
F160	5	0.24

Table 29. Moisture content, expressed as a percentage of total dry powder mass, at the time of compression for co-transformed powders prepared with different types and concentrations of sucrose esters.

that the material with the highest concentration of polyesters (F90) produced the largest plasticizing effect. The moisture levels at the time of compression for all the sucrose ester co-transformed powders are tabulated in Table 29 and are comparable to the rest of the co-transformed powders and it is therefore considered that any differences observed between these powders were mainly due to changes in the concentration of the mono- and higher esteric groupings.

3.2.3 Alternative Methods for Producing Plasticity in Transformed Sucrose.

With the exception of sucrose co-transformed with either 1% or 3% w/w maltodextrin and 1% w/w of gelatin B.S. 60 or B.S. 300, all other co-transformed products were found to have plasticity either similar to commercial direct compression excipients such as Fast-Flo, Dipac, Tablettose, Emcompress and Nutab or only slightly higher than transformed sucrose (see section 3.2.2). Other methods of producing plasticity were therefore investigated.

3.2.3.1 Transformed Sucrose Coated with Maltodextrin.

Fig. 101E (see Appendix I) shows the agglomerate type present in transformed sucrose coated with maltodextrin. The original rough surface morphology of transformed sucrose was slightly smoothed out, presumably by the overlapping of maltodextrin. It was hypothesised that the distribution of polymeric material on the surface of transformed sucrose could

increase polymeric inter-agglomerate contact and hence have a plasticizing effect on transformed sucrose. The influence of a maltodextrin coat on the NWF-compaction behaviour of transformed sucrose is shown in Fig. 96. The moisture content at the time of compression was 0.28%, which was comparable to the rest of the sucrose co-transformed samples. The maltodextrin coat was found to increase the NWF values of transformed sucrose at all compaction forces. However, the NWF values were lower than those obtained when sucrose was co-transformed with maltodextrin. It was therefore concluded that for maltodextrin the largest increase in NWF achievable was by co-transformation and when the concentration of maltodextrin was 1%.

3.2.3.2 Transformed Sucrose with Polyethylene Glycol.

Transformed sucrose was coated with two different molecular weights of polyethylene glycol (PEG 4,000 D & 6,000 D). A typical agglomerate present in both these powders is shown in Fig. 101F (see Appendix I). The influence of PEG coats on the NWF -compaction force profile is shown in Fig. 97. Both PEG 4,000 and PEG 6,000 coats increased the NWF of pure transformed sucrose, but no difference in NWF was visible when the molecular weight of PEG was increased from 4,000 to 6,000 D. The moisture level at the point of compression was 0.30%, expressed as a percentage of total dry powder mass. Increase in plasticity of transformed sucrose by a PEG coat was comparable to the plasticity induced when either 3% or 5% w/w of maltodextrin was co-transformed with sucrose (Fig. 79).

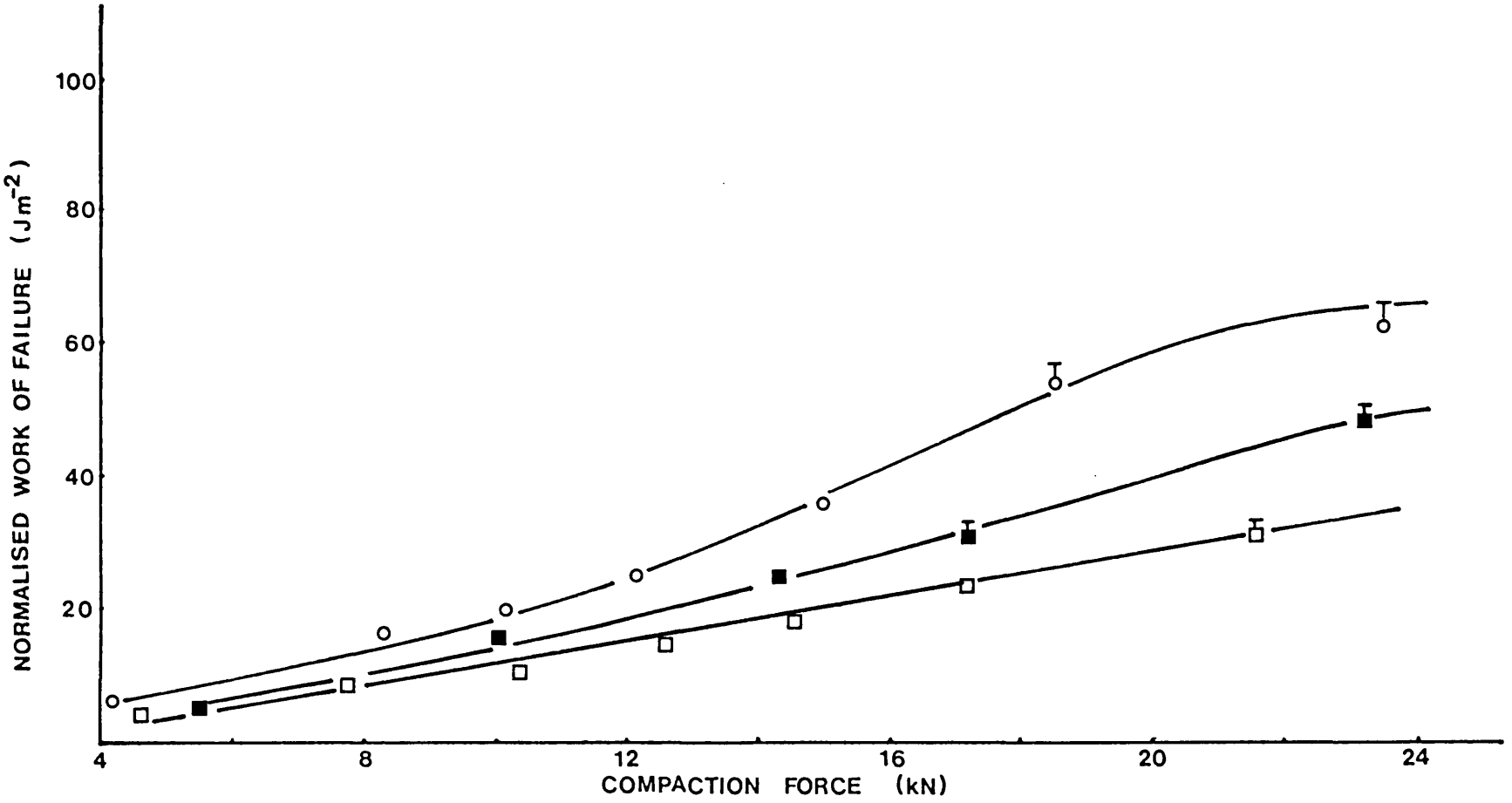

Figure 96. Influence of a 3% maltodextrin coat on transformed sucrose and compaction force on the normalised work of failure of tablets. (■) transformed sucrose coated with maltodextrin, (o) 3% w/w maltodextrin co-transformed with sucrose and (□) pure transformed sucrose.

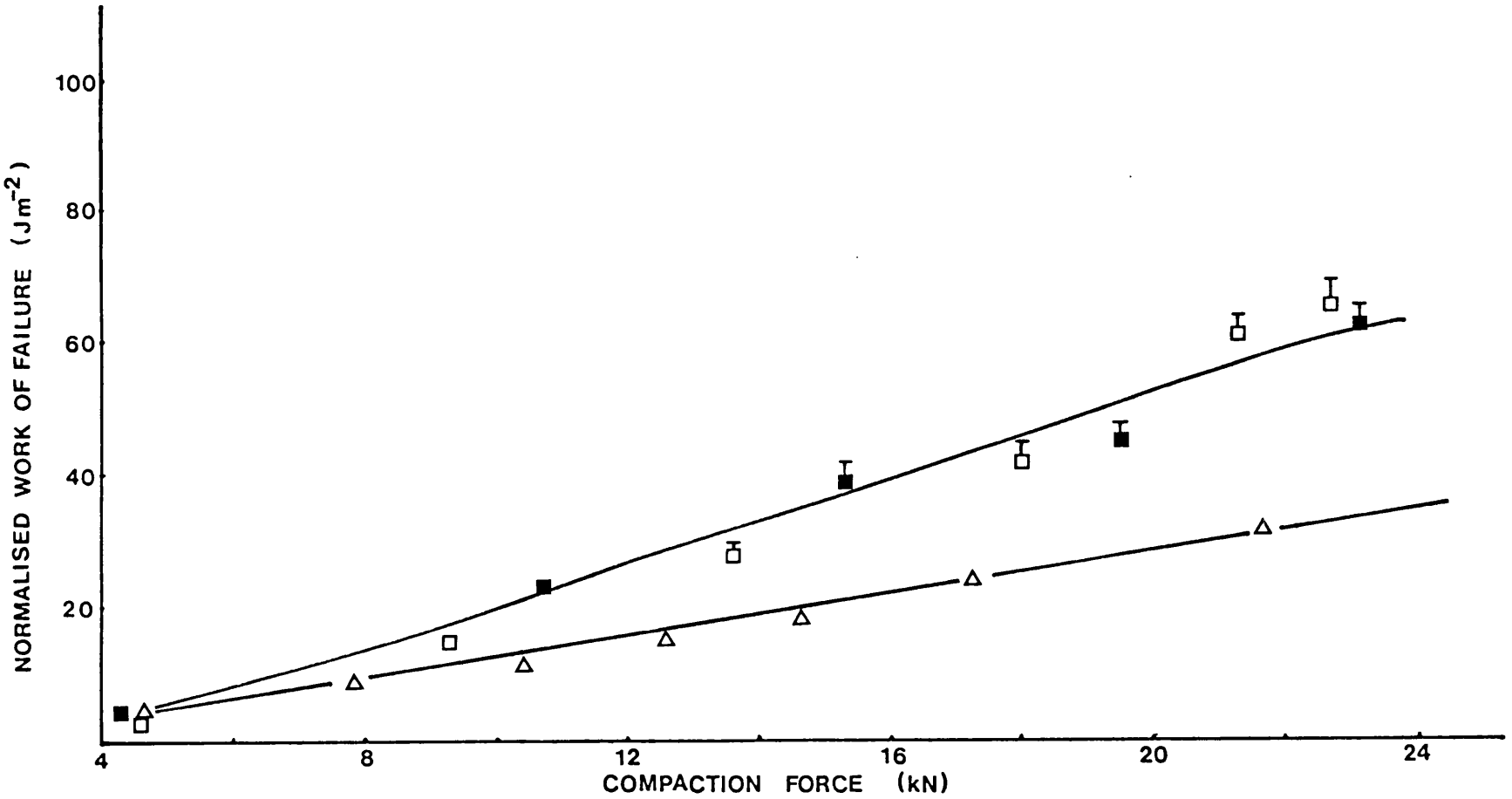

Figure 97. Influence of a polyethylene glycol coat on transformed sucrose and compaction force on the normalised work of failure of tablets. (□) polyethylene glycol (PEG) 4,000 and (■) PEG 6,000. (△) pure transformed sucrose.

3.2.4 Impure Sucrose Crystals.

In section 3.2.2 it was hypothesised that alteration of the sucrose lattice by crystal poisons could increase the plasticity of sucrose. Sucrose crystals with a large quantity of impurities are found in the third crop recovery of refinery sugar which is the residual product after a third re-crystallization stage of refining sugar. A commercial crystallized sucrose was used as a control. The moisture content at the time of compression for the third crop sample was approximately 0.32%.

Fig. 98 shows the influence of impurities in the sucrose crystals on the NWF-compaction force profile. Compared with pure sucrose crystals, the third crop crystals showed greater plasticity than pure sucrose or transformed sucrose (Fig. 75). Thus, these results suggested that the presence of impurites could be responsible for changes in the plasticity of sucrose crystals. However, when the third crop sucrose was examined by x-ray diffraction, the diffraction pattern and intensity (Table 30) were found to be similar to those for pure sucrose (c.f Table 18). Table 30 also shows the values for a sample of Brown Sugar (Domino Brown granulated sucrose, U.S Patent 3,194,682), which showed some changes in crystallinity, for example peak number 9, at a Bragg angle of 9.25° . The brown sugar showed lower crystallinity than the 3rd crop sample, but there was no siginificant shift in the position of the peaks suggesting that there was an absence of morphic changes in the different sucroses and that the crystalline structure of both these samples was similar. However the NWF of brown sugar tablets increased

sharply from approximately 35 J/m2 at a compaction force of 6kN to approximately 400 J/m2 at 24kN compaction force (Fig. 99). It is thought that the plasticity of sucrose was increased by caramelised sucrose or presence of impurities in brown sugar such as cane waxes.

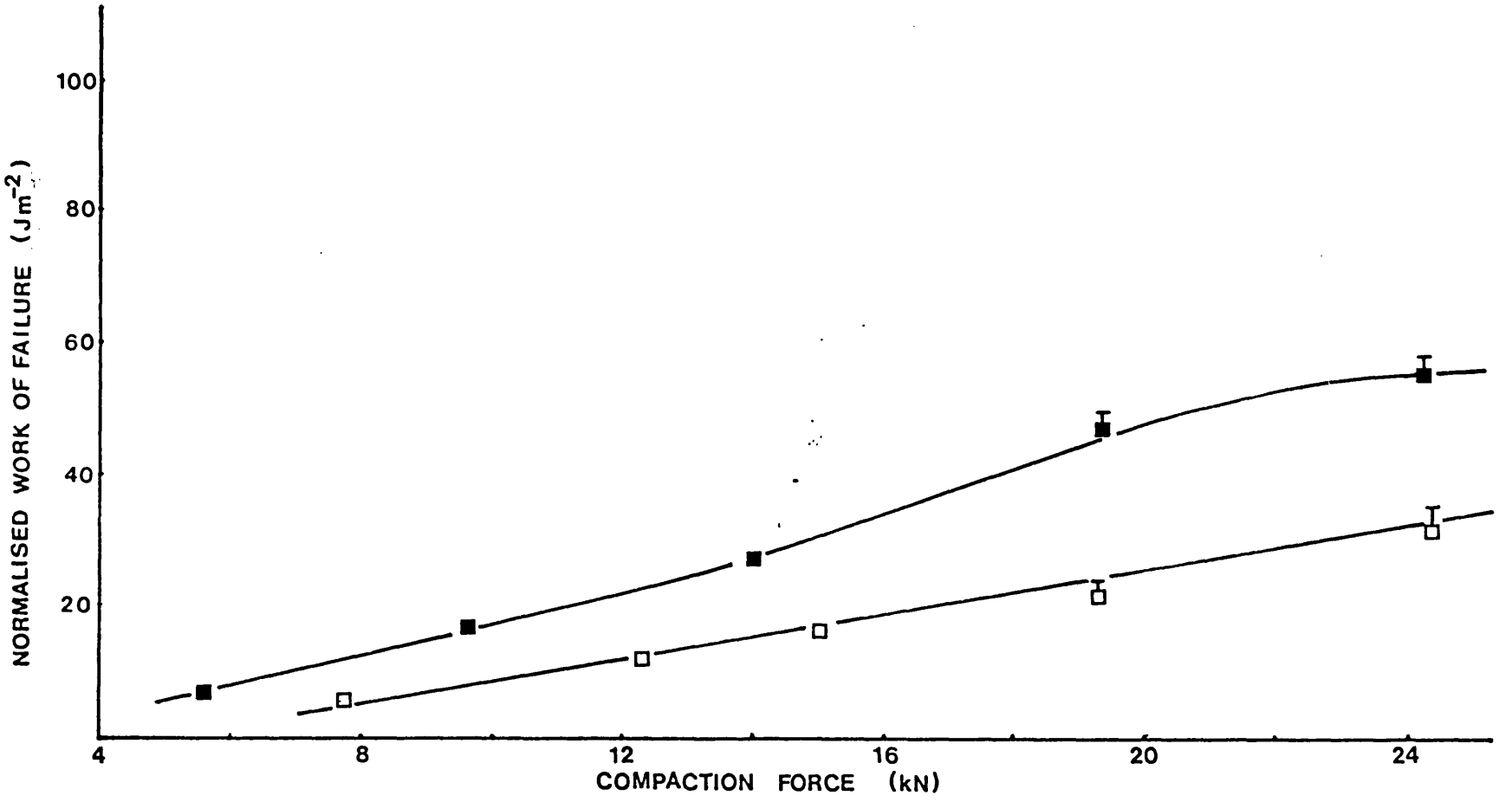

Figure 98. Influence of impurities in sucrose sample and compaction force on the normalised work of failure of tablets. (■) Third crop recovery sample, (□) pure sucrose crystals.

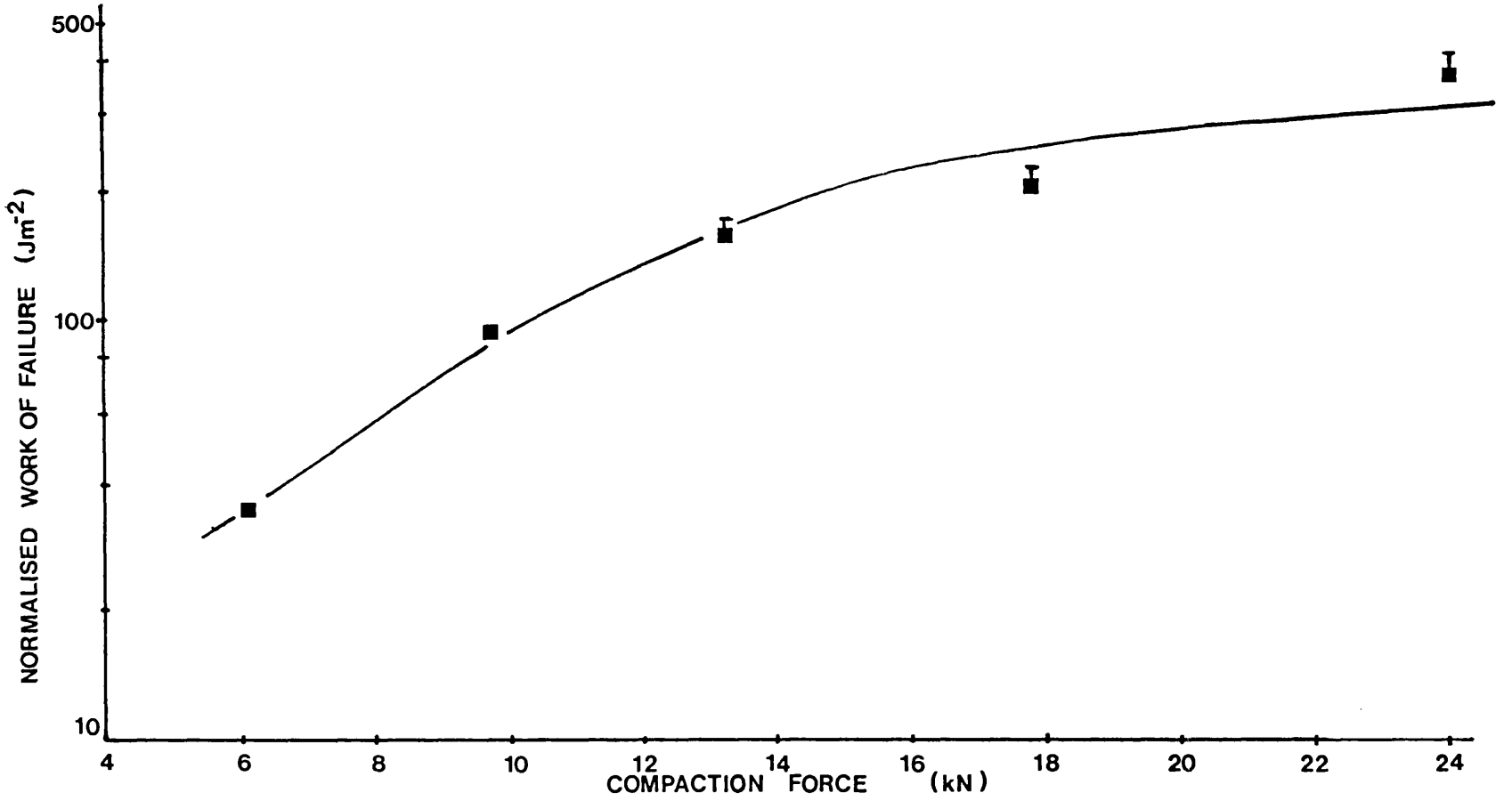

Figure 99. Relationship between normalised work of failure and compaction force of tablets compressed of "Brown sugar".

Peak No.	3rd Crop Sucrose Bragg angle	3rd Crop Sucrose Peak height	Brown Sucrose Bragg angle	Brown Sucrose Peak height
1	4.00°	15.0mm	4.00°	8.0mm
2	5.70	55.0	5.70	52.0
3	6.25	30.0	6.25	32.0
4	6.45	77.0	6.40	51.5
5	7.60	34.0	7.60	31.0
6	8.05	9.0	8.00	13.0
7	8.20	26.0	8.20	14.0
8	8.90	11.0	8.90	11.0
9	9.25	172.0	9.25	112.0
10	9.65	98.0	9.70	81.0
11	10.05	28.0	10.05	31.0
12	10.25	36.5	10.30	41.0
13	10.80	36.0	10.90	42.5
14	11.10	14.0	11.10	17.0
15	11.60	19.0	11.65	28.0
16	12.20	200.0	12.30	128.0
17	12.45	110.0	12.45	53.0
18	13.10	45.0	13.05	18.0
19	13.55	20.0	13.55	19.0
20	14.20	15.0	14.15	17.0

Table 30. Data derived from x-ray diffraction patterns for a 3rd crop recovery sample and commercial "Brown Sugar" sample.

4 CONCLUSIONS.

From the study of methods for characterization of the mechanical properties of tablets compressed from some direct compression excipients, it may be concluded that use of normalised work of failure determinations allowed quantitative differences in plasticity of Avicel PH102, anhydrous lactose, Fast-Flo, Dipac, Tablettose, Emcompress and Nutab to be distinguished.

A new parameter was developed to account for changes in strain rate application. Failure viscosity used the time component of tablet loading as a multiplier and was therefore found to have a similar sensitivity to changes in excipient plasticity to that obtained using NWF and it was concluded that both FV and NWF determinations gave a good indication of the plasticity of different excipients.

It was concluded that use of a second new parameter termed "power of failure", developed to take account of differences in crack propagation rates between tablet excipients, lacked the sensitivity required to distinguish small changes in plastic behaviour. Nevertheless it was considered a useful standard for comparative measure of tablet strength for tablets tested using equipment with different rates of loading.

It was concluded that the difference in fatigue behaviour for Avicel PH102, Microtal, Dipac, Emcompress and Tablettose tablets was due to differences in the rates of crack propagation through the tablets. The fatigue test developed in this study was

found to distinguish between the two main causes of tablet failure: ductile and brittle fracture. Differences in ductile fracture for Avicel and Microtal were also found to be distinguishable, however, it was concluded that the fatigue test was unable to differentiate between the plasticity of Microtal and Dipac tablets - differences which were apparent using NWF determinations. Monitoring the acoustic emissions from the tablets during fatigue testing showed that different modes of fatigue failure occurred prior to brittle or ductile fracture. In Avicel and Microtal tablets, the fatigue crack propagation (FCP) was retarded and was dependent on inter-particle bond strength. However, in Emcompress tablets, FCP occurred in rapid short bursts and was found to be independent of inter-particle bond strength.

Due to the high attenuation characteristics of the pharmaceutical powders used here, a study of FCP in tablets using SLAM proved impossible since images of the internal structure of stressed tablets could not be obtained.

It was concluded that an assumption widely accepted in the present literature, - namely that the work performed on the second compression without ejection, can be used to represent the work required for elastic deformation during tablet compression - was invalid. Since at least 10 multiple compressions for Avicel and 13 for Microtal and Emcompress were necessary in order to obtain the true value for the work performed during elastic deformation, it was further concluded that the values for work required for elastic deformation quoted in the literature are an

over-estimation resulting in an under-estimation of the true work of compaction. Determination of the true work of compaction was found not to be a good measure of the inherent capacity of an excipient to undergo irreversible deformation. It was also found that the method used to determine the true work of compaction influenced power of compaction determinations. It has been proposed that a plot of power of compaction versus tensile strength or NWF could be used to predict the probable compressional behaviour of formulations when transferring them from a slow tableting machine to faster pilot scale or production equipment, a problem frequently encountered in pre-formulation studies.

It was concluded that the rheological behaviour of direct compression excipients could be characterised by plotting creep compliance versus time. The curves were split up into three distinct regions corresponding to different rheological behaviour for each excipient: elastic; visco-elastic and plastic deformation. Starch 1500 was found to exhibit higher plastic properties than Avicel PH102 powder. However, Starch 1500 also possessed much larger elastic properties than Avicel and it was concluded that the low mechanical strength of Starch 1500 tablets reported in the literature probably resulted from bond disruption caused by excessive elastic recovery even though a large element of plastic deformation occurred on compression.

The principles of particle engineering were used to produce a range of direct compression excipients in the present study. The transformation of sucrose in the presence of polymeric

materials, such as maltodextrin, gelatin and various types of celluloses was found to increase the plasticity of tablets over that found with pure transformed sucrose. However, the plasticity of the product of sucrose co-transformation with either 5% dextran or 5% sucrose esters was found to be lower than that for pure transformed sucrose. It was concluded that the largest increase in sucrose plasticity was produced by co-transformation with maltodextrin or gelatin (B.S. 60, 300) at a concentration of 1%. It has been proposed that incorporation of such polymeric materials resulted in a weakening of the bonding between sucrose microcrystals so that during compaction, fracture occurred much more readily than that in pure transformed sucrose, thereby inducing greater inter-particle bonding. It was concluded that at concentrations greater than 1% the internal agglomerate structure may still be weakened but that bonding between dissimilar particles predominated thereby reducing the NWF values of tablets. It was found that several of the co-transformed products of sucrose with various types of polymeric materials exhibited higher plasticity than other commercially available sucrose-based direct compression excipients such as Dipac and Nutab and other direct compression excipients such as Fast-Flo, Tablettose and Emcompress.

5. SUGGESTIONS FOR FUTURE WORK.

I. A plot of tensile strength or NWF versus power of compaction has been proposed in the present study as a useful parameter for predicting the behaviour of formulations on transferring from a slow to fast tableting machine. However, the hypothesis requires testing using higher compaction rates than those used in the present study.

II. Non-destructive testing is presently widely used by structural engineerers to examine the internal structure of components for micro-cracks and cracks. The use of such techniques may be useful in understanding the occurrence of capping and lamination in tablets. Also this principle could be applied to on-line production to examine individual tablets for the presence and number of cracks which if correlated with tensile test data, could replace destructive testing and enable examination of every tablet manufactured.

III. The importance of rate of load application and removal on the deformation tendency of pharmaceutical powders is well documented (David and Augsburger, 1977; Rees and Rue, 1978b; Barton, 1978; Roberts and Rowe, 1985). In order to determine the rheological behaviour during production conditions, creep analysis should be performed at rates of loading higher than those used in the present study.

IV. There was no control over the rate of sucrose transformation in the present study due to massive crystallization pressure. However, conventional sucrose crystallization is a slow process and any polymeric material when incorporated should have sufficient time to come into close contact with one of the sucrose faces so that inclusion in the crystal can occur and may produce imperfections within the crystal lattice, leading to relaxation of the rigid sucrose crystal.

In order to investigate if the trend of increased plasticity with reduced polymeric concentration observed in maltodextrin and gelatin co-transformed sucrose, holds for other polymeric materials such as dextrans and Protein S, lower concentrations of these materials should be co-transformed with sucrose. In the present study, the lowest concentration of polymeric material co-transformed with sucrose was 1% w/w and it would therefore be of interest to investigate the effect of lowering the concentration of polymeric material below 1% w/w on the plasticizing effect. Consolidation of the powders has been inferred from normalised work of failure data and for comparative purposes, Heckel plots for these powders should be constructed in order to investigate the type of consolidation occurring during compaction (Rees and Hersey, 1970). Changes in consolidation behaviour with alteration of powder composition for binary mixes of transformed sucrose with Avicel PH102 and for transformed sucrose with maltodextrin could be followed by such Heckel plots. A sample of "Domino Brown Sugar" (Amrstar Co.) showed that there was no change in the sucrose crystallinity or presence of

polytypes, however, the plasticity was comparable to Avicel PH102. Knowledge of the true chemical composition of this product may give additional information for future particle engineering of sucrose based direct compression excipients.

Recently Staniforth (1985) compared the segregation tendencies exhibited by mixes of a model drug with various sucrose based direct compression excipients. It would be of interest to compare the segregation tendencies exhibited by some of the sucrose co-transformed products designed in the present study.

6 REFERENCES.

Armstrong, N.A and Haines-Nutt, R.F. 1970
J. Pharm. Pharmacol., 22, 8S-10S

Armstrong, N.A. and Haines-Nutt, R.F. 1972
J. Pharm. Pharmacol., 24, 135-136P

Armstrong, N.A. and Haines-Nutt, R.F. 1973
J. Pharm. Pharmacol., 25, 147p

Armstrong, N.A. and Morton, F.S.S. 1979
Pharm. Weekblad Sci., 1, 114, p1450-1458

Armstrong, N.A., Abourida, N.M.A. and Krijgsman, L. 1982
J. Pharm. Pharmacol, 34, p9-13

Armstrong, N.A., Abourida, N.M.A. and Gouch, A.M. 1983
J. Pharm. Pharmacol, 35, p320-321

Armstrong, N.A. and Lowndes, D.H.L. 1984
Int. J. Pharm. Tech. & Prod. Manf., 5(3), p251-255

Bangudu, A.B. and Pilpel, N. 1985
J. Pharm. Pharmacol., 37, p289-293

Barcellos, A. and Carneiro, F.L.L. 1954
R.I.L.E.M. Bulletin, 13, p97

Barry, B.W. and Warburton, B. 1968
J. Pharm. Pharmacol., 20, p725-744

Barry, B.W. 1970
J. Colloid. Interfac. Sci., 32, p551-560

Barry, B.W. and Grace, A.J. 1971a
J. Texture Studies 1, p259-279

Barry, B.W. and Grace, A.J. 1971b
J. Pharm. Sci., 60, p814-820

Barry, B.W. and Grace, A.J. 1971c
J. Pharm. Sci., 60, p1198-1203

Barton, D. 1978
M.Sc. Dissertation, University of Manchester, Manchester, England.

Battista, O.A. and Smith, P.A. 1962
Ind. Eng. Chem., 54, p20-29

Beevers, C.A. and Cochran, W. 1947
Proc. Roy. Soc. London Sec. A., 190, p257

Birks, A.H. and Muzzaffar, A. 1971
Proceedings of Powtech'71 Int. Powder Tech & Bulk Granular Solids Conf., Harrogate

Blitz, J. 1967
"Fundamentals of Ultrasonics" 2nd Ed., Butterworths.

Bloom, O.T. 1925
US Patent No. 1 540 979

Bolhuis, G.K., Lerk, C.F. and De Boer, A.H. 1974
Pharmaceutish Weekblad. 109, p945-955

Bowden, F.P. and Tabor, D. 1954
"Friction and Lubrication of Solids" Vol.1, Oxford Clarendon Press.

British Standards Methods 1976
B.S. 1796

Brown, G.M. and Levy, H.A. 1963
Science, 141, p921

Brown, G.M. and Levy, H.A. 1973
Acta. Crystallogr. Sect. 13, 29, p790

Brownley, C.A. and Lachman, L. 1964
J. Pharm. Sci., 53, p452

Carless, J.E. and Leigh, S. 1974
J. Pharm. Pharmacol., 26, p289

Castello, R.A. and Mattocks, A.M. 1962
J. Pharm. Sci., 51, p106

Chilamkurti, R.N., Schwartz, J.B. and Rhodes, C.T. 1983
Pharm. Acta. Helv., 58(9-10), p251-255

Chou, C.C. and Wnukowski, M. 1980
Pro. Tech. Sess. Cane Sugar Refin. Res., p1-25

Coffin-Beach, D.P. and Mollenbeck, R.G. 1983
Int. J. Pharm., 17, p313-324

Cohn, R., Nessel, R. and Reier, G. 1966
Indus. Pharm. Sect. 113th American Pharm. Ass., Dallas, Texas, USA.

Cottrell, A.H. 1953
"Dislocations and Plastic Flow in Crystals", Oxford University Press.

Davis, S.S. and Warburton, B. 1968

J. Pharm. Pharmacol., 20, p836-839

David, S.T. and Augsburger, L.L. 1977
J. Pharm. Sci., 66, p155-159

Deighton, M. and Mead, J.A. 1978
"Introduction of Material Science", BAS Printer Ltd.

Dieter, G.E. 1961
"Mechanical Metallurgy", McGraw-Hill.

Doelker, E., Gunny, R. and Mordier, D. 1980
Acta. Pharm. Tech., 26(3), p155-158

Down, G.R.B. 1983
Powder Tech., 35, p167-169

Durr, M., Hanseen, D. and Harwalik, H. 1972
Pharm. Ind., 34, p905-911

Endersby, V.A. 1940
Proc. Am. Soc. Test Mater., 40, p1154

Engle, R.B. and Dunegan, H.L. 1969
Int. J. NDT, 1, p109

Ferry, J.D. 1970
"Visco-elastic Properties of Polymers", 2nd Ed.,
John Wiley, New York.

Forsyth, P.J.E. 1963
Acta Metallurgica, 11, p703

Forsyth, P.J.E. 1965
J. Inst. Metals, 93, p456

Fox, C.D., Richman, M.D., Reier, G.E. and Shangraw, R. 1963
Drug & Cos. Ind., 92(2), p161-161 & p258-261

Frost, N.E. and Dugdale, D.S. 1958
J. Mech. Phys., 6, p92

Frost, N.E. 1962
J. Mceh. Eng. Sci., 4, p22

Fuehrer, C. 1962
Deut. Apotheker-Ztg., 102, p827

Fuwa, M., Bunsell, A.R. and Harris, B. 1974
Composites-Stand. Testing & Design, p77

Ganderton, D. and Shotton, E. 1961
J. Pharm. Pharmacol., 12, 93T-97T

Gilardi, R.D. and Flippen, J.L. 1975
J. Am. Chem. Sco., 97, p6264

Graf, E. and Sakr, A. 1978
Pharm. Ind., 40(2), p 165-170

Gregory, H.R. 1962
Trans. Inst. Chem. Eng., 40, p241

Griffith, A.A. 1920
Phil. Trans. Roy. Soc. London, A221, p163-198

Griffiths, R.V. and Armstrong, N.A. 1970
Pharm. Acta. Helv., 45, p585-588

Gunsel, W.C. and Lachman, L. 1963
J. Pharm. Sci., 52, p178

Gunsel, W.C. and Kanig, J.L. 1976
in "Theory & Practice of Industrial Pharmacy",
Editors, Lieberman, M., Lachman, L. and Kanig, J.L.

Guyot, J.C. 1978
Int. Conf. Powder Tech. Pharm., paper 3, p21

Hall, S.D. and Rees, J.E. , 1978
J. Pharm. Pharmacol., 30, 26P

Hanus, J.H. and King, L.D. 1968
J. Pharm. Sci., 57, p677-684

Hardman, J.S. and Lilley, B.A. 1970
Nature Physical Sci., 228, p353-355

Hardman, J.S. and Lilley, B.A. 1973
Proc. Roy. Soc. London, A333, p183-199

Hassid, W.Z., Doudoroff, M. and Barker, H.A. 1944
J. Am. Chem. Soc. 66, p1416

Hassid, W.Z. and Doudoroff, M. 1950
Adv. Enzymol., 10, p123

Hatschek, E. 1921
Kolloid - Z., 28, p210-213

Heckel, R.W. 1961a
Trans. Metall. Soc. of AIME., 221, p671-675

Heckel, R.W. 1961b
Trans. Metall. Soc. Of AIME., 221, p1001-1007

Henderson, N.L. and Bruno, A.J. 1970
J. Pharm. Sci., 59, p1336-1340

Hertzberg, R.W., Manson, J.A. and Norderg, H. 1970
J. Mater. Sci., 5, p52

Hertzberg, R.M., Manson, J.A. and Skibo, M.D. 1975
Polym. Eng. Sci., 11, p479

Hertzberg, R.M. and Manson, J.A. 1980
"Fatigue of Engineering Plastics", Academic Press.

Hertzberg, R.M., Manson, J.A., Skibo, M.D. and Donald, J.K. 1979
J. Mater. Sci., 14, p1754

Hiestand, E.N., Wells, J.E., Peot, C.B. and Ochs, J.F. 1977
J. Pharm. Sci., 66, p510-519

Higuchi, T., Arnold, R.D., Tucker, S.J. and Busse, L.W. 1952
J. Am. Pharm. Ass. Sci. Ed., 41(2), p93

Higuchi, T., Rao, A.N., Busse, L.W. and Swintosky, J.V. 1953
J. Am. Pharm. Ass. Sci. Ed., 42(4), p194-200

Hill, K. and Smith, R. 1969
NGTE-NT, p759

Huettenrauch, R. 1971
Pharmazie, 26, p645

Huffine, C.L and Bonilla, C.F. 1962
J. Am. Inst. Chem. Eng., 8(4), p490

Hult, J.A. 1966
"Creep in Engineering Structures", Blaisdell Publishers, London

Iley, D.F., and Fraser-Reid, B. 1975
Carbohydr. Res., 17, p465

Ingale, A. 1979
Eastern Pharmacist, 22, p45-48

Inglis, C.E. 1913
Proc. Inst. Naval Architects, p60

Irwin, G.R. 1958
"Handbuck der Physik", Vol. VI, Ed. Flugge, S. p551

Irwin, G.R. 1960
Trans. ASEM Ser., D82(2), p417

John, V.B. 1972
"Introduction to Engineering Materials", MacMillan Press Ltd., London. p55-75

Jones, T.M. 1977

"Formulation and Preparation of Dosage Forms", Ed., J. Polderman, North Holland Elsevier, p29-44

Juslin, M. and Jarvinen, M.J. 1971
Famr. Aikak., 4-5, p242-248

Kala, H., Moldehauer, H., Giese, R., Kedvessy, G., Selmeczi, B. and Pintye-Hodi, K. 1981
Pharmazie, 36, p833-838

Kanig, J.L. 1964
J. Pharm. Sci., 53, p187-192

Kanig, J.L. 1970
"Emcompress Synposuim", London

Kassem, M.A.A. 1981
Egypt J. Pharm. Sci., 22(1-4), p271-281

Kessler, L.W., Korpel, A. and Palermo, P.R. 1971
Nature, 232, July 9, p110-111

Kessler, L.W. and Yuhas, D.E. 1979
Proceedings of IEEE, 67, p526-536

Khan, K.A., Musikabhumma, P. and Warr, J.P. 1981
Drug Dev. Ind. Pharm., 7, p525-538

Krycer, I., Pope, D.G. and Hersey, J.A. 1982
Int. J. Pharm., 12, p133-134

Kurobe, T. and Wakashima, H. 1970
13th Jpn. Congr. Mater. Res. Non-metall. Mater., p192

Kurobe, T. and Wakashima, H. 1972
15th Jpn. Congr. Mater. Res. Non-metall. Mater., p137

Laakso, R., Sneck, K. and Kristofferson, E. 1982
J. Pharm. Sci., 54, p447

Lamberson, R.L. and Raynor, G.E. 1976
Manfr. Chem. & Aerosol News, 47, p6

Leaderman, H. 1963
"Elastic and Creep Properties of Filamentous Materials and Other High Polymers", Textile Foundation, Washington D.C.

Leigh, S., Carless, J.E. and Burt, B.W. 1967
J. Pharm. Sci., 56, p888

Lemieux, R.U. and Huber, G. 1953
J. Am. Chem. Soc., 75, p4188

Lieberman, H.A and Lachman, L. 1980

"Pharmaceutical Dosage Form", Vol.1, Marcel Dekker Inc., New York, p164-172

Livingstone, J.L. 1970
Manfr. Chem. & Aerosol News, 42, p23-25

Long, W.M. 1960
Powder Metall., 6, p73

Manson, J.A., Wu, W.C. and Hertzberg, R.W. 1973
ASTM STP, 536, p391

Mendell, E.J. 1972
Manfr. Chem. & Aerosol News, 143, p43-46

Murkherjee, B. and Burns, D.J. 1971
Exp. Mech., 11, p433

Morri, M., Takeguchi, N. and Horkoshi, I. 1973
Chem. Pharm. Bull., 21(3), p589-593

Newton, J.M. and Fell, J.T. 1968
J. Pharm. Pharmacol., 20, p657

Newton, J.M. and Fell, J.T. 1970
Pharm. Acta. Helv., 45, p520

Newton, J.M. and Fell, J.T. 1971a
Pharm. Acta. Helv., 46, p226-235

Newton, J.M. and Fell, J.T. 1971b
Pharm. Acta. Helv., 46, p425-430

Newton, J.M. and Fell, J.T. 1971c
Pharm. Acta. Helv., 46, p441-447

Newton, J.M. and Fell, J.T. 1971d
J. Pharm. Sci., 60, p1866-1869

Newton, J.M., Fell, J.T., Rowley, G., Peacock, D.G. and Ridgway, K. 1971
J. Pharm. Pharmacol., 23, 195S-201S

Newton, J.M., Al-Angari, A.A. and Kennerley, J.W. 1985
J. Pharm. Pharmacol., 37, p151-153

Newton, J.M. 1974
J. Pharm. Pharmacol., 26, p215

Nicol, W.M. 1974
U.K. Patent No. 1 460 614

Nyström, C. and Alderborn, G. 1982
Acta Pharm. Suec., 19, p147-156

Obiorah, B.A. 1978
Int. J. Pharm., 1, p249

Ondari, C.O., Kean, C.E. and Rhodes, C.T. 1983
Drug Develop. & Ind. Pharm., 9(8), p1555-1572

Orowan, E. 1948
Phys. Soc. Rep. Prog., 12, p186

Orowan, E. 1955
Weld. Res. Suppl., 34, 157S

Paris, P.C. 1964
Proc. Sagamore Army Mater. Res. Conf., 10th, p107

Paronen, P. and Juslin, M. 1983
J. Pharm. Pharmacol., 35, p627-635

Parrott, E.L. and Jarosz, P.J. 1982
Drug Develop. & Ind. Pharm., 8(3), p445-453

Pearson, S. 1968
RAE-TR 68232

Pilpel, N., Malamataris, S. and Bin-Baie, S. 1984
J. Pharm. Pharmacol., 36, p616-617

Plumbridge, W.J. and Ryder, D.A. 1969
Metall. Res. 136

Plumbridge, W.J. 1972
J. Mat. Sci., p939-962

Polderman, J., de Blaey, C.J., Braakman, D.R. and Burger, H. 1969
Pharm. Weekbl., 104, p575

Polderman, J. and de Blaey, C.J. 1970
Pharm. Weekbl., 105, p241-250

Polderman, J. and de Blaey, C.J. 1971a
Pharm. Weekbl., 106, p57-65

Polderman, J. and de Blaey, C.J. 1971b
Pharm. Weekbl., 106, p589-596

Polderman, J. and de Blaey, C.J. 1971c
Pharm. Weekbl., 106, p894-903

Powers, H.E.C. 1970
Sugar Technol. Rev., p85-190

Radon, J.C. and Culver, L.E. 1975

Polym. Eng. Sci. 15, p500

Ragnarsson, G. and Sjogren, J. 1983
J. Pharm. Pharmacol., 35, p201-204

Ragnarsson, G. and Sjogren, J. 1984a
Acta. Pharm. Suec., 21, p141-144

Ragnarsson, G. and Sjogren, J. 1984b
Acta. Pharm. Suec., 21, p321-330

Ragnarsson, G. and Sjogren, J. 1985
J. Pharm. Pharmacol., 34, p9-13

Rankine, A.O. 1906
Phil. Mag., 11, p447

Rees, J.E. and Shotton, E. 1966
J. Pharm. Pharmacol., 18, 160S

Rees, J.E. and Hersey, J.A. 1970
Particle Size Analysis Conference, Bradford, U.K.

Rees, J.E. and Shotton, E. 1971
J. Pharm. Sci., 60, p1704

Rees, J.E. and Hersey, J.A. 1971
Nature Physical Sci., 230, p96

Rees, J.E., Hersey, J.A. and Cole, E.T. 1975
Pharm. Acta. Helv., 50, p28-32

Rees, J.E., Rue, P.J. and Richardson, S.C. 1977
J. Pharm. Pharmacol., 29, 38P

Rees, J.E. and Rue, P.J. 1978a
J. Pharm. Pharmacol., 30. p642-643

Rees, J.E. and Rue, P.J. 1978b
J. Pharm. Pharmacol., 30, p601-607

Rees, J.E. and Rue, P.J. 1978c
Drug Develop & Ind. Pharm., 4(2), p157-174

Reier, G.E. and Shangraw, R.F. 1966
J. PHarm. Sci., 55, p510-514

Reiter, H. 1984
Personal communications.

Richman, M.D., Fox, C.D. and Shangraw, R.F. 1965
J. Pharm. Sci., 54, p447

Riddell, M.N. 1974

Plast. Eng., 30(4), 71

Ridgway, K., Glasby, J. and Rosser, P.H. 1969
J. Pharm. Pharmacol., 21, 24S

Roberts, R.J. and Rowe, R.C. 1985
J. Pharm. Pharmacol., 37, p377-384

Rowe, R.C., Elworthy, P.G. and Ganderton, D. 1973
J. Pharm. Pharmacol., 25, 12P-16P

Rubinstein, M.H., Jackson, I.M. and Ridgway, F. 1982
J. Pharm. Pharmacol., 34, 48P

Sauer, J.A. 1978
Polymer, 19, p859

Saunders, P.R. and Ward, A.G. 1954
Proc. 2nd Int. Congr. Rheology, Butterworth, London.

Schubert, H., Herrmann, W. and Rumpf, H. 1975
Powder Tech., 11, p121

Seager, H., Rue, P.J., Ryder, J. and Burt, I. 1980
Int. J. Pharm. Tech. & Prod. Manf., 1(3), p2-6

Seelig, R.P. and Wulff, J. 1946
Trans. Am. Inst. Min. Matall. Engrs., 166, p492-505

Seitz, J.A. and Flessland, G.M. 1965
J. Pharm. Sci., p1353-1357

Selkirk, A.B. 1974
J. Pharm. Pharmacol., 26, p554-555

Seth, P.L. 1956
PhD Thesis, Swiss Federal Inst. Techn., Zurich

Shafer, E.G., Wollish, E.G. and Engel, C.E. 1956
J. Am. Pharm. Ass. Sci. Ed., 45, p114

Shangraw, R.F., Wallace, J.W. and Bowers, F.M. 1981
Pharm. Technol. Sept-Oct.

Sheikh-Salem, H. and Fell, J.T. 1981
Int. J. Pharm. Tech. & Prod. Manf., 2(1), p19-22

Sherman, P. 1968
"Emulsion Science", Academic Press, London.

Sherman, P. 1970
"Industrial Rheology", Academic Press, London.

Shlanata, S. and Milosovich, G. 1964
J. Pharm. Sci., 53, p562-564

Sinnott, M.J. 1958
"The Solid State for Engineers", J.Wiley & Sons, N.Y

Sixsmith, D. 1982
J. Pharm. Pharmacol., 34, p345-346

Smith, H.L., Baker, C.A. and Wood. J.H. 1971
J. Pharm. Pharmacol., 23, 536-538

Sokolv, S. 1936
USSR Pat. No. 49; British Pat. No. 477 139, (1937)

Spring, M.S. 1977
J. Pharm. Pharmacol., 29, p513-514

Stamm, A. and Mathis, C. 1976
Acta. Pharm. Tech., Suppl.1, p7-16

Staniforth, J.N., Rees, J.E., Kayes, J.B., Priest, R.C. and
Cotterill, N.J. 1981
Drug Develop. & Ind. Pharm., 7(2), p179-190

Staniforth, J.N. 1982
Int. J. Pharm. Tech. & Prod. Manf., 3(Suppl.), p1-12

Staniforth, J.N. and McCluskey, J.A. 1982
Int. J. Pharm. Tech. & Prod. Manf., 3(3), p76-80

Staniforth, J.N. 1984
Int. J. Pharm. Tech. & Prod. Manf., 5(1), p1-12

Staniforth, J.N. 1985
J. Pharm. Pharmacol., 37, p692-697

Summers, M.P., Enever, R.P. and Carless, J.E. 1977
J. Pharm. Sci., 66, p1172-1175

Sutherland, D.N. and Paton, N. 1969
Int. Sugar J., 71, p131-135

Train, D. and Hersey, J.A. 1960
Powder Met., 6, p20

Travers, D.N. and Merriman, M.P.H. 1970
J. Pharm. Pharmacol., 22, 11S

Ueno, W. 1963
Rep. Progr. Polym. Phys., (Japan), 1, p175-178

Vaccuri, G., Accorsi, C.A. and Mantovani, G. 1981
Ind. Sac. Ital., 74, p147-152

VanHook, A. 1980

Proc. Tech. Sess. Cane Sugar Refin Res., p103-113

Vijayan, S. and Venkateswarlu, D. 1969
J. Inst. Eng.(India)., 49, p58-62

Walters, N.E. 1966
J. Mater. Sci., 1, p354

Wells, J.L. and Langridge, J.R. 1981
Int. J. Pharm. Tech. & Prod. Manf., 2(2), p1-8

Williams, R.S. and Reifsnider, K.L. 1974
J. Composite Mate., 8, p340

Yarton, D. and Davis, T.J. 1963
Powder Met., 11(1), p115

York, P. and Pilpel, N. 1972
J. Pharm. Pharmacol., 24, 47P

York, P. and Pilpel, N. 1973
J. Pharm. Pharmacol., 25, 1-11P

York, P. 1979
J. Pharm. Pharmacol., 31, p244-246

7. APPENDIX.

1

Figure 100:

A. Fractured surface of an Avicel tablet compressed at 6kN compaction force.

B. Fractured surface of an Emcompress tablet compressed at 8kN compaction force.

C. Surface morphology of a typical agglomerate present in a sample of sucrose co-transformed with 3% w/w maltodextrin.

D. Surface morphology of a typical agglomerate present in a sample of sucrose co-transformed with 1% w/w gelatin B.S. 300.

A

10um

B

10um

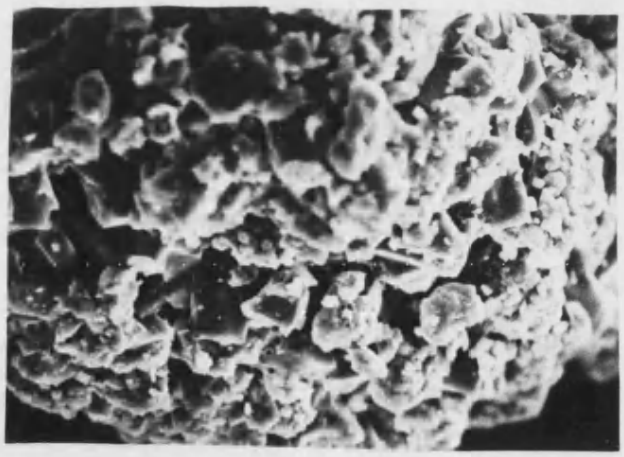

C

100um

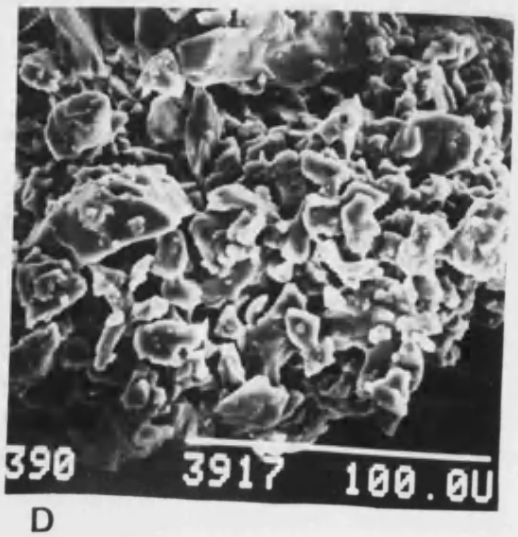

D

Figure 101 :

A. Sucrose crystals present in commercial sample.

B. Surface morphology of a typical sucrose crystal present in a sample of commercial sucrose.

C. General types of agglomerates present in a sample of transformed sucrose.

D. Surface morphology of a typical aggolmerate present in a sample of transformed sucrose.

E. Surface morphology of a typical aggolmerate present in a sample of transformed sucrose coated with 3% maltodextrin.

F. Surface morphology of a typical aggolmerate present in a sample of transformed sucrose coated with polyethylene glycol 4,000.

A

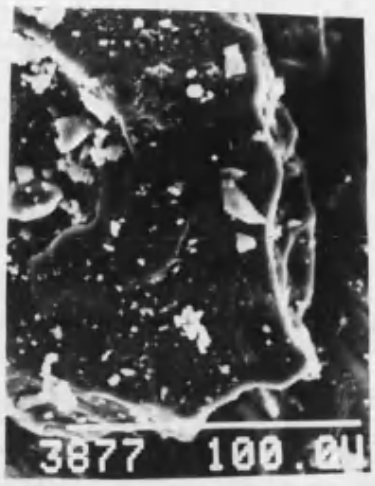

B

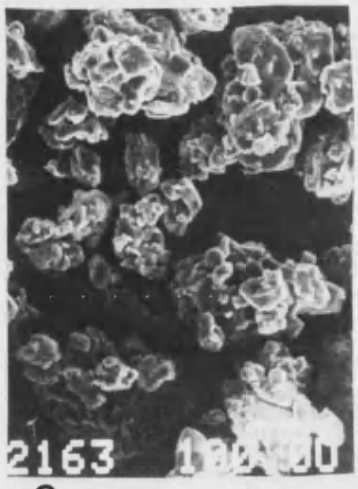

C

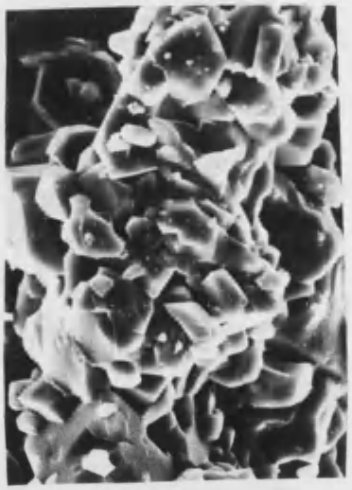

D 100um

E 100um

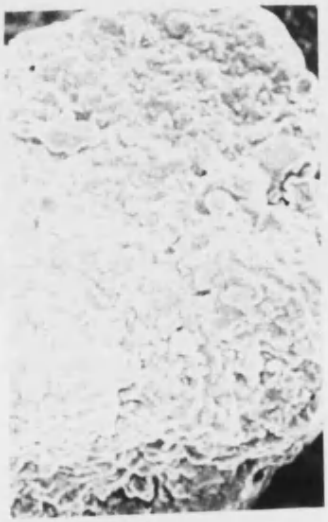

F 100um

Figure 102:

A. Surface morphology of a typical agglomerate present in a sample of sucrose co-transformed with 5% w/w dextran, with a relative molecular weight of 252,000 D.

B. Surface morphology of a typical agglomerate present in a sample of sucrose co-transformed with 10% w/w fibrous cellulose.

C. Surface morphology of a typical agglomerate present in a sample of sucrose co-transformed with 10% w/w cellulose acetate.

D. Surface morphology of a typical agglomerate present in a sample of sucrose co-transformed with 5% w/w sucrose ester, type F160.

A

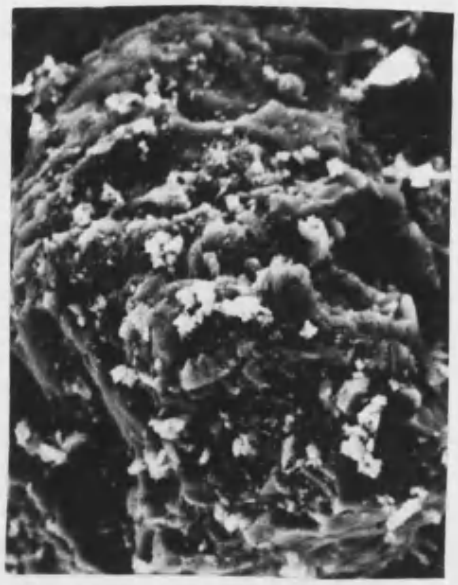

B

10um

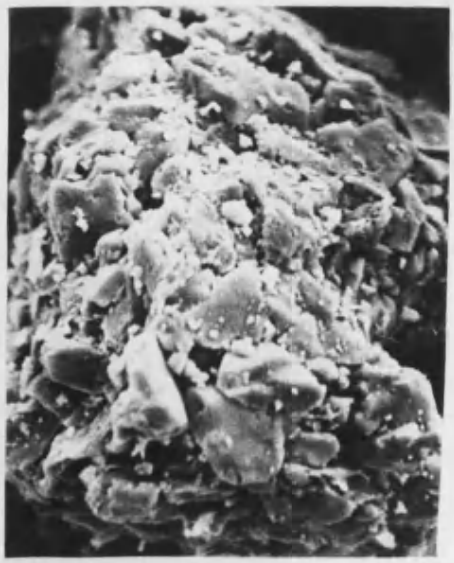

C

100um

D

10um